Journée des histiocytoses

Registre / centre de référence des histiocytoses

24 mai 2013 Paris

Comprendre et soigner les histiocytoses constituent la base des missions du centre de référence et du registre.

Les histiocytoses sont des maladies exceptionnelles, que de très nombreux praticiens et spécialistes sont amenés à voir, à diagnostiquer, à suivre. Elles donnent souvent du fil à retordre aux médecins impliqués dans le soin de leur patient et il va s'en dire aux patients et à leur famille. L'extrême rareté justifie pleinement qu'il puisse exister un centre ressource pour accumuler l'expérience et développer connaissance et expertise. Mais ce centre ressource n'a de sens que s'il s'appuie sur un large réseau de correspondants, que s'il produit des connaissances pour sortir ces maladies du flou qui les caractérisaient et enfin que s'il contribue à améliorer l'état de santé des personnes concernées.

Dans les 3 dernières années, nous voyons des progrès significatifs dans la compréhension moléculaire de ces maladies. Cette compréhension ouvre les perspectives de thérapie ciblée, ce qui était inespérée jusqu'alors et la preuve du concept nous est offerte par l'équipe de la pitié et Julien Haroche. Nous avons juste le sentiment de commencer à pouvoir tirer une ficelle qui nous donnera la bonne lecture de ces maladies. Toute la matinée va être dédiée à cette partie scientifique.

Au coeur de notre projet et qui justifie par dessus tout ces efforts, il y a les patients et bien sur d'abord des situations pénibles, voire parfois aussi dramatique. L'essai thérapeutique est l'étalon-or de l'évaluation des soins. Mais la rareté des cas, leur dispersion limitent les possibilités dans les histiocytoses. Il reste à partir d'une dimension plus modeste, l'étude rétrospective, la revue de la littérature pour dégager des consensus et avancer, pas à pas, aujourd'hui. La prise en charge des patients adultes, les atteintes neuro dégénérative sont abordées dans ce sens dans l'après midi.

Comme dans de nombreuses maladies rares, notre investissement est porté par des associations de patients, nationale comme *Histiocytose france*, ou locale comme *La petite maison dans la prairie* ou enfin plus généraliste comme *La Fédération Enfance et Santé*. Ces associations soutiennent notre projet et joignent leurs efforts à ceux des pouvoirs publics, la DGOS, l'Inserm, l'Invs qui, malgré une période économique difficile, nous permettent de continuer l'activité du registre et du centre de référence. Un dernier clin d'oeil à nos collègues hors France qui vont contribuer à cette journée, d'Égypte, d'Autriche, d'Allemagne et d'Angleterre..

Très bonne journée.

Jean Donadieu pour le centre de référence.

Table des matières

Pour chaque intervention, dans la mesure du possible nous avons fait figurer un article publié en rapport avec la présentation, sinon, nous laissons une page blanche pour des notes

Comité de pilotage commun : Centre de référence histiocytose et registre histiocytose

Coordinateur du centre de référence - Atteinte pulmonaire adulte: Pr A Tazi Service de pneumologie Hôpital Saint Louis 75010 Paris Tel 01 42 49 9718 Mail : abdellatif.tazi@sls.aphp.fr Et Dr G Lorillon Mail: gwenael.lorillon@sls.aphp.fr	Coordinateur du registre et de l'activité pédiatrique du centre de référence/ site Trousseau Dr J Donadieu Service d'hémato oncologie pédiatrique Hôpital Trousseau 75012 Paris Tel 01 44 73 53 14 Mail : jean.donadieu@trs.aphp.fr
Médecine interne Adulte Dr M De Menthon Service de médecine interne Hôpital Saint Louis 75010 Paris Mail : mathilde.de-menthon@sls.aphp.fr	*Médecine interne Adulte* Dr Julien Haroche Service de médecine interne Hôpital Pitié Salpêtrière 75013 Paris Mail : julien.haroche@psl.aphp.fr
Association des patients Histiocytose France Mme Debar Mail : asso.hystiocytose@voila.fr	Moniteur d'étude Clinique Mohamed Aziz Barkaoui Service d'hémato oncologie pédiatrique Hôpital Trousseau 75012 Paris mohamed-aziz.barkaoui@trs.aphp.fr Emmanuelle Bugnet Service de pneumologie Hôpital Saint Louis 75010 Paris E mail: emmanuelle.bugnet@sls.aphp.fr
Pédiatrie Site Nantes Dr C Thomas Service d'onco hémato pédiatrique CHU de Nantes Quai Moncousu Nantes 44 000 Mail : caroline.thomas@chu-nantes.fr	**Pédiatrie Site Montpellier** Dr Eric Jeziorski Service de pédiatrie Hôpital Arnaud de Villeneuve 371 avenue du Doyen Gaston Giraud 34295 MONTPELLIER CEDEX 5. e-jeziorski@chu-montpellier.fr
Neurologie Pr Khe Hoang Xuan Service de Neurologie Hopital de la Pitié Salpétriére **khe.hoang-xuan@psl.aphp.fr** Et Dr Ahmed IDBAIH Mail: **ahmed.idbaih@psl.aphp.fr**	**Pathologie** Pr Jean François Emile Laboratoire d'anatomo pathologie Hopital A Paré Boulogne **jean-francois.emile@apr.aphp.fr**

Programme

Le vendredi 24 mai 2013 : 9 h 30 -17 h 30

Accueil 9 h

Début 9 H 30

Biologie des histiocytoses: Ce qui change avec B raf 9 h 30 10 h 45

B raf Lien entre mutation et pathologies des macrophages JF Emile 15"
Corrélation B Raf et présentation clinique chez l'enfant J Donadieu 15'
B raf dans la maladie d'erdheim Chester et les formes mixtes de l'adulte J Haroche 15'

Les Inhibiteurs de B raf/ utilisation thérapeutiques 10 h 45 11 h 10
Expériences en cancérologie adultes; Inhibiteurs B raf et Inhibiteurs MEK L'exemple du Mélanome: C Lebbe St Louis 25'

Le sarcome histiocytaire: un cousin éloignée de l'Histiocytose langerhansienne ? 11 h 15 12 h
Le Sarcome histiocytaire: classification et évolution clinique JF Emile / F Charlotte K Moktari 15'
Sarcome histiocytaire cérébral et BRAF A Idbaih 10 '
Pathologies comparés Homme / Chiens: projet INCA Catherine André -Jérôme Abadie 20'

Voie NOTCH 1 et Histiocytose Langerhansienne: Caroline Hutter Vienne 30' 12 h 12 h 30

Ontogénie de la microglie et des cellules dendritiques hépatiques / modèle pathogénique de l'histiocytose langerhansienne : Elisa Gomez Perdiguero King's college Londres 30' 12 h 30 13 h

Repas à 13 h Lieu Le Bar du Théâtre

Après Midi 14 h Clinique et recommandations
Histiocytose Adulte 14 h 15 h 45
Enquête épidémiologique adulte à Paris 1 er résultats A Mahr St Louis 15'
Approches thérapeutiques de l'HL systémique de l'adulte table ronde/ Quel degré de preuve ?
M De menthon, A Tazi, J Haroche 1 H 20
Etude LCH A 1 A Tazi St Louis 15'
Utilisation de VLB et stéroide chez les adultes G Lorillon St Louis 15'
Utilisation du 2 cda chez l'adulte A Neel CHU Nantes 15 '
Diphosphonates Aracytine et autres traitements / Revue de la littérature M De Menthon St Louis 15 '
Radiothérapie chez l'adulte J Donadieu Trousseau 10'
Thalidomide (équipe St Louis) 10 '

Euro Histio net E Schaefer 15' 15 H 45 16 h

Pause 16 h 16 h 15

Coopération France / Egypte M Sedlki 15 '

Atteintes neurologiques Enfants et Adultes Recommandations pour le diagnostic et la prise en charge des: A Idbaih K Hoang Xuan E Bayen / propositions de recommandations 20 '

2 Cda Arac - Mise à jour. Trop toxicité ? Recommandations thérapeutiques version 2013 J Donadieu 15'

Fin de Journée 17 h 30

B raf Lien entre mutation et pathologies des macrophages
JF Emile A Paré Boulognes

Brief report

High prevalence of *BRAF V600E* mutations in Erdheim-Chester disease but not in other non-Langerhans cell histiocytoses

Julien Haroche,[1,2] *Frédéric Charlotte,[3] *Laurent Arnaud,[1,2] Andreas von Deimling,[4] Zofia Hélias-Rodzewicz,[5] Baptiste Hervier,[1,2] Fleur Cohen-Aubart,[1,2] David Launay,[6] Annette Lesot,[3] Karima Mokhtari,[7] Danielle Canioni,[8] Louise Galmiche,[8] Christian Rose,[9] Marc Schmalzing,[10] Sandra Croockewit,[11] Marianne Kambouchner,[12] Marie-Christine Copin,[13] Sylvie Fraitag,[8] Felix Sahm,[4] Nicole Brousse,[8] Zahir Amoura,[1,2] Jean Donadieu,[14] and Jean-François Emile[5,15]

[1]Department of Internal Medicine & French Reference Center for Rare Auto-immune & Systemic Diseases, Assistance Publique–Hôpitaux de Paris (AP-HP), Pitié-Salpêtrière Hospital, Paris, France; [2]Université Pierre et Marie Curie, Université Paris 06, Paris, France; [3]Department of Pathology, Hôpital Pitié-Salpêtrière, Paris, France and University Paris 6, Paris, France; [4]Department of Neuropathology, Institute of Pathology, Ruprecht-Karls-University, Heidelberg, and Clinical Cooperation Unit Neuropathology, German Cancer Research Center, Heidelberg, Germany; [5]EA4340, Versailles University, Boulogne, France; [6]Department of Internal Medicine, Hôpital Claude-Huriez, Centre Hospitalier Regional Universitaire Lille, Lille, France; [7]Department of Neuropathology, Raymond Escourolle, Hôpital Pitié-Salpêtrière, Paris, France and University Paris 6, AP-HP, Paris, France; [8]Department of Pathology, Hôpital Necker-Enfants Malades, Paris, France and University Paris 5, AP-HP, Paris, France; [9]Department of Onco-hematology, Hôpital Saint Vincent de Paul, UC de Lille, Université Nord de France, Lille, France; [10]Department of Rheumatology, University of Tübingen, Tübingen, Germany; [11]Department of Hematology, Radboud University Nijmegen Medical Center, Nijmegen, The Netherlands; [12]Department of Pathology, Hôpital Avicenne, AP-HP, Université Paris 13, Bobigny, France; [13]Department of Pathology, University Hospital, Lille, France; [14]Department of Pediatry, AP-HP, Centre de Référence des histiocytoses, Hôpital Trousseau, Paris, France; and [15]Department of Pathology, Hôpital Ambroise Paré, AP-HP, Boulogne, France

Histiocytoses are rare disorders of unknown origin with highly heterogeneous prognosis. *BRAF* mutations have been observed in Langerhans cell histiocytosis (LCH). We investigated the frequency of *BRAF* mutations in several types of histiocytoses. Histology from 127 patients with histiocytoses were reviewed. Detection of $BRAF^{V600}$ mutations was performed by pyrosequencing of DNA extracted from paraffin embedded samples. Diagnoses of Erdheim-Chester disease (ECD), LCH, Rosai-Dorfman disease, juvenile xanthogranuloma, histiocytic sarcoma, xanthoma disseminatum, interdigitating dendritic cell sarcoma, and necrobiotic xanthogranuloma were performed in 46, 39, 23, 12, 3, 2, 1, and 1 patients, respectively. *BRAF* status was obtained in 93 cases. $BRAF^{V600E}$ mutations were detected in 13 of 24 (54%) ECD, 11 of 29 (38%) LCH, and none of the other histiocytoses. Four patients with ECD died of disease. The high frequency of $BRAF^{V600E}$ in LCH and ECD suggests a common origin of these diseases. Treatment with vemurafenib should be investigated in patients with malignant $BRAF^{V600E}$ histiocytosis. (*Blood*. 2012;120(13):2700-2703)

Introduction

Histiocytoses encompass a wide range of rare and heterogeneous diseases characterized by the accumulation and/or the proliferation of histiocytes within various tissues. Since 1987, the classification for histiocytoses relies on the Langerhans and non-Langerhans cell origin.[1] The distinction was based on the presence of Birbeck granules and, more recently, on CD1a expression on formalin-fixed, paraffin-embedded samples.[2,3] The latest World Health Organization classifications has individualized Langerhans cell histiocytosis (LCH), Rosai-Dorfman disease, disseminated juvenile xanthogranuloma (JXG; synonym of Erdheim-Chester disease [ECD] and xanthoma disseminatum), interdigitating dendritic cell sarcoma, and histiocytic sarcomas.[4,5] Diagnosis of these conditions is mainly based on histopathology and corresponds to highly variable clinical syndromes, whose prognoses range from benign self-healing to highly malignant.

The RAS-RAF-MEK-ERK pathway is a cellular signaling pathway, which plays a major role in tumors.[6] $BRAF^{V600E}$ mutation, an activating mutation of the proto-oncogene BRAF, is present in several human tumors.[7] This mutation results in an activation of RAS-ERK pathway, independently of RAS activation. Inhibition of BRAF activation by vemurafenib improves survival of patients with $BRAF^{V600E}$ metastatic melanomas.[8] $BRAF^{V600E}$ mutations have been detected in patients with LCH.[9,10] We thus investigated whether this mutation was present in other subsets of histiocytoses.

Methods

Patients and samples

Patients were retrieved from the databases of the French Registry of Histiocytoses, and of 3 teaching hospitals (Pitié-Salpêtrière, Necker-Enfants Malades, and Ambroise Paré). Thirty-nine and 12 consecutive cases of LCH and cutaneous JXG were included, respectively. For other histicytoses, all cases available were included. Study was approved by the

Submitted May 18, 2012; accepted July 10, 2012. Prepublished online as *Blood* First Edition paper, August 9, 2012; DOI 10.1182/blood-2012-05-430140.

*F.C. and L.A. contributed equally to this study.

The online version of this article contains a data supplement.

The publication costs of this article were defrayed in part by page charge payment. Therefore, and solely to indicate this fact, this article is hereby marked "advertisement" in accordance with 18 USC section 1734.

ethic committee Ile de France III (#2011-A00447–34) and conducted in accordance with the Declaration of Helsinki. Clinical follow-up of patients with LCH and ECD was prospectively recorded according to previously described methodologies.[11,12]

All tissue samples were reviewed by at least 4 independent pathologists, trained in the field of histiocytoses (N.B., D.C., F.C., and J.-F.E.), and classified according to the World Health Organization classification.[4,5] Immunohistochemistry was performed with CD1a (Beckman-Coulter), CD68 (Dako Denmark), CD163 (Thermo Scientific), CD205 (Langerin; Novocastra), S100 protein (Dako Denmark), and factor XIIIa (Novocastra) when necessary. For ECD cases and a few other difficult cases, the diagnoses were achieved taking into account the clinical and radiologic aspects of the disease.[10] Patients with both LCH and ECD features were excluded.

Detection of $BRAF^{V600}$ mutations

Tumor DNA was extracted from formalin-fixed, paraffin-embedded tissues as described.[13] Four serial sections were performed for each sample. The first section was used for histology and selection of the areas of highest histiocyte density and the 3 others for dissection at ×10 magnification. When histiocyte infiltration was lower than 20%, sensitivity was considered as insufficient for *BRAF* heterozygous mutation detection. Detection of *BRAF* V600 mutations was performed by pyrosequencing with PyroMark Q24 (QIAGEN).

Immunochemistry with $BRAF^{V600E}$

Mouse monoclonal antibody VE1 was shown to be specific of $BRAF^{V600E}$ mutation.[14] Stainings were performed with Bond-Max (Leica Biosystems). Antigen retrieval was performed during 60 mn at 96°C in pH9 buffer Bond Epitope Retrieval Solution 2 (Leica Biosystems). VE1 hybridoma supernatant was diluted one-third and incubated at 37°C for 32 mn. Staining was revealed with Bond polymer refine red detection kit (Leica Biosystems). Staining was scored according to previously published criteria[14] by a pathologist who was not aware of genetic results.

Statistical analysis

Differences between groups of patients were tested using Mann-Whitney or Kruskal-Wallis tests for continuous data, and Fisher exact or χ^2 tests for categorical data. These analyses were followed by Bonferroni correction for multiple testing, when needed. All P values were 2-tailed, and statistical significance was defined as $P < .05$. Statistical analyses were performed using JMP8 (SAS Institute).

Results and discussion

Samples of the 127 patients mainly originated from bone (n = 29), skin (n = 27), lymph node (n = 18), perirenal infiltration (n = 12), and lung (n = 9; supplemental Table 1, available on the *Blood* Web site; see the Supplemental Materials link at the top of the online article). Diagnosis of ECD (n = 46), LCH (n = 39), Rosai-Dorfman disease (n = 23), JXG (n = 12), histiocytic sarcomas (n = 3), xanthoma disseminatum (n = 2), interdigitating dendritic cell sarcoma (n = 1), and NXG (n = 1) were established. In all ECD cases, histiocytes were $CD68^+$, $CD1a^-$, $S100^-$. Histiocytes were positive for factor XIII in 5 of 9 of ECD cases. All LCH cases contained $CD1a^+$, $S100^+$ histiocytes. *BRAF* mutational status was obtained by pyrosequencing in 93 (73%) of available cases. Failure to determine *BRAF* status was more frequent in bone and perirenal fat than in other sites of biopsies (49% vs 17%, $P = .0005$; supplemental Tables 1-3).

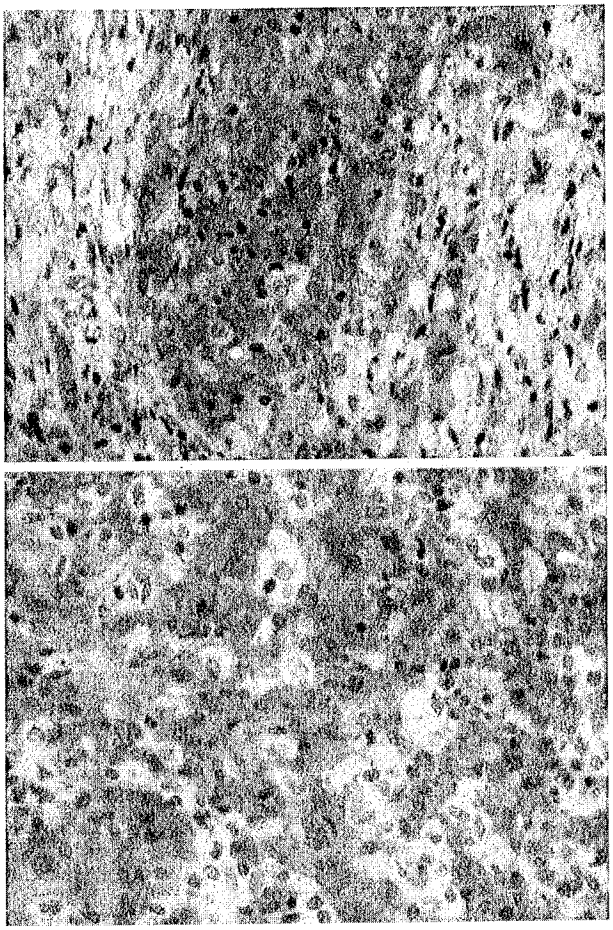

Figure 1. Identification of cells with BRAF mutation. Immunohistochemistry with $BRAF^{V600E}$ specific antibody VE1 disclosed cytoplasmic staining of histiocytes, whereas lymphocytes and fibroblasts were negative (top, original magnification ×100). Some histiocytes were not stained and correspond to reactive macrophages (bottom, original magnification ×200). Microphotographs were performed with a microscope BX41, eyepiece (WH 10×/22), objectives Olympus UPlanFI 10× and Olympus UPlanFI 20× (Olympus), Camera Axopcam ICc1, and AxioVision Rel Version 4.8 software (Carl Zeiss).

A $BRAF^{V600E}$ mutation was detected by pyrosequencing in 13 of 24 (54%) patients with ECD. For 2 patients, 2 different samples were available and both harbored the $BRAF^{V600E}$ mutation. The exact frequency of *BRAF* mutations in ECD patients remains to be confirmed in other series, as the present series may be biased by the fact that only 52% could be evaluated for *BRAF* status. The pathophysiology of histiocytoses remains to be determined. LCH was shown to be a clonal proliferation by HUMARA[15]; this result was confirmed with other methods. By contrast, there is an ongoing debate as to whether ECD should be considered as a tumor or an abnormal immune response. Indeed, the complex network of cytokines and chemokines associated with ECD underlines an intense systemic Th-1–oriented immune activation.[16] However, ECD was shown to be clonal in 5 patients, with either HUMARA[17] or cytogenetic.[18] The detection in the present study of *BRAF* mutations in 13 other ECD cases confirms that ECD is a clonal proliferation.

To determine which cells were mutated in ECD and further confirm the presence of the $BRAF^{V600E}$ mutation, we performed confirmatory immunohistochemistry analysis with $BRAF^{V600E}$ specific antibody on wild-type and mutated ECD samples. We recently confirmed in a series of melanomas that VE1 antibody was highly specific of $BRAF^{V600E}$ mutation, and shown it was more sensitive

Table 1. Main clinical characteristics of the 46 patients with ECD according to *BRAF*^{V600E} status

	WT (n = 11)	BRAF V600E (n = 13)	NA (n = 22)	*P* BRAF V600E versus WT*	*P* Across all 3 categories†
Median age at diagnosis, y (range)	55 (39-81)	55 (37-72)	57 (16-73)	.62	.83
Sex, male/female	9/2	8/5	16/6	.28	.54
Involvement					
CNS, n (%)	2 (18)	6 (46)	11 (50)	.15	.20
Heart, n (%)	4 (36)	7 (54)	10 (45)	.39	.73
Large vessels, n (%)	5 (45)	11 (85)	14 (64)	.04	.13
Exophthalmos, n (%)	3 (27)	7 (54)	7 (32)	.19	.32
Diabetes insipidus, n (%)	2 (18)	3 (23)	7 (32)	.77	.67
Lung, n (%)	4 (36)	4 (31)	10 (45)	.77	.67
Perirenal infiltration, n (%)	3 (27)	7 (54)	13 (59)	.19	.21
Xanthelasma, n (%)	4 (36)	4 (31)	6 (27)	.77	.87
Bone pain, n (%)	5 (45)	7 (54)	11 (50)	.68	.92
Death of disease progression, n (%)	2 (18)	2 (15)	5 (23)	.85	.86

*P values computed using Mann-Whitney test, χ^2 test, or Fisher test, as appropriate.

†P values computed using Kruskal-Wallis test or χ^2 test, as appropriate. None of these P values remains significant after Bonferroni correction for multiple testing.

than Sanger sequencing (E. Colomba, Z.H.-R., A.v.D., C. Marin, N. Terrones, D. Pechaud, S. Surel, J.-F. Côté, F. Peschaud, D. Capper, H. Blons, U. Zimmermann, T. Clerici, P. Saiag, J.-F.E., Detection of BRAF p.V600E mutations in melanomas: comparison of four methods argues for sequential use of immunohistochemistry and pyrosequencing, manuscript submitted, August 10, 2012). Seven positive and 6 negative ECD cases identified with pyrosequencing were tested, and immunohistochemistry with VE1 confirmed the *BRAF* status in all cases. Only histiocytes were stained, whereas lymphocytes, fibroblasts, and endothelial cells were negative (Figure 1). Both mononucleated histiocytes and Touton cells were positive, confirming that both mononucleated and multinucleated histiocytes derive from the same tumor progenitor. In some areas, BRAF-negative histiocytes were admixed with positive cells (Figure 1), probably corresponding to reactive inflammatory cells. Validation of the detection of *BRAF* mutations with immunohistochemistry for diagnostic use would be helpful for cases with low histiocyte infiltration.

A *BRAF*^{V600E} mutation was detected in 11 of 29 (38%) patients with LCH. This frequency was not statistically different from 13 of 24 (54%) that we observed in patients with ECD nor from 35 of 61 (57%) in the Badalian-Very series.[9] No mutations were detected in patients with Rosai-Dorfman disease (n = 23), cutaneous JXG (n = 12), histiocytic sarcomas (n = 3), xanthoma disseminatum (n = 2), interdigitating dendritic cell sarcoma (n = 1), or NXG (n = 1). Thus, ECD and LCH share similar oncogenic pathways, which are distinct from other histiocytoses. Interestingly, associations of ECD and LCH have been reported,[19] suggesting that both proliferations could derive from a common progenitor.

The treatment of ECD and LCH remains a challenge. Although some forms of LCH are benign and self-healing, some patients with ECD and LCH are resistant to several lines of chemotherapies.[12,20] Disease-related death occurred in 6 of 46 ECD and 3 of 39 LCH cases. Within this small series, the clinical characteristics of ECD patients did not appear to depend on *BRAF* status (Table 1); however, this outcome should be checked in a larger series.

Targeted therapies have recently been tested in both conditions[21,22]; however, it has limited efficacy. Prognosis of ECD has been substantially improved by IFN-α therapy, but many refractory forms subsist, especially those with CNS and cardiovascular involvements. Verumafenib, an inhibitor of BRAF, was recently approved for treating patients with metastatic melanoma and *BRAF*^{V600} mutations.[8] The poor prognosis of a substantial number of patients with multisystemic ECD and LCH warrants new therapeutic approaches that could involve BRAF inhibitors.

Acknowledgments

The authors thank Dominique Peschaud, Gladwys Faucher, Nathalie Terrones, Mariama Bakari, Yolaine Pothin, Sylvie Surel, and Catherine Le Gall for contributing to the *BRAF* mutation analyses.

This work was supported in part by Ligue Contre le Cancer, Association pour la Recherche et l'Enseignement en Pathologie (AREP), and Association pour la Recherche en Oncologie Digestive (AROLD) nonprofit associations.

Authorship

Contribution: J.H., F.C., J.D., Z.A., and J.-F.E. designed research; J.H., F.C., L.A., Z.H.-R., B.H., F.C.-A., D.L., A.L., K.M., D.C., L.G., C.R., M.S., S.C., M.K., M.-C.C., S.F., N.B., Z.A., J.D., and J.-F.E. collected data; L.A. performed statistical analysis; J.H., F.C., Z.A., and J.-F.E. analyzed and interpreted data; A.v.D., F.S., and J.-F.E. performed anti-VE1 immunohistochemical analysis; J.H., F.C., Z.H.-R., and J.-F.E. analyzed data; J.H., F.C., L.A., Z.A., and J.-F.E. wrote the manuscript; and all authors approved the final manuscript.

Conflict-of-interest disclosure: J.-F.E. received honoraria for counseling on diagnosis and/or treatment with BRAF inhibitors of patients with melanomas from Roche and Glaxo Smith Kline. The laboratory of J.-F.E. received grants from Roche for organization and external quality control assessment of *BRAF* mutation detection in France. D.C. and A.v.D. applied for a patent on the diagnostic use of BRAF V600E mutant-specific antibody VE1. All terms are being managed by the German Cancer Research Center in accordance with its conflict of interest policies. The remaining authors declare no competing financial interests.

Correspondence: Jean-François Emile, Pathology Department, Ambroise Paré Hospital, 9 Av. Charles de Gaulle, F-92104 Boulogne, France; e-mail: jean-francois.emile@apr.aphp.fr.

References

1. Writing Group of the Histiocyte Society. Histiocytosis syndromes in children. *Lancet.* 1987;329(I): 208-209.
2. Nezelof C, Basset F, Rousseau MF. Histiocytosis X histogenetic arguments for a Langerhans cell origin. *Biomedicine.* 1973;18(5):365-371.
3. Emile JF, Wechsler J, Brousse N, et al. Langerhans' cell histiocytosis: definitive diagnosis with the use of monoclonal antibody O10 on routinely paraffin-embedded samples. *Am J Surg Pathol.* 1995;19(6):636-641.
4. LeBoit PE, Burg G, Weedon D, Sarasin A. *World Health Organization Classification of Tumours: Pathology and Genetics of Tumours of the Skin.* Lyon, France: International Agency for Research in Cancer; 2006.
5. Swerdlow SH, Campo E, Lee Harris N, et al. *WHO Classification of Tumours of Haematopoietic and Lymphoid Tissues.* Lyon, France: International Agency for Research in Cancer; 2008.
6. Beeram M, Patnaik A, Rowinsky EK. Raf: a strategic target for therapeutic development against cancer. *J Clin Oncol.* 2005;23(27):6771-6790.
7. Davies H, Bignell GR, Cox C, et al. Mutations of the BRAF gene in human cancer. *Nature.* 2002; 417(6892):949-954.
8. Chapman PB, Hauschild A, Robert C, et al. Improved survival with vemurafenib in melanoma with BRAF V600E mutation. *N Engl J Med.* 2011; 364(26):2507-2516.
9. Badalian-Very G, Vergilio JA, Degar BA, et al. Recurrent BRAF mutations in Langerhans cell histiocytosis. *Blood.* 2010;116(11):1919-1923.
10. Satoh T, Smith A, Sarde A, et al. B-RAF mutant alleles associated with Langerhans cell histiocytosis, a granulomatous pediatric disease. *PLoS One.* 2012;7(4):e33891.
11. Guyot-Goubin A, Donadieu J, Barkaoui M, Bellec S, Thomas C, Clavel J. Descriptive epidemiology of childhood Langerhans cell histiocytosis in France, 2000-2004. *Pediatr Blood Cancer.* 2008;51(1):71-75.
12. Arnaud L, Hervier B, Néel A, et al. CNS involvement and treatment with interferon-α are independent prognostic factors in Erdheim-Chester disease: a multicenter survival analysis of 53 patients. *Blood.* 2011;117(10):2778-2782.
13. Moreau S, Saiag P, Aegerter P, et al. Prognostic value of *BRAF* (V600) mutations in melanoma patients after resection of metastatic lymph nodes [published online ahead of print July 7, 2012]. *Ann Surg Oncol.* doi:10.1245/s10434-012-2457-5.
14. Capper D, Preusser M, Habel A, et al. Assessment of BRAF V600E mutation status by immunohistochemistry with a mutation-specific monoclonal antibody. *Acta Neuropathol.* 2011;122(1): 11-19.
15. Willman CL, Busque L, Griffith BB, et al. Langerhans'-cell histiocytosis (histiocytosis X): a clonal proliferative disease. *N Engl J Med.* 1994; 331(3):154-160.
16. Arnaud L, Gorochov G, Charlotte F, et al. Systemic perturbation of cytokine and chemokine networks in Erdheim-Chester disease: a single-center series of 37 patients. *Blood.* 2011;117(10): 2783-2790.
17. Chetritt J, Paradis V, Dargere D, et al. Chester-Erdheim disease: a neoplastic disorder. *Hum Pathol.* 1999;30(9):1093-1096.
18. Vencio EF, Jenkins RB, Schiller JL, et al. Clonal cytogenetic abnormalities in Erdheim-Chester disease. *Am J Surg Pathol.* 2007;31(2):319-321.
19. Marchal A, Cuny JF, Montagne K, Haroche J, Barbaud A, Schmultz JL. Associated Langerhans cell histiocytosis and Erdheim-Chester disease. *Ann Dermatol Venereol.* 2011;138(11):743-747.
20. French Langerhans' Cell Histiocytosis Study Group. A multicentre retrospective survey of Langerhans' cell histiocytosis: 348 cases observed between 1983 and 1993. *Arch Dis Child.* 1996;75(1):17-24.
21. Montella L, Insabato L, Palmieri G. Imatinib mesylate for cerebral Langerhans'-cell histiocytosis. *N Engl J Med.* 2004;351(10):1034-1035.
22. Haroche J, Amoura Z, Charlotte F, et al. Imatinib mesylate for platelet-derived growth factor receptor-beta-positive Erdheim-Chester histiocytosis. *Blood.* 2008;111(11):5413-5415.

Corrélation B Raf et présentation clinique chez l'enfant J Donadieu Trousseau Paris

OPEN ACCESS Freely available online

PLoS one

B-RAF Mutant Alleles Associated with Langerhans Cell Histiocytosis, a Granulomatous Pediatric Disease

Takeshi Satoh[1☯], Alexander Smith[2☯], Aurelien Sarde[1☯], Hui-chun Lu[3], Sophie Mian[2], Celine Trouillet[1], Ghulam Mufti[2], Jean-Francois Emile[4], Franca Fraternali[3], Jean Donadieu[5], Frederic Geissmann[1]*

1 School of Medicine, Centre for Molecular and Cellular Biology of Inflammation (CMCBI), King's College London, London, United Kingdom, **2** Haematology Department, King's College London, London, United Kingdom, **3** Randall Division of Molecular Biophysics, King's College London, London, United Kingdom, **4** Hopital Ambroise-Pare, Pathology department, AP-HP, Paris, France, **5** Centre de Référence de l'Histiocytose, Hopital d'Enfants Armand Trousseau, Pediatric Hematology Unit, AP-HP, Paris, France

Abstract

Background: Langerhans cell histiocytosis (LCH) features inflammatory granuloma characterised by the presence of CD1a+ dendritic cells or 'LCH cells'. Badalian-Very et al. recently reported the presence of a canonical ^{V600E}B-RAF mutation in 57% of paraffin-embedded biopsies from LCH granuloma. Here we confirm their findings and report the identification of two novel B-RAF mutations detected in LCH patients.

Methods and Results: Mutations of B-RAF were observed in granuloma samples from 11 out of 16 patients using 'next generation' pyrosequencing. In 9 cases the mutation identified was ^{V600E}B-RAF. In 2 cases novel polymorphisms were identified. A somatic ^{600DLAT}B-RAF insertion mimicked the structural and functional consequences of the ^{V600E}B-RAF mutant. It destabilized the inactive conformation of the B-RAF kinase and resulted in increased ERK activation in 293 T cells. The ^{600DLAT}B-RAF and ^{V600E}B-RAF mutations were found enriched in DNA and mRNA from the CD1a+ fraction of granuloma. They were absent from the blood and monocytes of 58 LCH patients, with a lower threshold of sequencing sensitivity of 1%–2% relative mutation abundance. A novel germ line ^{T599A}B-RAF mutant allele was detected in one patient, at a relative mutation abundance close to 50% in the LCH granuloma, blood monocytes and lymphocytes. However, ^{T599A}B-RAF did not destabilize the inactive conformation of the B-RAF kinase, and did not induce increased ERK phosphorylation or C-RAF transactivation.

Conclusions: Our data confirmed presence of the ^{V600E}B-RAF mutation in LCH granuloma of some patients, and identify two novel B-RAF mutations. They indicate that ^{V600E}B-RAF and ^{600DLAT}B-RAF mutations are somatic mutants enriched in LCH CD1a$^+$ cells and absent from the patient blood. Further studies are needed to assess the functional consequences of the germ-line ^{T599A}B-RAF allele.

Citation: Satoh T, Smith A, Sarde A, Lu H-c, Mian S, et al. (2012) B-RAF Mutant Alleles Associated with Langerhans Cell Histiocytosis, a Granulomatous Pediatric Disease. PLoS ONE 7(4): e33891. doi:10.1371/journal.pone.0033891

Editor: Alice Y. W. Chang, Kaohsiung Chang Gung Memorial Hospital, Taiwan

Received October 20, 2011; **Accepted** February 19, 2012; **Published** April 10, 2012

Funding: TS is a fellow of the Japan Society for the Promotion of Science (JSPS) and FG is the Arthritis Research UK Chair of Inflammation Biology, at King's College London. This study was also funded by grants from the Histiocytosis Research Trust (HRT) and MRC G0900867 from the Medical Research Council (UK) to FG. The funders had no role in study design, data collection and analysis, decision to publish, or preparation of the manuscript.

Competing Interests: The authors have declared that no competing interests exist.

* E-mail: frederic.geissmann@kcl.ac.uk

☯ These authors contributed equally to this work.

Introduction

Langerhans cell histiocytosis (LCH) is a pediatric granulomatous disease with an incidence of four to eight cases per million children [1,2,3]. The clinical spectrum of LCH is remarkably broad, ranging from isolated skin or bone lesions to a disseminated disease that may require aggressive chemotherapy [1,4,5]. LCH can lead to severe dental and periodontal lesions [6]. LCH also frequently leads to diabetes insipidus [1,2,3]. Apart from diabetes insipidus, central nervous system involvement in Langerhans cell histiocytosis (LCH) is rare but represent a serious complication with neurological deterioration, including progressive cerebellar ataxia [7].

LCH lesions feature granulomatous collections of immature CD1a+ langerin/CD207+ DC ('LCH cells') presumed to be pathologic [8,9,10], admixed with abundant eosinophils [11], polyclonal T cells including abundant FoxP3$^+$ CD4$^+$ T cells [12], activated macrophages and osteoclast-like multinucleated giant cells [13]. These granuloma are therefore heterogeneous in cellular composition as well as anatomical distribution. The pathophysiology of LCH is largely unknown [10,14], although a genetic component is suggested by a higher concordance rate between monozygotic twins compared with dizygotic twins [15]. The tropism of skin lesions to flexures also suggests that external stimuli may trigger inflammation [16]. However, the nature of the initiating event(s), and the mechanisms of local tissue destruction by LCH and other inflammatory cells are still largely unknown.

Clonality of LCH granulomas has been reported in 1994 [17,18]. Its significance remained controversial, since specific genetic abnormalities were not consistently observed [19], until recently. Progress came from the identification by Badalian-Very

et al., of a ^{V600E}B-RAF mutation by pyrosequencing of formalin-fixed, paraffin-embedded material, from 35 out of 61 archived specimens (57%) [20]. This ^{V600E}B-RAF mutation is likely to be somatic, because a germ-line activating ^{V600E}B-RAF allele is embryonic lethal in mice [21]. B-RAF is a protein kinase activated by ras-coupled receptor tyrosine kinases (RTK) that is central to signaling via the Mitogen Activated Kinase (MAPK) and phosphorylates its downstream target MEK and ERK kinases [22]. The RAS-RAF-MAPK pathway coordinates a large variety of cellular responses involved in development, cell cycle regulation, cell proliferation and differentiation, cell survival and apoptosis, and many other physiological processes, by transmitting extracellular signals to various nuclear, cytoplasmic and membrane-bound targets [22].

Data obtained from murine model using Cre-mediated activation of a conditionnal B-RAF allele indicate that ^{V600E}B-RAF can contribute to tumour initiation [23]. For example, ^{V600E}B-RAF induces high levels of cyclin D1-mediated cell proliferation. However, ^{V600E}B-RAF also induces oncogene-induced senescence (OIS) that may restrain further development of the tumour [23,24]. In human, somatic ^{V600E}B-RAF mutation have been found in a number of benign and malignant tumors including non-malignant nacvi [25], melanoma [26], colon and thyroid tumors [21,22,24,26]. Thus ^{V600E}B-RAF may represent a first step toward the development of a malignant tumor, although the presence of a ^{V600E}B-RAF mutation is not synonymous with cancer.

Of note, the clinical features of LCH are not typical of cancer [10,14] and LCH lesions frequently regress, either spontaneously or after local treatment [1,4,5]. In addition, LCH CD1a+ cells, which are presumed to be pathologic, very slowly proliferate in most patients [12], while the expansion of a monocyte or dendritic cell compartment, which represent candidate precursors for these CD1a+ cells of the granuloma, was not consistently observed in the blood of LCH patients [12,27].

Identification of dysregulation of the RAS-RAF-MAPK pathway in LCH is nevertheless an important step towards a molecular understanding of the pathophysiology of this pediatric granuloma. It suggests possible novel therapeutic approaches, e.g. the use of B-RAF or MEK inhibitors. Moreover, if ^{V600E}B-RAF was detectable in the patient's blood, this could be of use for diagnostic, monitoring of treatment efficacy, and potentially prognostic purposes.

We therefore sought firstly to confirm the finding of Badalian-Very using another methodology i.e. analyzing flow sorted CD1a+ cells from fresh LCH granuloma tissue instead of paraffin embedded biopsies. We then aimed to compare relative mutation abundance of V600E B-RAF mutations between CD1a+ and CD1a− cells from LCH granuloma, and whether mutations can be detected in the peripheral blood of patients. Finally we investigated whether additional B-RAF mutations can be found in LCH patients, to further reinforce the link between LCH and the RAS-RAF pathway.

Results

B-RAF polymorphisms associated with LCH

We investigated the presence of B-RAF mutations by 'next generation' pyrosequencing (Roche GS FLX 454) in a series of 16 granuloma samples obtained at diagnosis from 16 patients with LCH from a cohort followed in the French LCH Registry (Tables 1 & 2). Among granuloma samples 11/16 carried B-RAF mutations as detected by pyrosequencing of granuloma genomic DNA (gDNA) and cDNA (Table 1). In 9/11 cases (patients #1–9) we found a g1799 T>A transition resulting in the previously described ^{V600E}B-RAF mutation [20] (Figure 1 A). In one patient (patient #10) we found a novel in-frame insertion of 12 nucleotides, leading to the insertion of 4 amino acids (Asp-Leu-Ala-Thr, or DLAT) (Figure 1 A). In one other patient we observed an A>G transversion, producing a ^{T599A}B-RAF allele (Table 2, Figure 1 A). The ^{T599A}B-RAF and ^{600DLAT}B-RAF alleles were not previously reported in the literature, dbSNP (v131), or in data from 1000 genomes project (Nov 10 release).

Somatic B-RAF mutations

The ^{V600E}B-RAF and ^{600DLAT}B-RAF, mutations were detected in granuloma from patients 1–10 with a high relative mutation abundance (RMA) (Table 2) We therefore investigated whether these alleles were germ-line or somatic mutants, and which cellular fraction of the granuloma was bearing the mutation. In 4 cases of ^{V600E}B-RAF mutation (Patients 4, 5, 8, 9) and in the sample carrying the ^{600DLAT}B-RAF mutation (patient #10) (Table 2), CD1a+ cells were enriched from fresh granuloma tissue using antibody-coupled beads [8]. The CD1a-depleted fractions (Effluent, Table 2) were also collected in 4 cases (Patients 5, 8, 9, 10, Table 2). Genomic DNA and cDNA were extracted from all samples and analysed by next generation sequencing. In all cases B-RAF mutated alleles were enriched in the CD1a+ fraction at the genomic DNA and cDNA level, in comparison with the CD1a-depleted fractions, with a relative mutation abundance of up to 48% (Table 2), suggesting that the CD1a+ 'LCH cells' carry a heterozygous B-RAF mutant allele, though we did not assess heterozygosity at the single cell level. We then investigated whether ^{V600E}B-RAF or ^{600DLAT}B-RAF mutations could be found in the patients circulating myeloid or lymphoid cells, either because of a germ-line mutation, or because of a mosaicism in bone marrow progenitors. Analysis by pyrosequencing of whole blood and of purified monocytes (CD14+) and lymphocytes (CD14−) from patient 1 indicated the absence of detectable B-RAF mutations, with a lower threshold of sequencing sensitivity of 1%–2% relative mutation abundance. Analysis of whole blood from patient 2 with the same method also failed to detect a ^{V600E}B-RAF mutation. Blood samples were not available for the 8 other patients with a ^{V600E}B-RAF or ^{600DLAT}B-RAF mutation.

We therefore investigated the presence of B-RAF mutations in peripheral blood mononuclear cells of an additional series of LCH patients for whom blood samples were available either at diagnosis or relapse (n = 22) (Table 3), or under treatment (n = 32). Neither ^{V600E}B-RAF or ^{600DLAT}B-RAF were detectable by pyrosequencing in these 56 peripheral blood mononuclear cell samples (Tables 2 & 3, and data not shown). Unfortunately granuloma samples were not availables for these patients, however based on the frequency of B-RAF mutation in LCH granuloma, 57% in the Badalian-Very study, and 11/16 (68%) in the present study, it is likely that several of the 56 patients had a B-RAF mutation in their granuloma.

In aggregate, these data indicate that ^{V600E}B-RAF and ^{600DLAT}B-RAF mutations are detectable in granuloma but not in the blood, and thus strongly suggest they are somatic events. In addition, lack of detection of B-RAF mutations in the blood from patients 1 and 2 and from the 22 others patients for whom blood samples were available at diagnosis or relapse suggests that detection of potential circulating B-RAF mutated cells will require a threshold of sensitivity below 1%.

Germline B-RAF polymorphisms

In contrast, the ^{T599A}B-RAF mutation was detected in both the granuloma and the whole blood of patient #16. ^{T599A}B-RAF was

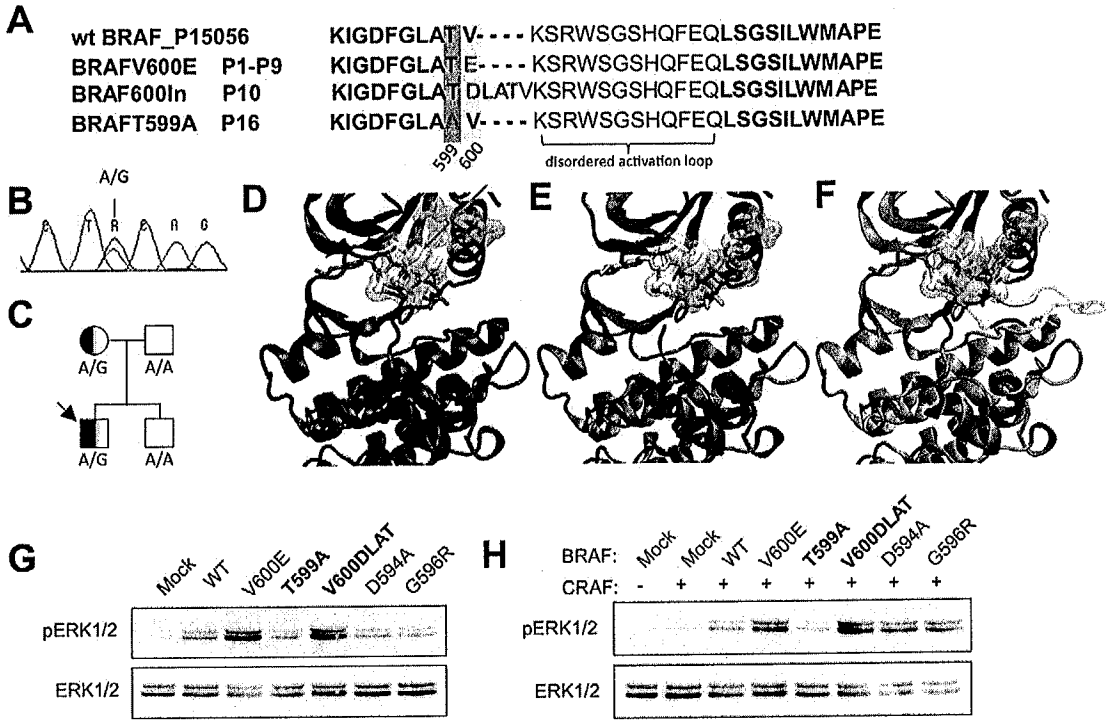

Figure 1. Analysis of B-RAF mutant. A. Sequence alignment, results from 454 pyrosequencing of granuloma cells from patients 1–10 and 16. **B.** 'Sanger' sequencing of patient 16 blood; A/G transition at nucleotide 1795. **C.** Pedigree of patient 16. Both the patient and his mother carry a ^{T599A}B-RAF allele, while his father is ^{wt}B-RAF. **D–E.** Comparison between ^{wt}B-RAF 5P_15056 (D, purple), ^{V600E}B-RAF structure (E, cyan) and the modeled mutant ^{600DLAT}B-RAF (F, grey). In D, Val600 (yellow) forms a hydrophobic contact with Phe468 (red arrow). In E and F charged residues Asp and Glu (in orange) disrupt the hydrophobic network of interactions, stabilising the active conformation of the P-loop. In F, insertion Asp-Leu-Ala-Thr shifted Val600 and disrupt the hydrophobic cluster. **G, H.** MEK phosphorylation in 293 T cells. 293 T cells were transiently transfected with with mock or B-RAF mutant expressing vectors (WT, V600E, T599A, 600DLAT, D594A, G596R), and with (H) or without (G) wtC-RAF. Twenty-four hours after transfection, the medium was changed to serum-free DMEM, followed by further 18 hours culture. Total cell lysates were immunoblotted with the indicated antibodies.
doi:10.1371/journal.pone.0033891.g001

Table 1. Age, sex, and clinical characteristics of patients 1 to 16.

Patient#	NUP	age at diagnosis (y)	sex	clinical features
#1	1506614	7.9	F	bone
#2	1506751	9	M	bone
#3	2106401	0.26	M	skin, lung, lympn node
#4	2106143	0.5	M	LETTERER SIWE hematological dysfunction, bone, liver, spleen
#5	1406259	8.4	F	bone
#6	1506706	19	M	Skin
#7	2106169	0.438	F	LETTERER SIWE hematological dysfunction, bone, liver, spleen, pituitary
#8	1406253	8.6	F	bone
#9	1406254	7.6	M	bone
#10	1406015	0	F	LETTERER SIWE hematological dysfunction, bone, liver, spleen, pituitary, lung, lymph nodes
#11	1406210	10	M	bone
#12	1506008	0.97	F	LETTERER SIWE hematological dysfunction, bone, lung, liver, spleen
#13	1406215	5.3	M	bone
#14	1406247	7.59	F	bone, lymph node
#15	1506766	11.79	F	bone
#16	1506646	1	M	skin, bone

doi:10.1371/journal.pone.0033891.t001

Table 2. Presence and relative abundance of B-RAF mutant clones identified in granuloma and blood from patients with LCH.

		granuloma							
		total	gDNA		cDNA		blood, gDNA		
Patient#	NUP	gDNA	CD1a+	effluent	CD1a+	effluent	whole blood	CD14+	CD14−
#1	1506614	V600E 13,5%					wt	wt	wt
#2	1506751	V600E 29,4%					wt		
#3	2106401	V600E 16%							
#4	2106143		V600E 35%		V600E 40%				
#5	1406259		V600E 38%	V600E 22%	V600E 46%	V600E 24%			
#6	1506706	V600E 8%							
#7	2106169	V600E 9%							
#8	1406253		V600E 21%	V600E 8%	V600E 48%	V600E 6%			
#9	1406254		V600E 35%	V600E 23%	V600E 47%	V600E 35%			
#10	1406015		600DLAT 11%	600DLAT 5%	600DLAT 28%	600DLAT 11%			
#11	1406210	wt							
#12	1506008	wt							
#13	1406215	wt							
#14	1406247	wt							
#15	1506766	wt						wt	wt
#16	1506646	T599A 44%					T599A 37%	T599A 37%	T599A 45%

doi:10.1371/journal.pone.0033891.t002

detected in the monocytic (CD14+) and lymphoid fractions (CD14−), at a high frequency of 37 to 45% relative mutation abundance, respectively, similar to its abundance in the granuloma (Table 2). This pattern suggested a germ-line mutation. Conventional 'Sanger' sequencing of peripheral blood mononuclear cells from the patient and from the patient's mother with an Applied Biosystem Genetic analyzer 3730xl confirmed the presence of an allelic mutation (Figure 1 B). Therefore the ^{T599A}B-RAF mutation was present in the peripheral blood of the patient and his mother, indicating a germ-line transmitted allele (Figure 1 C).

Altogether, these data indicate that ^{V600E}B-RAF and ^{600DLAT}B-RAF are somatic events while ^{T599A}B-RAF is a germ-line polymorphism.

B-RAF 600DLAT is an activating B-RAF mutant

Substitution of Val600 with Glu (^{V600E}B-RAF) strongly activates B-RAF [28,29]. ^{600DLAT}B-RAF is an in-frame insertion of 12 nucleotides leading to the insertion of 4 amino acids (Asp-Leu-Ala-Thr, or DLAT) starting from position 600 (Figure 1 A). This insertion, in the structural alignment superimposed to the V600 position, therefore effectively results in a B-RAFV600D substitution, leaving the insertion constituted only by a LATV segment. We have examined the residues surrounding D600 in the structure within a cut-off range of 6 Å. As reported by Wan et al. [29] the V600 residue is in a cluster of hydrophobic residues with Phe468, therefore the presence of a negative charge (residue D) will disrupt this cluster, resulting in destabilization of the inactive conformation of ^{600DLAT}B-RAF, exactly as for the V600E mutant (Figure 1 D–F). As expected from our structural modelisation study, ^{600DLAT}B-RAF resulted in increased MEK and ERK activation upon transient transfection in 293 T cells in comparison to wild-type B-RAF, similar to what is observed for ^{V600E}B-RAF [29] (Figure 1). However, we could not investigate the role of ^{V600E}B-RAF and ^{600DLAT}B-RAF in myeloid cells, since, when transfected in U937 and THP1 myeloid cell lines both ^{V600E}B-RAF and ^{600DLAT}B-RAF resulted in growth arrest and cell death (data not shown).

B-RAF T599A is a dead-kinase B-RAF mutant that does not transactivate C-RAF

Thr599 is a major phosphorylation site in the B-RAF activation domain [28], and substitution of Thr599 with alanine was shown in vitro to suppress B-RAF activity. Indeed, in contrast to ^{V600E}B-RAF and ^{600DLAT}B-RAF, ^{T599A}B-RAF substitutes a polar uncharged residue with a hydrophobic residue, causing the loss of short-ranged interactions with residues D576 and D594 (Figure 1 A, B). This does not predict a destabilization of the inactive conformation of B-RAF. Indeed transfection of ^{T599A}B-RAF in 293 T cells did not increase MEK and ERK phosphorylation, in comparison to wt control (Figure 1 G). Co-transfection of C-RAF did not increase MEK and ERK phosphorylation in the presence of ^{T599A}B-RAF (Figure 1 H). To further investigate the function of ^{T599A}B-RAF in myeloid cells, we retrovirally transfected ^{wt}B-RAF and ^{T599A}B-RAF in THP1 myeloid cells. As shown in Figure 2 C and 2 D ^{T599A}B-RAF did not induce MEK and ERK phosphorylation in THP1 cells above control (Figure 2 C). Thus ^{T599A}B-RAF may represent a mutant devoid of intrinsic kinase activity.

However, some B-RAF mutants found in cancer such as ^{D594A}B-RAF, albeit devoid of intrinsic B-RAF kinase activity, can transactivate C-RAF and the MEK/ERK pathway [30,31]. We thus compared the activity of ^{T599A}B-RAF with that of ^{wt}B-RAF and ^{D594A}B-RAF after retroviral transfection into U937 cells. Results indicated that unlike ^{D594A}B-RAF, ^{T599A}B-RAF did not induce MEK/ERK phosphorylation (Figure 2 D, E) or IL-8 production (Figure 2 F) by U937 cells.

Table 3. Age, sex, clinical features, and molecular findings in 22 patients with available blood samples at the time of diagnosis or relapse.

patient #	NUP	Clinical features	status at the time of blood sample	BRAF		
				whole blood	CD14+	CD14−
#17	1406220	bone skin, ENT, pituitary, neuro	active/progressive disease	na	wt	wt
#18	1506752	skin	active/progressive disease	wt	na	na
#19	1506604	Bone, skin, hematological dysfunction	active/progressive disease	wt	na	na
#20	1506648	Bone, skin, ENT, lung, liver, hematological dysfunction	active/progressive disease	wt	na	na
#21	1506882	Skin, ENT	active/progressive disease	wt	na	na
#22	1506863	Bone, skin, ENT, lung, liver, hematological dysfunction	active/progressive disease	wt	na	na
#23	1506009	Bone, skin, ENT, nodes, pituitary, lung, liver, spleen, hematological dysfunction	active/progressive disease	wt	na	na
#24	1507109	skin, ENT, pituitary	active/progressive disease	wt	na	na
#25	2106005	Bone, skin, ENT, CNS mass lesion	active/progressive disease	wt	na	na
#26	1509003	bone	at diagnosis, before treatment	wt	na	na
#27	1506819	bone	at diagnosis, before treatment	wt	na	na
#28	1507093	bone	at diagnosis, before treatment	wt	wt	na
#29	1506957	lung	at diagnosis, before treatment	wt	na	na
#30	1506973	bone, pituitary	at diagnosis, before treatment	wt	na	na
#31	1507062	Skin	at diagnosis, before treatment	wt	wt	wt
#32	1506869	bone	1 MONTH DIAGNOSIS	wt	na	na
#33	1507096	bone	<2 MONTH DIAGNOSIS	na	wt	wt
#34	1506754	skin	2 MONTHS DIAGNOSIS	wt	na	na
#35	1506865	bone	2 MONTH DIAGNOSIS	wt	na	na
#36	1507084	skin	2 MONTH DIAGNOSIS	wt	wt	wt
#37	1506932	bone	3 MONTH DIAGNOSIS	wt	wt	na
#38	1506984	skin	3 MONTH DIAGNOSIS	wt	na	na

doi:10.1371/journal.pone.0033891.t003

Clinical features of patients with B-RAF mutations

^{V600E}B-RAF mutations were found both in children with granuloma of bones or isolated skin disease, and in infants with early-onset multi-organ disease (Table 1). Among the 16 studied patients, we compared the proportion of patients with or without B-RAF mutations according to the extension of the disease by Fisher exact test and according to the age of diagnosis by Kruskall Wallis Test. No significant difference was observed as the p value was above 0.05 for all tests. However the sample size was small and may not be representative of a population based sample of patients. The patient with a ^{600DLAT}B-RAF insertion presented with early-onset multi-organ disease, but responded well to treatment (Patient #10, Table 1). The patient with a germ-line ^{T599A}B-RAF allele (Patient #16, Table 1) presented at the age of 10 months with persistent swelling of the left parietal bone. Two months after, clinical examination revealed 10 small skin nodules. Biopsy of one skin element demonstrated the histological diagnosis of LCH with the presence of CD1a+ cells. Patient #16 received therapy by vinblastine and steroid, as per the LCH III protocol, for a total duration of one year. No reactivation of the disease or sequellae was observed during a 7-year follow-up. His mother, who carried the same allelic mutation, is in good health and did not report a personal history of LCH.

Discussion

In this study we confirm the findings by Badalian-Very et al. [20], that ^{V600E}B-RAF mutations are detected in LCH granuloma, and identify two additional mutations ^{600DLAT}B-RAF and ^{T599A}B-RAF in two LCH patients. The ^{600DLAT}B-RAF mutants mimics ^{V600E}B-RAF at the structural and functional level. Our results also indicate that ^{V600E}B-RAF and ^{600DLAT}B-RAF mutations are enriched in CD1a+ 'LCH' granuloma cells and absent from the blood of 58 patients, suggesting the presence of somatic mutations in CD1a+ cells, and arguing against a mosaicism in the myeloid lineage or a bone marrow clonal disease, within the sensitivity limits of our deep-sequencing assay. We also identified a novel germ-line ^{T599A}B-RAF polymorphism in a patient with LCH, although it remains unclear whether ^{T599A}B-RAF is involved in the pathophysiology of LCH in this patient. The data presented here strengthen the association between B-RAF mutation and a dysregulation of the RAS-RAF-MEK pathway in CD1a+ LCH cells from LCH granuloma.

Both the study by Badalian-Very [20] and our present report fail to show a correlation between the presence of B-RAF mutations in LCH granuloma and the patient's age, clinical presentation, or outcome. However, the total number of cases analysed reported (77 in total) is still too small to allow a powerful

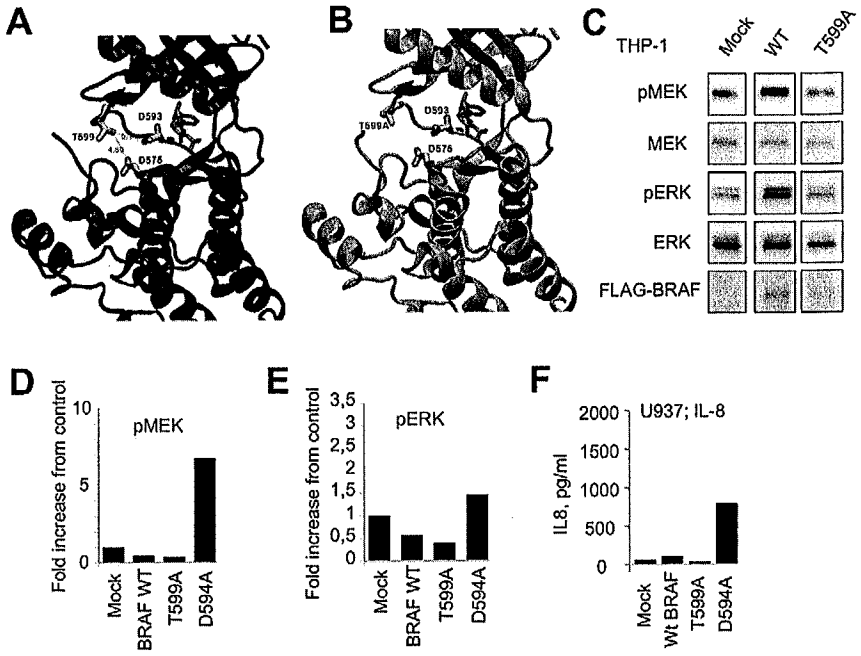

Figure 2. Analysis of ^{T599A}B-RAF. (**A, B**) Comparison between models of ^{WT}B-RAF 5P_15056 (A, violet) and ^{T599A}B-RAF (B, gold). ^{T599A}B-RAF substitutes a polar uncharged residue with a hydrophobic residue, causing the loss of short-ranged interactions with residues D576 and D594. **C.** Analysis of MEK and ERK phosphorylation in THP1 cell lines stably transfected with ^{WT}B-RAF-FLAG and ^{T599A}B-RAF-FLAG. Experiment was repeated twice with similar results. (**D–F**) Analysis of MEK and ERK phosphorylation and IL-8 production in U937 cell lines stably transfected with ^{WT}B-RAF, ^{T599A}B-RAF, and ^{D594A}B-RAF. Experiment was repeated twice with similar results.
doi:10.1371/journal.pone.0033891.g002

statistical analysis, given the marked clinical heterogeneity of the disease [1,4,5]. A statistical study of the possible association or lack of association of B-RAF somatic mutations with subgroups of LCH patients or with the natural history of the disease remains to be done, in a population based approach.

Our results indicate that both ^{600DLAT}B-RAF and ^{V600E}B-RAF mutations are somatic events which are not detected in the blood of patients. LCH granulomas may thus arise from a local process within affected tissues, rather than from the continuous recruitment of putative precursors, such as monocytes or dendritic cells carrying activating B-RAFV600E or B-RAF600DLAT alleles. Nevertheless, given the threshold sensitivity of 1%–2% of our deep-sequencing method, we cannot exclude the contribution of a minor myeloid-restricted clone in the bone marrow of patients, or of a subset of patients, and a prospective investigation is required to further investigate whether detection of rare circulating or bone marrow B-RAF mutated cells may be useful to monitor residual disease.

While substitution of Val600 with Glu (^{V600E}B-RAF) strongly activates B-RAF, substitution of Thr599 with Ala (^{T599A}B-RAF) impairs B-RAF kinase activity [28,29] given that Thr599 is the major phosphorylation site in the B-RAF activation domain [28]. Other mutations that affect intrinsic B-RAF kinase activity such as ^{D594A}B-RAF can also transactivate C-RAF and the MEK/ERK pathway, albeit less strongly [30,31]. However we have shown here that ^{T599A}B-RAF was both impaired in its intrinsic B-RAF kinase activity and unable to transactivate C-RAF. At this time, we do not have a molecular explanation for this observation. Further studies will therefore be needed to potentially unveil the functional consequences of the ^{T599A}B-RAF allele on cell activation. The patient's mother born in 1977 carried the same B-RAFT599A allele while in good health, and without a personal history of LCH. Therefore, although the ^{T599A}B-RAF allele is not a common polymorphism, there is no evidence that ^{T599A}B-RAF is involved in the pathophysiology of LCH in our patient. However the clinical spectrum of LCH is remarkably broad, and the age of onset highly variable [1,4,5], preventing us to definitely conclude to the absence of LCH in the mother of the patient. For instance, in one previously reported case of familial LCH, a monostotic lesion was diagnosed in a 20-year-old woman and then also in her daughter when aged 30 months [32].

Finally, ^{V600E}B-RAF mutations are observed in a number of benign and tumoral diseases (e.g. naevi and melanoma [25,26]). In itself this mutation thus do not characterize a malignant disease. It is posssible that the effects of activating B-RAF mutations such as ^{V600E}B-RAF and ^{600DLAT}B-RAF are different whenever they occur in stem cells or and differentiated cells, and depending on the lineage of the mutated cells, i.e. epithelial or myeloid. Therefore, more work is needed to understand the consequences of ^{V600E}B-RAF and ^{600DLAT}B-RAF in myeloid cells. We observed that retroviral transduction of either ^{V600E}B-RAF or ^{600DLAT}B-RAF in U937 and THP1 myeloid cell lines resulted in growth arrest and cell death. This suggests that an in vivo approach may be preferable, since an appropriate cellular environment could be required to support cell growth of ^{V600E}B-RAF or ^{600DLAT}B-RAF expressing myeloid cells. In this regard, mouse models of conditional expression of B-RAF mutant alleles in different cell lineages [23], should prove extremely useful.

Materials and Methods

Patients

Patients were registered in the National French Registry for Langerhans Cell Histiocytosis. LCH diagnosis was established on the basis of the patients' clinical history, histological examination and the mandatory presence of CD1a+ histiocytes in clinical

biopsy specimens, and reviewed by a national panel of pathologists. Patient's parents gave written informed consent for the study. The Study was approved by the Institutional Review Board of the University Hospital of Nantes, France. Characteristic of patients 1–16 are summarized in Table 1. Biopsies samples and/or blood were obtained at diagnosis from 15 patients with various clinical forms of the disease, isolated involvement of bone (n = 9), early-onset multisystem disease (n = 4), isolated skin (n = 1) and skin and lung disease (n = 1) (Table 1). Purified CD1a+ cells were isolated from biopsies from patients with eosinophilic granuloma of bone (n = 3) and early-onset multisystem disease (n = 3). Blood was obtain from patient 16 and his parents, and epithelial cells from patient 16, his parents and brother.

Preparation of DNA from granuloma samples, whole blood, and purified cellular fractions

Samples from CD1a+ LCH cells were obtained as previously described [8]. In brief, after frozen section examination, sterile tissue from eosinophilic granuloma was harvested in RPMI 1640 supplemented with 2 mM L-glutamine, 100 U/mL penicillin, 100 µg/mL streptomycin, and 10% heat-inactivated fetal calf serum (FCS) myoclone (all from GIBCO BRL, Gaithersburg, MD), referred to below as complete medium. Tissues were immediately gently dissociated through a nylon mesh. The cell suspension was washed 3 times and incubated with human IgG to block Fc receptor, and anti-CD1a antibody (BL6; Immunotech, Marseille, France). The cells were washed twice, incubated with antimouse microbeads (MACS; Miltenyi Biotec, Bergisch Gladbach, Germany) for 15 minutes at 4°C. Cells were washed again, and then CD1a+ LCH cells were separated by positive immunomagnetic selection by using a magnetic cell separator (MACS) according to the manufacturer's instructions. Between 2.105 and 6.105 CD1a+ cells were recovered from each sample. Purity of CD1a+ and CD1alow/neg sorted fraction was 80% or greater and mortality 10% or less. Genomic DNA and RNA from frozen granuloma cells, sorted CD1a+ cells and effluent fractions lysed and stored in Trizol were extracted using chloroform, the organic phase was transferred to a fresh tube to extract genomic DNA, and RNA was extracted using the RNA microkit from Qiagen. cDNA was obtained using the Superscript III Reverse-transcriptase kit (Invitrogen) according to the manufacturer's procedure. Genomic DNA extraction from paraffin sections (Patient 16) was performed as per Qiagen protocol for this material. Genomic DNA extraction from whole Blood was performed using the GenElute Blood genomic DNA kit mini prep from Sigma Aldrich according to the manufacturer procedure. Peripheral blood mononuclear cells (PBMCs) were obtained by the standard Ficoll-Hypaque method. CD14+ and CD14− fraction were separated by negative magnetic depletion by using hapten-conjugated CD3, CD7, CD19, CD45RA, CD56, and anti-IgE antibodies (MACS; Miltenyi Biotec) and a MACS according to the manufacturer's instructions. gDNA and RNA were extracted from CD14+ and CD14− MACS purificated monocytes fractions using the RNA/DNA AllPrep QIAgen Minikit (Quiagen).

B-RAF mutation detection

Pyrosequencing assay was performed using with 454 sequencing (Roche GS FLX platform). Primers sets were designed to amplify B-RAF exons 11 and 15 from both genomic DNA and cDNA, which incorporated a universal forward and reverse sequence tag. A second round of PCR was also performed utilizing the universal tags, to incorporate a sample specific 10 bp "barcode" sequence as well as additional tags utilized in the sequencing process (Roche GS FLX Titanium). Sequencing was performed to yield a 'depth' in excess of 500 clonal reads (500×) per exonic amplicon, per patient sample in most cases. This allowed detection of mutant clones down to around 1–2% relative mutation abundance, defined as the proportion of sequence reads that contain the mutation. Independent PCR and GS FLX sequencing experiments were carried out to confirm mutations and to reduce sampling error for calculations of mutation abundance. Somatic mutation in patient #16, his parents and his sibling were confirmed using a Applied Biosystem Genetic analyzer 3730xl (primers available on request).

B-RAF mutation modeling

The B-RAF patient mutations ^{600DLAT}B-RAF and ^{T599A}B-RAF have been modeled starting from the structure of the B-RAF kinase domain [29] using the Modeller 9v8 program [33]. The sequence alignment on this domain with the observed patient mutations was performed with the program Praline [34]. The structural alignment of the mutated sequences with the chosen template (pdb code 1WUH) was performed with the program T-coffee [35]. For each mutant, 200 structures have been generated and the ones with the best DOPE score have been selected for further investigations. The VMD program [36] has been used for graphical representations and for structural analyses.

Transfection of B-RAF alleles in 293 T cells

293 T (Lenti-X 293 T) was purchased from Clontech, and maintained in DMEM supplemented with 10% FBS, 100 units/ml Penicillin, and 100 mg/ml Streptomycin. cDNA fragments of human B-RAF (Genbank accession number: NM_004333) and C-RAF (Genbank accession number: NM_002880) were amplified by RT-PCR from human PBMC cDNA and cloned into pMXs-puro vector. V600E, T599A, D594A, and G596R B-RAF mutants construct were obtained by site-direct mutagenesis (Agilent Technologies). DLAT insertion B-RAF mutant construct was generated by PCR. The constructs were FLAG-tagged and cloned into pMXs-puro and pMXs-IRES-GFP vectors. The mutations were confirmed by DNA sequencing.

293 T was transiently transfected with pMXs-puro, FLAG-B-RAF WT, V600E, T599A, 600DLAT, D564A, G596R, or FLAG-CRAFvectors as indicated in the figure. Transfection was carried out with jetPEI according to the manufacture's instructions (Polyplus transfections, Inc.).

Generation of stable B-RAF transfectants using retroviral vector

Retrovirus packaging cell line, Plat-A was purchased from Cell Biolabs, Inc., and maintained in DMEM supplemented with 10% FBS, 100 units/ml Penicillin, and 100 mg/ml Streptomycin. U937 was kindly donated by Dr. Taams. THP-1 was kindly donated by Dr. Neil. These cell lines were maintained in RPMI supplemented with 10% FBS, 100 units/ml Penicillin, and 100 mg/ml Streptomycin (complete medium). Plat-A was transiently transfected with pMXs-IRES-GFP, FLAG-B-RAF WT, V600E, T599A, 600DLAT, D594A, and G596R vectors using jetPEI. Twenty-four hours after transfection, the medium was changed to fresh DMEM, and the cells were cultured for further 24 hours. The virus supernatants were collected and the debris was removed by centrifuge. The supernatants were mixed with DOTAP Liposomal Transfection Reagent (Roche) and added to U937 or THP-1 culture, followed by centrifuge at 30°C at 1100×g for 2 hours. Forty-eight hours after infection, GFP positive cells were sorted using BD FACSAria (BD Biosciences) and maintained in complete medium.

Western-Blot analysis

Twenty-four hours after transfection to 293 T cells, culture medium was changed to serum-free DMEM and cells starved for 18 hours. Cells were lysed with RIPA buffer (20 mM Tris-HCl (pH7.4), 150 mM NaCl, 2 mM EDTA, 1% Nonidet-P 40, 0.1% Sodium dodecyl sulfate, 0.1% Sodium deoxycolate, 50 mM Sodium fluoride, 1 mM b-Glycerophosphate, 1 mM Sodium orthovanadate, 1 mM Phenylmethylsulfonyl fluoride, and Protease inhibitor cocktail (Sigma-Aldrich)). For the experiment using THP-1 transfectant, 1×10^6 of growing cells were colllected by centrifuge and lysed in RIPA buffer. The cell lysates were separated on 10% SDS-PAGE gel and transferred onto nitrocellulose membranes (Bio-Rad). The membrane were blotted with anti-phospho-MEK1/2 mAb (41G9), anti-MEK1/2 mAb (L38C12), anti-phospho-ERK1/2 (D13.14.4E), anti-ERK1/2 mAb (L34F12) all from Cell Signaling Technology, Inc., and anti-FLAG M2 (Sigma Aldrich). Horseradish peroxidase-coupled secondary antibodies were used to detect the primary antibodies. Signal was revealed by enhanced chemiluminescence (SuperSignal West Pico Chemiluminescent Substrate, Pierce) using a molecular imager Chemidoc^{TM} XRS+, Biorad. Band intensity was quantified by ImageLab^{TM} Analysis Software.

Quantification of pMEK, pERK, and IL-8 from U937 transfectant by Bio-Plex

For the measurement of IL-8 secretion, 1×104 of U937 transfectants ware laid in a 96 well plate in 100 microL. After 24 hours, the plate were centrifuged and supernatants were collected. For pMEK and pERK, 1×104 of U937 were lysed using Bio-Plex Cell Lysis kit. The samples were analyzed according to manufactures instructions.

Statistics

Unsupervised students t-test on single comparisons was compared to analyse significance. A P value<0.05 was considered significant.

Acknowledgments

The authors thank patients and their families for participating to the study, Dempsey and his family, and the association Histiocytose france for constant support. We thank Dr Elisa Gomez-Perdigero and Dr Brigitte Senechal for helpful discussions.

Author Contributions

Conceived and designed the experiments: FG JD TS. Performed the experiments: A. Smith A. Sarde H-CL SM CT. Analyzed the data: FG FF JD. Contributed reagents/materials/analysis tools: GM JFE. Wrote the paper: FG.

References

1. Guyot-Goubin A, Donadieu J, Barkaoui M, Bellec S, Thomas C, et al. (2008) Descriptive epidemiology of childhood Langerhans cell histiocytosis in France, 2000–2004. Pediatr Blood Cancer 51: 71–75.
2. Salotti JA, Nanduri V, Pearce MS, Parker L, Lynn R, et al. (2009) Incidence and clinical features of Langerhans cell histiocytosis in the UK and Ireland. Arch Dis Child 94: 376–380.
3. Stalemark H, Laurencikas E, Karis J, Gavhed D, Fadeel B, et al. (2008) Incidence of Langerhans cell histiocytosis in children: a population-based study. Pediatr Blood Cancer 51: 76–81.
4. Group TFLCHS (1996) A multicentre retrospective survey of Langerhans' cell histiocytosis: 348 cases observed between 1983 and 1993. Arch Dis Child 75: 17–24.
5. Ceci A, de Terlizzi M, Colella R, Loiacono G, Balducci D, et al. (1993) Langerhans cell histiocytosis in childhood: results from the Italian Cooperative AIEOP-CNR-H.X '83 study. Med Pediatr Oncol 21: 259–264.
6. Madrigal-Martinez-Pereda C, Guerrero-Rodriguez V, Guisado-Moya B, Meniz-Garcia C (2009) Langerhans cell histiocytosis: literature review and descriptive analysis of oral manifestations. Med Oral Patol Oral Cir Bucal 14: E222–228.
7. Grois N, Prayer D, Prosch H, Lassmann H (2005) Neuropathology of CNS disease in Langerhans cell histiocytosis. Brain 128: 829–838.
8. Geissmann F, Lepelletier Y, Fraitag S, Valladeau J, Bodemer C, et al. (2001) Differentiation of Langerhans cells in Langerhans cell histiocytosis. Blood 97: 1241–1248.
9. Allen CE, Li L, Peters TL, Leung HC, Yu A, et al. (2010) Cell-specific gene expression in Langerhans cell histiocytosis lesions reveals a distinct profile compared with epidermal Langerhans cells. J Immunol 184: 4557–4567.
10. Egeler RM, van Halteren AG, Hogendoorn PC, Laman JD, Leenen PJ (2010) Langerhans cell histiocytosis: fascinating dynamics of the dendritic cell-macrophage lineage. Immunol Rev 234: 213–232.
11. Annels NE, Da Costa CE, Prins FA, Willemze A, Hogendoorn PC, et al. (2003) Aberrant chemokine receptor expression and chemokine production by Langerhans cells underlies the pathogenesis of Langerhans cell histiocytosis. J Exp Med 197: 1385–1390.
12. Senechal B, Elain G, Jeziorski E, Grondin V, Patey-Mariaud de Serre N, et al. (2007) Expansion of regulatory T cells in patients with Langerhans cell histiocytosis. PLoS Med 4: e253.
13. da Costa CE, Annels NE, Faaij CM, Forsyth RG, Hogendoorn PC, et al. (2005) Presence of osteoclast-like multinucleated giant cells in the bone and nonostotic lesions of Langerhans cell histiocytosis. J Exp Med 201: 687–693.
14. Gasent Blesa JM, Alberola Candel V, Solano Vercet C, Laforga Canales J, Semler C, et al. (2008) Langerhans cell histiocytosis. Clin Transl Oncol 10: 688–696.
15. Arico M, Nichols K, Whitlock JA, Arceci R, Haupt R, et al. (1999) Familial clustering of Langerhans cell histiocytosis. Br J Haematol 107: 883–888.
16. Weitzman S, Egeler RM (2008) Langerhans cell histiocytosis: update for the pediatrician. Curr Opin Pediatr 20: 23–29.
17. Willman CL, Busque L, Griffith BB, Favara BE, McClain KL, et al. (1994) Langerhans'-cell histiocytosis (histiocytosis X)–a clonal proliferative disease. N Engl J Med 331: 154–160.
18. Yu RC, Chu C, Buluwela L, Chu AC (1994) Clonal proliferation of Langerhans cells in Langerhans cell histiocytosis. Lancet 343: 767–768.
19. da Costa CE, Szuhai K, van Eijk R, Hoogeboom M, Sciot R, et al. (2009) No genomic aberrations in Langerhans cell histiocytosis as assessed by diverse molecular technologies. Genes Chromosomes Cancer 48: 239–249.
20. Badalian-Very G, Vergilio JA, Degar BA, Macconaill LE, Brandner B, et al. (2010) Recurrent BRAF mutations in Langerhans cell histiocytosis. Blood.
21. Mercer K, Giblett S, Green S, Lloyd D, DaRocha Dias S, et al. (2005) Expression of endogenous oncogenic V600EB-raf induces proliferation and developmental defects in mice and transformation of primary fibroblasts. Cancer Res 65: 11493–11500.
22. Wellbrock C, Karasarides M, Marais R (2004) The RAF proteins take centre stage. Nat Rev Mol Cell Biol 5: 875–885.
23. Pritchard C, Carragher L, Aldridge V, Giblett S, Jin H, et al. (2007) Mouse models for BRAF-induced cancers. Biochem Soc Trans 35: 1329–1333.
24. Dhomen N, Reis-Filho JS, da Rocha Dias S, Hayward R, Savage K, et al. (2009) Oncogenic Braf induces melanocyte senescence and melanoma in mice. Cancer Cell 15: 294–303.
25. Pollock PM, Harper UL, Hansen KS, Yudt LM, Stark M, et al. (2003) High frequency of BRAF mutations in nevi. Nat Genet 33: 19–20.
26. Dankort D, Curley DP, Cartlidge RA, Nelson B, Karnezis AN, et al. (2009) Braf(V600E) cooperates with Pten loss to induce metastatic melanoma. Nat Genet 41: 544–552.
27. Rolland A, Guyon L, Gill M, Cai YH, Banchereau J, et al. (2005) Increased blood myeloid dendritic cells and dendritic cell-poietins in Langerhans cell histiocytosis. J Immunol 174: 3067–3071.
28. Zhang BH, Guan KL (2000) Activation of B-Raf kinase requires phosphorylation of the conserved residues Thr598 and Ser601. Embo J 19: 5429–5439.
29. Wan PT, Garnett MJ, Roe SM, Lee S, Niculescu-Duvaz D, et al. (2004) Mechanism of activation of the RAF-ERK signaling pathway by oncogenic mutations of B-RAF. Cell 116: 855–867.
30. Kamata T, Hussain J, Giblett S, Hayward R, Marais R, et al. (2010) BRAF inactivation drives aneuploidy by deregulating CRAF. Cancer Res 70: 8475–8486.
31. Heidorn SJ, Milagre C, Whittaker S, Nourry A, Niculescu-Duvas I, et al. (2010) Kinase-dead BRAF and oncogenic RAS cooperate to drive tumor progression through CRAF. Cell 140: 209–221.
32. de Chadarevian JP, Pawel BR (1998) Hereditary Langerhans cell histiocytosis: instances of apparent vertical transmission. Med Pediatr Oncol 31: 559.
33. Eswar N, Eramian D, Webb B, Shen MY, Sali A (2008) Protein structure modeling with MODELLER. Methods Mol Biol 426: 145–159.
34. Simossis VA, Heringa J (2005) PRALINE: a multiple sequence alignment toolbox that integrates homology-extended and secondary structure information. Nucleic Acids Res 33: W289–294.

35. Notredame C, Higgins DG, Heringa J (2000) T-Coffee: A novel method for fast and accurate multiple sequence alignment. J Mol Biol 302: 205–217.

36. Humphrey W, Dalke A, Schulten K (1996) VMD: visual molecular dynamics. J Mol Graph 14: 33–38, 27–38.

B raf dans la maladie d'erdheim Chester et les formes mixtes de l'adulte J Haroché Pitié Paris

Dramatic efficacy of vemurafenib in both multisystemic and refractory Erdheim-Chester disease and Langerhans cell histiocytosis harboring the *BRAF* V600E mutation

*Julien Haroche,[1,2] *Fleur Cohen-Aubart,[1,2] *Jean-François Emile,[3] *Laurent Arnaud,[1,2] Philippe Maksud,[4] Frédéric Charlotte,[5] Philippe Cluzel,[6] Aurélie Drier,[7] Baptiste Hervier,[1,2] Neïla Benameur,[8] Sophie Besnard,[9] Jean Donadieu,[10] and Zahir Amoura[1,2]

[1]Department of Internal Medicine and French reference Center for Rare Auto-immune and Systemic Diseases, Assistance Publique–Hôpitaux de Paris (AP-HP), Pitié-Salpêtrière Hospital, Paris, France; [2]Université Pierre et Marie Curie, UPMC University Paris 6, Paris, France; [3]Research Unit (EA) EA4340 and Pathology Laboratory, Versailles University and AP-HP, Boulogne, France; Departments of [4]Nuclear Medicine, [5]Pathology, [6]Radiology, [7]Neuroradiology, and [8]Pharmacy, Hôpital Pitié-Salpêtrière, University Paris 6, AP-HP, Paris, France, [9]Department of Internal Medicine, Pontchaillou University Hospital, Rennes Cedex, France, and [10]Department of Pediatry, AP-HP, Centre de Référence des Histiocytoses, Hôpital Trousseau, Paris, France

Key Points

- Treatment with vemurafenib induced a dramatic response in 3 patients with histiocytosis harboring *BRAF* V600E mutations.
- Tumor response was observed in both Erdheim-Chester disease and Langerhans cell histiocytosis.

Histiocytoses are rare disorders of unknown origin with highly heterogeneous prognosis. *BRAF*^{V600E} gain-of-function mutations have been observed in 57% of cases of Langerhans cell histiocytosis (LCH) and 54% of cases of Erdheim-Chester disease (ECD), but not in other types of histiocytoses. Targeted therapy with an inhibitor of mutated BRAF (vemurafenib) improves survival of patients with melanoma. Here, we report vemurafenib treatment of 3 patients with multisystemic and refractory ECD carrying the *BRAF*^{V600E} mutation; 2 also had skin or lymph node LCH involvement. The patients were assessed clinically, biologically (CRP values), histologically (skin biopsy), and morphologically (positron emission tomography [PET], computed tomography and magnetic resonance imaging). For all patients, vemurafenib treatment led to substantial and rapid clinical and biologic improvement, and the tumor response was confirmed by PET, computed tomography, and/or magnetic resonance imaging 1 month after treatment initiation. For the first patient treated, the PET response increased between months 1 and 4 of treatment. The treatment remained effective after 4 months of follow-up although persistent disease activity was still observed. Treatment with vemurafenib, a newly approved BRAF inhibitor, should be considered for patients with severe and refractory *BRAF*^{V600E} histiocytoses, particularly when the disease is life-threatening. (*Blood*. 2013;121(9):1495-1500)

Introduction

Erdheim-Chester disease (ECD) is a rare non-Langerhans cell histiocytosis, characterized by the infiltration of tissues by foamy CD68$^+$ CD1a$^-$ histiocytes.[1] It is a systemic disease with diverse manifestations: the clinical course mainly depends on the extent and distribution of the disease, and ranges from asymptomatic bone lesions to life-threatening manifestations.[2] Rare cases of ECD associated with Langerhans cell histiocytosis (LCH) have been reported.[3]

Unlike ECD, LCH histiocytes are CD1a$^+$ and frequently infiltrate the epidermis in skin lesions.[4] Interferon α (IFN) is generally the first choice for ECD therapy and improves survival. It should be prescribed at high dose if there is central nervous system and/or cardiovascular involvement.[2] However, long-term IFN treatment can lead to severe side effects and some patients are refractory to treatment. Moreover some patients with CNS and/or cardiovascular infiltrations develop secondary resistance to high-dose of IFN. Alternative treatments include recombinant human interleukin-1 receptor antagonist, cladribine, thyrosine kinase inhibitors, autologous hematopoietic stem cell transplantation.[2] However, the optimal second line therapeutic strategy remains to be defined, mostly because these treatments have been evaluated in only small numbers of patients. Despite recent therapeutic progress the overall mortality remains high (18% of the 84 ECD patients seen at our institution). *BRAF*^{V600E} mutations have been observed in 38% to 69% of cases of LCH.[5-7] We recently reported *BRAF*^{V600E} mutations in 54% of 24 patients with ECD.[8] Vemurafenib, an inhibitor of mutant BRAF, has shown some efficacy against 2 diseases (melanoma and hairy-cell leukemia) associated with the *BRAF*^{V600E} mutation.[9,10]

Methods

This study was approved by the ethics committee Ile de France III (#2011-A00447-34) and conducted in accordance with the Declaration of Helsinki.

Patient no. 1

A 65-year-old man presented in October 2010 with elevated serum creatinine and C-reactive protein (CRP) levels found on routine blood testing. Abdominal computed tomography (CT) disclosed retroperitoneal

Submitted July 27, 2012; accepted November 18, 2012. Prepublished online as Blood First Edition paper, December 20, 2012; DOI: 10.1182/blood-2012-07-446286.

*J.H., F.C.-A., J.-F.E., and L.A. contributed equally to this work

There is an Inside *Blood* commentary on this article in this issue.

The publication costs of this article were defrayed in part by page charge payment. Therefore, and solely to indicate this fact, this article is hereby marked "advertisement" in accordance with 18 USC section 1734.

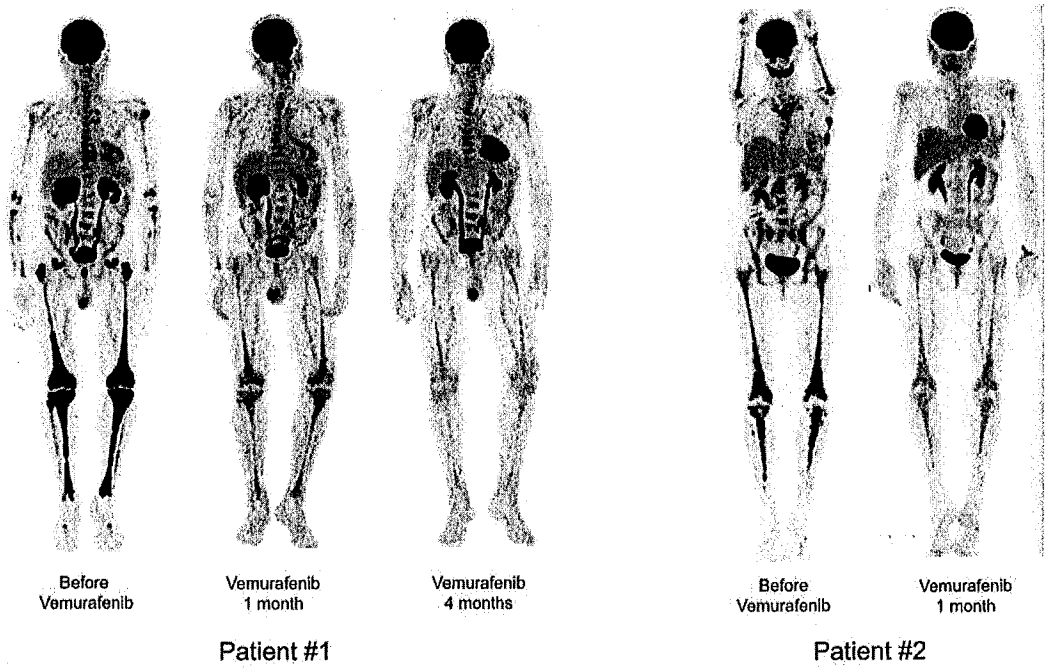

Figure 1. Sequential PET. Patient no. 1 (left): Sequential PET showing high initial pathologic uptake of ^{18}F-fluorodeoxyglucose in soft tissue and bones before vemurafenib treatment, and significantly less uptake after 1 month and major regression after 4 months of vemurafenib treatment. Patient no. 2 (right): Similar substantial reduction of ^{18}F-fluorodeoxyglucose uptake in all tissues involved. Reconstruction algorithm: OSEM_3D (5 iterations, 16 subsets, 9 mm Gauss filter). Volume rendering: Maximum Intensity Projection (Osirix Software). Display: BW inverse logarithmic table and range (min value = 0, max = 2.7 for SUV).

fibrosis complicated by bilateral hydronephrosis with sheathing of the abdominal aorta. Double ureteral pigtail stents were inserted and because hydronephrosis relapsed, bilateral nephrostomy was performed. Long-bone X-rays showed typical bilateral and symmetric cortical osteosclerosis in the lower limbs. A biopsy sample of the perirenal fibrosis showed numerous foamy CD68$^+$ CD1a$^-$ histiocytes. A diagnosis of ECD was established. Cerebral magnetic resonance imaging (MRI) showed sinus osteosclerosis; on cardiac MRI, the pericardium appeared thickened and there was specific infiltration of the auriculo-ventricular sulcus. Positron emission tomography (PET) revealed an intense uptake in the lower limbs and in the thoracic aorta.

Pegylated interferon α (PEG-IFN) treatment was started in July 2011, at 135 μg/w for 4 weeks, and was then increased to 180 μg/w due to cardiac involvement. Double ureteral pigtail stents were implanted to replace the nephrostomy and the blood creatinine concentration remained stable at 115μM. In January 2012, the CRP level was 21 mg/L, and the creatinine level was 137 μM. The patient developed pruritus, and gammaglutamyl transferase (GGT) activity was 936 U/L (normal 12-55) and alkaline phosphatase activity was 644 U/L (normal 40-120). Abdominal CT showed the persistence of sheathing of the whole aorta. Bilateral hydronephrosis had increased and there was a left renal artery stenosis. Liver MRI and biopsy showed no or only minor abnormalities, and in particular no histiocytes or signs of sclerosing cholangitis. PET revealed that the number of lesions and uptake by the lesion had increased, that is, hypermetabolism of the long bones of the lower limbs, and of thoracic and abdominal aorta, mediastinum and retroperitoneum (Figure 1). Cardiac MRI findings were unchanged. Angioplasty of the left renal artery with stent implantation was performed. In February 2012, the IFN dose was increased (to 180 μg/w PEG-IFN alternating with 270 μg/w) due to the absence of response to treatment; this was followed by depression and fatigue. The depressive symptoms persisted despite administration of antidepressant drugs, leading to the IFN treatment being stopped in March 2012. The creatinine level increased to 190μM, and consequently the double ureteral pigtail stents were replaced by thermoformable spiral metallic stents.

Patient no. 2

A 59-year-old woman was referred to us in February 2011 with a 2-year history of bone pain in the lower limbs. For the previous 6 months she had had diabetes insipidus, right orbital pain requiring morphine, and headaches. She had a history of bilateral breast cancer in 1998 treated by right mastectomy, radiotherapy, and chemotherapy. Thoracic and abdominal CT showed peri-aortitis (involving the arch, origin of the supra-aortic vessels, and the sub-renal aorta), nodular infiltration of the epiplon, and soft-tissue thickening of the pre- and retro-sternal spaces. Cardiac MRI showed a right pseudo-tumoral atrial infiltration. Orbital MRI found a right retro-orbital infiltration and compression of the optic nerve with intense enhancement after gadolinium administration. Bone scintigraphy was highly suggestive of ECD with intense uptake in the lower limbs. A monoclonal IgA κ component (12 g/L) was found, so a bone marrow biopsy was collected and revealed 30% plasma cell infiltration; renal function and calcemia were normal, hemoglobin was 12.5 g/dL, there was no proteinuria, and no lytic bone lesions were found. Stage I myeloma in the Durie-Salmon classification was diagnosed. Celioscopy in January 2011 found a peritoneal infiltration with foamy CD68$^+$ CD1a$^-$ histiocytes consistent with a diagnosis of ECD. At initial presentation, the patient had papulo-maculous squamous intertrigo-like lesions under the left breast: biopsies showed Langerhans cell infiltrate in the epidermis and non-Langerhans cell infiltrate in the hypodermis (Figure 2). Initial PET revealed intense uptake in the retro-orbital space, right atrium, and abdominal aorta, and bilateral and symmetric uptake in the diaphyseal and metaphyseal regions of the long bones (Figure 1) typical of ECD. These findings led to a diagnosis of ECD associated with histologic lesions of LCH in the skin. The most severe symptoms, requiring therapy, were due to ECD (peri-aortitis, bone pain, pseudo-tumoral atrial infiltration, mesenteric localization, and right retrorbital involvement). The associated IgAκ stage I myeloma only required monitoring.

Therapy with 135 μg/w PEG-IFN was initiated in March 2011. Partial improvement was observed, but pain in the right eye and cardiac abnormalities persisted. The PEG-IFN dose was increased to 180 μg/w in June 2011. In December 2011, the orbital pain had worsened and orbit MRI detected a

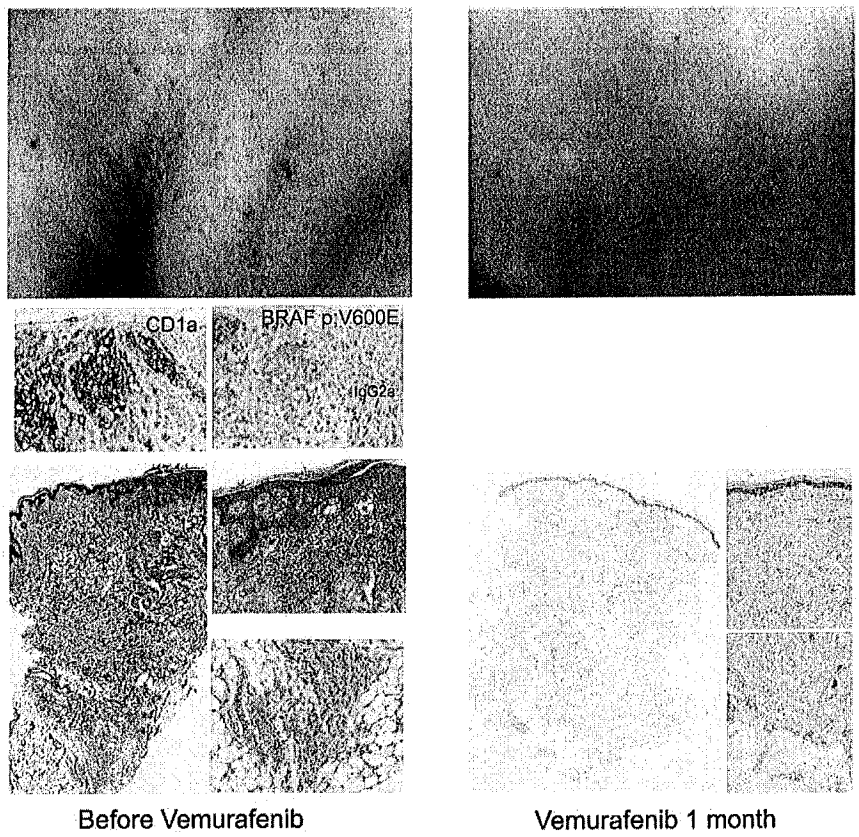

Figure 2. Skin lesions. LCH skin lesions in patient no. 2 disappeared after a few days of treatment with vemurafenib. Skin biopsy before treatment showing typical LCH infiltration of the epidermis and papillary dermis with $CD1a^+$ histiocytes; the hypodermis is infiltrated by foamy $CD68^+CD1a^-$ histiocytes (as in the peritoneal biopsy). Immunohistochemistry confirmed the expression of BRAF by histiocytes.

new hypersignal in the right optic nerve; PET revealed intense uptake in the long bones. PEG-IFN, which had been maintained at 180 μg/w, was stopped at the beginning of March 2012 due to depression, fatigue, neutropenia (≈ 500/mm^3), thrombocytopenia (46.000/mm^3), and inefficacy against the retro-orbital involvement. The patient was re-assessed on March 23: she had fever, CRP was 89 mg/L, and PET confirmed the worsening of the retro-orbital, bone, and mediastinal involvements. Orbit MRI also showed persistence of the retro-orbital lesion (Figure 3). Treatment with 100 mg/d anakinra was initiated on March 24 and effectively reduced the fever but not the CRP value (Figure 4). Concomitantly, the cutaneous lesions relapsed leading to anakinra discontinuation on April 17. The right retro-orbital pain worsened. Skin lesions were re-biopsied and the findings were unchanged (co-existence of LCH in the epidermis and ECD in the hypodermis).

Patient no. 3

A 31-year-old woman originating from Laos was referred to our department in April 2010 for subacute renal failure, diabetes insipidus, and elevated CRP level. Physical examination identified bilateral superior and inferior eyelid xanthelasma. Blood tests confirmed elevated creatinine and CRP levels (178μM and 147 mg/L, respectively). Abdominal CT-scan revealed retroperitoneal fibrosis and lymphadenopathy, and cerebral MRI showed that the pituitary axis was enlarged. Long bone ^{99}Tc scintigraphy showed intense metaphyseodiaphyseal uptake in femurs and tibias. Similar hypermetabolism in the long bones and also in the spleen, and retroperitoneal adenopathies were found on PET.

Biopsy of the palpebral xanthelasma confirmed the ECD localization with foamy histiocytes. Immunohistology was positive for CD68 and negative for PS100 with a few CD1a-positive cells. Biopsies of T4 vertebra and right inferior metaphyseal femur showed the same ECD patterns, and a biopsy of a retroperitoneal node displayed characteristics of LCH with strongly positive CD1a and PS100 staining.

In April 2010, treatment with PEG-IFN (135 μg/w) was started and double ureteral pigtail stents were inserted. Ten months later, in February 2011, the CRP level was 24 mg/L, creatinine had decreased to 138μM, and PET showed an improvement of long-bone uptake. In February 2012, the clinical status had deteriorated with new lower-limb pain and increased size of xanthelasmas. Abdominal CT scan showed enlargement of periaortic and periureteral infiltrations. Cardiac MRI, which had been normal on previous assessments, displayed a typical infiltration of the right atrial wall, atrioventricular groove, and gadolinium enhancement of the left ventricular wall, septum, and apex. The CRP level was 20 mg/L and PET disclosed a strong, new uptake in the basilar skull region. The PEG-IFN dose was increased to 180 μg/w on March 20, but was clinically ineffective: the CRP level increased to 42 mg/L. Treatment was stopped on May 9.

Histology and molecular analyses

All biopsies (perirenal, peritoneal, skin, and bone) obtained from the 3 patients before or after vemurafenib treatment were reviewed by 2 pathologists with specialist training in histiocytosis (F.C.-A., J.-F.E.). All patients provided consent for vemurafenib treatment after the provision of counseling. Each sample was processed for immunohistochemistry with antibodies against CD1a (Beckman-Coulter), CD68 (Dako), CD163 (Thermoscientific) and S100 protein (Dako), and with VE1 (a mouse monoclonal antibody specific for the $BRAF^{V600E}$ mutant, kindly provided by Prof A. von Deimling, Heidelberg University, Heidelberg, Germany). Clone L26 (anti-CD20) was used as IgG2a isotype matched control for the VE1 antibody.[11]

$BRAF^{V600E}$ mutations were detected as previously described.[12] DNA was extracted from formalin-fixed and paraffin-embedded (FFPE) tissues after histologic detection of histiocyte-rich areas, and pyrosequencing with PyroMark Q24 (QIAGEN) was used to detect $BRAF^{V600}$ mutations.

Results

$BRAF^{V600E}$ mutations were detected in ECD biopsies from all 3 patients, and in samples of LCH epidermal infiltration from

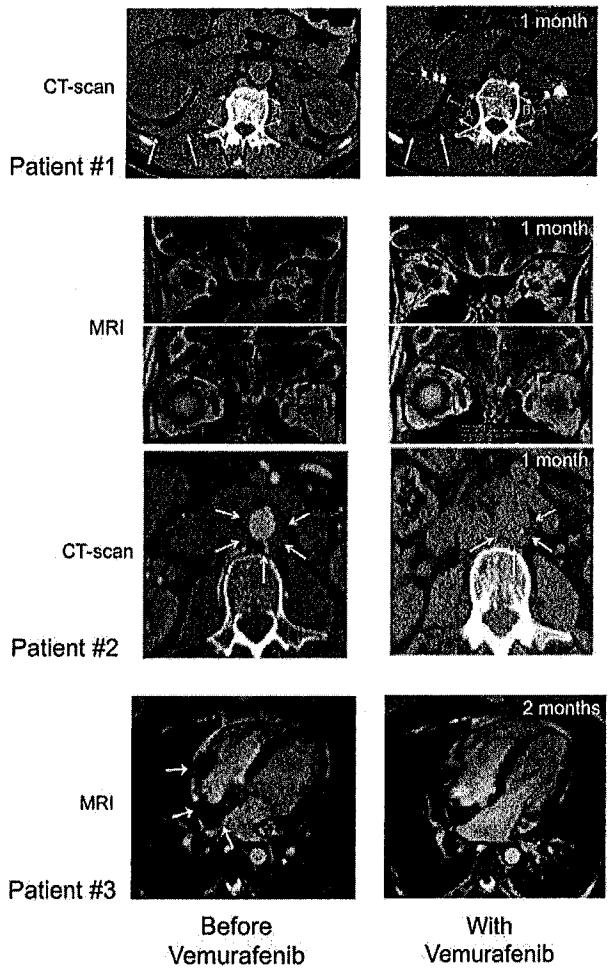

Figure 3. CT scan and MRI imaging assessment. Patient no. 1: Comparison of abdominal axial CT scans performed before (January 28, 2012; left) and on day 37 (May 23, 2012; right) of treatment showing regression of the infiltration around both kidneys (white arrows), evidenced by the decreased thickness (right kidney: 24.8 to 18.2 mm, left kidney 22 to 12.4 mm). Patient no. 2: Comparison of MRI performed before (left) and on day 36 (right) of vemurafenib treatment showing regression of ECD orbital infiltration. Comparison of abdominal axial CT scans performed before (March 29, 2012; left) and on day 39 (May 25, 2012; right) of vemurafenib treatment showing regression of the infiltration around abdominal aorta (white arrows): latero-aortic infiltration from 10.8 to 6.5 mm thick, and posterior infiltration from 6.5 to 4.6 mm thick. Patient no. 3: comparison of cardiac MRI, 4-chamber view: (A) February 21, 2012; see the infiltration of the atrial septum, the posterior wall and the free wall of the right atrium (white arrows); (B) July 19, 2012; note the regression of the infiltration.

patient no. 2. The expression of the V600E mutant BRAF protein in histiocytes from both ECD and LCH lesions was confirmed by immunohistochemistry (Figure 2).

The efficacy of vemurafenib

These 3 cases of refractory ECD with life-threatening manifestations associated with the *BRAF*^{V600E} mutation were all treated with vemurafenib. All patients provided consent for vemurafenib treatment after appropriate counseling.

Vemurafenib (initially given at 1920 mg/d) was tapered in all 3 patients to 960 mg/d (on days 30, 30, and 20, respectively) due to cutaneous side effects and was maintained until further follow-up. 2 These side effects were classified as grade 2 according to the Common Terminology Criteria for Adverse Effects (CTAE). No other toxicities or adverse events were observed. All patients showed clear clinical improvement within a few days of initiation of this treatment.

Patient no. 1. Vemurafenib was started at 1920 mg/d (b.i.d.) on April 19, 2012 and was tapered to 960 mg/d from day 30 due to erythema, and was thereafter maintained at this dose. Within a few days of the initiation of treatment, itching disappeared. Evaluation on day 30 showed an improvement of creatinine (190 to 161μM), GGT (936 to 300 U/l) and alkaline phosphatase (644 to 177 U/l) values. On day 62, GGT was 183 U/l, PAL 146 U/l, and creatinine 170μM. CRP was normalized by day 30 (Figure 4), and remained under 5 mg/L on day 62. PET was performed after 30 days of vemurafenib treatment and the findings compared with those obtained 4 months earlier: there was a substantial improvement of all lesions (Figure 1), with a mean Standardized Uptake Value (SUV) change of −70% (range, −66% to −80%); the change within soft tissue and bone was similarly −70% (range, −51% to −78%; supplemental data, available on the *Blood* Web site; see the Supplemental Materials link at the top of the online article). Thoraco-abdominal CT after 37 days of treatment showed a significant reduction of periaortic infiltration (Figure 3). This cannot be attributed to PEG-IFN treatment, withdrawn on March 31, 2012, because several

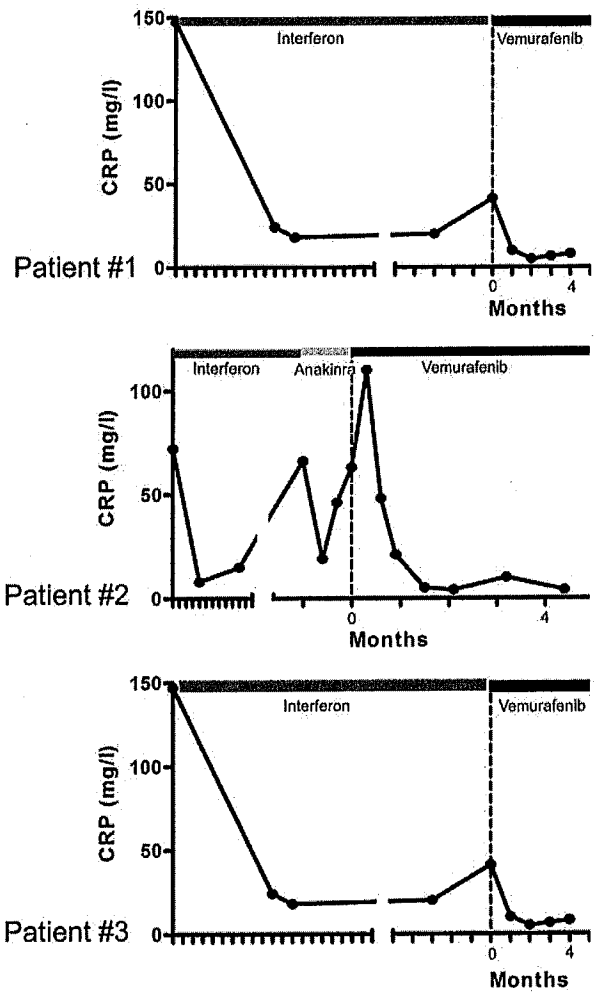

Figure 4. Evolution of CRP levels under treatment. Patient no. 1: Blood CRP concentrations, correlating with initial response and secondary resistance to PEG-IFN treatment, and returning to normal values (< 5 mg/L) under vemurafenib. Patient no. 2: an initial CRP increase was associated with headaches and fever (39°C); CRP concentrations returned to normal values after 1 month of treatment. Patient no. 3: CRP concentrations returned to normal values after one month of treatment. Time 0 corresponds to initiation of vemurafenib treatment, and each graduation corresponds to 1 month.

other markers clearly indicated that the patient was a nonresponder (high CRP values, hydronephrosis and pyelocalicial dilation, worsening of PET findings). Hydronephrosis and pyelocaliceal dilation resolved completely. Note that the PET assessment at 4 months showed that the decrease of FDG uptake had been sustained: uptake was lower than that observed after the first month (Figure 1). Aortic MRI after 4 months disclosed a marked regression of peri-aortic sheathing relative to that observed by CT-scan in May 2012. The CRP value remained low on day 123 of treatment (Figure 4).

Patient no. 2. Vemurafenib was administered at 1920 mg/d (b.i.d) from April 17 with a transient interruption of 2 days (days 12 to 14) due to headaches and fever at 39°C. The CRP value increased to 114 mg/L (May 1); lumbar puncture was normal, blood cultures were negative, and both physical examination and thoracic CT-scan ruled out pneumopathy. The clinical symptoms rapidly disappeared and CRP values declined (100 and 48 mg/L on May 2 and 3). We were able to resume treatment at full dose at day 14. Our impression was that this transient episode was perhaps a viral infection, or cytokine-related, but not due to the disease or vemurafenib treatment. The dose was tapered to 960 mg/d from day 30 due to itching, skin rash and keratosis pilaris lesions which had appeared a few days before. Itching was not attributed to LCH involvement but appeared to be a consequence of the cutaneous toxicity of vemurafenib. Skin manifestations disappeared within days of the reduction of the dose which was maintained at 960 mg/d until further follow-up.

After a few days, histiocytic skin lesions resolved (Figure 2), and the pain in the right eye disappeared such that morphine could be stopped. A new skin biopsy confirmed the absence of histiocytic infiltration of the epidermis and hypodermis. CRP was normalized by day 30 (Figure 4), and was 5.2 mg/L ($N < 5$) on day 48. PET 31 days after initiation of vemurafenib was compared with that performed 2 months earlier: the change in the mean SUV was −57% (range, −51% to −67%) and that in soft tissue and bone was −70% (range, −56% to −78%; Figure 1 and supplemental data). Orbit MRI on day 36 showed a 26% to 66% decrease of the retro-orbital infiltration (Figure 3 and supplemental data). Thoraco-abdominal CT on day 39 demonstrated a 30% to 40% decrease of the posterior and lateral peri-aortic infiltration (Figure 3), and the absence of the previously observed interlobular septa thickening, characteristic of pulmonary involvement of ECD. The CRP value remained below 5 mg/L on day 141 of treatment (Figure 4), and the patient was asymptomatic, with the absence of orbital pain.

Patient no. 3. Vemurafenib was administered at 1920 mg/d (b.i.d) from May 9 to May 29: the dose was tapered to 960 mg/d (b.i.d) due to pilar keratosis and erythema. One month later, the CRP level was 10 mg/L, the thickeness of xanthelasmas had diminished, and PET displayed significantly decreased uptake in the basilar region and by the long bones. In July 2012, the CRP value was normal. The most striking feature was the significant improvement of the cardiac MRI on July 19: right atrial wall infiltration had regressed substantially (Figure 3). On day 119 of treatment, the CRP value was still low, at 8 mg/L (Figure 4).

Discussion

This is the first report of the use of vemurafenib in ECD patients carrying the *BRAF*^{V600E} mutation, with a multisystemic form of the disease refractory to IFN. The treatment was extremely and rapidly effective in all 3 patients: clinical symptoms improved, CRP values normalized, all pathologic uptakes on PET regressed substantially, peri-vascular sheathing regressed, and heart infiltration improved markedly; the LCH skin lesions of patient no. 2 disappeared and the severity of the orbital lesion decreased.

PET assessment of treatment of cases of ECD has not previously documented such rapid efficacy. IFN treatment has a much more subtle and slow effect on the regression of uptakes.[13] For patient no. 1, there was a mean regression of 70% of visceral and bone ^{18}F-fluorodeoxyglucose uptakes at month 1, and the therapeutic response observed at month 4 was even better. Substantial regression of peri-vascular sheathing and disappearance of hydronephrosis (CT), as well as normalization of measures of CRP and liver enzymes confirmed the excellent therapeutic efficacy. The benefits of treatment were similar in patient no. 2, with 57% to 70% regression of visceral and bone ^{18}F-fluorodeoxyglucose uptakes, regression of peri-aortic and orbital infiltrations, and normalization of CRP values.

Imaging and analysis of biologic markers demonstrated tumor regression within 40 days in patients 1 and 2, and for patient no. 3 there was a major regression of heart infiltration by day 71. Moreover, the clinical benefits, with the resolution of pruritus for patient no. 1 and of skin lesions and orbital pain for patient no. 2, were apparent within a few days. The Pitié-Salpêtrière Hospital has cared for 84 ECD patients between 1991 and 2012, and there have been no previous cases of such remarkable and rapid clinical, biologic, and imaging improvements.

Typical LCH infiltration has been reported in some patients with confirmed ECD. In patient no. 2, the *BRAF*^{V600E} mutation was detected in both types of histiocytes. LCH skin lesions disappeared rapidly under vemurafenib and this was confirmed by biopsy, suggesting that LCH patients may also benefit from vemurafenib treatment; the value of such treatment should be assessed in patients with pure LCH disease.

Contrasting with other types of histiocytosis, *BRAF*^{V600E} mutations are present in approximately half of the patients with ECD or LCH.[6-8] Among the 84 ECD patients followed in our center, 17 (20.2%) have died of disease. Although an appropriate dosing schedule and treatment duration remain to be determined in clinical trials, our findings provide compelling evidence of the fast efficacy of BRAF inhibition in *BRAF*^{V600E}-associated ECD. The long-term efficacy of BRAF inhibition in ECD should also be studied, as secondary resistance develops in almost all cases of *BRAF*^{V600E}-associated melanoma.[14] Patient no. 1 was asymptomatic at 4 months and had normal CRP values. At that time, follow-up PET assessment only revealed persistent bone uptake, which we believe should rather be interpreted as being a typical hallmark of the disease than a marker of disease activity. Nevertheless, the durability of the therapeutic response to vemurafenib remains unknown and should be evaluated over longer periods.

In view of the remarkable efficacy in the 3 cases we report, we believe that BRAF inhibition should be considered in a larger cohort of *BRAF*^{V600E}-associated histiocytosis patients, particularly those with life-threatening disease.

Acknowledgments

The authors thank Prof A. von Deimling (Heidelberg, Germany) for providing the anti-BRAF^{V600E} mouse monoclonal antibody VE1.

This work was supported in part by grants from the nonprofit organism Association pour la Recherche en Pathologie (AREP).

Authorship

Contribution: J.H., F.C.-A., J.-F.E., L.A., and Z.A. designed the research; J.H., F.C.-A., J.-F.E., L.A., P.M., F.C., P.C., A.D., and Z.A. collected the data; J.H., F.C.-A., J.-F.E., L.A., P.M., F.C., P.C., A.D., B.H., N.B., S.B, J.D., and Z. A. analyzed and interpreted the data; J.H., F.C.-A., J.-F.E., L.A., P.M., F.C., P.C., A.D., B.H., N.B., S.B., J.D., and Z.A. wrote the manuscript; and all authors approved the final manuscript.

Conflict-of-interest disclosure: J.H. received honoraria from Glaxo Smith Kline for counseling of patients with histiocytosis on the treatments with targeted therapies. J.-F.E. received honoraria from Roche and Glaxo Smith Kline for counseling patients with melanomas on the diagnosis and/or treatment with BRAF inhibitors. The remaining authors declare no competing financial interests.

Correspondence: Dr Julien Haroche, MD, PhD, Service de Médecine Interne 2, Groupe Hospitalier Pitié-Salpêtrière, 47-83 bd de l'Hôpital, 75013, Paris, France;e-mail: julien.haroche@psl.aphp.fr.

References

1. Haroche J, Arnaud L, Amoura Z. Erdheim-Chester disease. *Curr Opin Rheumatol.* 2012; 24(1):53-59.
2. Arnaud L, Hervier B, Néel A, et al. CNS involvement and treatment with interferon-α are independent prognostic factors in Erdheim-Chester disease: a multicenter survival analysis of 53 patients. *Blood.* 2011;117(10):2778-82.
3. Marchal A, Cuny JF, Montagne K, et al. Associated Langerhans cell histiocytosis and Erdheim-Chester disease. *Ann Dermatol Venereol.* 2011; 138(11):743-7.
4. Emile JF, Wechsler J, Brousse N, et al. Langerhans' cell histiocytosis. Definitive diagnosis with the use of monoclonal antibody O10 on routinely paraffin-embedded samples. *Am J Surg Pathol.* 1995;19(6):636-41.
5. Badalian-Very G, Vergilio JA, Degar BA, et al. Recurrent BRAF mutations in Langerhans cell histiocytosis. *Blood.* 2010;116(11):1919-23.
6. Satoh T, Smith A, Sarde A, et al. B-RAF Mutant Alleles Associated with Langerhans Cell Histiocytosis, a Granulomatous Pediatric Disease. *PLoS One.* 2012;7(4):e33891.
7. Sahm F, Capper D, Preusser M, et al. BRAFV600E mutant protein is expressed in cells of variable maturation in Langerhans cell histiocytosis. *Blood.* 2012;120(12):e28-34.
8. Haroche J, Charlotte F, Arnaud L, et al. High prevalence of *BRAF V600E* mutations in Erdheim-Chester disease but not in other non-Langerhans cell histiocytoses. *Blood.* 2012; 120(13):2700-3.
9. Chapman PB, Hauschild A, Robert C, et al. Improved survival with vemurafenib in melanoma with BRAF V600E mutation. *N Engl J Med.* 2011; 364(26):2507-16.
10. Dietrich S, Glimm H, Andrulis M, et al. BRAF Inhibition in Refractory Hairy-Cell Leukemia. *N Engl J Med.* 2012;366:2038-40.
11. Capper D, Preusser M, Habel A, et al. Assessment of BRAF V600E mutation status by immunohistochemistry with a mutation-specific monoclonal antibody. *Acta Neuropathol.* 2011;122(1): 11-19.
12. Moreau S, Saiag P, Aegerter P, et al. Prognostic value of $BRAF^{V600}$ mutations in melanoma patients after resection of metastatic lymph nodes. *Ann Surg Oncol.* doi:2012;19(13):4314-4321.
13. Arnaud L, Malek Z, Archambaud F, et al. 18 F-Fluorodeoxyglucose–Positron Emission Tomography scanning is more useful in followup than in the initial assessment of patients with Erdheim-Chester disease. *Arthritis Rheum.* 2009;60(10): 3128-38.
14. Aplin AE, Kaplan FM, Shao Y. Mechanisms of resistance to RAF inhibitors in melanoma. *J Invest Dermatol.* 2011;131(9):1817-20.

Expériences en cancérologie adultes; Inhibiteurs B raf et Inhibiteurs MEK L'exemple du Mélanome: C Lebbe St Louis Paris

Le Sarcome histiocytaire: classification et évolution clinique JF Emile / F Charlotte K Moktari - A Paré Pitié Paris

Sarcome histiocytaire cérébral et BRAF A Idbaih Pitié Paris

Primary central nervous system histiocytic sarcoma (PCNS-HS) is a rare malignant disorder with a dismal prognosis. We report the case of a 40-year-old man suffering from progressive memory impairment and raised intracranial pressure syndrome. Magnetic resonance imaging revealed a contrast-enhanced left temporal tumor with acute hydrocephalus. After biopsy and cerebrospinal fluid (CSF) shunt, a comprehensive neurological and systemic workup demonstrated PCNS-HS with CSF spread. Molecular analysis of the tumor demonstrated a *BRAF* p.V600E mutation and multiple chromosomal imbalances. Vemurafenib treatment was started with dramatic clinical, radiological, and biological responses. Thus, the *BRAF* mutation is a potential driving mutation in PCNS-HS. This case supports molecular-based personalized medicine in neuro-oncology.

Pathologies comparés Homme / Chiens: projet INCA Catherine André -Jérôme Abadie CNRS Rennes / EVA Nantes

Hedan et al. BMC Cancer 2011, 11:201
http://www.biomedcentral.com/1471-2407/11/201

BMC Cancer

RESEARCH ARTICLE Open Access

Molecular cytogenetic characterization of canine histiocytic sarcoma: A spontaneous model for human histiocytic cancer identifies deletion of tumor suppressor genes and highlights influence of genetic background on tumor behavior

Benoit Hedan[1], Rachael Thomas[1,2], Alison Motsinger-Reif[2,3,4], Jerome Abadie[5], Catherine Andre[6], John Cullen[7] and Matthew Breen[1,2,8*]

Abstract

Background: Histiocytic malignancies in both humans and dogs are rare and poorly understood. While canine histiocytic sarcoma (HS) is uncommon in the general domestic dog population, there is a strikingly high incidence in a subset of breeds, suggesting heritable predisposition. Molecular cytogenetic profiling of canine HS in these breeds would serve to reveal recurrent DNA copy number aberrations (CNAs) that are breed and/or tumor associated, as well as defining those shared with human HS. This process would identify evolutionarily conserved cytogenetic changes to highlight regions of particular importance to HS biology.

Methods: Using genome wide array comparative genomic hybridization we assessed CNAs in 104 spontaneously occurring HS from two breeds of dog exhibiting a particularly elevated incidence of this tumor, the Bernese Mountain Dog and Flat-Coated Retriever. Recurrent CNAs were evaluated further by multicolor fluorescence *in situ* hybridization and loss of heterozygosity analyses. Statistical analyses were performed to identify CNAs associated with tumor location and breed.

Results: Almost all recurrent CNAs identified in this study were shared between the two breeds, suggesting that they are associated more with the cancer phenotype than with breed. A subset of recurrent genomic imbalances suggested involvement of known cancer associated genes in HS pathogenesis, including deletions of the tumor suppressor genes *CDKN2A/B*, *RB1* and *PTEN*. A small number of aberrations were unique to each breed, implying that they may contribute to the major differences in tumor location evident in these two breeds. The most highly recurrent canine CNAs revealed in this study are evolutionarily conserved with those reported in human histiocytic proliferations, suggesting that human and dog HS share a conserved pathogenesis.

Conclusions: The breed associated clinical features and DNA copy number aberrations exhibited by canine HS offer a valuable model for the human counterpart, providing additional evidence towards elucidation of the pathophysiological and genetic mechanisms associated with histiocytic malignancies. Extrapolation of data derived from canine histiocytic disorders to human histiocytic proliferation may help to further our understanding of the propagation and cancerization of histiocytic cells, contributing to development of new and effective therapeutic modalities for both species.

* Correspondence: Matthew_Breen@ncsu.edu
[1]Department of Molecular Biomedical Sciences, College of Veterinary Medicine, North Carolina State University, Raleigh, NC, USA
Full list of author information is available at the end of the article

Background

Histiocytic malignancies in human patients are rare but aggressive cancers associated with high mortality [1-4]. Pathologic and cytogenetic data for these malignancies are sparse, based on a few early case studies e.g.[5-7] and a single larger study of 18 histiocytic sarcomas (HS) [2]. On a molecular level, deletions of *CDKN2A/p14ARF, TP53, MDM2* and *PTEN* have been reported in human histiocytic disorders [4,8-14], but their etiology remains poorly understood. The clinical behavior of these diseases is also unclear, and the optimal course of treatment remains a matter of debate [4,15]. Elucidation of the genetic basis of many human cancers has been aided by identification of recurrent genomic DNA copy number aberrations (CNAs) affecting dosage of target genes involved in cancer pathogenesis. The diagnostic, prognostic and therapeutic significance of numerous CNAs in a variety of common cancers is well described [16]. However, for rare cancers, including HS, the limitations on sample availability preclude the generation of comprehensive data regarding recurrent CNAs.

Histiocytic cancers are uncommon within the domestic dog population in general, but there is a highly elevated incidence in several breeds, including the Bernese Mountain Dog (BMD) and Flat-Coated Retriever (FCR), suggesting heritable risk factors and indicating that these breeds may share genetic characteristics contributing to tumor initiation and progression [17-22]. Canine HS are histologically comparable to the corresponding human cancers, involving proliferation of members of both histiocytic lineages (dendritic cells (DC) and macrophages) with which they share pathologic features [17,18]. With only small numbers of available human samples, we propose that the canine model provides a unique opportunity to identify recurrent genomic lesions associated with spontaneous HS, and provide greater insight into the pathogenesis and genetic etiology in human patients.

For this study we hypothesized that recurrent CNAs exist in canine HS, detection of which would identify regions of the canine genome containing genes associated with HS initiation and progression. Approximately ~25% of all tumors diagnosed in the BMD are reported to be HS, and a recent study estimated that 80% of canine disseminated HS cases are diagnosed in the BMD, suggestive of a multigenic or multifactorial mode of transmission [22,23]. The typical age of onset in the BMD is 6.5 years, with 82% and 55% of cases involving an internal organ and multiple organs, respectively [22,23]. This latter presentation represents the disseminated form of the disease, often referred to as malignant histiocytosis. Tumor progression is rapid with a mean survival time following diagnosis of only 49 days [23]. With such an aggressive behavior and high prevalence in the breed, HS has a huge impact on BMD longevity. HS also is the most common malignant tumor identified in the FCR, accounting for at least 40% of all tumors diagnosed in this breed, with an average age of onset of 8.5 years [24,25]. Tumors in the FCR are generally located in the muscle region surrounding a joint, with a high rate of metastasis to local lymph nodes, spleen, thorax and abdominal organs. While treatments are available for palliation of clinical signs and extension of life, this tumor carries a poor prognosis in the FCR, with a reported median survival of only four months [25].

We evaluated genome-wide CNAs in a cohort of histologically confirmed canine HS cases using array comparative genomic hybridization (aCGH), supplemented with fluorescence *in situ* hybridization (FISH) and loss of heterozygosity (LOH) analysis. We identified recurrent CNAs common to HS in both breeds (BMD and FCR), indicating an association with tumor phenotype. These changes included genomic imbalances encompassing well defined cancer associated genes (*CDKN2A/B, RB1, PTEN*). Epidemiological data revealed a significant difference in the anatomical location of histiocytic tumors between the two breeds. A subset of CNAs was also associated significantly with breed. These data suggest that at least some of the CNAs are associated with breed and/or tumor location, rather than tumor phenotype.

Having defined aberrant genomic regions in two breeds of dog with a high incidence of HS, subsequent comparative molecular analysis of such regions, both in dog and human patients, will provide opportunities to gain greater insight into our understanding of the pathways implicated in histiocytic cancers, providing a first step on the road to developing new treatments.

Methods

Case recruitment and histological evaluation of canine histiocytic tumors

No animal experimentation was performed during this study. All patients evaluated in this study were from family owned dogs with a confirmed histiocytic malignancy. All blood and tumor samples were taken with informed owner consent by veterinarians between 2003-2008. One hundred and forty six patients were recruited for this study. Unfixed tumor biopsies were submitted from 125 cases that had not previously received treatment for their HS other than for palliative care. Tumor biopsies were obtained under sterile conditions, either as part of a routine diagnostic biopsy procedure, during surgery, or immediately following euthanasia. All FCR cases (n = 45) originated from the USA, while the BMD cases (n = 101) were derived from the USA (n = 68 patients) or France (n = 33 patients). The anatomical location of tumors evident at the time of diagnosis and/or necropsy

was recorded for each case in one of five categories: tumor present in i) one internal organ; ii) multiple internal organs (equivalent to disseminated HS); iii) lymph node only; iv) limb only; v) skin only. The last two locations were regarded as localized HS. A representative portion of the tumor was fixed in 10% neutral-buffered formalin. Histological specimens were evaluated by board-certified veterinary pathologists (JC, JA) using routine hematoxylin-eosin (H&E) staining and antibodies against CD3 (T-cell marker), CD18 (hematopoietic marker), CD79a (B-cell marker), MHC class II, E-cadherin and Thy-1. In rare cases where the pathology remained inconclusive (and where frozen tissue was available) tissues were evaluated further with CD11c and CD11d. In such cases, a diagnosis of HS was confirmed when tumor cells were positive for CD11c or CD11d markers and negative for CD3 and CD79a markers. Tumors were classified according to the criteria of Affolter and Moore (2002)[17].

Array comparative genomic hybridization (aCGH) analysis

Genomic DNA was isolated from representative specimens of unfixed tumor tissue. aCGH analysis was performed as described previously [26] using a custom genomic microarray comprising canine bacterial artificial chromosome (BAC) clones distributed at ~1 Mb intervals within the 7.6× canine genome sequence assembly [27]. All BAC clones had been previously verified to map to a unique chromosomal location by multicolor fluorescence *in situ* hybridization (FISH) analysis [26]. Equimolar quantities of blood-derived DNA isolated from five or more unrelated, cancer free individuals were used as breed matched reference samples. Data analysis was performed as described elsewhere [26,28]. Tumor-associated genomic imbalances were detected using the aCGH-Smooth algorithm [29] with threshold limits for detection of CNAs set at $\log_2$ ratio values of tumor DNA vs. reference DNA equivalent to 1.15:1 (copy number gain) and 0.85:1 (copy number loss). CNAs were defined as recurrent or highly recurrent when common to ≥30% and ≥50% of cases, respectively. The megabase (Mb) location of dog genes along the corresponding chromosome were based on the canFam v2 genome sequence assembly [27] accessed via the UCSC genome browser http://genome.ucsc.edu/.

Loss of heterozygosity (LOH) analysis

Genomic regions exhibiting recurrent DNA copy number loss in HS were further evaluated for LOH using the M13-tailed primer method [30]. PCR primers flanking microsatellite sequences [31] located within these regions are listed in Additional file 1: Table S1. Each locus was amplified independently from paired tumor- and blood-derived DNA from each patient evaluated. PCR was conducted in 10 μl reactions containing 0.8 units Taq polymerase (Go Taq, Promega), 1.0 μl 10× reaction buffer (Promega), 0.25 mM each dNTP, 0.15 μM each microsatellite-specific primer, 0.1 μM 5' fluorescently labeled M13 primer and 50 ng template DNA. The M13 primer was tagged at the 5' end either with PET, VIC, FAM or NED (Applied Biosystems) to facilitate multiplexing of products. Amplification conditions were as follows: 95°C for 2 min followed by 35 cycles of 94°C for 30 s, 58°C for 30 s and 72°C for 30 s, followed by a 2-min final extension at 72°C. Amplicons were visualized and evaluated by capillary-electrophoresis (3730xl DNA Analyzer, Applied BioSystems). Two parameters were calculated for each sample: the allelic ratio (AR) and allelic balance (AI). The AR was calculated by AR = (peak area 1)/(peak area 2); AI by AI = AR (tumor)/AR (blood). When AI ≥ 1.5 or ≤ 0.67, the region was considered to be deleted.

Cytogenetic and fluorescence *in situ* hybridization (FISH) analysis

Where viable tumor tissue was available, interphase nuclei and chromosome preparations were generated for FISH analysis. Primary tumor specimens were disaggregated using Collagenase B (Roche) and the resulting cell suspensions harvested directly, or from low passage (n <2) primary cell cultures, using conventional techniques of colcemid arrest, hypotonic treatment and methanol/glacial acetic acid fixation, as described elsewhere [32]. Multicolor FISH analysis was carried out as described previously [33] using BAC clones representing regions of the genome highlighted by aCGH analysis. All probes were hybridized first onto metaphase chromosome preparations from a pool of clinically healthy dogs to confirm the expected copy number for each probe at the expected chromosomal location. Image data were assessed from a minimum of 30 representative cells from each control/case evaluated.

Statistical analysis

aCGH, clinical and demographic data were compared with Mann-Whitney U tests in the case of continuous outcome variables, and with Fisher's Exact tests in the case of categorical outcomes. These methods are non-parametric, requiring no distributional assumptions to retain validity. Principal components analysis (PCA) is well-established in human genetics to detect geographic and racial background differences in human populations [34,35]. PCA was performed to evaluate potential population substructure in the USA and French BMD populations, and to test for differences in CNA frequency between the two breeds [36-38]. Association analyses were performed with Fisher's Exact tests to test for association between aberration frequencies and breed. To

control family-wise error rates and correct for multiple comparisons, permutation testing was performed, deriving empirically p-value cut-offs of significance corresponding to a family-wise error rate of 0.05 [39]. Statistical analyses were performed using JMP Genomics v4 and SAS 9.1.3 (SAS Institute, Cary, NC) and Stata v.11 http://www.stata.com.

Results

Statistical evaluation of epidemiological data

Evaluation of the 113 HS cases recruited from within the USA provided an opportunity for direct comparison of their epidemiological characteristics. The USA cohort comprised 68 BMD (33 male, 35 female) and 45 FCR (20 male, 25 female), all of whom were registered with the American Kennel Club. The mean age at diagnosis was 8.6 years ± 1.7 for the FCR (range 5 to 12 years) and 7.7 years ± 1.9 for the BMD (range 2 to 12 years), which also showed a secondary peak at 10 years of age (Figure 1). These data indicate that within the US patients the age of onset of HS was significantly higher in the FCR than the BMD ($p = 0.01$, Mann-Whitney U test).

The anatomical location of the tumor(s) also showed significant variation between the two breeds (Figure 2), with 87% of BMDs presenting with HS affecting one or more internal organs compared with 48% of FCRs ($p < 0.001$, Fisher's Exact test). Moreover, occurrence of HS on a limb was >10 times more frequent in the FCR than in the BMD (38.4% versus 3.2%). With the assumption that isolated skin and limb tumors correspond to localized HS, we may surmise that the prevalence of localized HS is seven times more frequent in the FCR than in the BMD (46.1% versus 6.5%) and that of disseminated HS is approximately two fold higher in the BMD than the FCR (50.8% versus 25.6%).

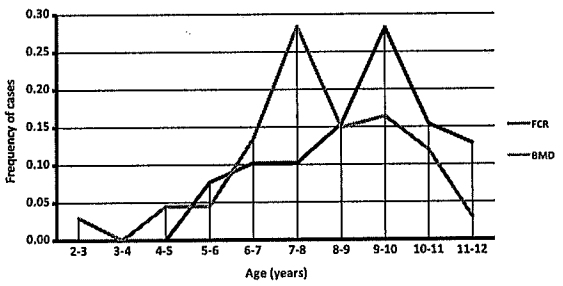

Figure 1 Distribution of the age of diagnosis of HS in US-resident BMD (68 cases) and FCR (45). The mean age of HS diagnosis is significantly different between BMD (7.7 yrs) and FCR (8.6 yrs) (pval = 0.01, Mann-Whitney U test).

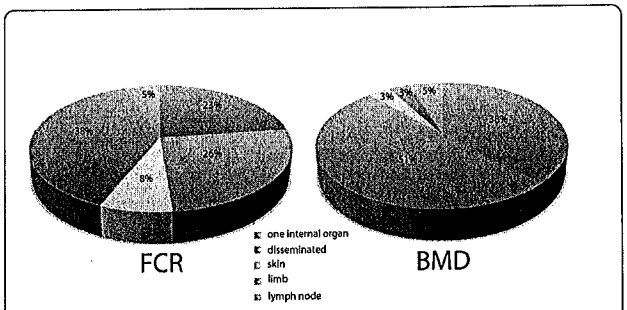

Figure 2 Anatomical distribution of histiocytic tumors in FCR and BMD. Anatomical location of HS is significantly different between the two breeds (p value < 0.001, Fisher Exact test).

Overview of DNA copy number aberrations revealed by aCGH

Metaphase preparations were generated from >20 HS tumor biopsies from both BMD and FCR. The domestic dog karyotype comprises 38 pairs of single-armed chromosomes and a pair of bi-armed sex chromosomes (2n = 78). Conventional cytogenetic evaluation of HS cases revealed highly variable chromosome numbers in both breeds, which were generally in the range 42-58. All cases evaluated exhibited an abundance of aberrant bi-armed chromosomes. These data suggest that in addition to numerical changes there also are large numbers of structural changes that merit further evaluation in a subsequent study.

Of the 146 HS cases available to this study (68 BMD and 45 FCR from the USA, and 33 BMD from France), unfixed tumor biopsies were obtained for 125 (Additional file 2: Table S2). Tumor specimens from 104 cases (33 FCRs, 71 BMDs) yielded DNA of sufficient quality to permit aCGH analysis, of which 86 (82.6%) (30 FCRs, 56 BMDs) presented with detectable CNAs. The remaining 18 cases (17.3%) (3 FCR and 15 BMD) did not demonstrate any detectable CNAs at 1 Mb resolution, presumably either due to an abundance of non-malignant tissue in the biopsy received, or the presence of a highly polyclonal cell population with few shared aberrations. Since these 18 cases provided no evidence for CNAs they were excluded from subsequent analyses.

Typically, aCGH profiles for individual canine HS cases demonstrated numerous CNAs, both gains and losses, throughout the genome (Figure 3a), which were supported by FISH analysis of select regions (Figures 3b, c and 3d). When considered as a single population of 86 aberrant cases, the genome wide aCGH profiles for canine HS shared numerous CNAs (Figure 4). Thirty-one regions of the canine genome presented with recurrent DNA copy number increases (present in ≥30% of the combined cohort), comprising eight regions of gain and 23 regions of loss. Of these 31 regions, six were highly recurrent (present in ≥50% of the combined

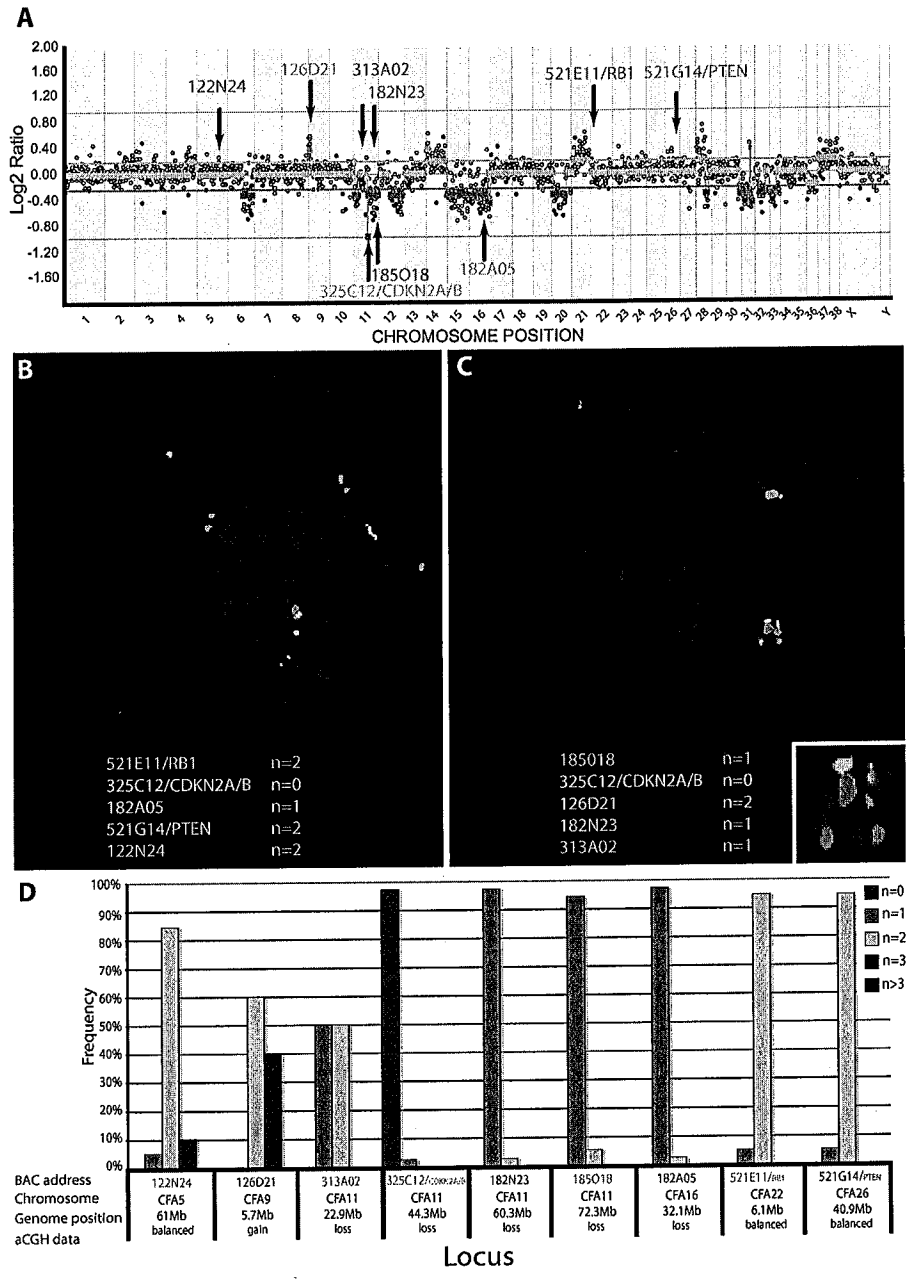

Figure 3 Molecular cytogenetic evaluation of a canine histiocytic malignancy using aCGH and FISH. A. Example of whole genome aCGH profile of a HS in a five year old female FCR. Log_2 ratios representing thresholds of genomic gain and loss are indicated by horizontal bars above (green line) and below (red line) the midline (orange line), which represents normal copy number. The chromosome copy number status line for the tumor appears as an orange overlay of the center-line when there is a normal copy number, and as either green (gain) or red (loss) in the regions where genomic imbalances were apparent, as determined by the aCGH Smooth algorithm [29]. The aCGH profile is annotated with the clone address of nine BAC clones from the 1 Mb array that were used in subsequent FISH analysis of this case. Three of these nine clones have been shown previously to contain the full coding sequence of a key cancer-associated gene (*CDKN2A*, *RB1*, *PTEN*) [26]. The color of the text denotes the fluorochrome with which the BAC clone was labeled. **B, C** Targeted FISH analysis of tumor metaphase chromosome spreads from the same case using nine differentially labeled BAC clones (highlighted in **A**) combined in two separate groups. The modal copy number for each clone is indicated. **D**. Summary of copy number data of all nine loci evaluated by FISH analysis of at least 30 tumor interphase nuclei or metaphase spreads. The aCGH copy number status of these regions (gain, loss, balance) are indicated, demonstrating concordance between FISH data and aCGH data.

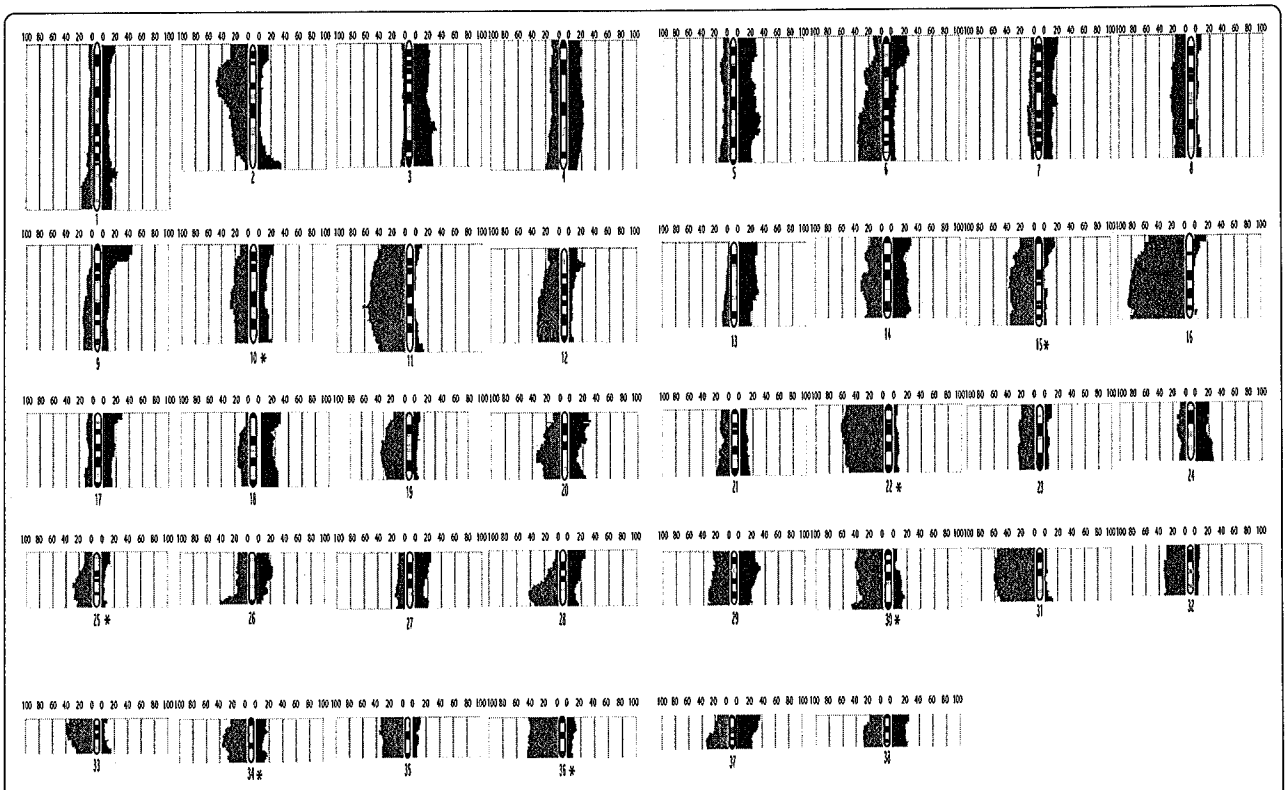

Figure 4 Whole genome CNA penetrance plot showing the percentage of all HS cases in the cohort (BMD+FCR; n = 86 cases) that presented with detectable DNA copy number gain (green) and loss (red) along the length of each dog chromosome (CFA 1 to CFA 38), surveyed at 1 Mb intervals. The asterisks indicate those seven chromosomes (CFA 10, 15, 22, 25, 30, 35 and 36) that have regions of CNAs differing significantly between BMD and FCR.

cohort), all of which were deletions; located on dog chromosome 2 (*Canis familiaris*, CFA 2) (50% cases), CFA 11 (62.8% of cases), CFA 16 (86% of cases), CFA 22 (64% of cases) and CFA 31 (61.6% of cases). Overall the mean number and size of CNAs in both breeds was highly comparable (Table 1), although the proportion of cases that showed no detectable CNAs was 2.3 fold greater in the BMD (21%) than in the FCR (9%). Figure 5 shows the size distribution of regions of CNA within the FCR and BMD, indicating that in both breeds more than 50% of the observed deletions were >30 Mb in size, while half of the gains were <15 Mb.

Table 1 Summary of the overall DNA copy number status in the study population.

	BMD	FCR	Mean (+/- st.dev)
mean number of CNAs	30.3 ± 17.8	32.2 ± 17.8	30.7 ± 17.6
mean number of losses	15.9 ± 9.3	18.1 ± 7.2	16.7 ± 8.6
mean number of gains	13.8 ± 10.3	14.1 ± 12.3	13.9 ± 10.9
ratio losses:gains	1.15:1	1.27:1	1.22:1
mean size of loss (Mb)	30.7 ± 21	35.7 ± 20.5	32.5 ± 21
mean size of gain (Mb)	23.3 ± 23.7	22.4 ± 20.5	23.1 ± 22.6

(CNAs = Copy Number Aberrations, BMD = Bernese Mountain Dog, FCR = Flat Coated Retriever, Mb = Megabase).

Identification of recurrent population associated aberrations

Segregation of aCGH data by breed revealed remarkable genome-wide similarity in the gross distribution of genomic gains and losses between BMD and FCR (Figure 6), indicating that most of the CNAs identified were

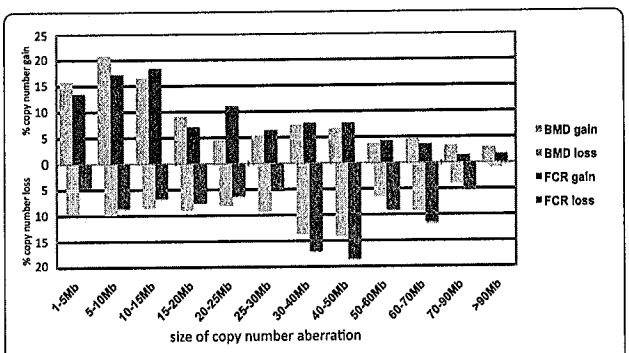

Figure 5 Distribution of the size of the CNAs identified by aCGH analysis of HS of BMD and FCR.

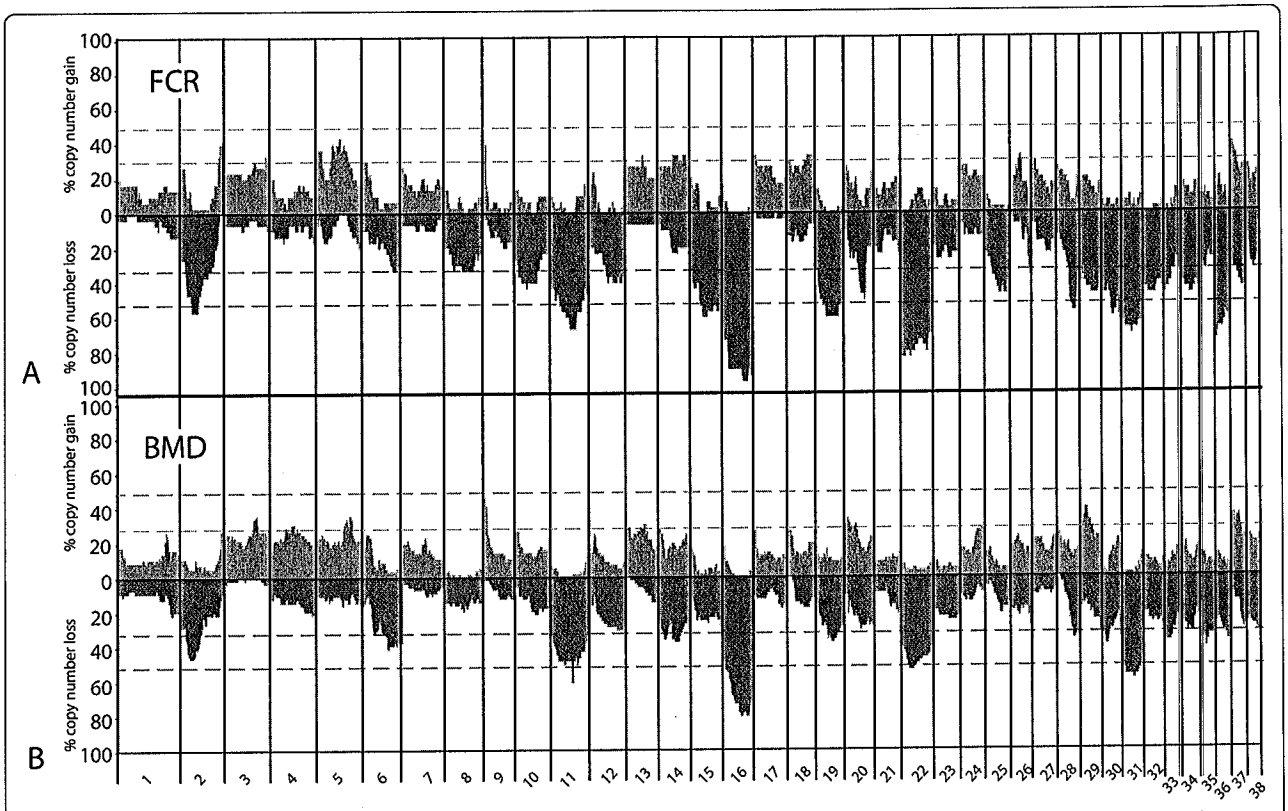

Figure 6 Whole genome CNA penetrance plots separated by breed A) FCR and B) BMD, where each indicates percentage of HS cases identified with DNA copy number gain (green) and deletion (red) along the length of each dog chromosome (CFA 1 to CFA 38) in 1 Mb intervals. The dashed horizontal red and green lines indicate thresholds of recurrence (≥33% incidence) and high recurrence (≥50% incidence).

common to both breeds. To identify whether the geographical origin of a patient (USA or France) had any significant effect on its genome wide CNA profile, principal component analysis (PCA) was used to investigate potential population substructure within the BMD cohort. Visual inspection of the scree plot of the first ten potential components indicated just a single significant component (Figure 7a). Eigen values for the first three components are represented in three-dimensional space in Figure 7b, which demonstrates that there is no division between BMD patients by geographical origin. Mann-Whitney U tests showed no significant association between the eigen values from the first five components and the geographic origin of the patient ($p > 0.05$ for each test). These results indicate there is no substantial population substructure between American and French BMDs. Based on these results the American and French BMDs were evaluated as one single population in subsequent association analysis.

PCA was also used to assess evidence for global differences in the distribution of genome-wide DNA copy number aberrations between the two breeds (Figure 8a). These results indicate four significant components that define the global data. The eigen values were generated corresponding to the first four components and were tested for association with breed using nonparametric Mann-Whitney U tests (Table 2). The results of these association tests indicate a statistically significant association between breed and the second principal component ($p < 0.0001$). Figure 8b shows that there is a strong division between the two breeds defined by the second component, visually representing the association demonstrated in Table 2. Tumor location was also tested for association with the eigen values for the first four principal components (Table 2), the results indicating a significant association between tumor location and the second principal component. Since there is a highly significant association between breed and tumor location, it is not possible to determine if it is the breed or the tumor location that is driving the association and so this must be considered when interpreting the results of breed association with CNA.

Fisher's exact tests of associations were performed for each region of DNA copy number gain or loss and breed, to identify specific regions of aberrations that define this global difference (Table 3). The permutation

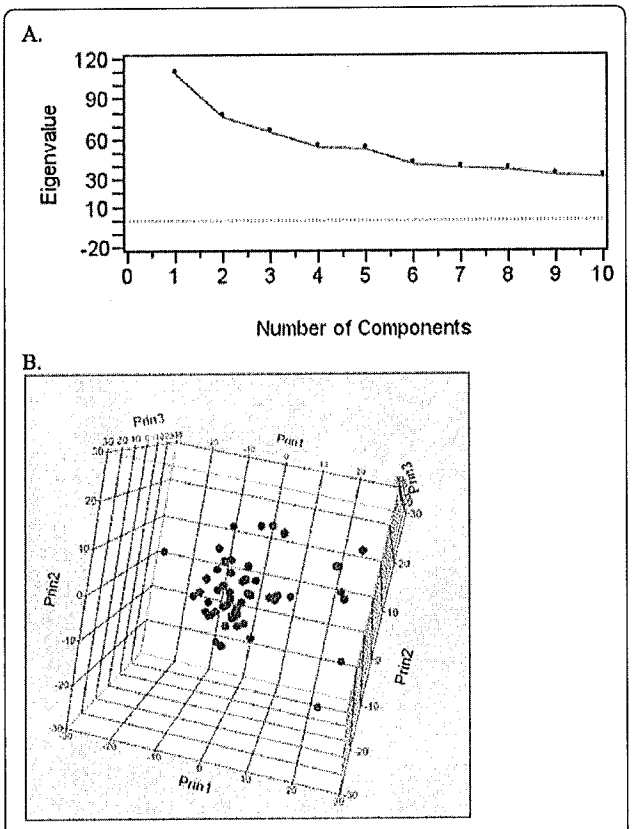

Figure 7 Principal Component Analysis (PCA) to identify potential population substructure between French and American BMD cases of HS. A). Scree plots of the eigen values first 10 components. B). Three dimensional plot of the first three components. American BMD patients are indicated in red while French BMD patients are indicated in blue.

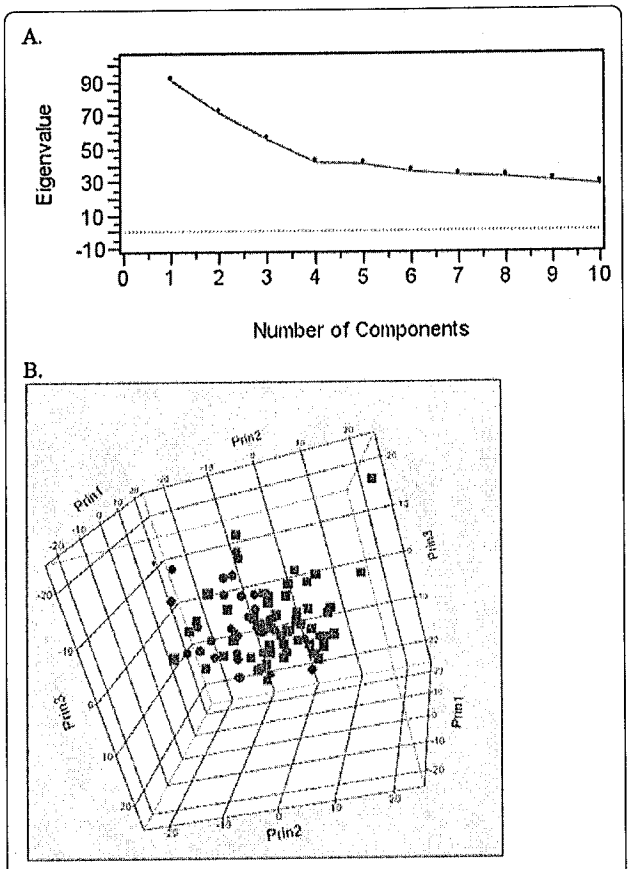

Figure 8 Principal Component Analysis (PCA) to assess global variation in aberration frequency between BMD and FCR. A) Scree plots of the eigenvalues first 10 components. B) Three dimensional plot of the first three components. BMD patients are indicated in red and FCR patients are indicated in blue.

distribution indicated that an uncorrected p-value < 0.01 was statistically significant at a family-wise error rate (FWER) of 0.05. Copy number aberrations involving 13 regions on seven different chromosomes (CFA 10, 15, 22, 25, 30, 34, and 36) were significantly associated with breed.

Evaluation of tumor suppressor gene deletions in canine HS

A subset of recurrent CNAs identified in this study involved regions of the genome that contain known cancer associated genes and were investigated further. Deletion of CFA 11q16 at ~44 Mb, which includes the tumor suppressor gene *CDKN2A/B*, was identified in 62.8% of HS cases (60.7% of BMD and 66.7% of FCR) (Figure 6). This region was further evaluated by LOH analysis of 26 BMD and 20 FCR cases, each of which exhibited CFA 11q16 deletion in aCGH analysis, and had high quality DNA available from both peripheral blood and tumor specimens. Genotyping of seven microsatellites surrounding the *CDKN2A/B* locus demonstrated LOH of at least one microsatellite within this region in all 46 cases, consistent with the loss of CFA 11q16 identified by aCGH (data not shown). Moreover, LOH analysis of an additional 11 cases, in which loss of this region of CFA 11 was not apparent from aCGH analysis, revealed that six (54%) showed LOH of at least one marker close to the *CDKN2A/B* locus (data not shown). The common region deleted in both breeds was centered on the *CDKN2A/B* locus. Two of the cases used for this analysis showed $\log_2$ tumor DNA:reference DNA ratios < -1.0 at the *CDKN2A/B* locus, highly suggestive of an homozygous deletion. Subsequent FISH analysis using a BAC clone containing the *CDKN2A/B* locus confirmed homozygous deletion of this region in these tumors (see Figure 3 for an example).

The most frequent DNA copy number aberration observed by aCGH in the HS cohort was deletion of CFA 16, with a 6 Mb segment of this chromosome (extending from 47-53 Mb) deleted in 86% of all cases (80.4% of BMD and 96.7% of FCR). These data were

Table 2 Test of association between the first eigenvalues for the first four principal components and breed (BMD/FCR) or tumor location (internal/external)

Component	P-value for association test with breed	P-value for association test with tumor location
1	0.4174	0.08205431
2	<0.00001	7.12E-05
3	0.1291	0.06926817
4	0.2995	0.82846813

supported by FISH analysis (see Figure 3 for an example) and LOH analysis on a subset of 26 BMDs and 20 FCRs for which matched blood and tumor DNA samples were available (data not shown). The second most frequently observed CNA in our cohort was deletion of CFA 22q11 at ~60.5 Mb, which includes the tumor suppressor gene *RB1*. DNA copy number loss of this region was identified in 55.8% of all cases, with deletions twice as common in the FCR (83.3% of FCRs and 41.1% of BMDs). The *TP53* tumor suppressor gene locus (CFA 5q21 at ~35.5 Mb) was gained in 26.7% of all cases, with the frequency in the FCR (40%) being twice that of the BMD (19.6%). Further, gain of this region was almost three times more frequent than loss (26.7% gain vs 9.3% loss) across all cases and also within both breeds when considered separately (10.7% loss in BMDs, 6.6% loss in FCRs). aCGH indicated that deletion of the full length of CFA 26 was evident in approximately 10-20% of cases. In both breeds, however, deletion of the distal end of CFA 26, a region that contains *PTEN*, was deleted in 40.7% of cases (42.9% of BMD, 36.7% of FCR), representing the highest frequency of loss along this chromosome. FISH analysis with BAC clones representing *CDNK2A/B*, *RB1*, *TP53* and *PTEN* supported the copy number status identified by aCGH in those cases evaluated.

Table 3 Thirteen regions along seven dog chromosomes showed significant differences between BMD and FCR tumors.

CFA	position (Mb)	P-value
10	25-30	<0.0057
15	19-22	<0.0063
15	29-49	<0.0094
15	52-54	<0.0059
22	00-12	<0.0023
22	31-48	<0.0089
22	54-57	<0.0064
25	09-12	<0.0046
25	14-18	<0.0062
30	26-28	<0.0040
30	30-33	<0.0076
34	45-46	<0.0094
36	00-20	<0.0099

The megabase (Mb) position of these regions on different chromosomes (CFA) is indicated. The uncorrected p-value is shown.

Discussion

We hypothesized that spontaneous canine HS exhibit recurrent CNAs of genes involved in histiocytic cancerization, and that identification of these CNAs may advance our understanding of the molecular characteristics of these cancers in both canine and human patients. The pathophysiologies of several dog and human cancers share many similarities and our previous studies have demonstrated that CNAs in a variety of human cancers are evolutionarily conserved in the corresponding canine cancer [40-42]. These findings support the idea of a fundamental and evolutionarily conserved association between cytogenetic abnormalities and tumor phenotype, indicating similar biological consequences in both species [41]. In testing our hypothesis we recruited client owned BMD and FCR patients, each with a confirmed diagnosis of HS, and performed genome-integrated aCGH analysis of 104 cases to identify recurrent CNAs at 1 Mb resolution. We also performed statistical analysis of clinical and demographic data from our HS cohort in order to expand knowledge of the epidemiological basis of this disease in these breeds.

Disseminated canine HS was first described as malignant histiocytosis in the BMD [19,20], and while this condition has been documented in other breeds [17], it appears that this clinical form continues to be reported more frequently in the BMD than other breeds. Conversely, Fidel et al. (2006) [25] described that the majority of HS in the FCR were restricted to a joint and/or muscle/skin, corresponding to a localized form of HS. Epidemiological data from our cohort are consistent with previous reports. Our data showed also that the anatomical location of the histiocytic tumors differed significantly between the two breeds investigated: BMDs present more frequently with tumors of internal organs and also with a high frequency of dissemination, while FCRs more often develop a localized tumor of the skin or leg. To our knowledge this study represents the first to provide statistical significance for these parameters. The contrasting patterns of anatomical location of HS in the BMD and FCR suggest that the genetic backgrounds of these two breeds may play a key role in

determining risk, location and progression of this neoplasm, which could be assessed using genome wide association analyses. Prior human and mouse studies have identified specialized DC subtypes with heterogeneous functions [43] and so it is possible that the HS diagnosed in FCR and BMD represent malignancies of different DC subtypes, which might explain the different behavior of these cancers in the two breeds.

Identification of breed-associated genomic copy number aberrations

No statistical differences were found between CNAs detected in HS of BMDs from two distinct geographic areas (France/USA). These data suggest that it is reasonable to sample BMDs from different geographic areas to increase the number of cases available for subsequent statistical analyses. This is not surprising considering the BMD has its roots in Switzerland in the late 19th century, was admitted to the AKC registry in 1937, and experienced numerous international 'line-exchanges' over the ensuing 74 years. These data suggest a relatively homogeneous international population, supporting the conclusion of Quignon et al. [44] who proposed the use of international BMD cohorts for genetic studies. From a population genetics perspective, since the main populations of BMD are located in the USA and Europe, and there are no apparent differences in CNAs evident at 1 Mb resolution between the two BMD populations, we surmise that the genomic changes associated with HS are common to all BMDs regardless of geographic origin. This in turn may indicate that any risk factors for the development and progression of HS are linked tightly to the genetic makeup of the breed and independent of geography. Advances in understanding of the biological mechanism of HS in BMDs in the USA should therefore apply also to BMDs in other countries, extending the value of such studies.

Most of the CNAs identified in this study were common to both the BMD and the FCR, and so it is likely that such aberrations may also be evident in other breeds presenting with these malignancies. We identified 13 regions of the genome on seven chromosomes that showed a significant association between DNA copy number and breed of the patient (Table 1). Further, PCA indicated a significant association between specific CNAs and either breed (BMD/FCR) or anatomical location(s) of the tumor(s). Since breed and tumor location are so closely correlated, it is not possible from this study to determine whether the association between CNAs and breed was driven by breed itself or by the anatomical location of the tumor in that breed. Aberrations may be associated with location of affected organ/tissue, and/or dissemination/metastatic nature of HS. These aberrations could confer a proliferative advantage to the tumor in one particular organ, or elevate the risk of metastasis. An alternative hypothesis is that some of these aberrations are linked specifically with the genetic background of each breed. Since it has been shown previously that individual genetic backgrounds, as defined by breed in dogs, influence tumor karyotypes [40,45], we could hypothesize that some pathways are inactivated by germline mutations in one breed, creating a genetic risk for HS, but are inactivated by somatic modifications (genomic loss, mutation) in the second breed. Evaluation of HS in additional breeds that also present with a disseminated form of the disease, such as the Rottweiler, will aid in determining whether the apparent separation between BMD and FCR is driven by breed or by anatomical features of the cancer [9].

Identification of highly recurrent CNAs shared by the FCR and the BMD - candidate regions for human HS

Despite the high level of genome reorganization evident in canine HS and the varying anatomical location of the tumors between breeds, we identified numerous CNAs within our sample population shared between the both breeds. Several of these were classified as recurrent (≥30% frequency) or highly recurrent (≥50% frequency). Among the most highly recurrent CNAs detected were loss of regions of CFA 2, CFA 11, CFA 16, CFA 22 and CFA 31, all of which were highly frequent (50-86%) in both breeds. The presence of highly recurrent abnormalities common to both breeds, along with their presence in both the localized and disseminated forms of HS, is suggestive of an association more with the cancer phenotype than with breed. These regions likely contain genes that may play a key role in malignant transformation of histiocytes, independent of anatomical location. This is especially so for the most frequent CNA, deletion of CFA 16, an aberration that was detected in 86% of HS cases (80.4% of BMD, 96.7% of FCR).

At first glance many of the recurrent aberrations identified in this study involved large contiguous tracts of the canine genome (Figures 4 and 5), and so identification of candidate genes is challenging. Closer consideration of subchromosomal differences in aberration frequency may however be used to determine minimal regions of interest. For example, Figures 4 and 5 indicate that while the full length of CFA 16 is deleted in at least 50% of all HS cases (both FCR and BMD), there are regional differences in the frequency of deletion along the length of the chromosome. The highest frequency of recurrent deletion (86%) along CFA 16 involved a 6 Mb region (47-53 Mb) towards the telomeric end of the chromosome. There are several annotated candidate genes within this region of the canine genome http://genome.ucsc.edu/cgi-bin/hgGateway?db=canFam2 that are known either to be involved in

regulation of apoptosis, or which are suspected to be tumor suppressor genes; including *CDKN2A interacting protein (CDKN2AIP), FAT tumor suppressor homolog1 (FAT1), Tumor suppressor candidate 3 (TUSC3), Mitochondrial Tumor Suppressor gene 1 (MTUS1)* and *pericentriolar material-1 (PCM1)*. Of comparative significance specific to HS, *CDKN2AIP* is known to interact with *CDKN2A/p14ARF, TP53*/p53 and *MDM2*, all of which have been shown to be involved in human histiocytic disorders [4,8,9,11-14,46] and so this merits further investigation in future studies.

Similarly, a neighboring 2.4 Mb region of CFA 16 (41.8 Mb-44.2 Mb) was deleted in 84.9% of HS cases. Of possible comparative significance, this region of CFA 16 is in part orthologous to human chromosome (HSA) 8p22-p21.3, a region that is frequently deleted in numerous tumors, including multiple myeloma, prostate cancer, hepatocellular carcinoma and neck squamous cell carcinoma [47-50]. These data indicate that in both human and canine cancers, this region exhibits a strikingly high and comparable level of CNA. Further evaluation of both human and canine patients will be required to determine whether this shared deletion contains genes and regulatory elements associated with HS, or if its presence is merely a generalized passenger aberration.

aCGH profiling of canine HS suggests that disruption of the p53 and Rb pathways is a common event

Segments of CFA 11 (q22), 22 (q11) and 26 (q25) all showed a high incidence of copy number loss in canine HS. Each of these three regions contain key cancer associated genes involved in the p53 and Rb pathways: *CDKN2A/B* (CFA 11q22), *RB1* (CFA 22q11) and *PTEN* (CFA 26q25). *CDKN2* encodes three distinct tumor suppressor genes (*ARF, $p15^{INK4b}$ $p16^{INK4a}$*) that code for proteins regulating cell cycle progression via the Rb and p53 pathways. While $p15^{INK4b}$ and $p16^{INK4a}$ regulate the Rb-pathway, ARF inactivates MDM2 protein and so regulates p53 [51,52]. The human region orthologous to CFA 11q22 is HSA 9p21, which is among the most frequent sites of DNA copy number loss in human cancers [53]. Genes within this region, especially $p16^{INK4a}$, have also been shown to be inactivated in several dog cancers including lymphoma, melanoma, hemangiosarcoma and osteosarcoma [42,54-59]. Since direct inactivation of $p16^{INK4a}$ by point mutation, deletion or promoter methylation is evident in approximately one third of human hematopoietic tumors [53,60], it is not surprising to find this locus is involved in human histiocytic disorders. Significantly, monosomy of HSA 9, including the *CDKN2* locus, has been observed in different human dendritic proliferations including plasmacytoid DC sarcoma [8] and follicular DC sarcoma [9]. Moreover deletion of HSA 9p has been reported as the second most frequently observed aberration in Langerhans cell histiocytosis (LCH) of the lung [10]. In mice, loss of *INK4a* allows macrophages to bypass senescence [61] and Pten and Ink4a/Arf have a cooperative role in restricting macrophage growth. The same is true in human HS where inactivation of *PTEN* and *INK4a/ARF* tumor suppressors are critical steps in the pathogenesis of this cancer [4,11]. It is therefore of interest that in this study >50% of HS cases presented with a deletion of the *CDKN2* locus. Other mechanisms, such as DNA sequence mutations or methylation, may also inactivate these tumor suppressor genes. In future studies it will be important to investigate whether HS cases presenting with no apparent deletion of *CDKN2* have an increased rate of DNA sequence mutation of this locus, resulting in aberrant expression for reasons other than gene dosage.

Also belonging to these key pathways is the gene *Retinoblastoma 1 (RB1)*, which is disrupted in a variety of human solid tumors including pituitary adenomas, esophageal carcinoma, gliomas and ovarian cancer [62]. Deletion of HSA 13q14, containing *RB1*, is also a common event in a wide variety of acute/chronic myeloid disorders as well as in human dendritic sarcomas (plasmacytoid DC and follicular DC sarcomas) [8,63]. In our study, loss of the *RB1* locus on CFA 22 was highly recurrent across the cohort (55.8% of HS cases) although it was detected twice as frequently in HS tumors of FCRs than of BMDs (83.3% of FCR cases vs 41.1% of BMD cases).

Deletion of HSA 17p, containing *TP53*, has been described in human LCH [10,12], while other studies reported an elevated expression of p53 in this disease [13,14]. In the present study, 36% of canine HS cases demonstrated CNA of *TP53*, representing copy number loss in 9.3% cases and gain in 26.7% of cases. Further studies are needed to assess if gene dosage of *TP53*, as well as other mechanisms, result in altered expression of p53 that may be correlated with elevated expression of this protein in Langerhans cell proliferation.

Deletion of CFA26 was present in approximately 20% of canine HS cases, but the telomeric end of this chromosome, a region encoding the *PTEN* locus, was deleted in ~41% of cases, regardless of breed. *PTEN* plays a significant role in inducing cycle arrest and programming apoptosis. It is an antagonist of the *PI3K/AKT* pathway, and in turn regulates the *Rb* pathway [64]. It also controls p53 protein levels and transcriptional activity through both phosphatase-dependent and independent mechanisms [65]. *PTEN* has been shown to be deleted or mutated in a wide range of human tumors [64] and also in several canine tumors [58,66]. While *PTEN* influences p53 transcriptional activity and p53 stability [65], no association was found in our data between gain/loss of *TP53* and *PTEN* loss (Fisher's Exact test, data not shown).

Copy number aberrations common to both breeds, combined with their likely consequential impact on the same pathways in human and canine HS, support the relevance of the dog as a model of HS. In addition to the genes discussed above we suspect that other tumor suppressors on CFA 2, CFA 16 and CFA 31 (deleted in 50%, 86% and 61.6% of HS tumors, respectively) also may play an important role in histiocytic cancerization. Their identity likely will become apparent with increased resolution and functional analysis of genes within these regions.

Conclusions

This study demonstrates that histiocytic sarcomas of two dog breeds with distinct genetic backgrounds (BMD and FCR), but sharing a high incidence of the disease, present with highly aberrant genome-wide DNA copy number profiles. The presence of numerous highly recurrent CNAs shared by both BMD and FCR tumors suggests that these are associated more with the cancer phenotype than breed. The small number of breed associated CNAs identified may contribute to the major differences in the varying tumor location evident in these two breeds. The most highly recurrent aberrations revealed in this study are evolutionarily conserved with those reported in human histiocytic proliferations, suggesting that human and dog HS share a conserved pathogenesis. The breed associated clinical features and chromosomal aberrations of canine HS offer a valuable spontaneous model for the human counterpart, aiding elucidation of the pathophysiological and genetic mechanisms associated with histiocytic malignancies and providing new opportunities for developing effective therapeutic modalities for both species.

Additional material

Additional file 1: Table S1. List of microsatellite markers used for LOH study. The position of each sequence is shown as the base pair location in the canine genome assembly, canFam2. Forward primers of CFA 11 markers had an M13-tail and were used with an M13 primer fluorescently tagged at the 5' end either with PET, VIC, FAM or NED to facilitate multiplexing.

Additional file 2: Table S2. Signalment and clinical data for all 125 canine histiocytic sarcoma cases for which unfixed tumor biopsies were available. Unshaded cases indicate 86 cases used for aCGH data analysis. Cases that did not yield sufficient quality DNA and those that did not contain evident CNAs are highlighted in grey.

Acknowledgements

This study was supported by funds from the American Kennel Club Canine Health Foundation (award numbers 2667 and 760 [MB and JC] and 336b/337 [CA]). We thank the staff of the NCSU Histopathology Service for their help and expertise and are especially grateful to the owners of Bernese Mountain Dogs and Flat Coated Retrievers who provided the samples required for this study. We are especially grateful to the Health and Genetics Committees of the BMDCA and the FCRSA and to Joye Neff, Pat Long, Vicky Nickerson, Gay Coffin and Shirleen Roeder. We thank the French and Italian Bernese Mountain Dog clubs (AFBS, SIBB: Alberto Vittoni Award) for funding support and all European clubs, breeders, owners, French histopathology laboratories and veterinarians for their active participation in this study.

Author details

[1]Department of Molecular Biomedical Sciences, College of Veterinary Medicine, North Carolina State University, Raleigh, NC, USA. [2]Center for Comparative Medicine and Translational Research, North Carolina State University, Raleigh, NC, USA. [3]Bioinformatics Research Center, North Carolina State University, Raleigh, NC, USA. [4]Department of Statistics, North Carolina State University, Raleigh, NC, USA. [5]UMR 707 IECM, AMaROC team, ONIRIS, Nantes, FRANCE. [6]Institut de Génétique et Développement, UMR 6061 CNRS/Université de Rennes1, Faculté de Médecine, Rennes, FRANCE. [7]Department of Population Health and Pathobiology, College of Veterinary Medicine, North Carolina State University, Raleigh, NC, USA. [8]Cancer Genetics Program, UNC Lineberger Comprehensive Cancer Center, Chapel Hill, NC 27599, USA.

Authors' contributions

MB conceptualized and designed the project. MB and CA obtained all the samples for the study, for which JC and JA conducted the pathology review. BH performed and analyzed the aCGH, FISH and LOH data with input from RT and MB. AMR was responsible for statistical design. BH and AMR conducted the statistical evaluation of the aCGH data. BH, MB and RT wrote the manuscript. All authors read, edited and approved the final manuscript.

Competing interests

The authors declare that they have no competing interests.

Received: 22 December 2010 Accepted: 26 May 2011
Published: 26 May 2011

References

1. Jaffe ES: **Pathology and genetics of tumours of haematopeietic tissues.** Lyon: World Health Organization of Tumours. International Agency for Research on Cancer; 2001.
2. Pileri SA, Grogan TM, Harris NL, Banks P, Campo E, Chan JK, Favera RD, Delsol G, De Wolf-Peeters C, Falini B, *et al*: **Tumours of histiocytes and accessory dendritic cells: an immunohistochemical approach to classification from the International Lymphoma Study Group based on 61 cases.** *Histopathology* 2002, **41(1)**:1-29.
3. Favara BE, Feller AC, Pauli M, Jaffe ES, Weiss LM, Arico M, Bucsky P, Egeler RM, Elinder G, Gadner H, *et al*: **Contemporary classification of histiocytic disorders. The WHO Committee On Histiocytic/Reticulum Cell Proliferations. Reclassification Working Group of the Histiocyte Society.** *Med Pediatr Oncol* 1997, **29(3)**:157-166.
4. Carrasco DR, Fenton T, Sukhdeo K, Protopopova M, Enos M, You MJ, Di Vizio D, Nogueira C, Stommel J, Pinkus GS, *et al*: **The PTEN and INK4A/ARF tumor suppressors maintain myelolymphoid homeostasis and cooperate to constrain histiocytic sarcoma development in humans.** *Cancer Cell* 2006, **9(5)**:379-390.
5. Teyssier JR, Behar C, Pignon B, Caulet T, Patey M, Bajolle F, Adnet JJ: **Chromosomal changes in a documented case of malignant histiocytosis: significance of polyploidy.** *Cancer Genet Cytogenet* 1986, **21(1)**:85-91.
6. Mecucci C, Donti E, Tabilio A, Martelli MF, Van den Berghe H: **Clinical and cytogenetic findings in monocyte-macrophage system malignancies with initial spontaneous regression.** *Cancer Genet Cytogenet* 1983, **9(4)**:317-327.
7. Schouten TJ, Hustinx TW, Scheres JM, Holland R, de Vaan GA: **Malignant histiocytosis. Clinical and cytogenetic studies in a newborn and a child.** *Cancer* 1983, **52(7)**:1229-1236.
8. Leroux D, Mugneret F, Callanan M, Radford-Weiss I, Dastugue N, Feuillard J, Le Mee F, Plessis G, Talmant P, Gachard N, *et al*: **CD4(+), CD56(+) DC2 acute leukemia is characterized by recurrent clonal chromosomal changes affecting 6 major targets: a study of 21 cases by the Groupe Francais de Cytogenetique Hematologique.** *Blood* 2002, **99(11)**:4154-4159.
9. Sander B, Middel P, Gunawan B, Schulten HJ, Baum F, Golas MM, Schulze F, Grabbe E, Parwaresch R, Fuzesi L: **Follicular dendritic cell sarcoma of the spleen.** *Hum Pathol* 2007, **38(4)**:668-672.

10. Dacic S, Trusky C, Bakker A, Finkelstein SD, Yousem SA: **Genotypic analysis of pulmonary Langerhans cell histiocytosis.** *Hum Pathol* 2003, **34(12)**:1345-1349.
11. Kumar R, Khan SP, Joshi DD, Shaw GR, Ketterling RP, Feldman AL: **Pediatric histiocytic sarcoma clonally related to precursor B-cell acute lymphoblastic leukemia with homozygous deletion of CDKN2A encoding p16(INK4A).** *Pediatr Blood Cancer* 2010.
12. Murakami I, Gogusev J, Fournet JC, Glorion C, Jaubert F: **Detection of molecular cytogenetic aberrations in langerhans cell histiocytosis of bone.** *Hum Pathol* 2002, **33(5)**:555-560.
13. Bank MI, Rengtved P, Carstensen H, Petersen BL: **p53 expression in biopsies from children with Langerhans cell histiocytosis.** *J Pediatr Hematol Oncol* 2002, **24(9)**:733-736.
14. Weintraub M, Bhatia KG, Chandra RS, Magrath IT, Ladisch S: **p53 expression in Langerhans cell histiocytosis.** *J Pediatr Hematol Oncol* 1998, **20(1)**:12-17.
15. De Pas T, Spitaleri G, Pruneri G, Curigliano G, Noberasco C, Luini A, Andreoni B, Testori A, de Braud F: **Dendritic cell sarcoma: an analytic overview of the literature and presentation of original five cases.** *Crit Rev Oncol Hematol* 2008, **65(1)**:1-7.
16. Mitelman F, Johansson B, Mertens F: **The impact of translocations and gene fusions on cancer causation.** *Nat Rev Cancer* 2007, **7(4)**:233-245.
17. Affolter VK, Moore PF: **Localized and disseminated histiocytic sarcoma of dendritic cell origin in dogs.** *Vet Pathol* 2002, **39(1)**:74-83.
18. Moore PF, Affolter VK, Vernau W: **Canine hemophagocytic histiocytic sarcoma: a proliferative disorder of CD11d+ macrophages.** *Vet Pathol* 2006, **43(5)**:632-645.
19. Moore PF, Rosin A: **Malignant histiocytosis of Bernese mountain dogs.** *Vet Pathol* 1986, **23(1)**:1-10.
20. Rosin A, Moore P, Dubielzig R: **Malignant histiocytosis in Bernese Mountain dogs.** *J Am Vet Med Assoc* 1986, **188(9)**:1041-1045.
21. Dobson J, Villiers E, Roulois A, Gould S, Mellor P, Hoather T, Watson P: **Histiocytic sarcoma of the spleen in flat-coated retrievers with regenerative anaemia and hypoproteinaemia.** *Vet Rec* 2006, **158(24)**:825-829.
22. Padgett GA, Madewell BR, Keller ET, Jodar L, Packard M: **Inheritance of histiocytosis in Bernese mountain dogs.** *J Small Anim Pract* 1995, **36(3)**:93-98.
23. Abadie J, Hedan B, Cadieu E, De Brito C, Devauchelle P, Bourgain C, Parker HG, Vaysse A, Margaritte-Jeannin P, Galibert F, *et al*: **Epidemiology, Pathology, and Genetics of Histiocytic Sarcoma in the Bernese Mountain Dog Breed.** *J Hered* 2009.
24. Dobson J, Hoather T, McKinley TJ, Wood JL: **Mortality in a cohort of flat-coated retrievers in the UK.** *Vet Comp Oncol* 2009, **7(2)**:115-121.
25. Fidel J, Schiller I, Hauser B, Jausi Y, Rohrer-Bley C, Roos M, Kaser-Hotz B: **Histiocytic sarcomas in flat-coated retrievers: a summary of 37 cases (November 1998-March 2005).** *Vet Comp Oncol* 2006, **4(2)**:63-74.
26. Thomas R, Duke SE, Karlsson EK, Evans A, Ellis P, Lindblad-Toh K, Langford CF, Breen M: **A genome assembly-integrated dog 1 Mb BAC microarray: a cytogenetic resource for canine cancer studies and comparative genomic analysis.** *Cytogenet Genome Res* 2008, **122(2)**:110-121.
27. Lindblad-Toh K, Wade CM, Mikkelsen TS, Karlsson EK, Jaffe DB, Kamal M, Clamp M, Chang JL, Kulbokas EJ, Zody MC, *et al*: **Genome sequence, comparative analysis and haplotype structure of the domestic dog.** *Nature* 2005, **438(7069)**:803-819.
28. Thomas R, Duke SE, Bloom SK, Breen TE, Young AC, Feiste E, Seiser EL, Tsai PC, Langford CF, Ellis P, *et al*: **A cytogenetically characterized, genome-anchored 10-Mb BAC set and CGH array for the domestic dog.** *J Hered* 2007, **98(5)**:474-484.
29. Jong K, Marchiori E, Meijer G, Vaart AV, Ylstra B: **Breakpoint identification and smoothing of array comparative genomic hybridization data.** *Bioinformatics* 2004, **20(18)**:3636-3637.
30. Boutin-Ganache I, Raposo M, Raymond M, Deschepper CF: **M13-tailed primers improve the readability and usability of microsatellite analyses performed with two different allele-sizing methods.** *Biotechniques* 2001, **31(1)**:24-26, 28.
31. Clark LA, Tsai KL, Steiner JM, Williams DA, Guerra T, Ostrander EA, Galibert F, Murphy KE: **Chromosome-specific microsatellite multiplex sets for linkage studies in the domestic dog.** *Genomics* 2004, **84(3)**:550-554.
32. Breen M, Bullerdiek J, Langford CF: **The DAPI banded karyotype of the domestic dog (Canis familiaris) generated using chromosome-specific paint probes.** *Chromosome Research* 1999, **7(5)**:401-406.
33. Breen M, Hitte C, Lorentzen TD, Thomas R, Cadieu E, Sabacan L, Scott A, Evanno G, Parker HG, Kirkness EF, *et al*: **An integrated 4249 marker FISH/RH map of the canine genome.** *BMC Genomics* 2004, **5(1)**:65.
34. Reich D, Price AL, Patterson N: **Principal component analysis of genetic data.** *Nat Genet* 2008, **40(5)**:491-492.
35. Price AL, Zaitlen NA, Reich D, Patterson N: **New approaches to population stratification in genome-wide association studies.** *Nat Rev Genet* 2010, **11(7)**:459-463.
36. Reich DE, Goldstein DB: **Detecting association in a case-control study while correcting for population stratification.** *Genet Epidemiol* 2001, **20(1)**:4-16.
37. Hoggart CJ, Parra EJ, Shriver MD, Bonilla C, Kittles RA, Clayton DG, McKeigue PM: **Control of confounding of genetic associations in stratified populations.** *Am J Hum Genet* 2003, **72(6)**:1492-1504.
38. Pritchard JK, Stephens M, Rosenberg NA, Donnelly P: **Association mapping in structured populations.** *Am J Hum Genet* 2000, **67(1)**:170-181.
39. Dwass M: **Modified Randomization Tests for Nonparametric Hypotheses.** *The Annals of Mathematical Statistics* 1957, **28**:181-187.
40. Thomas R, Duke SE, Wang HJ, Breen TE, Higgins RJ, Linder KE, Ellis P, Langford CF, Dickinson PJ, Olby NJ, *et al*: **'Putting our heads together': insights into genomic conservation between human and canine intracranial tumors.** *J Neurooncol* 2009, **94(3)**:333-349.
41. Breen M, Modiano JF: **Evolutionarily conserved cytogenetic changes in hematological malignancies of dogs and humans–man and his best friend share more than companionship.** *Chromosome Res* 2008, **16(1)**:145-154.
42. Fosmire SP, Thomas R, Jubala CM, Wojcieszyn JW, Valli VE, Getzy DM, Smith TL, Gardner LA, Ritt MG, Bell JS, *et al*: **Inactivation of the p16 cyclin-dependent kinase inhibitor in high-grade canine non-Hodgkin's T-cell lymphoma.** *Vet Pathol* 2007, **44(4)**:467-478.
43. Shortman K, Liu YJ: **Mouse and human dendritic cell subtypes.** *Nat Rev Immunol* 2002, **2(3)**:151-161.
44. Quignon P, Herbin L, Cadieu E, Kirkness EF, Hedan B, Mosher DS, Galibert F, Andre C, Ostrander EA, Hitte C: **Canine population structure: assessment and impact of intra-breed stratification on SNP-based association studies.** *PLoS ONE* 2007, **2(12)**:e1324.
45. Tamburini BA, Trapp S, Phang TL, Schappa JT, Hunter LE, Modiano JF: **Gene expression profiles of sporadic canine hemangiosarcoma are uniquely associated with breed.** *PLoS ONE* 2009, **4(5)**:e5549.
46. Dakic A, Wu L: **Hemopoietic precursors and development of dendritic cell populations.** *Leuk Lymphoma* 2003, **44(9)**:1469-1475.
47. Sutlu T, Alici E, Jansson M, Wallblom A, Dilber MS, Gahrton G, Nahi H: **The prognostic significance of 8p21 deletion in multiple myeloma.** *Br J Haematol* 2009, **144(2)**:266-268.
48. Hornstein M, Hoffmann MJ, Alexa A, Yamanaka M, Muller M, Jung V, Rahnenfuhrer J, Schulz WA: **Protein phosphatase and TRAIL receptor genes as new candidate tumor genes on chromosome 8p in prostate cancer.** *Cancer Genomics Proteomics* 2008, **5(2)**:123-136.
49. Di Benedetto M, Pineau P, Nouet S, Berhouet S, Seitz I, Louis S, Dejean A, Couraud PO, Strosberg AD, Stoppa-Lyonnet D, *et al*: **Mutation analysis of the 8p22 candidate tumor suppressor gene ATIP/MTUS1 in hepatocellular carcinoma.** *Mol Cell Endocrinol* 2006, **252(1-2)**:207-215.
50. Ye H, Pungpravat N, Huang BL, Muzio LL, Mariggio MA, Chen Z, Wong DT, Zhou X: **Genomic assessments of the frequent loss of heterozygosity region on 8p21.3-p22 in head and neck squamous cell carcinoma.** *Cancer Genet Cytogenet* 2007, **176(2)**:100-106.
51. Kim WY, Sharpless NE: **The regulation of INK4/ARF in cancer and aging.** *Cell* 2006, **127(2)**:265-275.
52. Gil J, Peters G: **Regulation of the INK4b-ARF-INK4a tumour suppressor locus: all for one or one for all.** *Nat Rev Mol Cell Biol* 2006, **7(9)**:667-677.
53. Sharpless NE: **INK4a/ARF: a multifunctional tumor suppressor locus.** *Mutat Res* 2005, **576(1-2)**:22-38.
54. Koenig A, Bianco SR, Fosmire S, Wojcieszyn J, Modiano JF: **Expression and significance of p53, rb, p21/waf-1, p16/ink-4a, and PTEN tumor suppressors in canine melanoma.** *Vet Pathol* 2002, **39(4)**:458-472.
55. Levine RA, Fleischli MA: **Inactivation of p53 and retinoblastoma family pathways in canine osteosarcoma cell lines.** *Vet Pathol* 2000, **37(1)**:54-61.

56. Modiano JF, Breen M, Valli VE, Wojcieszyn JW, Cutter GR: **Predictive value of p16 or Rb inactivation in a model of naturally occurring canine non-Hodgkin's lymphoma.** *Leukemia* 2007, **21(1)**:184-187.
57. Yonemaru K, Sakai H, Murakami M, Kodama A, Mori T, Yanai T, Maruo K, Masegi T: **The significance of p53 and retinoblastoma pathways in canine hemangiosarcoma.** *J Vet Med Sci* 2007, **69(3)**:271-278.
58. Dickerson EB, Thomas R, Fosmire SP, Lamerato-Kozicki AR, Bianco SR, Wojcieszyn JW, Breen M, Helfand SC, Modiano JF: **Mutations of phosphatase and tensin homolog deleted from chromosome 10 in canine hemangiosarcoma.** *Vet Pathol* 2005, **42(5)**:618-632.
59. Thomas R, Scott A, Langford CF, Fosmire SP, Jubala CM, Lorentzen TD, Hitte C, Karlsson EK, Kirkness E, Ostrander EA, *et al*: **Construction of a 2-Mb resolution BAC microarray for CGH analysis of canine tumors.** *Genome Res* 2005, **15(12)**:1831-1837.
60. Ruas M, Peters G: **The p16INK4a/CDKN2A tumor suppressor and its relatives.** *Biochim Biophys Acta* 1998, **1378(2)**:F115-177.
61. Randle DH, Zindy F, Sherr CJ, Roussel MF: **Differential effects of p19(Arf) and p16(Ink4a) loss on senescence of murine bone marrow-derived preB cells and macrophages.** *Proc Natl Acad Sci USA* 2001, **98(17)**:9654-9659.
62. Presneau N, Manderson EN, Tonin PN: **The quest for a tumor suppressor gene phenotype.** *Curr Mol Med* 2003, **3(7)**:605-629.
63. Della Porta M, Rigolin GM, Bugli AM, Bardi A, Bragotti LZ, Bigoni R, Cuneo A, Castoldi G: **Differentiation of follicular dendritic sarcoma cells into functional myeloid-dendritic cell-like elements.** *Eur J Haematol* 2003, **70(5)**:315-318.
64. Di Cristofano A, Pandolfi PP: **The multiple roles of PTEN in tumor suppression.** *Cell* 2000, **100(4)**:387-390.
65. Freeman DJ, Li AG, Wei G, Li HH, Kertesz N, Lesche R, Whale AD, Martinez-Diaz H, Rozengurt N, Cardiff RD, *et al*: **PTEN tumor suppressor regulates p53 protein levels and activity through phosphatase-dependent and -independent mechanisms.** *Cancer Cell* 2003, **3(2)**:117-130.
66. Thomas R, Wang HJ, Tsai PC, Langford CF, Fosmire SP, Jubala CM, Getzy DM, Cutter GR, Modiano JF, Breen M: **Influence of genetic background on tumor karyotypes: evidence for breed-associated cytogenetic aberrations in canine appendicular osteosarcoma.** *Chromosome Res* 2009, **17(3)**:365-377.

Pre-publication history
The pre-publication history for this paper can be accessed here:
http://www.biomedcentral.com/1471-2407/11/201/prepub

doi:10.1186/1471-2407-11-201
Cite this article as: Hedan *et al.*: Molecular cytogenetic characterization of canine histiocytic sarcoma: A spontaneous model for human histiocytic cancer identifies deletion of tumor suppressor genes and highlights influence of genetic background on tumor behavior. *BMC Cancer* 2011 11:201.

Voie NOTCH et Histiocytose Langerhansienne: Caroline Hutter Vienne

Notch is active in Langerhans cell histiocytosis and confers pathognomonic features on dendritic cells

Caroline Hutter,[1,2] Max Kauer,[2] Ingrid Simonitsch-Klupp,[3] Gunhild Jug,[2] Raphaela Schwentner,[2] Judith Leitner,[4] Peter Bock,[5] Peter Steinberger,[4] Wolfgang Bauer,[6] Nadia Carlesso,[7] Milen Minkov,[1,2] Helmut Gadner,[1,2] Georg Stingl,[6] Heinrich Kovar,[2] and Ernst Kriehuber[6]

[1]St Anna Children's Hospital, Department of Pediatrics, Medical University of Vienna, Vienna, Austria; [2]Children's Cancer Research Institute, St Anna Kinderkrebsforschung, Vienna, Austria; [3]Clinical Institute of Pathology, Medical University of Vienna, Vienna, Austria; [4]Institute of Immunology, Center for Pathophysiology, Infectiology and Immunology, Medical University of Vienna, Vienna, Austria; [5]Department of Orthopedic Surgery, Danube Hospital, Vienna, Austria; [6]Department of Dermatology, Division of Immunology, Allergy and Infectious Diseases, Medical University of Vienna, Vienna, Austria; and [7]Department of Pediatrics, Herman B. Wells Center, Indiana University Simon Cancer Center, Indiana University School of Medicine, Indianapolis, IN

Langerhans cell histiocytosis (LCH) is an enigmatic disease defined by the accumulation of Langerhans cell-like dendritic cells (DCs). In the present study, we demonstrate that LCH cells exhibit a unique transcription profile that separates them not only from plasmacytoid and myeloid DCs, but also from epidermal Langerhans cells, indicating a distinct DC entity. Molecular analysis revealed that isolated and tissue-bound LCH cells selectively express the Notch ligand Jagged 2 (*JAG2*) and are the only DCs that express both Notch ligand and its receptor. We further show that *JAG2* signaling induces key LCH-cell markers in monocyte-derived DCs, suggesting a functional role of Notch signaling in LCH ontogenesis. *JAG2* also induced matrix-metalloproteinases 1 and 12, which are highly expressed in LCH and may account for tissue destruction in LCH lesions. This induction was selective for DCs and was not recapitulated in monocytes. The results of the present study suggest that *JAG2*-mediated Notch activation confers phenotypic and functional aspects of LCH to DCs; therefore, interference with Notch signaling may be an attractive strategy to combat this disease. (*Blood.* 2012;120(26):5199-5208)

Introduction

Langerhans cell histiocytosis (LCH) is a disease characterized by the accumulation of eponymous CD1a$^+$Langerin$^+$ Langerhans cell (LC)–like dendritic cells (DCs) of largely unknown origin.[1] It is a rare disease that may affect any age group, although its most severe clinical course predominantly affects young children.[2] One intriguing feature of LCH is the wide spectrum of clinical presentations, which can range from single system disease such as osteolytic bone lesions, which can resolve spontaneously, to fulminant multisystem disease that requires intensive chemotherapy and BM transplantation.[3] The etiology of LCH is not known, and it is even unclear whether it is an inflammatory disorder or neoplastic disease.[4] Therefore, targeted therapeutic approaches do not exist, although the recent discovery of *BRAF* mutations in a majority of LCH samples[5] could pave the way for RAF inhibitors in the treatment of LCH.

Recently, a comprehensive gene-expression profiling study of LCH cells has been conducted and revealed more than 2000 differentially expressed transcripts compared with normal LCs.[6] However, the relationship between LCH cells and other naturally occurring dendritic cells had not yet been investigated.

In the present study, we performed comparative gene-expression analysis of highly purified LCH cells derived from different locations and disease courses and 3 major, functionally divergent naturally occurring human DC lineages: epidermal LCs, myeloid dendritic cells (mDC1s), and plasmacytoid dendritic cells (pDCs).[7] Our results indicate that LCH cells form a distinct DC entity. Furthermore, we have identified transcripts that are uniquely expressed by LCH cells and that in functional analyses induced LCH-specific features in human DCs.

Methods

Cell isolation

LCH biopsies were obtained from patients undergoing surgery. Cell suspensions were prepared by dissociating collagenase IV (Worthington Biochemical)–treated, minced tissue using a cell dissociation sieve (Sigma-Aldrich). Cells were pelleted, resuspended in ice-cold RPMI 1640/10% FCS, and immunostained with CD1a (BD Biosciences) and CD207/Langerin (Coulter) Abs. Isolation of epidermal Langerhans cells, pDCs, and mDC1s was performed as described previously[8] and as outlined in supplemental Methods (available on the *Blood* Web site; see the Supplemental Materials link at the top of the online article). All protocols for obtaining and studying human tissues and cells were approved by the institutional review boards and according to the regulations of the Declaration of Helsinki.

RNA purification, amplification, and hybridization

Sorted cells were lysed in TRIzol reagent (Sigma-Aldrich) and RNA was isolated according to the manufacturer's recommendations. cRNA target synthesis, amplification, hybridizations to GeneChip Human Genome U133 Plus 2.0 Arrays (Affymetrix), and scanning were done according to standard protocols recommended by the manufacturer.

Submitted February 13, 2012; accepted September 22, 2012. Prepublished online as *Blood* First Edition paper, October 16, 2012; DOI 10.1182/blood-2012-02-410241.

The online version of this article contains a data supplement.

The publication costs of this article were defrayed in part by page charge payment. Therefore, and solely to indicate this fact, this article is hereby marked "advertisement" in accordance with 18 USC section 1734.

Analysis of gene-expression data and functional annotation

Raw and normalized microarray experiments have been submitted to the Gene Expression Omnibus (GEO; accession number GSE35340). Normalization of CEL files and all further analyses were performed in the R statistical environment using Bioconductor packages. Affymetrix CEL files of LCH and DC samples were normalized together using gcrma and preprocessed as described previously.[9] Briefly, probe sets that did not differ significantly from nontargeting probe sets were excluded and the most informative (variable) probe set was selected for each gene. This procedure yielded a final number of 10 007 probe sets that were used for all further analyses. Differential expression between the different DCs and LCH samples was measured by a moderated t test statistic and P values were corrected for multiple testing using the Benjamini-Hochberg method.[10]

Principal component analysis, multidimensional scaling, and hierarchical clustering

Analyses were based on a matrix of pairwise correlations (Pearson correlation coefficient) over all filtered genes among the 17 samples (used as distances: 1-cor). For multidimensional scaling, the R function "sammon" was used with default parameters. For hierarchical clustering and the heat map shown in supplemental Figure 1, the R function "hclust" was used in combination with the "heatmap.2" function using the "average linkage" algorithm.

Generation of Euler diagrams

Area proportional Euler diagrams were generated using VennMaster Version 0.37.5 software.[11] Differentially regulated genes (adjusted $P < .05$, fold change > 2) in LCH cells compared with the individual DC subsets were used for analysis.

Immunohistochemistry and immunofluorescence

Paraffin sections were stained according to standard protocols, as described previously[12] and as detailed in the supplemental materials. For immunofluorescence analysis, frozen sections were fixed at −20°C in acetone or at room temperature in 4% paraformaldehyde. Sections were blocked in 1% BSA and 10% goat or rabbit serum before Ab labeling and then counterstained with DAPI. Images were captured with a fluorescence microscope (Axioplan 2; Zeiss) using the ISIS Fluorescence Imaging System (MetaSystems) or an inverted Axiovert 200M microscope (Zeiss) equipped with the laser-scanning module LSM510 (Zeiss). IHC stains were acquired on a Olympus BX51 microscope equipped with a ProgRes C12 Jenoptic Optical Systems digital camera with the operational ProgRes MAC CapturePro 2.7 application software. Figure 2B and Care shown with a original magnification of 40×, using a Olympus Plan Apo 40×/0.85 objective, the insets and Figure 2D show the original magnification of 100× operating with a Olympus U Plan Apo 100×/1.35 objective.

Quantitative PCR

Total RNA was reverse transcribed using a Superscript III first-strand synthesis kit (Invitrogen) and quantitative PCR was performed under standard conditions with an ABI 7500 fast real-time PCR machine (Applied Biosystems). Samples were run in triplicate for each probe and quantification was based on ΔΔCT calculations. Samples were normalized to β-microglobulin. Predesigned TaqMan probes were purchased from Applied Biosystems. The following probes were used: *B2M*: Hs 99999907, *TGF-B*: Hs 000998133, *MMP1*: Hs 00899658, *MMP12*: Hs 00899662, and *ADAMDEC1*: Hs 00936068.

DC differentiation

PBMCs were isolated from buffy coats from healthy donors by density gradient centrifugation using Ficoll-Paque. Monocytes were isolated by magnetically activated cell sorting using CD14 MicroBeads (Miltenyi Biotec). Alternatively, cells were isolated by counterflow centrifugal elutriation (Elutra Cell Separation System). For DC differentiation, CD14-enriched monocytes were cultured in 100 ng/mL of human recombinant GM-CSF (rGM-CSF) and 100 ng/mL of human rIL-4 (both PeproTech) in culture medium consisting of RPMI 1640 medium supplemented with 50 U/mL of penicillin, 50 μg/mL of streptomycin, 2mM glutamine (all from Invitrogen), and 10% FCS (Hyclone). Where indicated, TGF-β1 (PeproTech) was added to a final concentration of 10 ng/mL. Cultures were maintained for 7 days on a confluent layer of MS5 cells transduced with human *Jagged2* (*JAG2*) or empty vector (MSCV-IRES-GFP).[13]

DC stimulation

Immature monocyte-derived DCs (MoDCs) were washed twice in ice-cold RPMI 1640 medium and resuspended in RPMI 1640 medium supplemented with 10% FCS, 50 U/mL of penicillin, 50 μg/mL of streptomycin, and 2mM glutamine at a density of 2×10^6 cell/mL. DCs were either stimulated with recombinant human TNFα (R&D Systems) at a final concentration of 10 ng/mL in flat-bottom, 96-well culture plates or seeded on a confluent layer of MS5 cells transduced with human *JAG2* or empty vector.[13,14]

FACS staining

Three-color immunolabeling was performed as described previously.[15] Briefly, cells were washed twice in ice-cold PBS, resuspended in MACS buffer (0.5% BSA and 2mM EDTA in PBS, pH 7.4) containing the mAb mixture and incubated on ice for 30 minutes. The cells were then washed, resuspended in PBS, and analyzed on a FACScan flow cytometer (BD Biosciences).

Immunoblot analysis

Pieces of frozen tumor samples (approximately 2 mm^3) were homogenized in lysis buffer (20mM Tris, pH 7.5, 150mM NaCl, 1mM EDTA, 1mM EGTA, 1% Triton X-100, and proteinase inhibitors). Lysates were run on polyacrylamide gels, transferred to Protran Nitrocellulose Membranes (Whatman), blocked with Roche Western Blocking Reagent, and hybridized with Abs to activated NOTCH1 (Cleaved Notch1 Val1744 [D3B8] rabbit; Cell Signaling Technology) and Langerin (mab2088; R&D Systems). Blots were rinsed in 0.1% Tween 20/PBS, incubated with HRP-conjugated secondary Ab, and visualized with SuperSignal Femto Chemoluminescent Substrate (Pierce).

Results

LCH cells form a distinct entity among naturally occurring DCs

Investigation of LCH cells poses major challenges because of the paucity of biopsy material and the heterogeneity of lesional composition. Therefore, to obtain the most comprehensive molecular information on these disease-causing DCs, in the present study, we performed purification and subsequent analysis of transcriptional profiles of LCH cells. In addition, we compared the transcriptional profiles of LCH with those from different naturally occurring human DCs to address lineage relationships between LCH cells and indigenous DCs. Biopsies of 8 different LCH patients were analyzed (Table 1): 5 patients had single site bone lesions, 1 had a skin lesion, and 1 had mucosal manifestations. All patients had single system disease, although 1 had multifocal bone lesions, and 1 was classified as single system reactivation of a multisystem disease. CD1a and Langerin immunolabeling identified LCH cells in the biopsy materials, and > 95% pure populations were obtained using FACS (Figure 1A-B). In addition to LCH cells, 3 major DC lineages, LCs, mDC1s, and pDCs, were isolated from skin (for LCs) and peripheral blood (for mDC1s and pDCs) of healthy donors.

Cells were lysed immediately after ex vivo purification without an intercalated culture step. Therefore, RNA reflects most closely

Table 1. Summary of clinical and demographic details of LCH sample donors

Sample no.	Sex	Age, y	Localization	Staging
Gene expression array				
LCH1	F	1	Skull	SS
LCH2	M	11	Rib	SS
LCH3	M	3	Skull	SS
LCH4	M	16	Skull	SS
LCH5	M	2	Skull	Multifocal bone
LCH6	F	0.5	Skin	SS
LCH7	M	4	Pelvis	SS
LCH8	F	14	Mucosa	SS*
Western blot (Figure 2F)				
LCH9	F	7	Bone	MS
LCH10	M	10	Bone	SS
LCH11	M	3	Bone	SS
LCH12	M	16	Bone	SS
LCH13	M	10	Bone	SS
LCH14	ND	ND	Bone	SS
Immunohistochemistry (Figure 2B-E)				
LCH13				
LCH15	F	8	Skull	SS
LCH16	M	6	Bone	SS

*This patient had a multisystem disease as an infant. At time of the biopsy, she had a single system relapse confined to the mucosa. Since then (3 years ago), she has not had another relapse.

ND indicates not determined; SS, single system; and MS, multisystem.

the in vivo gene expression of investigated DCs. We first investigated the lineage relationships between the different DC subsets and the LCH cells. Using the whole dataset obtained with the Affymetrix whole genome expression arrays in an unsupervised approach to define groups of samples, principal component analysis placed LCH samples in an independent cluster apart from LCs and the other DCs (Figure 1C). Even though LCH cells were obtained from different organs and at different stages of the disease, they had a remarkably high degree of homogeneity, indicating that these cells form an entity (Figure 1C and supplemental Figure 1). Surprisingly, LCs and mDC1s were equidistantly positioned from LCH samples (Figure 1C and supplemental Figure 1B). In addition, the Pearson correlation coefficients between LCH:LCs and LCH:mDC1s were virtually identical (0.77 in both comparisons; Figure 1D), which is a further indication that LCH cells differ from LCs and mDC1s to a similar extent. This was demonstrated most directly by the fact that 2419 differentially regulated transcripts separated pDCs from LCH cells, whereas lower and similar numbers of differentially regulated transcripts were observed when comparing LCH cells with LCs and mDC1s (1488 and 1431, respectively; Figure 1G-H). Therefore, no preferential ties of LCH cells with either LCs or mDC1s could be established, leading to the conclusion that LCH cells are equidistantly related to mDC1s and LCs, whereas pDCs displayed a lower degree of similarity in all analyses performed.

This lineage independency compared with normally occurring DCs is further underscored by the unique combination of hallmark lineage antigens: LCH cells share CD1a and Langerin expression with LCs and can be discerned by these discriminative markers from other DCs analyzed (supplemental Figure 2). Conversely, LCH cells express CD14, a marker not found on epidermal LCs and mDC1s, and share BDCsA4 expression with pDCs. In addition, CD163 and ITGAM, 2 markers of myeloid DCs, were expressed in the LCH samples (supplemental Figure 2).[7]

From a transcriptomic view, we conclude that LCH cells form a separate entity distinct from indigenous occurring DCs and, on average, are more closely related to LCs and mDC1s than to pDCs.

Sets of genes defining LCH identity

Based on the observation that LCH cells form a separate entity apart from indigenous DCs, we hypothesized that transcripts involved in LCH pathogenesis are likely to be differentially regulated in LCH cells compared with naturally occurring DCs. We first identified differentially expressed (P value adjusted for multiple testing, $< .05$, fold change, > 2) transcripts between LCH and individual DC subsets (Figure 1D-F). In total, 1488 genes (684 down-regulated and 804 up-regulated) were differentially expressed comparing LCH cells with LCs (Figure 1E), 1431 genes (560 down-regulated and 871 up-regulated) in mDC1s (Figure 1F), and 2419 genes (1035 down-regulated and 1384 up-regulated) in pDCs (Figure 1G). To assess whether these differentially regulated genes in the respective DC lineages contained the same transcripts or whether each comparison resulted in a separate set of genes, we generated Euler diagrams to illustrate the number of regulated genes and the extent to which they overlapped (Figure 1H-I). Figure 1H shows that the majority of up-regulated genes in LCH cells compared with mDC1s are also up-regulated compared with pDCs and to a smaller extent compared with LCs. A total of 203 transcripts were jointly overexpressed in LCH cells compared with all 3 indigenous DC subsets, thus defining the "private" or LCH cell unique transcriptional profile. Among the down-regulated genes, the diversity between the DCs was higher, but 53 genes were down-regulated in LCH cells compared with all other DCs (Figure 2I). To single out common biologic functions of significantly up- and down-regulated genes, we assembled them into functional groups. Regulated genes were assigned molecular functions using databases of gene-function relationships and significantly enriched annotations were then clustered (supplemental Figure 3). These analyses showed that genes involved in the immune response were up-regulated in LCH cells compared with all 3 individual DC subsets. Cell-cycle–related genes were up-regulated in LCH cells compared with mDC1s and pDCs but not LCs. In addition, genes involved in apoptosis formed a prominent LCH-enriched group in all of the comparisons (supplemental Figure 4).

Among the selectively regulated transcripts, we found several signaling molecules and cytokine receptors tightly associated with cellular proliferation (Table 2): LCH cells selectively displayed c-kit ligand. Because the c-kit ligand has been reported to drive expansion of $CD34^+$ hematopoietic progenitor cell Langerhans cell precursors in vitro,[16] this signaling pathway could be an attractive candidate to account for LCH cell expansion. Other molecules associated with cellular proliferation and/or survival were IL7R and FGF2, which has not yet been reported on DCs.[17] Interestingly, *FLT3*, which is tightly associated with the expansion of DC progenitors,[18] was selectively absent in LCH cells (Table 2). A previous study showed that Flt3 is not required for the appearance of LCs in mice,[19] indicating that the development of cells with LC features does not rely on FLT3 signaling.

Among the immunoregulatory factors that were selectively up-regulated in LCH cells, we identified IL22RA2, the decoy receptor for IL22,[20] and ghrelin, which has been shown to repress leptin-induced cytokine release[21] (Table 2). In addition, LCH cells selectively

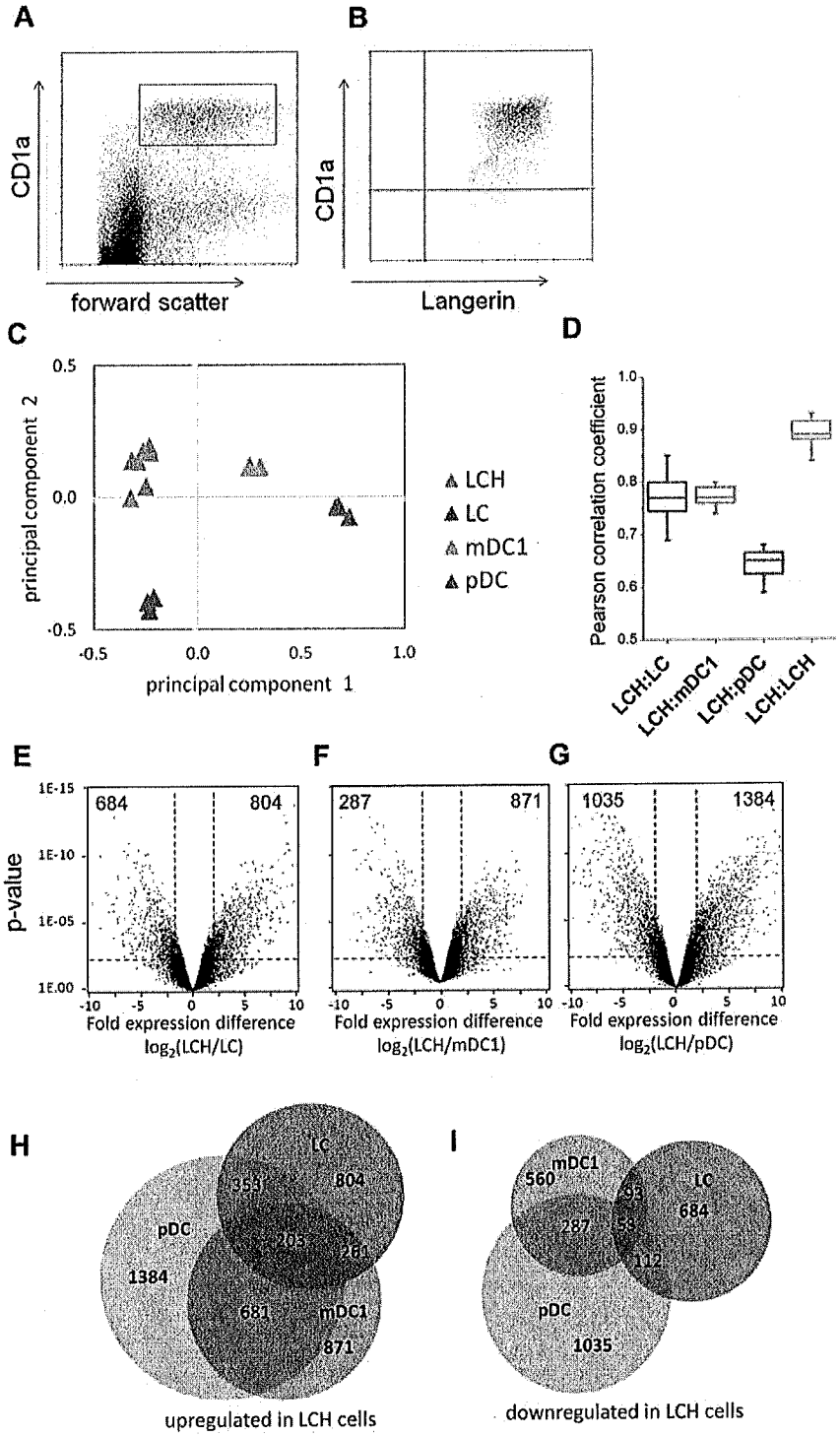

Figure 1. LCH cells form a distinct entity among indigenous human DCs. (A-B) LCH cell purification. Cell suspensions obtained from LCH biopsies carried out at the time of diagnosis contain a high number of LCH cells identified by CD1a expression and forward scatter properties. LCH cells were sorted to > 95% purity and reanalyzed for CD1a and Langerin expression. (C) Principal component analysis of LCH cells and 3 indigenous DC subsets. LCs and mDC1s cells are approximately equidistant from LCH cells, although in different axes (dimensions) of the gene space (ie, different gene sets separate LCH from LCs and mDCs). Each DC subset sample is presented by a triangle. LCs, mDC1s, and pDCs (n = 3 for each subset) were isolated from healthy subjects; LCH cells (n = 8) were isolated as shown in panel A. Because of superimpositions, not all symbols can be optically discerned in the displayed figure. (D) Similarity of LCH cells to indigenous DCs. Mean Pearson correlation coefficients of each replicate of LCs, mDC1s, pDCs, and LCH cells versus each replicate of LCH cells are depicted. Correlation coefficients are the highest among LCH samples, followed by mDC1s and LCs, indicating the highest similarity among LCH samples followed by virtually equal similarity of LCH cells to mDC1s and LCs. Results are shown as box plots displaying the medians and 25th and 75th percentiles as boxes and outliers as whiskers. (E-G) Identification of LCH transcripts selectively regulated compared with individual indigenous DC subsets. Volcano plot analysis (−log10-transformed *P* values from a moderated *t* test statistic vs log2-fold change of all genes) of gene-expression differences between LCH cells and LCs (E), mDC1s (F), and PDCs (G). Fold change and *P* value thresholds are indicated by dashed lines. Transcript highlighted by red circles is JAG2. Numbers in boxed areas indicate the number of transcripts. (H-I) Identification of LCH unique transcriptional profile: Venn diagram (Euler diagram) of significantly regulated (log-fold change > 2, *P* value adjusted for multiple testing < .05) genes comparing LCH with LCs, pDCs, and mDC1s. The relative sizes of circles indicate the relative sizes of gene sets. The overlapping areas of circles indicate the number of genes that are shared by 2 or more DC lineages. Among the regulated genes, 203 were up-regulated and 53 were down-regulated in all 3 DC lineages compared with LCH cells.

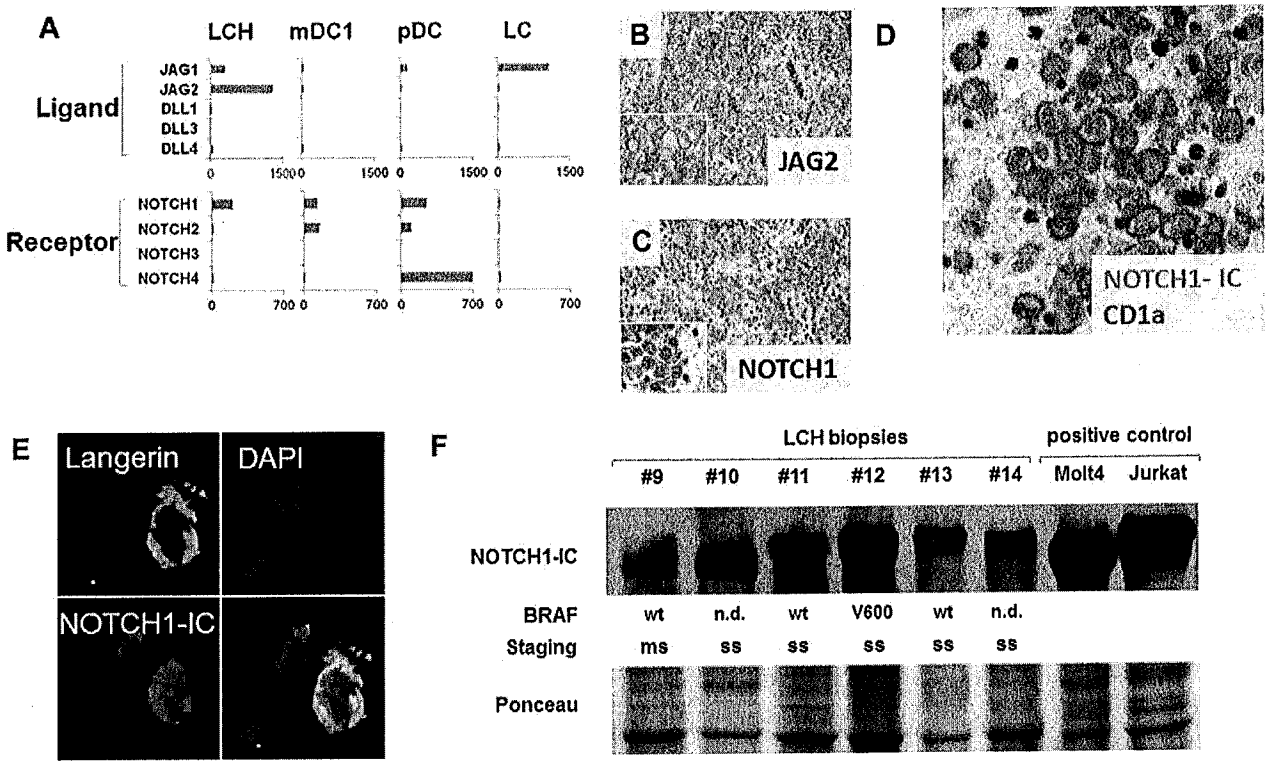

Figure 2. JAG2 and active NOTCH1 are detected in lesional LCH cells in situ. (A) LCH cells are the only DCs that coexpress Notch receptor and ligand. RMA normalized expression values for Notch-receptors and Notch-ligands. (B-D) Immunohistochemical analysis of paraffin-embedded LCH material. Sections were stained with Abs to JAG2 (B), full-length NOTCH1 (C), and activated NOTCH1 (D-E). Corresponding isotype controls are shown in supplemental Figure 5B. LCH samples LCH13 (B-C), LCH15 (D), and LCH16 (E) are shown. Immunofluorescence staining of a frozen LCH section showing staining for Langerin (green), DAPI (blue), and activated NOTCH1 (red). (F) Immunoblot analysis showing activated NOTCH1 in biopsy material from LCH patients. MOLT-4 and Jurkat cell lines were used as positive controls. Ponceau staining was used to ensure comparable loading.

displayed transcripts for matrix-degrading enzymes matrix metalloproteinase 1 (MMP1), MMP9, and MMP12,[22] which have already been described in LCH lesions using immunohistochemistry.[6,23]

Analysis of LCH-specific genes also revealed potential auto- and/or paracrine signaling loops. The TNF family member TRAIL was selectively detected in LCH cells (Table 2 and supplemental Figure 5), whereas high-level expression of functional receptors (TNFRSF10A and B) was shared with other DCs. TRAIL is a potent inducer of cell death via TRAIL receptors, and expression of TRAIL by tumor cells is viewed as a tumor-escape mechanism by eliminating tumor-reactive T cells.[24] LCH cells selectively coexpressed TNRSF10C (Table 2), a nonsignaling decoy receptor for TRAIL, indicating potential protection of LCH cells against TRAIL-induced death stimuli.

LCH cells coexpress *JAG2* and its cognate receptor, *NOTCH1*

Another receptor-ligand pair that was coexpressed by LCH cells was *NOTCH1* and its ligand, *JAG2*.[25] *JAG2* was highly expressed in all LCH samples, whereas all other DCs were devoid of this molecule (Figure 2A and Table 2). LCH cells also expressed *NOTCH1*, and this expression was shared with mDC1s and pDCs. However, LCH cells were the only DCs that coexpressed transcripts for the NOTCH receptor(s) together with one of its cognate ligands (Figure 2A).

Immunohistochemical validation of JAG2 and NOTCH1 was performed on LCH sections. Anti-JAG2 Ab prominently stained the membrane of LCH cells (Figure 2B). Within the lesions, these JAG2$^+$ LCH cells were densely packed, indicating that these aggregates provide a structural basis for JAG2-Notch activation in LCH cells in *trans*.

Staining of LCH biopsies with an Ab against full-length NOTCH1 showed staining in both the plasma membrane region and the nucleus (Figure 2C). Because nuclear translocation of Notch is a hallmark feature of Notch activation,[25] this indicated that NOTCH1 is active in LCH.

NOTCH1 is activated in lesional LCH cells in situ

To further validate whether NOTCH1 was activated in LCH, we stained LCH lesions with an Ab that specifically recognizes activated NOTCH1. Figure 2D shows that staining for activated NOTCH1 can be detected in the majority of CD1a$^+$ LCH cells. In addition, immunofluorescence staining corroborated nuclear distribution for NOTCH1 in LCH cells (Figure 2E). To further confirm this finding, activated NOTCH1 was detected by Western blotting in protein lysates from LCH biopsies (Figure 2F). Ten of 12 patients displayed detectable Langerin reactivity by Western blotting, which was indicative of detectable LCH material in lysates and thus qualified for further analysis. Among these 10 patients, 9 displayed activated NOTCH1 (Figure 2E and supplemental Table 1). Of 7 patients analyzed by immunohistochemistry, 7 displayed detectable nuclear staining of activated NOTCH1. In total, intracellular NOTCH (NOTCH-IC) was detected in 15 of 17 patients with traceable LCH cells. No active NOTCH1 could be detected in the Langerin$^-$ samples or a biopsy taken from a Wilms tumor (supplemental Table 1 and data not shown), suggesting that activated NOTCH1 is specifically found in LCH cells, most likely because of stimulation by JAG2. Consistent with this finding, 3 patients with a different histiocyte disorder, juvenile xanthogranuloma, tested negative for *NOTCH1* expression (supplemental Figure 5C) and therefore activated NOTCH1 (data not shown).

Table 2. Transcripts selectively regulated in LCH cells

	LCH:LC	LCH:mDC	LCH:pDC	↑/↓
Matrix-degrading and tissue-remodeling enzymes				
MMP1				
FC	25	55	67	↑
P	6×10^{-8}	2×10^{-9}	1×10^{-9}	
MMP9				
FC	4	1541	2352	↑
P	3×10^{-5}	6×10^{-16}	2×10^{-16}	
MMP12				
FC	16	3300	4067	↑
P	5×10^{-6}	1×10^{-12}	9×10^{-13}	
ADAMDEC1				
FC	28	29	29	↑
P	4×10^{-3}	4×10^{-3}	4×10^{-3}	
Signaling molecules				
JAG2				
FC	33	28	50	↑
P	4×10^{-7}	8×10^{-7}	1×10^{-9}	
TNFSF10				
FC	45	7	64	↑
P	1×10^{-11}	3×10^{-7}	2×10^{-12}	
FGF2				
FC	11	11	12	↑
P	1×10^{-3}	1×10^{-3}	1×10^{-3}	
KITLG				
FC	9	9	9	↑
P	1×10^{-3}	1×10^{-3}	1×10^{-3}	
GHRL				
FC	12	5	8	↑
P	1×10^{-7}	5×10^{-5}	1×10^{-6}	
SEMA3C				
FC	−47	−36	−76	↓
P	2×10^{-9}	7×10^{-9}	4×10^{-10}	
PDGF C				
FC	−19	−5	−7	↓
P	7×10^{-8}	8×10^{-5}	2×10^{-5}	
Cytokine receptors				
IL7R				
FC	47	148	247	↑
P	1×10^{-5}	3×10^{-7}	9×10^{-8}	
IL22RA2				
FC	10	293	295	↑
P	7×10^{-7}	1×10^{-12}	1×10^{-12}	
TNFRSF9				
FC	16	42	72	↑
P	1×10^{-6}	2×10^{-8}	3×10^{-9}	
TNFRSF10C				
FC	13	11	14	↑
P	4×10^{-6}	1×10^{-5}	4×10^{-6}	
FLT3				
FC	−87	−406	−341	↓
P	4×10^{-12}	4×10^{-14}	6×10^{-14}	
INSR				
FC	−5	−134	−93	↓
P	1×10^{-3}	5×10^{-10}	1×10^{-9}	

Transcripts that were up- or down-regulated (fold change [FC] > 2, adjusted $P < .05$) in LCH cells compared with all 3 indigenous DC lineages as delineated in the Venn diagrams in Figure 1 were clustered into functional groups related to LCH disease. Genes involved in matrix remodeling and signaling are shown. Arrows indicate whether transcripts were up-regulated (↑) or down-regulated (↓) in LCH cells compared with all other DC lineages. FC and *P* values (by Student *t* test) are also indicated.

JAG2 cooperates with TGF-β1 in the differentiation of LCH like cells

Although Notch signaling has been implicated in DC differentiation,[26] no specific evidence for the role of JAG2 in this process exists to date. In the present study, we investigated whether JAG2 might contribute to the development of LCH-like cells. We incubated peripheral blood monocytes with *JAG2*-expressing MS5 cells and the DC-promoting cytokine GM-CSF and assayed for induction of LCH-defining markers. JAG2 readily induced CD1a expression on MoDCs (Figure 3A). CD1a induction by JAG2 depended on GM-CSF (data not shown), but did not require IL-4 or TGF-β1 (Figure 3A). We then investigated whether the addition

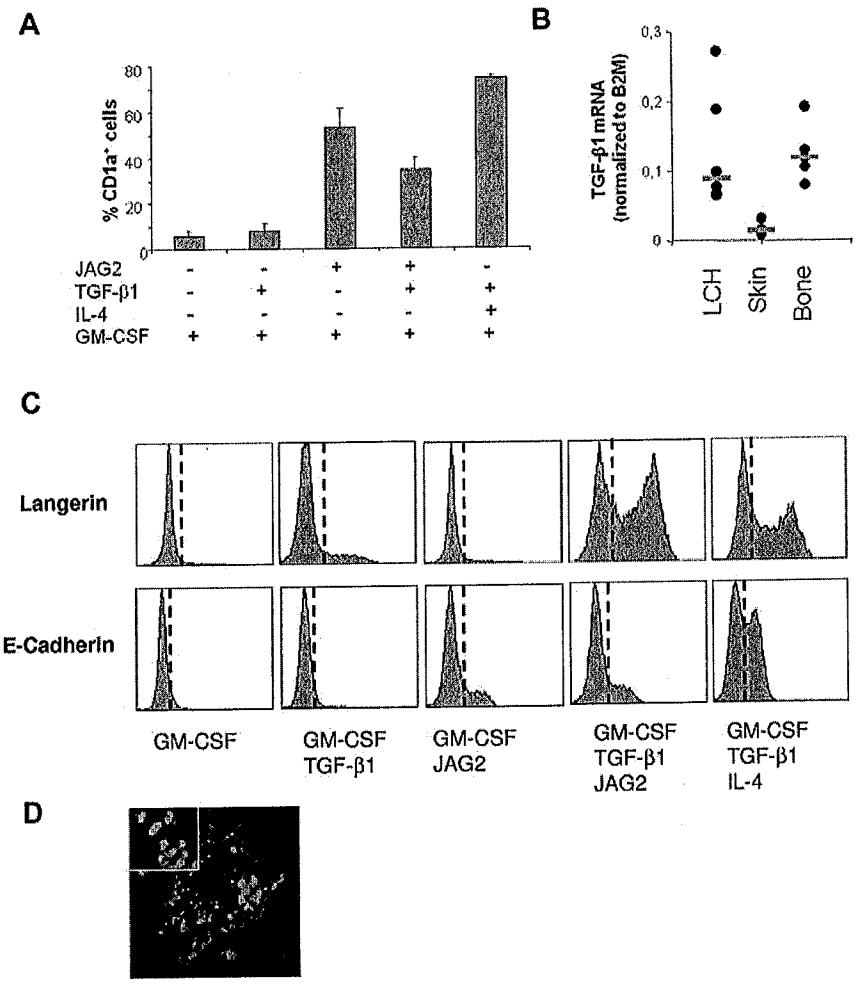

Figure 3. JAG2 induces an LCH-like phenotype in vitro. Monocytes were cultured with the indicated cytokines in the presence of JAG2 or control transfected CD45$^-$ MS5 feeder cells for 5 days. Cells were collected and stained for CD45 to allow separation of monocyte-derived cells from feeder cells, along with Abs against the LCH-associated markers CD1a and Langerin. (A) Induction of CD1a shown as the percentage of CD1a$^+$ cells among the CD45$^+$ population. (B) Detection of TGF-β1 mRNA in frozen biopsy material taken from LCH lesions and from healthy human skin and bone. TGF-β1 expression is normalized to B2M. (C) CD1a$^+$ cells were further analyzed for the coexpression of Langerin and E-cadherin. Histogram plots show Langerin and E-cadherin expression of CD1a$^+$CD45$^+$ cells shown in panel A. (C) DCs generated in the presence of GM-CSF, TGFβ1, and JAG2. Langerin staining (red) reveals the presence of numerous rod-shaped Langerin$^+$ organelles in the cytoplasm indicative of the presence of Birbeck granules. Cell borders were determined by phase contrast (cyan).

of the LC-promoting factor TGF-β1 could induce a more complete LCH-like phenotype. TGF-β1 promoted Langerin and E-cadherin expression in GM-CSF- and IL-4–containing conditions, but failed to do so when IL-4 was omitted (Figure 3C). In contrast, substitution of IL-4 by JAG2 permitted high-level induction of Langerin, but not E-cadherin, by TGF-β1 (Figure 3C). This is remarkable because LCH cells display no or only very low levels of E-cadherin transcripts,[1,6,27] whereas E-cadherin is highly expressed on LCs.[28] We conclude that JAG2 cooperates with TGF-β1 in the formation of CD1a$^+$Langerin$^+$ E-cadherin$^-$ DCs that are strikingly similar to LCH cells. Furthermore, JAG2 renders DC generation from human monocytes independently of IL-4 stimulation.

Because the observed LCH-like phenotype was dependent on JAG2 and TGF-β1, we next investigated whether LCH lesions contained TGF-β1 in addition to JAG2 (Figure 3B) and sought to compare LCH lesions with regard to TGF-β1 message with normal human tissues. As shown in Figure 3B, LCH lesions contained TGF-β1 message at higher levels than normal human dermis and at levels comparable to those seen in normal human bone. Because bone is a predilection site for LCH, it is tempting to speculate that elevated levels of TGF-β1 in the bone may contribute to LCH formation in that location. Our data indicate that 2 key ligands that can promote LCH-cell–like differentiation in vitro, JAG2 and TGF-β1, are found in LCH lesions in situ and cooperate in vitro to differentiate LCH-like cells in an IL-4–independent fashion.

JAG2 stimulates MMP production by DCs but not monocytes

Tissue destruction is frequently observed in LCH lesions. This process may be explained by the production of tissue-degrading enzymes, particularly MMPs that are expressed in LCH lesions.[6,23] Therefore, we investigated whether JAG2 might also be implicated in the pathogenesis of LCH lesions by MMP induction. MoDCs were stimulated with JAG2 and with TNFα, which is a known strong inducer of MMPs as a control.[29] Strikingly, JAG2 induced 2 of the 3 MMPs that were selectively expressed in LCH cells, MMP1 and MMP12. MMP1 in particular was massively up-regulated by JAG2, but MMP12 also showed a low, but consistent elevation (Figure 4A). In contrast, ADAMDEC1, another member of the family of metalloproteinases up-regulated in LCH (Table 2), was not regulated by JAG2 (Figure 4).

We also investigated whether MMP induction by JAG2 was specific for DC differentiation. MMP1 was only induced in differentiated DCs, not in their progenitor cells (ie, monocytes), indicating that MMP1 induction by JAG2 is a distinct feature of DCs (Figure 4B). We conclude that MMP expression in LCH is likely to occur by JAG2-mediated Notch stimulation on LCH cells.

Discussion

In the present study, we compared the transcriptional profiles of LCH cells with those of 3 indigenous types of DCs, LCs, pDCs,

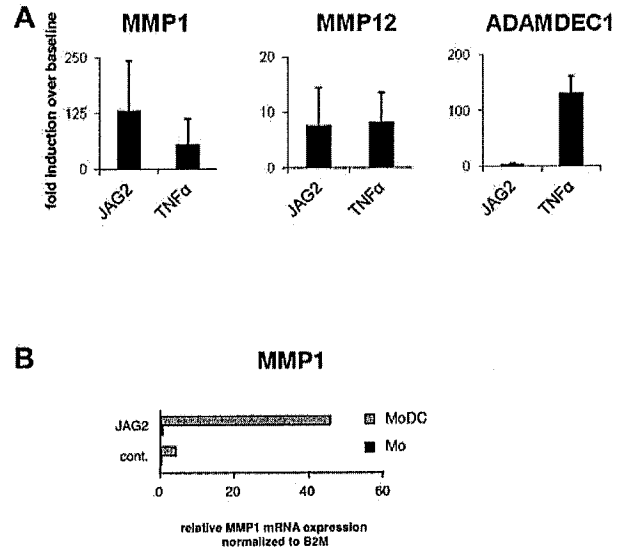

Figure 4. JAG2 induces MMP expression in MoDCs. (A) GM-CSF– and IL-4–generated MoDCs were cocultured with JAG2 or control transfected MS5 feeder cells for 15 hours. As a benchmark for protease induction, TNFα was added instead of JAG2 or control feeder cells. Cells were harvested and analyzed for induction of MMP1, MMP12, and ADAMDEC1. Transcripts were normalized to β_2-microglobulin and induction over control transfected feeder cells is shown. Feeder cells alone did not show significant induction of transcripts. Error bars show the SD. The results of 1 of 6 independent experiments with 3 different donors are shown. (B) Induction of MMP1 expression in monocytes and MoDCs. Cells were plated onto feeder cells expressing JAG2 or control cells and harvested after 14 hours. MMP1 RNA induction was normalized to β_2-microglobulin and relative expression values are shown. The results of 1 of 3 independent experiments with 5 different donors are shown.

and mDC1s, constituting a representative cross-section of naturally occurring DC lineages in humans: pDCs are key to fighting viral infections[30] and myeloid DCs constitute a heterogeneous entity that comprises dermal DCs and peripheral blood–derived mDC1s and mDC2s.[30] Myeloid DCs can adapt to disease conditions and display phenotypes and functions not observed in healthy subjects.[31] LCs are regarded as a unique DC subset that forms dense networks in the skin or mucosal epithelium.[32] This approach enabled us to investigate: (1) whether homogeneity exists among LCH cells of different patients, and (2) the relationship of LCH cells to naturally occurring DC subsets. Principal component analysis showed that LCH samples were surprisingly homogeneous and formed a separate cluster apart from indigenous DC subsets, a result further corroborated by multidimensional scaling and unsupervised hierarchical clustering (supplemental Figure 1). This is intriguing because LCH samples were derived from different body sites and disease stages, which suggests a common LCH-wide differentiation program. To further investigate relationships among naturally occurring DCs and LCH cells, 2 independent statistical methods were used. The numbers of differentially regulated transcripts among LCH cells and indigenous DCs were calculated (Figure 1H-I), and mean Pearson correlation coefficients (r) were examined (Figure 1D).

Both statistical methods revealed that LCH samples differed from LCs and that mDC1s differed to a similar extent with regard to r values and differentially regulated transcripts, whereas pDCs were clearly less closely related to LCH. LCH forms a separate, well-defined entity apart from naturally occurring DCs that is at the transcriptomic level similarly related to mDC1s and LCs.

All DC subsets analyzed were purified ex vivo in an immature state and subjected to chip profiling without any intercalated culture or activation step. LCH cells have also been described as immature DCs in situ.[1,33] This was corroborated by our present results because maturation-associated markers such as B7 family members and HLA-DR–related transcripts were observed in similar numbers as in comparator DCs (supplemental Figure 2). Hallmarks of DC maturation such as CCR7 and CD83 were either absent or expressed at a comparable level as in immature LCs (data not shown). Therefore, transcriptional profiling of LCH cells confirms an immature phenotype and relationships between LCH cells and indigenous DCs obtained in silico are not skewed by different activation and or maturational stages.

The notion that LCH cells form a separate DC entity that displays a similar relationship to mDC1s and LCs has several implications. As the name implies, LCH cells are currently considered to be aberrant LCs.[1] Therefore, LCH is categorized by the World Health Organization (WHO) classification as a hematologic disease derived from LCs based on the expression of the key LC discriminating markers CD1a and Langerin.[34] The finding that LCH transcriptional profiles are equidistant to LCs and mDC1s challenges this dogma, which is consistent with observations made by other investigators.[6,32] Therefore, LCH cells should be viewed as a DC entity distinct from LCs. Whether LCH cells represent a separate lineage originating from an as-yet-unidentified precursor or if they are derived from differentiated DCs such as LCs or mDCs that adopted the LCH-specific phenotype during pathogenesis remains to be investigated.

Given the fact that LCH cells form a well-defined entity, we next identified LCH transcripts that displayed significant regulation compared with any other DC subset. A total of 203 transcripts were selectively up-regulated in LCH cells, among them JAG2, a member of the Notch-signaling pathway. Because dysregulation of Notch signaling is associated with several human diseases,[25] we explored the impact of this pathway on LCH. We showed that LCH cells selectively expressed the Notch ligand *JAG2* and coexpressed the *NOTCH1* receptor. Although our LCH study cohort primarily consisted of patients with early-stage, single system disease manifestations, a previous study that included multisystem LCH also revealed up-regulation of *JAG2* in those patient samples.[6]

We verified expression of *JAG2* and *NOTCH1* in LCH cells by immunohistochemistry and explored activation of Notch signaling in LCH with a 2-tailed approach: First, activated NOTCH1 was detected in LCH cells and nuclear translocation was demonstrated. Second, activated NOTCH1 was detected in lysates derived from LCH biopsies, further corroborating activity of this signaling cascade in LCH lesions. Overall, 15 of 17 patients analyzed displayed activated NOTCH1. Failure to detect NOTCH-IC in 2 patients may indicate insufficient sensitivity of either the detection methods used or the pathways active in a subset of LCH patients who may compensate for NOTCH signaling. Both NOTCH-IC$^-$ patients were contained in the single-system LCH pool (11 patients), whereas 6 of 6 multisystem patients displayed NOTCH activation (supplemental Table 1). *BRAF* status was successfully determined in 7 patients and the V600EE mutation was identified in 2 patients. However, all patients with known *BRAF* status displayed activated NOTCH, indicating that mutated *BRAF* in principle does not impede NOTCH1 activation in LCH (supplemental Table 1). Larger cohort sizes will be required to correlate NOTCH activity with LCH subsets.

Only transcripts for *NOTCH1*, not for any other Notch receptors, were detected in LCH cells, leading to the conclusion that biologic effects of JAG2 are conferred via *NOTCH1*. Notch signaling regulates a variety of developmental processes, and the Notch ligands JAG1 and Delta-like ligand (DLL) have been shown to affect DC function and phenotype.[35-38] However, a distinct

functionality of Notch ligands has been suggested and the role of JAG2 has not yet been explored in DC ontogeny. Therefore, we investigated whether JAG2 might modulate DC differentiation from monocytes. Surprisingly, high numbers of CD1a$^+$ DCs were readily obtained on culture of monocytes in GM-CSF and JAG2, a process usually requiring IL-4[39] and not previously described in the literature. Further addition of TGF-β1 induced high levels of Langerin on MoDCs. Therefore, JAG2 efficiently promotes the expression of LCH hallmark antigens and renders DC development independently of IL-4 in vitro. JAG2 suppressed TGF-β1–driven E-cadherin induction on MoDCs. Synergism between TGF-β1 and a different Notch ligand, DLL1, in the induction of CD1a and Langerin has been reported previously, and DLL1 has been shown to induce sizable quantities of this molecule,[35] whereas our present data suggest a suppressive effect of JAG2 on E-cadherin expression. This discrepancy that may be reconciled by the notion that individual Notch ligands elicit divergent biologic effects.[40] CD1a$^+$Langerin$^+$E-cadherin$^-$ DCs induced by JAG2 display striking similarity to LCH cells, which, in sharp contrast to LCs, express E-cadherin at low levels or not at all.[1,27,41] Therefore, it can be speculated that the LCH phenotype may be at least in part due to JAG2-mediated NOTCH1 activation on LCH cells. Although these data were generated by in vitro differentiation of monocytes, this hypothesis is further corroborated by the observation that LCH cells coexpress Notch receptor and ligands. Activation of NOTCH1 signaling could therefore be a LCH cell–autonomous process, which consequently could confer some degree of independence from signals from the surrounding tissue on LCH cells and thus enable them to reside in such diverse locations as skin and bone. To ultimately test this hypothesis, inhibition of Notch signaling in LCH-derived pathologic cells would be required, which is currently not possible because of the lack of a suitable culture system or animal model.

The concept of a cell-autonomous interplay of Notch receptor and ligands has been recently elaborated in granulocyte regulation,[42] but has not yet been investigated in DC biology. However, JAG2 derived from mesenchymal stem cells was shown to be critically important in conferring regulatory functions onto DCs[43] and regulatory T cells were induced by forced expression of Jag1 in murine DCs.[44] This is particularly interesting because regulatory T-cell expansion has been observed in LCH patients,[45] and it is conceivable that JAG2 activation of LCH cells may contribute to this phenomenon. However, the role of Notch in DC biology is not limited to the induction of tolerance: IL-12 independent Th_1 differentiation has been reported by Dll4,[46] and in humans JAG1 was shown to induce DC maturation rather than an arrest at an immature state, as was suggested in the mouse.[38] It therefore appears that Notch plays a vital role in DC biology and that the individual contributions of each Notch ligand in different species still need to be elaborated.

The occurrence of densely packed DCs aggregates is a feature unique to LCH, so it is conceivable that efficient stimulation of the Notch signaling pathway occurs in LCH-DCs in *trans*.[47] We also examined whether JAG2 may have an impact on pathognomonic LCH features. We and others observed induction of tissue-degrading enzymes in LCH[6,48] that may explain the tissue destruction in LCH lesions most prominently recognized in eosinophilic granuloma of the bone. Data presented herein show that JAG2 is a potent inducer of MMP1 in DCs. MMP1 induction by JAG2 appears to be DC selective: monocytes did not induce MMP1 mRNA levels in response to JAG2. Other Notch ligands tested displayed weak induction of MMP1 in MoDCs, further underscoring the pivotal role of JAG2 in this system and suggesting divergent roles of different notch ligands. MMP1 is the only enzyme able to initiate breakdown of the major collagens of skin, bone, and vasculature, and is also involved in migratory and invasive processes.[22] It is therefore conceivable that JAG2-mediated MMP1 is a crucial factor in LCH-mediated tissue destruction.

Currently, treatment of multisystem LCH consists of combination chemotherapy, and the most promising approach for high-risk patients who fail to respond to standard initial treatment is hematopoietic stem cell transplantation after reduced-intensity conditioning.[49] However, among multisystem patients with risk of organ involvement, mortality is still approximately 20%.[49] These patients would clearly profit from targeted therapies. The finding that NOTCH1 is active in LCH lesions and that JAG2 signaling induces an LCH-like phenotype in Mo-DCs tempts speculation that interference with the Notch signaling pathway might provide a new therapeutic approach to the treatment of LCH. Interestingly, the involvement of the Notch signaling in LCH has been discussed before based on the detection of an activating *NOTCH1* mutation in one LCH patient with a previous T-ALL,[50] underscoring a potential role of this pathway in LCH.

In conclusion, the results of the present study show that LCH cells form a distinct DC entity that differs from LCs and mDC1s to a similar extent. Furthermore, we have identified the Notch signaling pathway as being a potentially important factor in LCH pathogenesis. We have also demonstrated that Notch is constitutively active in LCH cells in vivo and provided evidence that the Notch signaling pathway can contribute to LCH cell phenotype and function. We conclude that targeting Notch activity in LCH may be a promising approach to fighting this disease.

Acknowledgments

The authors thank Andreas Heitger for contributing monocytes; Baerbel Reininger, Angela Schumich, and Dieter Printz for help with FACS analysis; Isabella Mosberger and Andrea Ziegler for help with the immunofluorescence and immunohistochemical analyses; Maximilan Zeyda and Thomas Stulnig for help with skin cell preparations; Ingrid M. Rading at the Microarray Resource Center at Lund University for excellent help with the microarray analysis; and Cesar Cobaleda and Herbert Auer for comments on the manuscript.

This work was supported by the Oesterreichische Nationalbank Anniversary Fund (grant 13434 to C.H. and grant 13668 to E.K.). R.S. is the recipient of a DOC-fFORTE fellowship of the Austrian Academy of Science.

Authorship

Contribution: C.H., I.S.-K., G.J., R.S., J.L., W.B., and E.K. performed the experiments; M.K. conducted the bioinformatics analysis; C.H., M.K., I.S.-K., P.S., H.G., G.S., H.K., and E.K. analyzed and interpreted the experiments; M.M., P.B., and N.C. provided reagents; and C.H. and E.K. devised the project, designed the experiments, obtained the funding, and wrote the manuscript.

Conflict-of-interest disclosure: E.K. is an employee of Novartis Institute for Biomedical Research Inc. The remaining authors declare no competing financial interests.

The current affiliation of E.K. is Novartis Institute for Biomedical Research Inc, Wien, Austria.

Correspondence: Ernst Kriehuber, Department of Dermatology, Division of Immunology, Allergy and Infectious Diseases (DIAID), Medical University of Vienna, Vienna, Austria; e-mail: ernst.kriehuber@gmail.com; or Caroline Hutter, St Anna Kinderspital, Kinderspitalgasse 6, 1090 Vienna, Austria; e-mail: caroline.hutter@stanna.at.

References

1. Laman JD, Leenen PJ, Annels NE, Hogendoorn PC, Egeler RM. Langerhans-cell histiocytosis 'insight into DC biology'. *Trends Immunol.* 2003;24(4):190-196.
2. Weitzman S, Egeler RM. Langerhans cell histiocytosis: update for the pediatrician. *Curr Opin Pediatr.* 2008;20(1):23-29.
3. Gadner H, Grois N, Potschger U, et al. Improved outcome in multisystem Langerhans cell histiocytosis is associated with therapy intensification. *Blood.* 2008;111(5):2556-2562.
4. Badalian-Very G, Vergilio JA, Degar BA, Rodriguez-Galindo C, Rollins BJ. Recent advances in the understanding of Langerhans cell histiocytosis. *Br J Haematol.* 2012;156(2):163-172.
5. Badalian-Very G, Vergilio J-A, Degar BA, et al. Recurrent BRAF mutations in Langerhans cell histiocytosis. *Blood.* 2010;116(11):1919-1923.
6. Allen CE, Li L, Peters TL, et al. Cell-specific gene expression in Langerhans cell histiocytosis lesions reveals a distinct profile compared with epidermal Langerhans cells. *J Immunol.* 2010; 184(8):4557-4567.
7. Ziegler-Heitbrock L, Ancuta P, Crowe S, et al. Nomenclature of monocytes and dendritic cells in blood. *Blood.* 2010;116(16):e74-80.
8. Kriehuber E, Breiteneder-Geleff S, Groeger M, et al. Isolation and characterization of dermal lymphatic and blood endothelial cells reveal stable and functionally specialized cell lineages. *J Exp Med.* 2001; 194(6):797-808.
9. Kauer M, Ban J, Kofler R, et al. A molecular function map of Ewing's sarcoma. *PLoS ONE.* 2009; 4(4):e5415.
10. Smyth GK. Linear models and empirical bayes methods for assessing differential expression in microarray experiments. *Stat Appl Genet Mol Biol.* 2004;3:Article3.
11. Kestler HA, Muller A, Kraus JM, et al. VennMaster: area-proportional Euler diagrams for functional GO analysis of microarrays. *BMC Bioinformatics.* 2008;9: 67.
12. Chott A, Haedicke W, Mosberger I, et al. Most CD56+ intestinal lymphomas are CD8+CD5-T-cell lymphomas of monomorphic small to medium size histology. *Am J Pathol.* 1998;153(5):1483-1490.
13. Fernandez L, Rodriguez S, Huang H, et al. Tumor necrosis factor-alpha and endothelial cells modulate Notch signaling in the bone marrow microenvironment during inflammation. *Exp Hematol.* 2008;36(5):545-558.
14. Höflinger S, Kesavan K, Fuxa M, et al. Analysis of Notch1 function by in vitro T cell differentiation of Pax5 mutant lymphoid progenitors. *J Immunol.* 2004;173(6):3935-3944.
15. Kriehuber E, Bauer W, Charbonnier AS, et al. Balance between NF-kappaB and JNK/AP-1 activity controls dendritic cell life and death. *Blood.* 2005; 106(1):175-183.
16. Szabolcs P, Moore MA, Young JW. Expansion of immunostimulatory dendritic cells among the myeloid progeny of human CD34+ bone marrow precursors cultured with c-kit ligand, granulocyte-macrophage colony-stimulating factor, and TNF-alpha. *J Immunol.* 1995;154(11):5851-5861.
17. Turner N, Grose R. Fibroblast growth factor signalling: from development to cancer. *Nat Rev Cancer.* 2010;10(2):116-129.
18. Waskow C, Liu K, Darrasse-Jeze G, et al. The receptor tyrosine kinase *FLT3* is required for dendritic cell development in peripheral lymphoid tissues. *Nat Immunol.* 2008;9(6):676-683.
19. Ginhoux F, Liu K, Helft J, et al. The origin and development of nonlymphoid tissue CD103+ DCs. *J Exp Med.* 2009;206(13):3115-3130.
20. Xie MH, Aggarwal S, Ho WH, et al. Interleukin (IL)-22, a novel human cytokine that signals through the interferon receptor-related proteins CRF2-4 and IL-22R. *J Biol Chem.* 2000;275(40): 31335-31339.
21. Baatar D, Patel K, Taub DD. The effects of ghrelin on inflammation and the immune system. *Mol Cell Endocrinol.* 2011;340(1):44-58.
22. Kessenbrock K, Plaks V, Werb Z. Matrix metalloproteinases: regulators of the tumor microenvironment. *Cell.* 2010;141(1):52-67.
23. Rust R, Kluiver J, Visser L, et al. Gene expression analysis of dendritic/Langerhans cells and Langerhans cell histiocytosis. *J Pathol.* 2006; 209(4):474-483.
24. Gonzalvez F, Ashkenazi A. New insights into apoptosis signaling by Apo2L/TRAIL. *Oncogene.* 2010;29(34):4752-4765.
25. Radtke F, Fasnacht N, Macdonald HR. Notch signaling in the immune system. *Immunity.* 2010; 32(1):14-27.
26. Cheng P, Zhou J, Gabrilovich D. Regulation of dendritic cell differentiation and function by Notch and Wnt pathways. *Immunol Rev.* 2010;234(1): 105-119.
27. Geissmann F, Emile JF, Andry P, et al. Lack of expression of E-cadherin is associated with dissemination of Langerhans' cell histiocytosis and poor outcome. *J Pathol.* 1997;181(3):301-304.
28. Tang A, Amagai M, Granger LG, Stanley JR, Udey MC. Adhesion of epidermal Langerhans cells to keratinocytes mediated by E-cadherin. *Nature.* 1993;361(6407):82-85.
29. Bahar-Shany K, Ravid A, Koren R. Upregulation of MMP-9 production by TNFalpha in keratinocytes and its attenuation by vitamin D. *J Cell Physiol.* 2010;222(3):729-737.
30. Siegal FP, Kadowaki N, Shodell M, et al. The nature of the principal type 1 interferon-producing cells in human blood. *Science.* 1999;284(5421): 1835-1837.
31. Klechevsky E, Liu M, Morita R, et al. Understanding human myeloid dendritic cell subsets for the rational design of novel vaccines. *Hum Immunol.* 2009;70(5):281-288.
32. Merad M, Ginhoux F, Collin M. Origin, homeostasis and function of Langerhans cells and other langerin-expressing dendritic cells. *Nat Rev Immunol.* 2008;8(12):935-947.
33. Geissmann F. Differentiation of Langerhans cells in Langerhans cell histiocytosis. *Blood.* 2001; 97(5):1241-1248.
34. Swerdlow S, Campo E, Harris NL, eds; International Agency for Research on Cancer. *WHO Classification of Tumours of Haematopoietic and Lymphoid Tissue.* Geneva: World Health Organization; 2008.
35. Ohishi K, Varnum-Finney B, Serda RE, Anasetti C, Bernstein ID. The Notch ligand, Delta-1, inhibits the differentiation of monocytes into macrophages but permits their differentiation into dendritic cells. *Blood.* 2001;98(5):1402-1407.
36. Bugeon L, Gardner LM, Rose A, Gentle M, Dallman MJ. Cutting edge: Notch signaling induces a distinct cytokine profile in dendritic cells that supports T cell-mediated regulation and IL-2-dependent IL-17 production. *J Immunol.* 2008; 181(12):8189-8193.
37. Pérez-Cabezas B, Naranjo-Gomez M, Bastos-Amador P, Requena-Fernandez G, Pujol-Borrell R, Borras FE. Ligation of Notch receptors in human conventional and plasmacytoid dendritic cells differentially regulates cytokine and chemokine secretion and modulates Th cell polarization. *J Immunol.* 2011;186(12):7006-7115.
38. Weijzen S, Velders MP, Elmishad AG, et al. The Notch ligand Jagged-1 is able to induce maturation of monocyte-derived human dendritic cells. *J Immunol.* 2002;169(8):4273-4278.
39. Geissmann F, Prost C, Monnet JP, Dy M, Brousse N, Hermine O. Transforming growth factor beta1, in the presence of granulocyte/macrophage colony-stimulating factor and interleukin 4, induces differentiation of human peripheral blood monocytes into dendritic Langerhans cells. *J Exp Med.* 1998; 187(6):961-966.
40. Van de Walle I, De Smet G, Gartner M, et al. Jagged2 acts as a Delta-like Notch ligand during early hematopoietic cell fate decisions. *Blood.* 2011;117(17):4449-4459.
41. Leenen PJ, Egeler RM. Langerhans' cell histiocytosis is caused by dysregulation of the E-cadherin-beta-catenin cascade: a hypothesis. *Immunol Cell Biol.* 1999;77(5):460-467.
42. Radke AL, Reynolds LE, Melo RC, Dvorak AM, Weller PF, Spencer LA. Mature human eosinophils express functional Notch ligands mediating eosinophil autocrine regulation. *Blood.* 2009; 113(13):3092-3101.
43. Zhang B, Liu R, Shi D, et al. Mesenchymal stem cells induce mature dendritic cells into a novel Jagged-2-dependent regulatory dendritic cell population. *Blood.* 2009;113(1):46-57.
44. Cheng P, Nefedova Y, Corzo CA, Gabrilovich DI. Regulation of dendritic-cell differentiation by bone marrow stroma via different Notch ligands. *Blood.* 2007;109(2):507-515.
45. Senechal B, Elain G, Jeziorski E, et al. Expansion of regulatory T cells in patients with Langerhans cell histiocytosis. *PLoS Med.* 2007;4(8):e253.
46. Skokos D, Nussenzweig MC. CD8- DCs induce IL-12-independent Th1 differentiation through Delta 4 Notch-like ligand in response to bacterial LPS. *J Exp Med.* 2007;204(7):1525-1531.
47. Sprinzak D, Lakhanpal A, Lebon L, et al. Cis-interactions between Notch and Delta generate mutually exclusive signalling states. *Nature.* 2010;465(7294):86-90.
48. da Costa CET. Presence of osteoclast-like multinucleated giant cells in the bone and nonostotic lesions of Langerhans cell histiocytosis. *J Exp Med.* 2005;201(5):687-693.
49. Minkov M. Multisystem Langerhans cell histiocytosis in children: current treatment and future directions. *Paediatr Drugs.* 2011;13(2):75-86.
50. Rodig SJ, Payne EG, Degar BA, et al. Aggressive Langerhans cell histiocytosis following T-ALL: clonally related neoplasms with persistent expression of constitutively active NOTCH1. *Am J Hematol.* 2008;83(2):116-121.

Ontogénie de la microglie et des cellules dendritiques hépatiques / modèle pathogénique de l'histiocytose langerhansienne : Elisa Gomez Perdiguero King's college Londres

GLIA

GLIA 61:112–120 (2013)

Development and Homeostasis of "Resident" Myeloid Cells: The Case of the Microglia

ELISA GOMEZ PERDIGUERO,[1,2] CHRISTIAN SCHULZ,[1,2] AND FREDERIC GEISSMANN[1,2]*
[1]*Centre for Molecular and Cellular Biology of Inflammation (CMCBI), King's College London, Great Maze Pond, London, United Kingdom*
[2]*Peter Gorer Department of Immunobiology, King's College London, Great Maze Pond, London, United Kingdom*

KEY WORDS
hematopoiesis; myb; yolk sac; macrophages; fetal liver

ABSTRACT
Microglia, macrophages of the central nervous system, play an important role in brain homeostasis. Their origin has been unclear. Recent fate-mapping experiments have established that microglia mostly originate from *Myb*-independent, FLT3-independent, but *PU.1*-dependent precursors that express the CSF1-receptor at E8.5 of embryonic development. These precursors are presumably located in the yolk sac (YS) at this time before invading the embryo between E9.5 and E10.5 and colonizing the fetal liver. Indeed, the E14.5 fetal liver contains a large population of *Myb*-independent YS-derived myeloid cells. This myeloid lineage is distinct from hematopoietic stem cells (HSCs), which require the transcription factor *Myb* for their development and maintenance. This "yolky" beginning and the independence from conventional HSCs are not unique to microglia. Indeed, several other populations of F4/80-positive macrophages develop also from YS *Myb*-independent precursors, such as Kupffer cells in the liver, Langerhans cells in the epidermis, and macrophages in the spleen, kidney, pancreas, and lung. Importantly, microglia and the other *Myb*-independent macrophages persist, at least in part, in adult mice and likely self-renew within their respective tissues of residence, independently of bone marrow HSCs. This suggests the existence of tissue resident macrophage "stem cells" within tissues such as the brain, and opens a new era for the molecular and cellular understanding of myeloid cells responses during acute and chronic inflammation.

MICROGLIA—RESIDENT MACROPHAGES OF THE CNS

Microglia are macrophages of the central nervous system (CNS) (Lawson et al., 1992; Perry et al., 1985). They account for 5 to 20% of the non-neuronal glial cells. Their estimated total number in adult mice is 3.5 $\times$ 10^6 cells per brain but their density varies in different brain regions (from 22 to 165 cells/mm^2) (Lawson et al., 1990). They are proposed to monitor the functional status of neuronal cells (Wake et al., 2009), tissue metabolism, inflammation (Saijo et al., 2009), and cell death (Nimmerjahn et al., 2005; Wake et al., 2009). Here, we review experimental evidence that indicate that microglia are part of a novel family of *Myb*-independent "resident" macrophages.

HEMATOPOIETIC STEM CELLS

The founders of the adult hematopoietic system are the hematopoietic stem cells (HSCs). The current model proposes that HSCs emerge from the dorsal aortic endothelium in the aorto-gonado-mesonephros (AGM) region, in a *Runx1*-dependant manner (Bertrand et al., 2010; Kissa and Herbomel, 2010). In mouse embryos this process takes place 10.5 days after fecondation (embryonic day 10.5, E10.5) (Boisset et al., 2010). HSCs from the E10.5 AGM are able of long-term repopulation activity when transferred into irradiated recipient adult mice (Medvinsky and Dzierzak, 1996; Muller et al., 1994). HSCs migrate from the AGM to the fetal liver, where they expand and differentiate before definitive hematopoiesis shifts to the spleen and bone marrow (BM) (Cumano and Godin, 2007; Orkin and Zon, 2008). This sequence of events has been directly documented *in vivo*. For example, Murayama et al. used an *in situ* photoactivable cell tracer system to follow the migration of definitive hematopoietic precursors from the zebrafish AGM to the caudal hematopoietic tissue—equivalent of the fetal liver of the mouse—where they differentiated, expanded, and further migrated to the kidney—equivalent of the mammalian bone marrow—and the thymus (Murayama et al., 2006). Several transcription factors are essential in this process, in addition to *Runx1*. For example, *Myb* is detected in the AGM at sites of HSC emergence (Labastie et al., 1998; Vandenbunder et al., 1989). *Myb* is also expressed on HSCs in chicken, mice, and humans (Ivanova et al., 2002). *Myb*-deficient AGM and fetal liver do not present HSCs activity (Kasper et al., 2002) and *Myb*-deficient mice lack HSC-derived erythrocytes and die with anemia between E15 and E17 (Mucenski et al., 1991; Mukouyama et al., 1999; Schulz et al., 2012; Sumner et al., 2000).

In adult mice, granulocytes, blood monocytes, classical dendritic cells (cDC), and plasmatocytoid dendritic cells

Elisa Gomez Perdiguero and Christian Schulz contributed equally to this work.

Grant sponsor: German National Academy of Sciences Leopoldina; Grant number: LPDS 2009-31 (to C.S.); Arthritis Research UK Chair of Inflammation Biology, at KCL (to F.G.); Medical Research Council (MRC), UK; Grant number: G0900867; European Research Council; Grant number: ERC-2010-StG-261299 MPS2010 (to F.G.).

*Correspondence to: Frederic Geissmann, KCL, CMCBI, New Hunt's House, First Floor, Great Maze Pond, London SE1 1UL, UK.
E-mail: frederic.geissmann@kcl.ac.uk

Received 4 May 2012; Accepted 26 June 2012

DOI 10.1002/glia.22393

Published online 28 July 2012 in Wiley Online Library (wileyonlinelibrary.com).

(pDC), as well as a number of tissue macrophages are short-lived and continuously replaced from HSCs-derived precursors (Auffray et al., 2009; Fogg et al., 2006; Liu et al., 2007, 2009; Naik et al., 2007; Onai et al., 2007). Bone marrow transplantation and adoptive transfer of precursors indeed result in a high level of chimerism for these cells (Auffray et al., 2009; Fogg et al., 2006; Liu et al., 2009; Onai et al., 2007) (reviewed in (Geissmann et al., 2010)). A monocyte/macrophage and DC precursor (MDP) gives rise to monocytes and to the common DC precursor (CDP). The CDP gives rise to pDCs and cDCs of the lymphoid organs and peripheral tissues via pre-cDCs, which circulate in the blood and seed tissues. The Ly6C+ subset of blood monocytes can give rise to inflammatory macrophages, i.e. macrophages that acutely infiltrate inflamed tissues such as the brain (King et al., 2009; Mildner et al., 2009) and monocyte-derived DCs (Geissmann et al., 2003, 2010). Monocytes or their precursor can also give rise to DCs and macrophages in the intestinal lamina propria (Varol et al., 2009) and the intima of arteries (Choi et al., 2011). The Ly6C− subset of monocytes and their human putative counterparts seem to have a surveillance role in the circulation (Auffray et al., 2007; Cros et al., 2010). They are absent from mice deficient in the orphan nuclear receptor NR4A1/Nur77 (*Nr4a1*$^{-/-}$), while Ly6C+ monocytes are still present (Hanna et al., 2011). The putative bone marrow precursors of the Ly6C− monocytes that remain in the BM of *Nr4a1*$^{-/-}$ mice are arrested in S phase of the cell cycle and undergo apoptosis. Thus, NR4A1 may function as a master regulator of the differentiation of these "patrolling" Ly6C− monocytes from their BM proliferating precursor (Hanna et al., 2011).

"PRIMITIVE" MACROPHAGES

On the other hand, several lines of observation suggest that AGM-derived hematopoietic stem cells may not be universal lineage founders responsible for all tissue macrophages and dendritic cells.

First, yolk sac macrophages were shown to enter the embryo before E10.5 and the onset of HSCs (Fig. 1). From E8, macrophages and erythrocytes of zygotic origin develop outside the embryo in the YS blood islands (Bertrand et al., 2005). These macrophages express F4/80, CX3CR1, and CSF1R (Bertrand et al., 2005; Rae et al., 2007; Sasmono et al., 2003). They appear to colonize the whole embryo between E9.5 and E10.5 (Fig. 1), and were first described in the brain of mouse embryos as early as day E9.5 (Alliot et al., 1999; Fantin et al., 2011), and in rat (Ashwell 1991; Sorokin et al., 1992) and avian (Cuadros et al., 1993) embryos at comparable stages of embryonic development (E11 and HH15, respectively). Of note, Herbomel et al. also described a specific lineage of early macrophages in zebrafish that differentiate in the YS and which migrate along epithelial structures to invade the brain and epidermis (Herbomel et al., 2001). The growth factor and chemotactic factor receptor CSF1R (MCSF-receptor) seems essential to this process, because in the zebrafish *panther* mutant, which lacks a functional *csf1r* gene, macrophages differentiate normally in the YS, but fail to invade embryonic tissues (Herbomel et al., 2001).

Secondly microglia, Kupffer cells, and epidermal Langerhans cells, are "radioresistant" and can remain of host origin for extended periods of time after syngeneic bone marrow transplantation (Ajami et al., 2007; Katz et al., 1979; Merad et al., 2002; Mildner et al., 2007; Perreault et al., 1984), suggesting that they are either long lived, or can renew independently of bone marrow HSCs. Microglia can be replaced up to a chimerism of 10 to 20% following irradiation and transplantation (de Groot et al., 1992; Hickey and Kimura, 1988; Hickey et al., 1992; Krall et al., 1994; Lassmann et al., 1993; Massengale et al., 2005). However, in other studies, including in parabiotic mice where the vascular system of two animals is surgically joined, circulating myeloid cells do not replace brain microglia, even in the setting of brain inflammation (Ajami et al., 2011; Ginhoux et al., 2010; Matsumoto and Fujiwara, 1987). Similar observations were made in other tissues, in particular for epidermal Langerhans cells (Merad et al., 2002). Nevertheless, bone marrow-derived cells can enter the CNS, or the epidermis, in some experimental models, mostly associated with gamma or UV irradiation (Barcellos-Hoff et al., 2005; Ginhoux et al., 2006; Mildner et al., 2007). Infiltrating monocytes can disappear after disease resolution (Ajami et al., 2011; Mildner et al., 2007), and do not contribute to the long-term parenchymal microglia pool (Ajami et al., 2011). BM-derived cells could represent perivascular microglia, as opposed to resident parenchymal microglia (Hickey and Kimura, 1988).

Thirdly, renewal of some tissue macrophages may not require bone marrow-derived precursors, because they can proliferate locally. Microglia, epidermal LCs, and macrophages in the liver, peritoneum, and pleura can proliferate during inflammation and may self renew independently from BM-derived precursors in steady state (Bouwens et al., 1986; Chorro et al., 2009; Davies et al., 2011; Jenkins et al., 2011; Klein et al., 2007; Lawson et al., 1992; Shankaran et al., 2007; Thored et al., 2009). In the case of Langerhans cells, CX3CR1+ precursors are recruited from the dermis into the stratified epidermis at the time of its differentiation at E16.5, and later massively proliferate *in situ* and differentiate into adult-type LCs during the first week of postnatal life (Chorro et al., 2009). In adult mice, LC proliferation is detectable in steady-state and the proliferation rate increases in response to inflammatory stimuli (Chorro et al., 2009; Gschnait and Brenner, 1979; Miyauchi and Hashimoto, 1987).

Lastly, in human patients, recent reports have described germ-line mutations in the *GATA2* (Hsu et al., 2011) and *IRF8* (Hambleton et al., 2011) genes, two transcription factors that control hematopoietic precursor cells. Patients with *GATA2* or *IRF8* mutations show severe defects in BM-derived monocytes and DCs, but many tissue macrophages such as epidermal LC were unaffected (Bigley et al., 2011; Hambleton et al., 2011).

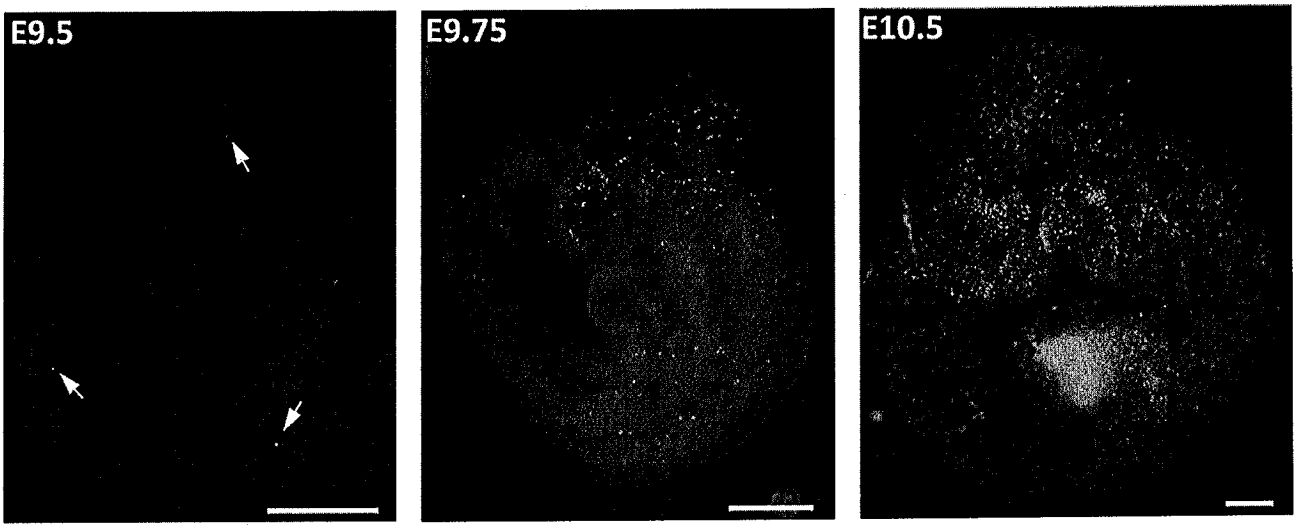

Fig. 1. CX3CR1+ macrophages invade the mouse embryo before E10.5. Epifluorescence images of *Cx3cr1*$^{gfp/+}$ macrophages in E9.5 (left panel), E9.75 (middle panel), and E10.5 (right panel) whole embryos. Arrows points to gfp+ macrophages. Bar is 500 μm (adapted from Schulz et al., 2012).

Following limb transplantation in human, epidermal Langerhans cells were also shown to remain of donor (limb) origin 4.5 years after graft (Kanitakis et al., 2004). Interestingly, in ~ 50% of pediatric patients with Langerhans cell histiocytosis—an inflammatory granulomatous disease that can affect the skin, brain, liver, and bone—somatic mutations of the *B-RAF* gene are detected in lesional macrophages, but were not detected in the germ-line and blood leucocytes (Badalian-Very et al., 2010; Satoh et al., 2012).

DEVELOPMENTAL ORIGINS SPECIFY FUNCTIONAL SUBSETS

Although little direct experimental evidence was available until recently, it was therefore conceivable that subsets of macrophages and DCs may have distinct developmental origins (Fig. 2A) (Geissmann et al., 2010). In theory, different developmental origins and molecular mechanisms could be involved in parallel for the maintenance of distinct subsets, or they could happen sequentially in time for a given subset, upon ageing or depending on inflammation (Fig. 2A). Of note, the capacity for a macrophage to be "radioresistant," long-lived, and to proliferate locally and self-renew does not rule out an HSC developmental origin. Therefore, in order to determine the developmental origin of macrophages and DC subsets, it was necessary to distinguish genetically the primitive macrophages from the HSCs, to identify their molecular signature, and to fate-map their progeny.

There is a biological and medical relevance to this question since "resident" macrophages/DC, including microglia, and monocyte-derived inflammatory cells most likely have diverse functions in acute inflammation and tissue homeostasis. Many proposed therapies aim at preventing the recruitment of inflammatory cells, e.g. by blocking chemokine gradients that direct immune cell migration (McDonald et al., 2010). Approaches based on a detailed knowledge of the biology of macrophages could increase effectiveness and also limit side effects. In any case, macrophages are not necessarily always causative of inflammation, and may also play useful roles in scavenging dead cells and toxic waste.

Experimental evidence for a lineage of MYB-independent YS-derived macrophages

As discussed above, *Myb* is a critical regulator of hematopoiesis and is required for the development of HSCs derived cells (Mucenski et al., 1991). In adult mice, loss of MYB by conditional deletion also causes failure of hematopoiesis (Lieu and Reddy, 2009; Schulz et al., 2012). On a molecular level MYB interacts with transcription factors such as C/EBPalpha (Oelgeschlager et al., 1996), the ETS family (including Pu.1) (Shapiro, 1995), and GATA1 (Bartunek et al., 2003). Activation of target gene transcription requires the transactivating domain, which recruits the coactivators p300 (Sandberg et al., 2005) and CREB-binding protein (Dai et al., 1996). Myb directly activates Gfi1 and Cited2 (Zhao et al., 2011), genes that are important for HSC maintenance (Kranc et al., 2009).

However, studies in mice and zebrafish suggested that absence of *Myb* might have little effect on yolk sac hematopoiesis (Mucenski et al., 1991; Soza-Ried et al., 2010). Myelomonocytic colony assays are only moderately impaired in *Myb*$^{-/-}$ YS (Sumner et al., 2000) and F4/80+ macrophages are present in normal numbers in the yolk sac at E10.5 (Schulz et al., 2012), suggesting that *Myb* is dispensable for YS myelopoiesis. Indeed, the fetal liver of *Myb*-deficient embryos at E14.5 and E16.5 contain a large population of F4/80+ CD11b+ cells, although KIT+ hematopoietic progenitors are absent

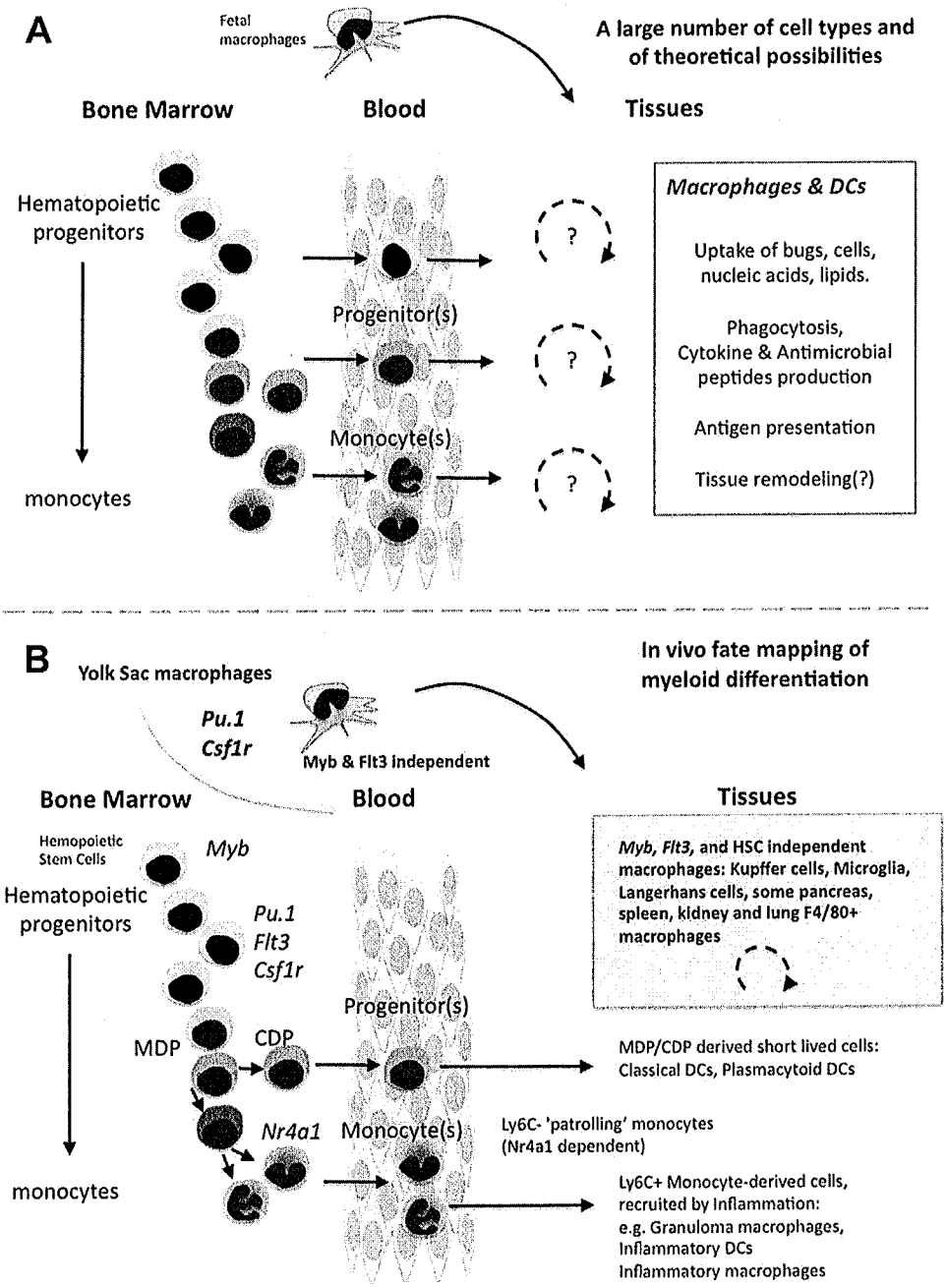

Fig. 2. Biology of phagocytes in steady state, and during inflammation and infection. **A**. Theoretical possibilities (top): monocyte-derived macrophages and dendritic cells differentiate from HSC via short-lived intermediates such as monocytes and common precursors (MDP/CDP). Macrophages/DC may also arise directly from fetal macrophage precursors. Macrophages and DCs subsets could be maintained through local proliferation (and self-renew) or through recruitment of new bone marrow-derived cells. These different mechanisms of macrophages/DCs development and maintenance could operate in parallel for distinct subsets or sequentially for a given subset, depending on local or inflammatory signals and ageing. **B**. Experimental evidence (bottom): CSF1R+ yolk sac progenitors give rise to microglia and F4/80+ macrophages/DC in many tissues (epidermal Langerhans cells, liver Kupffer cells, etc.). These macrophages are *Pu.1*-dependent but *Myb*-independent, and also develop largely independent of Flt3+ multipotent hematopoietic precursors. In contrast, other DC subsets and monocytes derive from HSC via Flt3+ MDP and CDP in a *Myb*-dependent manner. Csf1r, macrophage colony-stimulating factor (M-CSF) receptor; Flt3, fms-like tyrosine kinase receptor-3; BM, bone marrow; DC, dendritic cell; CDP, common DC precursor; HSC, hematopoietic stem cell; MDP, macrophage/DC precursor.

(Schulz et al., 2012). Moreover, brain microglia, as well as the populations of F4/80^{bright} tissue macrophages of the developing skin, liver, pancreas, lung, and spleen develop in normal numbers in *Myb*-deficient embryos (Fig. 3A and (Schulz et al., 2012)).

This is in contrast to the absence of CD11b^{bright} myeloid cells in the blood and all tissues of *Myb*-deficient fetuses. When conditional deletion of the *Myb* gene is induced in adult *Cd45.2*;*Mx1*Cre;*Myb*$^{flox/flox}$ mice, blood monocytes and granulocytes are rapidly depleted, and a

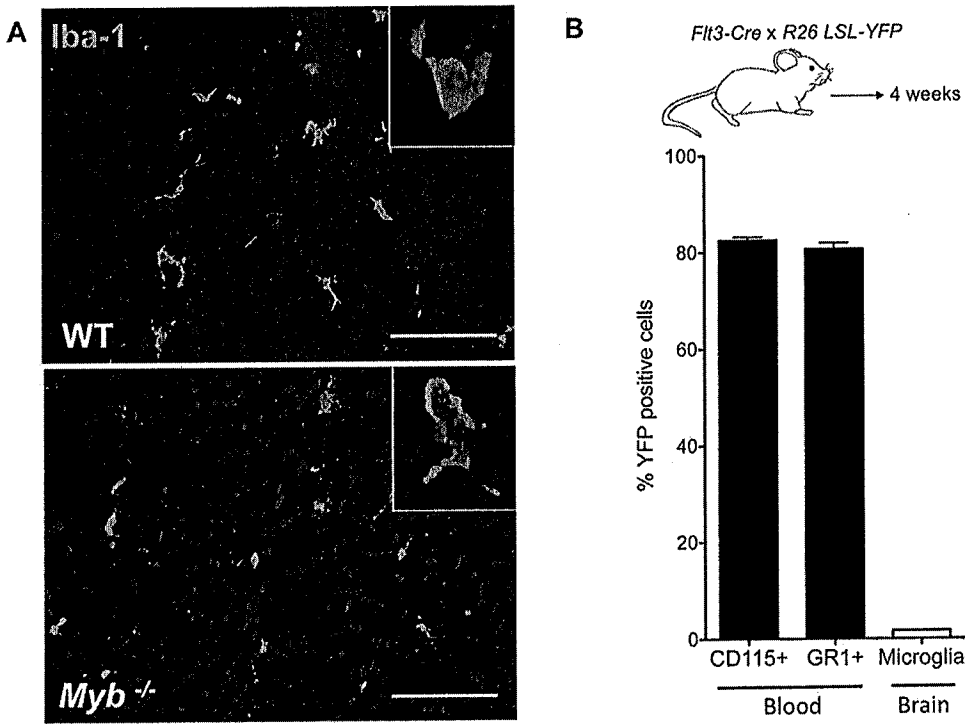

Fig. 3. Microglia are *Myb* and FLT3 independent. **A.** Normal development of microglia in E14.5 $Myb^{-/-}$ mouse embryos. Immunofluorescence imaging of neuroectoderm sections from E14.5 $Myb^{-/-}$ (bottom) and WT (top) embryos stained for Iba-1 (red) and DAPI (blue). Bar is 100 μm (pictures from K. Kierdorf and M. Prinz, Schulz et al., 2012). **B.** Flt3 fate mapping. Fate mapping of FLT3 expression in blood and brain microglia of 4-week-old *Flt3*-Cre x R26LSL-YFP mice. Bars represent percentage of YFP-positive cells (means ± SEM, $n = 3$). Microglia were gated on CD45+ CD11b+. No YFP was detected in Cre– littermates.

syngeneic $Myb^{+/+}$ bone marrow engrafts without irradiation (Schulz et al., 2012). Monocytes and granulocytes, as well as $CD11b^{bright}$ myeloid cells in the spleen, liver, kidney, and pancreas are completely replaced by donor bone marrow-derived cells, whereas microglia, epidermal LC, and Kupffer cells remain of host, *Myb*-deficient, origin 3 months after bone marrow transplantation.

Myb-dependency therefore distinguishes HSCs-derived from YS-derived myeloid cells. HSCs-derived myeloid cells are dependent on *Myb* for their maintenance and renewal in adult tissues, while microglia and others YS-derived "resident" macrophages persist in tissues in the presence of wt HSCs, and in the absence of *Myb*.

Myb-Independent Microglia and Macrophages are PU-1 Dependent

In contrast to *Myb*, the transcription factor *Pu.1* is required for the development of all macrophages (Dakic et al., 2005; McKercher et al., 1996; Nerlov and Graf 1998; Schulz et al., 2012) although it is dispensable for the development of HSC. This is likely due to the fact that PU.1 transactivates the proximal promoter of the *csf1r* gene (Reddy et al., 1994) and *csf1r* expression was not detected in *Pu.1*-deficient embryos (DeKoter et al., 1998) and *Pu.1*-deficient ES cells (Olson et al., 1995). *Csf1r* is also required for the development of all macrophages, including microglia (Erblich et al., 2011) and Langerhans cells (Merad et al., 2002). Lichanska et al. described cells expressing *csf1r* by *in situ* hybridization in *Pu.1*-deficient yolk sac and embryo at E10.5 and suggested that microglia can develop in a *Pu.1*-independent fashion (Lichanska et al., 1999). However, in other studies, consistent with the known roles of *Pu.1*, no F4/80+ macrophages were detected in the YS at E10.5 (Schulz et al., 2012), no $F4/80^{bright}$ or $CD11b^{bright}$ macrophages were detected in tissues at E14.5, and no Iba-1+ or isolectin B4+ microglia cells were detected in brains from *Pu.1*-deficient embryos (McKercher et al., 1996) on a C57Bl6 background (Fantin et al., 2011; Schulz et al., 2012). Therefore it is likely that microglia, like the other macrophages, are *Pu.1* dependent.

Myb-Independent Microglia and Macrophages are Largely FLT3 Independent

FLT3 is a cytokine receptor expressed on multipotent hematopoietic progenitors (Buza-Vidas et al., 2011), MDPs (Auffray et al., 2009), cDC progenitor (Onai et al., 2007), and common lymphoid progenitors in the bone marrow (Buza-Vidas et al., 2011). In a gene expression array analysis of E10.5 YS macrophages, E16.5 $F4/80^{bright}$ macrophages, and E16.5 $CD11b^{bright}$ macrophages, expression of FLT3 was restricted to $CD11b^{bright}$ macrophages. FLT3 thus represents a good candidate for a fate mapping analysis of bone marrow-derived *versus*

YS-derived macrophages in adult mice. In adult F1 *Flt3*-Cre (Benz et al., 2008) and R26LSL-YFP (Srinivas et al., 2001) mice, YFP labeling represents the present or past expression of FLT3 by labeled cells or by their precursor(s). Microglia are not labeled, and YFP expression is overall restricted to blood leucocytes and *Myb*-dependent macrophages (Fig. 3B) (Schulz et al., 2012) indicating that the development of *Myb*-independent macrophages occurs largely independently of $FLT3^+$ precursors.

Myb-Independent Microglia and Macrophages Originate from a CSF1-R Yolk Sac Progenitor

The development of temporally controlled gene expression in mice using Tamoxifen-induced Cre recombinase activation (Feil et al., 1996; Metzger et al., 1995) allows permanent and temporally controlled "pulse-labeling" of cell populations (Imayoshi et al., 2006) and subsequent fate mapping of their progeny. However, fate mapping of YS progenitors has been hampered by the fact that, while genes specific for HSCs and their progeny exists, e.g. *FLT3*, most genes that are expressed by YS hematopoietic cells are also expressed in HSCs, and are in addition frequently required for the development or maintenance of the definitive hematopoiesis, e.g. *Runx1* and *SCL* (reviewed in (Cumano and Godin, 2007). This makes fate-mapping analysis of YS progenitors technically difficult.

A recent fate-mapping study, employing *in utero* OH-Tamoxifen (TAM)-induced activation of Cre in E7.25-7.5 *Runx1-MER-iCre-MER* and R26LSL-YFP embryos resulted in the labeling of the microglia (Ginhoux et al., 2010). However, TAM-induced labeling in E7.25-7.5 *Runx1-MER-iCre-MER* embryos also results in labeling of 10% of HSCs (Samokhvalov et al., 2007). Thus, this model is not ideal to distinguish the progeny from HSCs and from YS-derived macrophages, and kinetics analyses can be difficult to interpret.

However, early expression of *csf1r* in YS precursors allows to pulse label these CSF1R+ progenitors between E8.5 and E9.5 in the YS, and to follow their progeny into adulthood, without labeling the progeny of HSCs. *In utero* administration of TAM into E8.5 *Csfr1*-MER-iCre-MER (Qian et al., 2011) and R26LSL-YFP embryos results in the YFP labeling of adult microglia and other *Myb*- and FLT3-independent macrophages, such as epidermal Langerhans cells and liver Kupffer cells, but *Myb*-dependent HSC-derived cells such as blood leukocytes are not labeled (Schulz et al., 2012). Thus, E8.5 *Myb*-independent precursors give rise to macrophages, such as microglia, that persist in adults.

PERSPECTIVES: A LINEAGE OF *MYB*-INDEPENDENT MACROPHAGES

Macrophages and DCs are present in all tissues and are critical effectors and regulators of immune responses. The data discussed in this review suggest

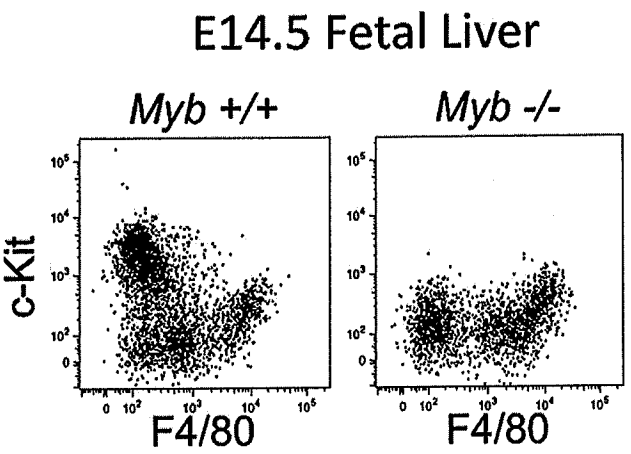

Fig. 4. E.14.5 fetal liver contains a large population of *Myb*-independent myeloid cells. Flow cytometry analysis of E14.5 fetal liver from $Myb^{+/+}$ and $Myb^{-/-}$ littermates, gated on CD45+ cells. Kit+ precursors are absent in $Myb^{-/-}$ fetal liver while F4/80+ cells are present (from Schulz et al., 2012).

that functionally distinct subsets of macrophages, which co-exist in embryo and in adult mice, also differ in their embryonic origin and in the genes and mechanisms that control their homeostasis and expansion. These are on the one hand *Myb*- and *Flt3*-independent macrophages, among them the microglia, and on the other hand *Myb*-dependent HSC-derived macrophages such as blood monocyte-derived cells. Several lines of investigation should arise from this model of myeloid differentiation.

Microglia and others *Myb*-independent macrophages integrate their target tissues at the time of their organization during embryogenesis and form stable networks within these tissues. They are literally interweaved with the ectodermal structures such as neurons and epithelial cells. Their activation by local cues (Chorro et al., 2009) may contribute to the pathogenesis of inflammatory diseases. Thus, it will be essential to investigate tissue molecular cues that may selectively control the renewal, proliferation, and effector functions of *Myb*-independent macrophages.

Although it is also likely that these resident cells can be replaced by bone marrow precursors-derived cells in some pathological circumstances, and maybe also during aging, local self-renewal suggests the existence of macrophage stem cells in the brain and other tissues, at least in young animals. It will thus be important to characterize these putative local "macrophage stem cells" and the cell autonomous molecular and cellular mechanisms that maintain the networks of macrophages and mediate their activation and expansion during inflammation. For example, Langerhans cell histiocytosis is a granulomatous disease that can affect the brain where a somatic mutation has been identified in a macrophage compartment, but is absent—or at least remains undetected—in the blood. It is therefore possible that this type of disease arise from a "resident" macrophage progenitor.

Finally, and in part because these cells could have a therapeutic potential, it will be important to better characterize the early CSF1R+ precursors that give rise to

Myb-independent macrophages in embryos. The E8.5-E9.5 CSF1R+ precursors that we described are likely to be located in the YS, and may correspond to the "C" YS-derived precursors (Bertrand et al., 2001) and to Mac-CFC or HPP-CFC (Palis et al., 1999, 2001). These cells enter the embryo around day 9.5, probably via the vitelline vein, and colonize the fetal liver. The fetal liver contains a large population of *Myb*-independent F4/80+ CD11b+ cells (Fig. 4), possibly *en route* to other tissues as well as precursors for local macrophages. Thereof, it contains a mix of *Myb*-independent and *Myb*-dependent precursors, and it should be useful to re-examine hematopoietic and myeloid precursors present in the fetal liver.

In this regard, it would therefore be naive to oppose macrophages that originate from the fetal liver to macrophages that originate from the YS. A genetic definition of HSC-derived *Myb*-dependent and YS-derived *Myb*-independent macrophages seems preferable to us.

ACKNOWLEDGMENTS

The authors are indebted to K. Kierdorf and M. Prinz, Department of Neuropathology, and BIOSS Centre for Biological Signalling Studies, University of Freiburg, Germany, for microglia immunohistochemistry.

REFERENCES

Ajami B, Bennett JL, Krieger C, McNagny KM, Rossi FM. 2011. Infiltrating monocytes trigger EAE progression, but do not contribute to the resident microglia pool. Nat Neurosci 14:1142–1149.

Ajami B, Bennett JL, Krieger C, Tetzlaff W, Rossi FM. 2007. Local self-renewal can sustain CNS microglia maintenance and function throughout adult life. Nat Neurosci 10:1538–1543.

Alliot F, Godin I, Pessac B. 1999. Microglia derive from progenitors, originating from the yolk sac, and which proliferate in the brain. Brain Res Dev Brain Res 117:145–152.

Ashwell K. 1991. The distribution of microglia and cell death in the fetal rat forebrain. Brain Res Dev Brain Res 58:1–12.

Auffray C, Fogg D, Garfa M, Elain G, Join-Lambert O, Kayal S, Sarnacki S, Cumano A, Lauvau G, Geissmann F. 2007. Monitoring of blood vessels and tissues by a population of monocytes with patrolling behavior. Science 317:666–670.

Auffray C, Fogg DK, Narni-Mancinelli E, Senechal B, Trouillet C, Saederup N, Leemput J, Bigot K, Campisi L, Abitbol M, Molina T, Charo I, Hume DA, Cumano A, Lauvau G, Geissmann F. 2009. CX3CR1+ CD115+ CD135+ common macrophage/DC precursors and the role of CX3CR1 in their response to inflammation. J Exp Med 206:595–606.

Badalian-Very G, Vergilio JA, Degar BA, MacConaill LE, Brandner B, Calicchio ML, Kuo FC, Ligon AH, Stevenson KE, Kehoe SM, Garraway LA, Hahn WC, Meyerson M, Fleming MD, Rollins BJ. 2010. Recurrent BRAF mutations in Langerhans cell histiocytosis. Blood 116:1919–1923.

Barcellos-Hoff MH, Park C, Wright EG. 2005. Radiation and the microenvironment—Tumorigenesis and therapy. Nat Rev Cancer 5:867–875.

Bartunek P, Kralova J, Blendinger G, Dvorak M, Zenke M. 2003. GATA-1 and c-myb crosstalk during red blood cell differentiation through GATA-1 binding sites in the c-myb promoter. Oncogene 22:1927–1935.

Benz C, Martins VC, Radtke F, Bleul CC. 2008. The stream of precursors that colonizes the thymus proceeds selectively through the early T lineage precursor stage of T cell development. J Exp Med 205:1187–1199.

Bertrand JY, Chi NC, Santoso B, Teng S, Stainier DY, Traver D. 2010. Haematopoietic stem cells derive directly from aortic endothelium during development. Nature 464:108–111.

Bertrand JY, Jalil A, Klaine M, Jung S, Cumano A, Godin I. 2005. Three pathways to mature macrophages in the early mouse yolk sac. Blood 106:3004–3011.

Bigley V, Haniffa M, Doulatov S, Wang XN, Dickinson R, McGovern N, Jardine L, Pagan S, Dimmick I, Chua I, Wallis J, Lordan J, Morgan C, Kumararatne DS, Doffinger R, van der Burg M, van Dongen J, Cant A, Dick JE, Hambleton S, Collin M. 2011. The human syndrome of dendritic cell, monocyte, B and NK lymphoid deficiency. J Exp Med 208:227–234.

Boisset JC, van Cappellen W, Andrieu-Soler C, Galjart N, Dzierzak E, Robin C. 2010. In vivo imaging of haematopoietic cells emerging from the mouse aortic endothelium. Nature 464:116–120.

Bouwens L, Baekeland M, De Zanger R, Wisse E. 1986. Quantitation, tissue distribution and proliferation kinetics of Kupffer cells in normal rat liver. Hepatology 6:718–722.

Buza-Vidas N, Woll P, Hultquist A, Duarte S, Lutteropp M, Bouriez-Jones T, Ferry H, Luc S, Jacobsen SE. 2011. FLT3 expression initiates in fully multipotent mouse hematopoietic progenitor cells. Blood 118:1544–1548.

Choi JH, Cheong C, Dandamudi DB, Park CG, Rodriguez A, Mehandru S, Velinzon K, Jung IH, Yoo JY, Oh GT, Steinman RM. 2011. Flt3 signaling-dependent dendritic cells protect against atherosclerosis. Immunity 35:819–831.

Chorro L, Sarde A, Li M, Woollard KJ, Chambon P, Malissen B, Kissenpfennig A, Barbaroux JB, Groves R, Geissmann F. 2009. Langerhans cell (LC) proliferation mediates neonatal development, homeostasis, and inflammation-associated expansion of the epidermal LC network. J Exp Med 206:3089–3100.

Cros J, Cagnard N, Woollard K, Patey N, Zhang SY, Senechal B, Puel A, Biswas SK, Moshous D, Picard C, Jais JP, D'Cruz D, Casanova JL, Trouillet C, Geissmann F. 2010. Human CD14dim monocytes patrol and sense nucleic acids and viruses via TLR7 and TLR8 receptors. Immunity 33:375–386.

Cuadros MA, Martin C, Coltey P, Almendros A, Navascues J. 1993. First appearance, distribution, and origin of macrophages in the early development of the avian central nervous system. J Comp Neurol 330:113–129.

Cumano A, Godin I. 2007. Ontogeny of the hematopoietic system. Annu Rev Immunol 25:745–785.

Dai P, Akimaru H, Tanaka Y, Hou DX, Yasukawa T, Kanei-Ishii C, Takahashi T, Ishii S. 1996. CBP as a transcriptional coactivator of c-Myb. Genes Dev 10:528–540.

Dakic A, Metcalf D, Di Rago L, Mifsud S, Wu L, Nutt SL. 2005. PU.1 regulates the commitment of adult hematopoietic progenitors and restricts granulopoiesis. J Exp Med 201:1487–1502.

Davies LC, Rosas M, Smith PJ, Fraser DJ, Jones SA, Taylor PR. 2011. A quantifiable proliferative burst of tissue macrophages restores homeostatic macrophage populations after acute inflammation. Eur J Immunol 41:2155–2164.

de Groot CJ, Huppes W, Sminia T, Kraal G, Dijkstra CD. 1992. Determination of the origin and nature of brain macrophages and microglial cells in mouse central nervous system, using non-radioactive in situ hybridization and immunoperoxidase techniques. Glia 6:301–309.

DeKoter RP, Walsh JC, Singh H. 1998. PU.1 regulates both cytokine-dependent proliferation and differentiation of granulocyte/macrophage progenitors. EMBO J 17:4456–4468.

Erblich B, Zhu L, Etgen AM, Dobrenis K, Pollard JW. 2011. Absence of colony stimulation factor-1 receptor results in loss of microglia, disrupted brain development and olfactory deficits. PLoS One 6:e26317.

Fantin A, Schwarz Q, Davidson K, Normando EM, Denti L, Ruhrberg C. 2011. The cytoplasmic domain of neuropilin 1 is dispensable for angiogenesis, but promotes the spatial separation of retinal arteries and veins. Development 138:4185–4191.

Feil R, Brocard J, Mascrez B, LeMeur M, Metzger D, Chambon P. 1996. Ligand-activated site-specific recombination in mice. Proc Natl Acad Sci USA 93:10887–10890.

Fogg DK, Sibon C, Miled C, Jung S, Aucouturier P, Littman DR, Cumano A, Geissmann F. 2006. A clonogenic bone marrow progenitor specific for macrophages and dendritic cells. Science 311:83–87.

Geissmann F, Jung S, Littman DR. 2003. Blood monocytes consist of two principal subsets with distinct migratory properties. Immunity 19:71–82.

Geissmann F, Manz MG, Jung S, Sieweke MH, Merad M, Ley K. 2010. Development of monocytes, macrophages, and dendritic cells. Science 327:656–661.

Ginhoux F, Greter M, Leboeuf M, Nandi S, See P, Gokhan S, Mehler MF, Conway SJ, Ng LG, Stanley ER, Samokhvalov IM, Merad M. 2010. Fate mapping analysis reveals that adult microglia derive from primitive macrophages. Science 330:841–845.

Ginhoux F, Tacke F, Angeli V, Bogunovic M, Loubeau M, Dai XM, Stanley ER, Randolph GJ, Merad M. 2006. Langerhans cells arise from monocytes in vivo. Nat Immunol 7:265–273.

Gschnait F, Brenner W. 1979. Kinetics of epidermal Langerhans cells. J Invest Dermatol 73:566–569.

Hambleton S, Salem S, Bustamante J, Bigley V, Boisson-Dupuis S, Azevedo J, Fortin A, Haniffa M, Ceron-Gutierrez L, Bacon CM, Menon G, Trouillet C, McDonald D, Carey P, Ginhoux F, Alsina L, Zumwalt TJ, Kong XF, Kumararatne D, Butler K, Hubeau M, Feinberg J, Al-Muhsen S, Cant A, Abel L, Chaussabel D, Doffinger R, Talesnik E, Grumach A, Duarte A, Abarca K, Moraes-Vasconcelos D, Burk D, Berghuis A, Geissmann F, Collin M, Casanova JL, Gros P. 2011. IRF8 mutations and human dendritic-cell immunodeficiency. N Engl J Med 365:127–138.

Hanna RN, Carlin LM, Hubbeling HG, Nackiewicz D, Green AM, Punt JA, Geissmann F, Hedrick CC. 2011. The transcription factor NR4A1 (Nur77) controls bone marrow differentiation and the survival of Ly6C- monocytes. Nat Immunol. 12:778–785.

Herbomel P, Thisse B, Thisse C. 2001. Zebrafish early macrophages colonize cephalic mesenchyme and developing brain, retina, and epidermis through a M-CSF receptor-dependent invasive process. Dev Biol 238:274–288.

Hickey WF, Kimura H. 1988. Perivascular microglial cells of the CNS are bone marrow-derived and present antigen in vivo. Science 239:290–292.

Hickey WF, Vass K, Lassmann H. 1992. Bone marrow-derived elements in the central nervous system: An immunohistochemical and ultrastructural survey of rat chimeras. J Neuropathol Exp Neurol 51:246–256.

Hsu AP, Sampaio EP, Khan J, Calvo KR, Lemieux JE, Patel SY, Frucht DM, Vinh DC, Auth RD, Freeman AF, Olivier KN, Uzel G, Zerbe CS, Spalding C, Pittaluga S, Raffeld M, Kuhns DB, Ding L, Paulson ML, Marciano BE, Gea-Banacloche JC, Orange JS, Cuellar-Rodriguez J, Hickstein DD, Holland SM. 2011. Mutations in GATA2 are associated with the autosomal dominant and sporadic monocytopenia and mycobacterial infection (MonoMAC) syndrome. Blood 118:2653–2655.

Imayoshi I, Ohtsuka T, Metzger D, Chambon P, Kageyama R. 2006. Temporal regulation of Cre recombinase activity in neural stem cells. Genesis 44;233–238.

Ivanova NB, Dimos JT, Schaniel C, Hackney JA, Moore KA, Lemischka IR. 2002. A stem cell molecular signature. Science 298:601–604.

Jenkins SJ, Ruckerl D, Cook PC, Jones LH, Finkelman FD, van Rooijen N, MacDonald AS, Allen JE. 2011. Local macrophage proliferation, rather than recruitment from the blood, is a signature of TH2 inflammation. Science 332:1284–1288.

Kanitakis J, Petruzzo P, Dubernard JM. 2004. Turnover of epidermal Langerhans' cells. N Engl J Med 351:2661–2662.

Kasper LH, Boussouar F, Ney PA, Jackson CW, Rehg J, van Deursen JM, Brindle PK. 2002. A transcription-factor-binding surface of coactivator p300 is required for haematopoiesis. Nature 419:738–743.

Katz SI, Tamaki K, Sachs DH. 1979. Epidermal Langerhans cells are derived from cells originating in bone marrow. Nature 282:324–326.

King IL, Dickendesher TL, Segal BM. 2009. Circulating Ly-6C+ myeloid precursors migrate to the CNS and play a pathogenic role during autoimmune demyelinating disease. Blood 113:3190–3197.

Kissa K, Herbomel P. 2010. Blood stem cells emerge from aortic endothelium by a novel type of cell transition. Nature 464:112–115.

Klein I, Cornejo JC, Polakos NK, John B, Wuensch SA, Topham DJ, Pierce RH, Crispe IN. 2007. Kupffer cell heterogeneity: Functional properties of bone marrow derived and sessile hepatic macrophages. Blood 110:4077–4085.

Krall WJ, Challita PM, Perlmutter LS, Skelton DC, Kohn DB. 1994. Cells expressing human glucocerebrosidase from a retroviral vector repopulate macrophages and central nervous system microglia after murine bone marrow transplantation. Blood 83:2737–2748.

Kranc KR, Schepers H, Rodrigues NP, Bamforth S, Villadsen E, Ferry H, Bouriez-Jones T, Sigvardsson M, Bhattacharya S, Jacobsen SE, Enver T. 2009. Cited2 is an essential regulator of adult hematopoietic stem cells. Cell Stem Cell 5:659–665.

Labastie MC, Cortes F, Romeo PH, Dulac C, Peault B. 1998. Molecular identity of hematopoietic precursor cells emerging in the human embryo. Blood 92:3624–3635.

Lassmann H, Schmied M, Vass K, Hickey WF. 1993. Bone marrow derived elements and resident microglia in brain inflammation. Glia 7:19–24.

Lawson LJ, Perry VH, Dri P, Gordon S. 1990. Heterogeneity in the distribution and morphology of microglia in the normal adult mouse brain. Neuroscience 39:151–170.

Lawson LJ, Perry VH, Gordon S. 1992. Turnover of resident microglia in the normal adult mouse brain. Neuroscience 48:405–415.

Lichanska AM, Browne CM, Henkel GW, Murphy KM, Ostrowski MC, McKercher SR, Maki RA, Hume DA. 1999. Differentiation of the mononuclear phagocyte system during mouse embryogenesis: The role of transcription factor PU.1. Blood 94:127–138.

Lieu YK, Reddy EP. 2009. Conditional c-myb knockout in adult hematopoietic stem cells leads to loss of self-renewal due to impaired proliferation and accelerated differentiation. Proc Natl Acad Sci USA 106:21689–21694.

Liu K, Victora GD, Schwickert TA, Guermonprez P, Meredith MM, Yao K, Chu FF, Randolph GJ, Rudensky AY, Nussenzweig M. 2009. In vivo analysis of dendritic cell development and homeostasis. Science 324:392–397.

Liu K, Waskow C, Liu X, Yao K, Hoh J, Nussenzweig M. 2007. Origin of dendritic cells in peripheral lymphoid organs of mice. Nat Immunol 8:578–583.

Massengale M, Wagers AJ, Vogel H, Weissman IL. 2005. Hematopoietic cells maintain hematopoietic fates upon entering the brain. J Exp Med 201:1579–1589.

Matsumoto Y, Fujiwara M. 1987. Absence of donor-type major histocompatibility complex class I antigen-bearing microglia in the rat central nervous system of radiation bone marrow chimeras. J Neuroimmunol 17:71–82.

McDonald B, Pittman K, Menezes GB, Hirota SA, Slaba I, Waterhouse CC, Beck PL, Muruve DA, Kubes P. 2010. Intravascular danger signals guide neutrophils to sites of sterile inflammation. Science 330:362–366.

McKercher SR, Torbett BE, Anderson KL, Henkel GW, Vestal DJ, Baribault H, Klemsz M, Feeney AJ, Wu GE, Paige CJ, Maki RA. 1996. Targeted disruption of the PU.1 gene results in multiple hematopoietic abnormalities. EMBO J 15:5647–5658.

Medvinsky A, Dzierzak E. 1996. Definitive hematopoiesis is autonomously initiated by the AGM region. Cell 86:897–906.

Merad M, Manz MG, Karsunky H, Wagers A, Peters W, Charo I, Weissman IL, Cyster JG, Engleman EG. 2002. Langerhans cells renew in the skin throughout life under steady-state conditions. Nat Immunol 3:1135–1141.

Metzger D, Clifford J, Chiba H, Chambon P. 1995. Conditional site-specific recombination in mammalian cells using a ligand-dependent chimeric Cre recombinase. Proc Natl Acad Sci USA 92:6991–6995.

Mildner A, Schmidt H, Nitsche M, Merkler D, Hanisch UK, Mack M, Heikenwalder M, Bruck W, Priller J, Prinz M. 2007. Microglia in the adult brain arise from Ly-6ChiCCR2+ monocytes only under defined host conditions. Nat Neurosci 10:1544–1553.

Mildner A, Mack M, Schmidt H, Brück W, Djukic M, Zabel MD, Hille A, Priller J, Prinz M. 2009. CCR2+Ly-6Chi monocytes are crucial for the effector phase of autoimmunity in the central nervous system. Brain 132:2487–2500.

Miyauchi S, Hashimoto K. 1987. Epidermal Langerhans cells undergo mitosis during the early recovery phase after ultraviolet-B irradiation. J Invest Dermatol 88:703–708.

Mucenski ML, McLain K, Kier AB, Swerdlow SH, Schreiner CM, Miller TA, Pietryga DW, Scott WJ, Jr., Potter SS. 1991. A functional c-myb gene is required for normal murine fetal hepatic hematopoiesis. Cell 65:677–689.

Mukouyama Y, Chiba N, Mucenski ML, Satake M, Miyajima A, Hara T, Watanabe T. 1999. Hematopoietic cells in cultures of the murine embryonic aorta-gonad-mesonephros region are induced by c-Myb. Curr Biol 9:833–836.

Muller AM, Medvinsky A, Strouboulis J, Grosveld F, Dzierzak E. 1994. Development of hematopoietic stem cell activity in the mouse embryo. Immunity 1:291–301.

Murayama E, Kissa K, Zapata A, Mordelet E, Briolat V, Lin HF, Handin RI, Herbomel P. 2006. Tracing hematopoietic precursor migration to successive hematopoietic organs during zebrafish development. Immunity 25:963–975.

Naik SH, Sathe P, Park HY, Metcalf D, Proietto AI, Dakic A, Carotta S, O'Keeffe M, Bahlo M, Papenfuss A, Kwak JY, Wu L, Shortman K. 2007. Development of plasmacytoid and conventional dendritic cell subtypes from single precursor cells derived in vitro and in vivo. Nat Immunol 8:1217–1226.

Nerlov C, Graf T. 1998. PU.1 induces myeloid lineage commitment in multipotent hematopoietic progenitors. Genes Dev 12:2403–2412.

Nimmerjahn A, Kirchhoff F, Helmchen F. 2005. Resting microglial cells are highly dynamic surveillants of brain parenchyma in vivo. Science 308:1314–1318.

Oelgeschlager M, Nuchprayoon I, Luscher B, Friedman AD. 1996. C/EBP, c-Myb, and PU.1 cooperate to regulate the neutrophil elastase promoter. Mol Cell Biol 16:4717–4725.

Olson MC, Scott EW, Hack AA, Su GH, Tenen DG, Singh H, Simon MC. 1995. PU. 1 is not essential for early myeloid gene expression but is required for terminal myeloid differentiation. Immunity 3:703–714.

Onai N, Obata-Onai A, Schmid MA, Ohteki T, Jarrossay D, Manz MG. 2007. Identification of clonogenic common Flt3+M-CSFR+ plasmacytoid and conventional dendritic cell progenitors in mouse bone marrow. Nat Immunol 8:1207–1216.

Orkin SH, Zon LI. 2008. Hematopoiesis: An evolving paradigm for stem cell biology. Cell 132:631–644.

Palis J, Robertson S, Kennedy M, Wall C, Keller G. 1999. Development of erythroid and myeloid progenitors in the yolk sac and embryo proper of the mouse. Development 126:5073–5084.

Palis J, Chan RJ, Koniski A, Patel R, Starr M, Yoder MC. Spatial and temporal emergence of high proliferative potential hematopoietic precursors during murine embryogenesis. 2001. Proc Natl Acad Sci USA 10; 98:4528–4533.

Perreault C, Pelletier M, Landry D, Gyger M. 1984. Study of Langerhans cells after allogeneic bone marrow transplantation. Blood 63:807–811.

Perry VH, Hume DA, Gordon S. 1985. Immunohistochemical localization of macrophages and microglia in the adult and developing mouse brain. Neuroscience 15:313–326.

Priller J, Flugel A, Wehner T, Boentert M, Haas CA, Prinz M, Fernandez-Klett F, Prass K, Bechmann I, de Boer BA, Frotscher M, Kreutzberg GW, Persons PA, Dirnagl U. 2001. Targeting gene-modified hematopoietic cells to the central nervous system: Use of green fluorescent protein uncovers microglial engraftment. Nat Med 7:1356–1361.

Qian BZ, Li J, Zhang H, Kitamura T, Zhang J, Campion LR, Kaiser EA, Snyder LA, Pollard JW. 2011. CCL2 recruits inflammatory monocytes to facilitate breast-tumour metastasis. Nature 475:222–225.

Rae F, Woods K, Sasmono T, Campanale N, Taylor D, Ovchinnikov DA, Grimmond SM, Hume DA, Ricardo SD, Little MH. 2007. Characterisation and trophic functions of murine embryonic macrophages based upon the use of a Csf1r-EGFP transgene reporter. Dev Biol 308:232–246.

Reddy MA, Yang BS, Yue X, Barnett CJ, Ross IL, Sweet MJ, Hume DA, Ostrowski MC. 1994. Opposing actions of c-ets/PU.1 and c-myb protooncogene products in regulating the macrophage-specific promoters of the human and mouse colony-stimulating factor-1 receptor (c-fms) genes. J Exp Med 180:2309–2319.

Saijo K, Winner B, Carson CT, Collier JG, Boyer L, Rosenfeld MG, Gage FH, Glass CK. 2009. A Nurr1/CoREST pathway in microglia and astrocytes protects dopaminergic neurons from inflammation-induced death. Cell 137:47–59.

Samokhvalov IM, Samokhvalova NI, Nishikawa S. 2007. Cell tracing shows the contribution of the yolk sac to adult haematopoiesis. Nature 446:1056–1061.

Sandberg ML, Sutton SE, Pletcher MT, Wiltshire T, Tarantino LM, Hogenesch JB, Cooke MP. 2005. c-Myb and p300 regulate hematopoietic stem cell proliferation and differentiation. Dev Cell 8:153–166.

Sasmono RT, Oceandy D, Pollard JW, Tong W, Pavli P, Wainwright BJ, Ostrowski MC, Himes SR, Hume DA. 2003. A macrophage colony-stimulating factor receptor-green fluorescent protein transgene is expressed throughout the mononuclear phagocyte system of the mouse. Blood 101:1155–1163.

Satoh T, Smith A, Sarde A, Lu HC, Mian S, Trouillet C, Mufti G, Emile JF, Fraternali F, Donadieu J, Geissmann F. 2012. B-RAF mutant alleles associated with langerhans cell histiocytosis, a Granulomatous pediatric disease. PLoS One 7:e33891.

Schulz C, Gomez Perdiguero E, Chorro L, Szabo-Rogers H, Cagnard N, Kierdorf K, Prinz M, Wu B, Jacobsen SE, Pollard JW, Frampton J, Liu KJ, Geissmann F. 2012. A lineage of myeloid cells independent of Myb and hematopoietic stem cells. Science 336:86–90.

Shankaran M, Marino ME, Busch R, Keim C, King C, Lee J, Killion S, Awada M, Hellerstein MK. 2007. Measurement of brain microglial proliferation rates in vivo in response to neuroinflammatory stimuli: Application to drug discovery. J Neurosci Res 85:2374–2384.

Shapiro LH. 1995. Myb and Ets proteins cooperate to transactivate an early myeloid gene. J Biol Chem 270:8763–8771.

Sorokin SP, Hoyt RF Jr, Blunt DG, McNelly NA. 1992. Macrophage development: II. Early ontogeny of macrophage populations in brain, liver, and lungs of rat embryos as revealed by a lectin marker. Anat Rec 232:527–550.

Soza-Ried C, Hess I, Netuschil N, Schorpp M, Boehm T. 2010. Essential role of c-myb in definitive hematopoiesis is evolutionarily conserved. Proc Natl Acad Sci USA 107:17304–17308.

Srinivas S, Watanabe T, Lin CS, William CM, Tanabe Y, Jessell TM, Costantini F. 2001. Cre reporter strains produced by targeted insertion of EYFP and ECFP into the ROSA26 locus. BMC Dev Biol 1:4.

Sumner R, Crawford A, Mucenski M, Frampton J. 2000. Initiation of adult myelopoiesis can occur in the absence of c-Myb whereas subsequent development is strictly dependent on the transcription factor. Oncogene 19:3335–3342.

Thored P, Heldmann U, Gomes-Leal W, Gisler R, Darsalia V, Taneera J, Nygren JM, Jacobsen SE, Ekdahl CT, Kokaia Z, Lindvall O. 2009. Long-term accumulation of microglia with proneurogenic phenotype concomitant with persistent neurogenesis in adult subventricular zone after stroke. Glia 57:835–849.

Vandenbunder B, Pardanaud L, Jaffredo T, Mirabel MA, Stehelin D. 1989. Complementary patterns of expression of c-ets 1, c-myb and c-myc in the blood-forming system of the chick embryo. Development 107:265–274.

Varol C, Vallon-Eberhard A, Elinav E, Aychek T, Shapira Y, Luche H, Fehling HJ, Hardt WD, Shakhar G, Jung S. 2009. Intestinal lamina propria dendritic cell subsets have different origin and functions. Immunity 31:502–512.

Wake H, Moorhouse AJ, Jinno S, Kohsaka S, Nabekura J. 2009. Resting microglia directly monitor the functional state of synapses in vivo and determine the fate of ischemic terminals. J Neurosci 29:3974–3980.

Zhao L, Glazov EA, Pattabiraman DR, Al-Owaidi F, Zhang P, Brown MA, Leo PJ, Gonda TJ. 2011. Integrated genome-wide chromatin occupancy and expression analyses identify key myeloid pro-differentiation transcription factors repressed by Myb. Nucleic Acids Res 39:4664–4679.

Enquête épidémiologique adulte à Paris . 1 er résultats A Mahr St Louis

Approches thérapeutiques de l'HL systémique de l'adulte table ronde/ Quel degré de preuve ? M De menthon, A Tazi, J Haroche

Trois documents sont joints pour introduire cette partie: 2 articles pédiatriques concernant des guidelines (EU et France) et un document adulte publié par Euro Histio net récemment dans OJRD.

Pediatr Blood Cancer

Langerhans Cell Histiocytosis (LCH): Guidelines for Diagnosis, Clinical Work-Up, and Treatment for Patients Till the Age of 18 Years

Riccardo Haupt, MD,[1] Milen Minkov, MD,[2] Itziar Astigarraga, MD,[3] Eva Schäfer, MSc,[4] Vasanta Nanduri, MD,[5] Rima Jubran, MD,[6] R. Maarten Egeler, MD, PhD,[7] Gritta Janka, MD,[8] Dragan Micic, MD,[9] Carlos Rodriguez-Galindo, MD,[10] Stefaan Van Gool, MD,[11] Johannes Visser, MBChB,[12] Sheila Weitzman, MD,[7] Jean Donadieu, MD, PhD[4]* and for the Euro Histio Network

These guidelines for the management of patients up to 18 years with Langerhans cell histiocytosis (LCH) have been set up by a group of experts involved in the Euro Histio Net project who participated in national or international studies and in peer reviewed publications. Existing guidelines were reviewed and changed where new evidence was available in the literature up to 2012. Data and publications have been ranked according to evidence based medicine and when there was a lack of published data, consensus between experts was sought. Guidelines for diagnosis, initial clinical work-up, and treatment and long-term follow-up of LCH patients are presented. Pediatr Blood Cancer

Key words: clinical work-up; diagnosis; follow-up; guidelines; Langerhans cell histiocytosis; therapy

INTRODUCTION

Langerhans cell histiocytosis (LCH) is a heterogeneous disease, characterized by accumulation of dendritic cells with features similar to epidermal Langerhans cells in various organs. Any organ or system of the human body can be affected, but those more frequently involved are the skeleton (80% of cases), the skin (33%), and the pituitary (25%). Other organs involved are the liver, spleen, the hematopoietic system and the lungs (15% each), lymph nodes (5–10%), and the central nervous system excluding the pituitary (2–4%). The clinical course may vary from a self-limiting disease to a rapidly progressive one that might lead to death. Between 30% and 40% of patients may develop permanent adverse sequelae. Treatment options vary depending on the extent of the disease and the severity at onset. Response to front-line treatment is an important information to adapt the therapeutic strategy. As LCH is a rare disease, only a limited number of large surveys or of randomized clinical trials are available in the literature and many aspects of the management of patients remain obscure or controversial. The presented guidelines are based on published evidence and the clinical expertise of the authors. They are intended to provide guidance with respect to diagnosis and clinical work-up of LCH occurring in patients <18 years old. The recommendations can neither replace the physician's own professional judgement nor consider all special clinical circumstances which may apply to individual cases.

METHODS

This document is derived from the project Euro Histio Net 2008, a reference network (www.eurohistio.net) for LCH and associated syndromes in the European Union which received funding within the framework of the Public Health Program. The guidelines were designed and established by European and North American physicians considered to be experts in the field of pediatric histiocytic disorders. They are active members of the international medical society of histiocytoses "Histiocyte Society" (HS), of the European national societies of Hematology/Oncology, and of their respective national groups for the study and treatment of these diseases. The guidelines have been developed for use as recommended practice in the evaluation and treatment of children and teenagers up to 18 years with LCH. Scientific articles published in peer-reviewed journals up to January 2012 were systematically reviewed. In addition to the medical literature, the following guidelines are a synthesis of different international and national guidelines and recommendation documents.

Evidence was ranked in four levels [1,2]: (A) meta-analyses, high quality systematic reviews, or randomized controlled trials with a low risk of bias; (B) systematic reviews of case–control or cohort studies; (C) non-analytic studies; for example, case reports, case series, small retrospective studies; (D) expert opinion. Level of agreement between experts and data was ranked in three classes: (2) general agreement between all experts or between available studies; (1) discussed recommendation, but no formal objections between experts or mild difference between studies, without contradiction for the main endpoint; (0) divergence of opinion or contradictory results for the main endpoint.

Additional Supporting Information may be found in the online version of this article.

Abbreviations: LCH, Langerhans cell histiocytosis; MRI, magnetic resonnance imaging; CNS, central nervous system; DI, diabetes insipidus; MS-LCH, multi system Langerhans cell histiocytosis; SS-LCH, single system Langerhans cell histiocytosis; RO, risk organs.

[1]Department of Hematology and Oncology, Epidemiology and Biostatistics Section, Istituto G. Gaslini, Genova, Italy; [2]Children's Cancer Research Institute, St. Anna Children's Hospital, Vienna, Austria; [3]Hospital Universitario Cruces Barakaldo, Barakaldo, Spain; [4]Reference Centre for Histiocytosis at Hopital Trousseau, Assistance Publique – Hopitaux de Paris, France; [5]Watford General Hospital, Watford, UK; [6]Children's Hospital of Los Angeles, Los Angeles, California; [7]Hospital for Sick Children, Toronto, Ontario, Canada; [8]University Medical Center Hamburg-Eppendorf, Hamburg, Germany; [9]Mother and Child Health Institute of Serbia "Dr Vukan Cupic," Belgrade, Serbia; [10]Dana Farber Cancer Institute, Children's Hospital Boston, Boston, Massachusetts; [11]University Hospital Gasthuisberg, Leuven, Belgium; [12]University Hospitals of Leicester, Leicester Children's Hospital, Leicester, UK

Conflict of interest: Nothing to declare.

*Correspondence to: Jean Donadieu, MD, PhD, Service d'Hémato Oncologie Pédiatrique, Hopital Trousseau, 26 avenue du Dr Netter, F 75012 Paris, France. E-mail: jean.donadieu@trs.aphp.fr

Received 13 May 2012; Accepted 18 September 2012

DOI 10.1002/pbc.24367
Published online in Wiley Online Library (wileyonlinelibrary.com).

TABLE I. Differential Diagnosis for Manifestations of Langerhans Cell Histiocytosis

Involvement	Manifestation	Possible other condition
Skin	Vesicles and bullae (most common in early infancy)	Erythema toxicum
		Herpes simplex
		Varicella
	Dermatitis (most frequently scalp, diaperarea, or axilla, may occur up to late infancy)	Seborrheic dermatitis (eczema; usually no petechiae and marked scaling)
	Nodules	Mastocytosis
		Juvenile xanthogranuloma
		Neuroblastoma
		Infant leukemia
	Pruritus	Scabies (other family members may be affected)
	Petechiae	
Bone	Vertebra plana	Ewing sarcoma
		Septic osteomyelitis
		Chronic relapsing multifocal osteomyelitis (CRMO)
		Leukemia
		Lymphoma
		Aneurysmal bone cyst
		Juvenile xanthogranuloma
		Myeloma (only described in adults)
		Osteoporosis
	Temporal bone	Chronic otitis media
		Mastoiditis
		Cholesteatoma
		Soft tissue sarcoma
	Orbit	Acute infection (preseptal cellulitis)
		Dermoid cyst
		Rhabdomyosarcoma
		Neuroblastoma
		Erdheim–Chester disease
		Pseudoinflammatory tumor
	Other lytic lesions of the long bones	Septic osteomyelitis
		Chronic recurrent multifocal osteomyelitis (CRMO)
		Aneurysmal bone cyst
		Bone angiomatosis (Gorham disease)
		Fibrous dysplasia
		Atypical mycobacterial infection
		Osteogenic sarcoma
		Ewing's sarcoma
Lung	In particular systemic symptoms and cavitated pulmonary nodules	Pneumocystis jirovecii cavitated infection
		Mycobacterial or other pulmonary infections
		Sarcoidosis
		Bronchiolar–alveolar carcinoma (only described in adults)
		Lymphangio–Leiomyosarcoma (only described in young adult women)
		Septic emboli
Liver	Jaundice with direct hyperbilirubinemia	Chronic destructive cholangitis
	Hypoalbuminemia	Metabolic disease
		Hepatitis
		Neoplasia obstructing biliary tract
		Inherited deficient conjugation of bilirubin
		Toxic (Reye syndrome)
		Chronic inflammatory bowel disease
		Neonatal hemochromatosis
Endocrine	Diabetes insipidus	Central nervous sysytem germ cell tumor
		Hypophisitis

Langerhans Cell Histiocytosis Diagnosis

Since LCH may affect any organ or system of the body, the condition should be considered whenever suggestive clinical manifestations occur in the skin, bone, lung, liver, or CNS. Table I shows a list of differential diagnoses to be considered depending on presenting complaints, signs, or symptoms. The diagnosis is clinicopathologic and should only be made in the appropriate clinical setting to prevent a misdiagnosis in the presence of normal reactive Langerhans cells, particularly in regional lymph nodes. In addition to clinical and radiological features, LCH diagnosis should always be based on histological and immunophenotypic examination of lesional tissue (agreement: 2), that

should be taken from the most easily accessible, yet representative lesion.

There is a well defined histologically characteristic appearance of the LCH lesions on hematoxylin and eosin stained sections, but positive CD1a and/or CD207 (Langerin) staining of the lesional cells is required for a definitive diagnosis [3–6] (agreement: 2). Electron microscopy is no longer needed (agreement: 2), since it has been shown that the expression of Langerin correlates with the ultrastructural presence of Birbeck granules. Diagnostic confirmation may be a challenge in some circumstances (e.g., liver specimens), where Birbeck granules are not present and CD1a and/or Langerin may be negative because LCH cells have regressed after having caused sclerosing cholangitis and Cirrhosis [7].

In rare cases the risk of biopsy may outweigh the need for a definitive diagnosis, and therefore the risk/benefit ratio should be carefully assessed. This is the case in patients with isolated involvement of a vertebral body without an adjacent soft tissue component, as in case of vertebra plana, or with isolated involvement of the odontoid peg. If the decision to avoid or postpone a biopsy is made, every effort should be made to rule out other conditions that might lead to a similar radiological finding (Table I).

Patients without a histologically confirmed diagnosis need to be carefully monitored by appropriate imaging for at least the next 6 months in order to reassess the need for biopsy and its justification, in order to exclude a malignancy.

Pretreatment Clinical Evaluation

Once the diagnosis of LCH has been ascertained it is important to collect further baseline information in order to decide on a therapeutic approach. A complete history should include special reference to the nature and duration of symptoms. Specific symptoms to be sought are: pain, swelling, skin rashes, otorrhea, fever, loss of appetite, diarrhea, poor weight gain, growth failure, polydipsia, polyuria, respiratory symptoms, irritability, behavioral, and neurological changes. A detailed examination should be performed at the onset and at each follow-up visit. Currently there is no specific biological marker of disease activity, however, there is a general agreement (agreement: 2) that biochemical and imaging evaluation at diagnosis and at disease reactivation should include the mandatory investigations listed in Table II. Certain scenarios might require additional testing; the recommended laboratory investigations, imaging, or specialized clinical assessments upon specific indication are shown in Table III; the detailed protocol for head MRI is provided in (Supplemental Appendix I).

TABLE II. Laboratory and Radiographic Evaluation of Children With LCH

Evaluation
Full blood count
Hemoglobin
White blood cell and differential count
Platelet count
Blood chemistry
Total protein
Albumin
Bilirubin
ALT (SGPT)
AST (SGOT)
γGT
Creatinine
Electrolytes
Erythrocyte sedimentation rate (ESR)
Abdominal ultrasound (in particular for young children)
Size and structure of liver and spleen
Abdominal lymph-nodes
Coagulation studies
INR/PT
APTT/PTT
Fibrinogen/factor I
Chest Radiograph (CXR)
Skeletal radiograph survey[a,b]

ALT (SGPT), alanine transaminase (serum glutamic pyruvic transaminase); APTT/PTT, activated partial thromboplastin time/partial thromboplastin time; AST (SGOT), aspartate transaminase (serum glutamic oxaloacetic transaminase); γGT, gamma-glutamyltransferase; INR/PT, international normalized ratio/prothrombin time; MRI, magnetic resonance imaging; PET, positron emission tomography; Tc, technetium. [a]Note that other imaging techniques as bone Tc scan, PET scan, or MRI are not an alternative to the standard skeletal survey. The real value of these images in LCH is still under study. In particular information from bone scan should not be considered for evaluation of disease extent and decision-making. PET scan has proven to be the most sensitive functional test used in the identification of LCH lesions and in evaluating patient response to therapy. However, it is currently expensive, exposes the patient to a significant radiation dose and is not widely available [56]. [b]It is not recommended to change the method of bone evaluation (skeletal radiograph), as it may lead to discrepancy between assessments. It is important also to consider the ALARA principle (as low as reasonably achievable) for ionizing radiation and, if possible, during follow up, limit the evaluation to the anatomic region initially involved.

Defining Organ Involvement, Risk Organs, and CNS (Central Nervous System) Risk Lesions

The findings of the pretreatment clinical evaluation allow definition of organ involvement based on the clinical, biological, and radiological criteria shown in Table IV. Disease involvement of certain organs is considered as a marker of higher risk of (a) dying from disease (risk organs) or (b) developing neuro-degenerative complications more commonly named as CNS risk lesions.

Risk organs include the hematologic system, the spleen and the liver (evidence: B, agreement: 2) [8–10]. The lung had been considered for many decades as a risk organ, but its individual prognostic impact has recently been questioned [11]. In fact, in the absence of involvement of other risk organs, lung disease is only in exceptional cases the ultimate cause of death [12,13], and this usually occurs through "mechanical complications" such as an uncontrolled pneumothorax [14], or as a late event due to chronic emphysematous changes. In the upcoming clinical trial for LCH in children (LCH-IV), the lung will be no longer considered a risk organ.

Involvement of some skull bones might predispose to diabetes insipidus (DI) and CNS manifestations [15–17]. The term CNS risk lesions, representing a more recent concept [16], suggests that these patients are more likely to develop neuro-degenerative CNS disease, which may be an irreversible complication of LCH and may have a debilitating course [18]. Therefore, skull bone lesions, with the exception of the vault, are considered as CNS risk

TABLE III. Specific Clinical Scenarios and Recommended Additional Testing in Children With LCH

Clinical scenario and recommended additional testing
History of polyuria or polydipsia
Early morning urine specific gravity and osmolality
Blood electrolytes
Water deprivation test if possible
MRI of the head[a]
Bicytopenia, pancytopenia, or persistent unexplained single cytopenia
Other causes of anemia or thrombocytopenia has to be ruled out according to standard medical practice. If no other causes are found, the cytopenia is considered LCH-related
Bone marrow aspirate and trephine biopsy to exclude causes other than LCH b as exposant
Evaluation for features of macrophage activation and hemophagocytic syndrome (triglycerides and ferritin in addition to the coagulation studies in Table IIa[c]
Liver dysfunction
If frank liver dysfunction (liver enzymes >5-fold upper limit of normal/bilirubin >5-fold upper limit of normal): consult a hepatologist and consider liver MRI which is preferable to retrograde cholangiography
Liver biopsy is only recommended if there is clinically significant liver involvement and the result will alter treatment (i.e., to differentiate between active LCH and sclerosing cholangitis)
Lung involvement (further testing is only needed in case of abnormal chest X-ray or symptoms/signs suggestive of lung involvement, or pulmonary findings not characteristic of LCH or suspicion of an atypical infection)
Lung high resolution computed tomography (HR-CT) or preferably low dose multi-detector HR-CT if available. Note that cysts and nodules are the only images typical of LCH; all other lesions are not diagnostic. In children already diagnosed with MS-LCH (see section "Clinical Classification") low dose CT is sufficient in order to assess extent of pulmonary involvement, and reduce the radiation exposure
Lung function tests (if age appropriate)
Bronchoalveolar lavage (BAL): >5% CD1a + cells in BAL fluid may be diagnostic in a non-smoker[d]
Lung biopsy (if BAL is not diagnostic)
Suspected craniofacial bone lesions including maxilla and mandible
MRI of head[a] including the brain, hypothalamus–pituitary axis, and all craniofacial bones. If MRI not available, CT of the involved bone and the skull base is recommended
Aural discharge or suspected hearing impairment/mastoid involvement
Formal hearing assessment
MRI of head[a] or HR-CT of temporal bone
Vertebral lesions (even if only suspected)
MRI of spine to assess for soft tissue massess and to exclude spinal cord compression
Visual or neurological abnormalities
MRI of head[a]
Neurological assessment
Neuropsychometric assessment
Suspected other endocrine abnormality (i.e., short stature, growth failure, hypothalamic syndromes, precocious, or delayed puberty)
Endocrine assessment (including dynamic tests of the anterior pituitary and thyroid)
MRI of head[a]
Unexplained chronic diarrhea, failure to thrive, or evidence of malabsorption
Endoscopy
Biopsy

(HR-)CT, (high resolution) computed tomography; MRI, magnetic resonance imaging. [a]See Appendix 1 for details. b The clinical significance of CD1a positivity in the bone marrow remains to be proven. An isolated finding of histiocytic infiltration on the bone marrow with no cytopenia is not a criterion for diagnosis or reactivation [57,58]. [c]Hemophagocytic syndrome with macrophage activation is a common finding in patients with hematological dysfunction [59,60]. [d]See discussion in Refs. [12,13].

lesions, assuming that risk factors for DI can also be considered as risk factors of neuro-degenerative changes (evidence C; agreement: 1).

Clinical Classification

The current classification differentiates between single system disease (SS-LCH) and multisystem disease (MS-LCH), a distinction based on the extent of involvement at diagnosis. In SS-LCH, only one organ or system is involved such as bone (either as a single bone or more than one bone), skin, lymph node (not the draining lymph node of another LCH lesion), lungs, hypothalamic-pituitary/central nervous system, or others such as thyroid or thymus. In MS-LCH, two or more organs, or systems are involved either with or without involvement of risk organs.

General Considerations for Treatment

Treatment of single-system LCH. Patients with SS-LCH may be initially referred to a range of medical specialists depending on the localization and presentation of the lesions, thus it is difficult to organize and execute coordinated international trials. This section combines the limited published evidence with the authors' experience (evidence: C, agreement: 1).

TABLE IV. Definition of Organ Involvement in Langerhans Cell Histiocytosis

Criteria	CNS risk lesions	Risk organ
Bone involvement		
General bone involvement: all radiologically documented lesions, which are not mentioned below		
Craniofacial bone involvement: lesions in the orbital, temporal, mastoid, sphenoidal, zygomatic, or ethmoidal bones; the maxilla or paranasal sinuses; or cranial fossa; with intracranial soft tissue extension	Yes	
Vertebral involvement without soft tissue extension, for example, vertebra plana		
Vertebral involvement with intraspinal soft tissue extension or lesions in the odontoid peg		
An abnormality on Tc bone scan or an MRI hypersignal, not correlated with symptoms, or with an X-ray image is not considered bony disease!		
Central nervous system (CNS) involvement	Yes	
Tumoral: all intracerebral expansive lesions predominantly affecting the brain or meninges		
Neurodegeneration on MRI: MRI imaging compatible with neurodegenerative disease[a], that is, abnormal signal intensity localized in the dentate nuclei or cerebellum or cerebral atrophy NOT explained by corticosteroids		
Clinical neurodegeneration: presence of suggestive symptoms (either cerebellar syndrome or learning difficulty) with compatible MRI imaging		
Ear involvement		
Ear involvement with external otitis, otitis media, or otorrhea	Yes	
Eye involvement		
Orbital involvement with proptosis or exophthalmos	Yes	
Hematopoietic involvement		Yes
Mild (both of the following categories should be present)		
Hemoglobin between 10 and 7 g/dl (not due to other causes, e.g., iron deficiency)		
Thrombocytopenia with platelets between 100,000 and 20,000/mm^3		
Severe (both of the following categories should be present)		
Hemoglobin <7 g/dl (not due to other causes, e.g., iron deficiency)		
Platelets <20,000/mm^3		
Liver involvement (the patient can show a combination of these symptoms)		Yes
Enlargement >3 cm below the costal margin at the mid clavicular line, confirmed by ultrasound or dysfunction documented by: hyperbilirubinemia >3 times normal hypoalbuminemia (<30 g/dl), γ GT increased >2 times normal, ALT (SGPT)–AST (SGOT) >3 times normal, ascites, edema, or intra hepatic nodular mass		
Lung involvement		(Yes)[b]
Typical imaging (nodules or cysts) on CT scan		
Any atypical mass needs to be explored by BAL or biopsy in order to have histopathological/cytological diagnosis		
Mucosa involvement		
Oral involvement with lesions in the oral mucosa, gums		
Genital or anal involvement		
Pituitary involvement		
Any pituitary hormone deficiency or tumor appearance in the hypothalamic-pituitary axis		
Skin involvement		
Any rash documented by histological examination or any lesion (erythematous and crusted macules, papules, or nodules, with or without ulceration, or petechiae, or seborrhea-like picture) compatible with the diagnosis, if LCH is confirmed by biopsy of another organ		
Spleen involvement		Yes
>3 cm below the costal margin at the mid clavicular line, confirmed by ultrasound		

ALT (SGPT), alanine transaminase (serum glutamic pyruvic transaminase); AST (SGOT), aspartate transaminase (serum glutamic oxaloacetic transaminase); BAL, bronchoalveolar lavage; CT, computed tomography; MRI, magnetic resonance imaging. [a]The term radiological neurodegeneration has been coined to describe a certain pattern of MRI findings, but this terminology may be misleading as it does not necessarily correlate with histopathology. [b]See section "Risk organs."

Single system unifocal bone involvement (isolated bone lesions). Unifocal bone lesions are the predominant clinical form of LCH. Spontaneous regression may occur, and the clinical course is probably not greatly influenced by any form of treatment. The decision on the most appropriate approach should be based on clinical symptoms, the size and location of the disease, and on any evidence of healing on imaging. Often, simple curettage during the diagnostic biopsy will result in healing, and further intervention may not be necessary [19]. Indications for additional treatment include involvement of weight-bearing bones, imminent spinal cord compression, unacceptable deformity, intense pain, and functional disability.

Complete excision of bone lesions (curettage) may be indicated if the lesion is small (<2 cm) and is combined with the diagnostic confirmation. However, radical excision of large lesions (>5 cm) is not indicated since it increases the size of the bony defect, could prolong the time to healing, and might result in permanent skeletal defects. For lesions 2–5 cms in diameter, a biopsy and partial curettage is an option. Depending on the size and location of the lesion, an intralesional injection of methylprednisolone may be administered [20] to promote healing (evidence: C). Immobilization of the limb may need to be considered and discussed with the orthopedic surgeon in rare cases. "Vertebra plana" *per se* is not an indication for an orthopedic corset, and expert physiotherapy assessment should be considered; however, temporary immobilization may be required for symptomatic relief in the early phases of vertebral involvement. Patients with temporal bone lesions and recurrent otorrhea, may have a secondary cholesteatoma which may need specific treatment [21].

In certain functionally critical anatomical sites, such as the odontoid peg or other vertebral lesions with intraspinal soft tissue extension there may be an immediate risk to the patient because of the potential for disease progression and the hazards involved in attempting a biopsy; however, these are exceptional situations, and a biopsy should always be considered. Isolated disease involving functionally critical anatomical sites may justify systemic therapy.

Because of the potential for development of sequelae, systemic therapy is indicated in patients with lesions involving the skull base, temporal bone, orbits, and vertebral column, where there is also involvement of the adjacent soft tissues.

Single system multifocal bone involvement. LCH which presents with only multiple bone lesions at diagnosis (SS-LCH multifocal bone) usually remains confined to the skeleton, and only rarely extends to other organs like the skin and pituitary gland. However, the incidence of reported reactivations in cases of multifocal bone disease is higher than for unifocal bone disease [22–24]. Regardless of the treatment approaches that vary from observation only to systemic chemotherapy, survival rates approaching 100% are reported for this disease form in almost all the published series. Therefore, the benefit of therapies should be evaluated in terms of localization and length of disease activity, and hence, risk of permanent consequences and quality of life. Unfortunately, due to discrepancy in anatomic bone lesions and outcome assessment, published data are difficult to compare and therefore no definitive conclusions can be reached. The most commonly used therapy for multifocal skeletal LCH consists of steroids and vinblastine (VBL), a relatively non-toxic, and well tolerated combination.

Single system skin involvement (isolated cutaneous LCH). LCH confined to the skin is rare and accounts for about 5% of the LCH population. It can occur at any age, but is most common in newborns and infants. In most of these cases LCH tends to regress spontaneously, but progression to MS-LCH is common. Therefore, close follow-up and reassessment of the need for treatment is warranted in all young patients with this disease form.

Cutaneous lesions can appear either as isolated nodules or as a skin rash; in patients with isolated nodules surgical excision may be indicated, but radical surgery is never warranted. In children with a skin rash, topical steroids are often suggested in standard textbooks, but their efficacy has never been proven. Moreover, most patients with isolated cutaneous LCH are often diagnosed after unsuccessful treatment with topical steroids for other presumed diagnoses such as eczema [25]. Topical caryolysine (20% nitrogen mustard ointment) has been shown to be effective on skin LCH [26]. Even with potential mutagenesis effect, no secondary tumor deleterious effect has been reported in relation to this drug for this indication. Unfortunately, it is not easily available and necessitates application by trained personnel.

In cases of ineffective local therapy or involvement of an extensive area, systemic therapy with steroids (±VBL), or oral low dose methotrexate can be used, but the level of evidence is low (D) [27–29]. In the most severe cases, treatments, including thalidomide associated with neurological toxicity, pain and fatigue [29], azathioprine, or PUVA-therapy which have been shown to be effective in some adult patients, might also be considered in children (evidence: D, agreement: 1).

Single System LCH of the Lymph Nodes

This is an extremely rare presentation of LCH [30]. Excision biopsy may be the only treatment required for a solitary lymph node.

Single system LCH of the lung (primary pulmonary LCH). This rare disease form occurs predominantly in adolescent and adult smokers. The impact of systemic therapy is not well documented in children, and adult pulmonologists do not consider it as the standard approach [12,13]. Smoking withdrawal is necessary, and usually results in significant clinical improvement and often complete resolution. However, isolated lung involvement can be very challenging due to the risk of acute severe complications such as pneumothorax, or cardiopulmonary arrest. Pneumothoraces should be treated by standard techniques such as drainage and possibly pleurodesis. Pleurectomy should be avoided as lung transplantation may ultimately be considered in patients with severe progressive disease. In case of persisting and progressive lung disease, systemic therapy with low dose steroids is most commonly used, but 2-chlorodeoxyadenosine (2-CdA), and the combination of VBL and steroids have also been used (evidence: D, agreement: 1).

Isolated diabetes insipidus and pituitary involvement. DI occurs due to involvement of the posterior pituitary (neurohypophysis) and may become manifest either before, concurrently, or after LCH diagnosis. Isolated DI is not considered an indication for systemic therapy *per se*, except when active disease is unequivocally documented by the presence of thickening of the pituitary stalk or a mass lesion of the hypothalamic-pituitary axis. A lesion of the hypothalamus–pituitary axis is usually considered as active if it had local neurological consequences like alteration

of the visual field or if its volume is increasing on sequential MRI. In the experience of experts, DI is with few exceptions uniformly irreversible, although DDAVP needs may vary.

There are some earlier anecdotal reports suggesting that treatment with 2-CdA [31], etoposide [32], or radiation [33,34] soon after DI onset may reverse the condition (evidence: D).

Brain lesions. In addition to pituitary stalk lesions, any brain, or meningeal lesion (except local reaction to a skull vault lesion) is considered an indication for systemic therapy. The standard therapy with vinblastine and steroid can be effective in this situation [35] or 2-CdA monotherapy [36].

Treatment of multisystem LCH. As mentioned before, the major clinical challenges of MS-LCH are mortality in young children with involvement of risk organs, and bouts of reactivation resulting in morbidity and permanent consequences which can occur in all age groups. Patients with risk organ involvement are at risk of death, and a poor response to therapy defines a subgroup with a particularly dismal prognosis. Patients without involvement of risk organs, although not at risk for mortality, need systemic therapy in order to control the disease activity, reduce reactivations, and reduce permanent consequences. Several international protocols for MS-LCH treatment have been designed within the framework of the HS [8–10]. Their main conclusions are (evidence: B, agreement: 2) (i) standard treatment is based on steroids and VBL, (ii) Clinical response after the first 6 weeks of treatment is a good marker of further disease evolution. (iii) Prolonged treatment for at least 1 year reduces the risk of disease reactivations.

Front Line Treatment and Evaluation of Response

Front line treatment of MS-LCH is based on the association of VBL 6 mg/m^2 i.v. weekly bolus for 6 weeks, with prednisone 40 mg/m^2/day given orally in three divided doses for 4 weeks and then tapered over the following 2 weeks. After the first 6 weeks of treatment, disease status should be reevaluated and treatment continued accordingly. The evaluation of the disease response is usually classified as "better" in case of complete resolution or regression of the disease, "worse" in case of progression of the disease, and "intermediate," in case of stable or mixed response with new lesions in one site, and regression in another site. Other evaluation methods have been proposed such as the disease activity score [37].

In case of a good response (especially in the risk organs) but with some active disease still present in other sites, treatment with VBL, and steroids should be continued for another 6 weeks with: VBL 6 mg/m^2 i.v. weekly bolus, and prednisone 40 mg/m^2/day orally in three divided doses for 3 days every week. One or two intensive courses according to the above mentioned schedule should be followed by maintenance therapy for a total duration of up to 12 months with VBL 6 mg/m^2 i.v. bolus every 3 weeks, and prednisone 40 mg/m^2/day orally in three divided doses for 5 days every 3 weeks and 6 MP at a dose of 50 mg/m^2/day is added if risk organ involvement is present.

Second Line Therapy

Refractory disease in patients with hematological involvement or liver dysfunction is a rare but life-threatening situation [10,38]. We suggest that such patients need to be referred to a specialized centre (evidence: D, agreement: 2). Therapeutic options (evidence: C) include combination chemotherapy with cladribine (2-CdA) and cytarabine (Ara-C) [39] or hematopoietic stem cell transplantation using reduced intensity conditioning regimen [40]. If there is evidence of disease progression in "non-risk organs," treatment with 2-CdA as monotherapy [41] or even with further courses of a combination of VBL and steroids should be considered.

Radiotherapy

Most experts in this field would no longer recommend radiotherapy due to the risk of long term sequelae, including the potential risk of developing a malignant tumor in the field of the radiotherapy [38]. However, there are some physicians who consider that radiotherapy may be useful for a single bone lesion in teenager (evidence: C, agreement: 2).

Neurodegenerative Complications

Neurodegenerative complications represent a complex situation and such patients need to be managed by a multidisciplinary team. Several therapies have been attempted but with possibly occasional transitory responses. The treatment options include: retinoic acid (evidence: C) [42], combination treatment with vincristine and Ara-C (evidence: C) [43], intravenous immunoglobulin (evidence: D) [44], and cladribine (evidence: D) [45]. To date, intensive therapies have not shown any effect and should thus be avoided, especially as they may add to the morbidity.

Monitoring and Supportive Care for Permanent Consequences

Although LCH is predominantly a benign and treatable disease, it can result in sequelae affecting various tissues involved [46]. Some may be present at diagnosis, while others may become manifest up to years and decades later. It is thus important to monitor these patients at least until growth is completed and possibly into adult life. The most common permanent consequences are endocrine, auditory, and orthopedic. Neurocognitive, pulmonary, and hepatic sequelae are rare but may cause significant morbidity. The recommended investigations and tests are shown in Table V. A scoring system for sequelae has been developed in order to observe the evolution and to standardize the recording of such problems [47].

Endocrine complications. DI is the most frequent endocrinopathy associated with LCH with a frequency from 15% to 30% of cases [30]. It is thus important to investigate thirst and polyuria in LCH patients, even many years after the diagnosis of LCH.

Growth hormone deficiency is the most frequent anterior pituitary hormone loss and occurs in up to 10% of patients. Measurement of height and weight and assessment of puberty is therefore recommended every 6 months or 1 year until growth is completed. Any child whose growth is below that expected may need to be investigated as suggested by the consensus guidelines of the GH Research Society [48].

Other hormone deficiencies may occur. These include delayed puberty and rarely panhypopituitarism. Puberty should be assessed according to Tanner stages and need investigation in the following cases: delayed onset of puberty (B2 >13 years in

TABLE V. Recommendations for Follow-Up of Patients With LCH After Diagnosis

Indication	Assesment
All patients	Routine assessment at clinically appropriate intervals including: History of thirst, polyuria Height, weight, pubertal status, neurological assesment FBC (CBC), ESR, Liver enzymes, Albumin
Bone involvement	X-ray oriented to the pathologic area at 6 weeks, 3 and 6 months and then depending on clinical findings
If vertebral involvement	Monitor for scoliosis especially during periods of rapid growth
If jaw involvement	Monitor dental development and jaw growth
Pulmonary involvement	Spirometry should be performed regularly (every 6–12 months) and if abnormal X-ray and high resolution computed tomography of chest may be needed
Endocrine involvement	
If endocrine signs and symptoms develops	See text for indications for endocrine testing and repeat depending on clinical findings and specialized advice
If proven hypothalamic-pituitary dysfunction	Head MRI, repeated after 1 year and then at 2, 4, 7, and 10 years
CNS involvement	
If neurological symptoms/signs develops	Neuropsychological tests, cerebellar function assessment and MRI of the head; repeat depending on clinical findings and specialized advice
If tumorous a lesion has been identified in the CNS	Repeat head MRI after 6 weeks (in symptomatic patients and those with tumorous lesions) and 3 months. Further images should be decided on the basis of the results of the first two examinations
If neurodegenerative findings on MRI, even without symptoms	Repeat head MRI is performed after 1 year and then at 2, 4, 7, and 10 years
Liver involvement	Consider ultrasound scan/MRI of liver or cholangiography and repeat depending on clinical findings and specialized advice
Ear/temporal bone involvement	Audiogram at end of treatment and reassessed at start of school and if any new symptoms develop

CT, computed tomography; MRI, magnetic resonance imaging, CBC, complete blood count; ESR, erytrocyte sedimentation rate; CNS, central nervous system; DI, diabetes insipidus, ENT: ear nose throat; BAL, broncho-alveolar lavage, GH, growth hormone.

girls, P2, T2 >14 years in boys), delayed onset of period in girls (>14 years), precocious puberty (B2 <8 years in girls, P2, T2 <9 years in boys), arrest, or regression of pubertal development.

In case of delayed growth/puberty, bone age should be assessed by X-ray, and anterior pituitary function tests should be performed to assess secretion of GH, LH, FSH, ACTH, and thyroid function. If hormone deficiency is confirmed by the stimulation tests, MRI scan of head (Appendix 1) should be performed. Bone mineral density (DEXA) scan needs to be monitored in patients with GH deficiency, delayed puberty, or panhypopituitarism.

Orthopedic. When several vertebrae are affected, scoliosis may become manifest later in life, in particular during periods of rapid growth such as puberty. Children should be assessed clinically at least annually in order to identify any early signs of scoliosis. They should be referred to the orthopedic surgeon in order to start preventive physical therapies (e.g., orthopedic corset/brace or neck collar) in order to manage this proactively. If facial bones are affected, facial asymmetry may become manifest and reconstructive surgery may be required.

Hearing. Subjects with involvement of the middle or inner ear and the temporal bone should be monitored with audiometry at diagnosis and at end of treatment and reassessed at start of school and if any new symptoms develop. Early diagnosis and interventional strategies such as hearing aids can avoid deterioration of school performance and significantly improve learning outcome.

Oral tissue and jaw. Children with involvement of gums and jaw should be monitored for dental development and growth of the jaw.

Neurological. Children with multisystem LCH should be regularly followed up clinically since they are at risk of developing late neuropsychological sequelae, in particular cerebellar ataxia and learning difficulties. In children with relevant history and/or abnormal neurological examination, further investigations including neuropsychological tests, cerebellar function assessment [49,50], and MRI of the head as described in Appendix 1 should be performed.

Lungs. In those with a history of lung involvement, spirometry should be performed regularly and if abnormal or progressive, X-ray and computed tomography of chest may be needed. The dangers of smoking should be explained and smoking avoided. Pulmonary involvement may also lead to respiratory insufficiency due to fibrosis and emphysema.

Liver. Liver involvement is rare, but can cause serious morbidity. In those with abnormal liver function consider ultrasound scan, MRI of liver, or cholangiography as clinically indicated. A subset of young children with liver involvement may subsequently develop sclerosing cholangitis that progresses to cirrhosis; treatment for these children includes liver transplantation.

Associated Malignancies

There is a recognized association between LCH and malignancies [17]. The malignancies may precede, occur concurrently or

follow the diagnosis of LCH and should be considered at every clinical visit. Acute lymphoblastic leukemia and lymphoma more often occur prior to the diagnosis of LCH but may be diagnosed within 5 years after LCH. Myeloid leukemias usually follow LCH especially in those patients exposed to etoposide, alkylating agents and/or radiotherapy. Solid tumors may occur concurrently or follow the diagnosis of LCH. Most of those that followed LCH developed in a previous radiation field. With the current treatment strategies it is expected that these types of secondary malignancy will be rare. Patients treated with radiotherapy should see their doctor in case of symptoms involving the irradiated area.

Follow-Up/Duration and Frequency

Recommendations for follow-up are shown in Table V. They are inspired by the long term follow-up for childhood cancer survivors [51,52]. Every patient should be followed by the local physician and if at any time a particular issue needs to be addressed, referral to a specialist is recommended. All patients should be followed for a sufficient time period, defined as (i) at least 5 years after the end of therapy; or (ii) 5 years after the last disease reactivation, in those who did not receive systemic therapy; or (iii) until final growth and pubertal development have occurred.

Perspectives. LCH is a rare disease potentially resulting in death or permanent sequelae. The burden of therapy may also be extremely heavy. There is an obvious need for a full assessment of each patient with a rational treatment tailored to the risks of the individual patient, which contributes to further fundamental and clinical research in this field.

In 2010, Badalian-Very et al. [53], reported somatic mutations of the BRAF oncogene in about half of the LCH patients in their series, and this finding was recently confirmed by other teams [54,55]. This discovery may have a significant potential impact if we consider the possibility of treating LCH with the new class of BRAF inhibitors. However, this promising discovery will need to be verified and concretized before these drugs can be used for treatment of LCH. The group(s) of LCH patients who may benefit from BRAF inhibitor treatment must be determined and balanced with toxicities as in the case of melanoma [56,57]. Knowledge about drug schedule and safety, especially long-term effects [57] and mechanisms of resistance [58] must be acquired.

Progress may be expected from collaborations organized at national and international levels, among specialist groups and expert networks. Collection of tissue and blood samples in biobanks is essential for improving the understanding of the biology of this rare and fascinating condition. New international protocols will soon be opened and continue to represent an opportunity to develop global research in LCH (see www.histiocytesociety.org and www.histio.net).

Euro Histio Net Partners—Institutions. Euro Histio Net is a project funded by the European Commission/DG Sanco and associated both medical institutions and patients associations as listed below. 1 Reference Centre for Histiocytosis, Hopital Trousseau, Assistance Publique – Hopitaux de Paris, France. Jean Donadieu, MD, PhD, Coordinator, Abdelatif Tazi, MD, PhD, Jean François Emile, MD, PhD, Milen Minkov, MD, PhD, Associated Partners, 2 Hospital Universitario Cruces Barakaldo, Spain. Itziar Astigarraga, MD, Associated Partner, 3 Children's Cancer Research Institute, St. Anna Children's Hospital, Vienna, Austria. 4 Istituto G. Gaslini, Genova, Italy. Riccardo Haupt, MD, Associated Partner, 5 Johns Hopkins, Baltimore, Maryland, USA. Robert J. Arceci, MD, PhD, Collaborating Partner, 6 Azienda Ospedaliero-Universitaria Meyer, Firenze, Italy. Maurizio Aricò, MD, PhD, Collaborating Partner, 7 Elisabethinen Hospital, Linz, Austria. Michael Girschikofsky, MD, Collaborating Partner, 8 Karolinska Institutet, Stockholm, Sweden. Jan-Inge Henter, MD, PhD, Collaborating Partner, 9 Children's University Hospital, Hamburg, Germany. Gritta Janka, MD, PhD, Collaborating Partner, 10 Hotel Dieu de France Hospital, Beirut, Lebanon. Claudia Djambas Khayat, MD, Collaborating Partner, 11 Hellenic Air Force & Veterans General Hospital, Athens, Greece. Polyzois Makras, MD, PhD, Collaborating Partner, 12 Hospital de Clínicas de Porto Alegre, Brasil. Mariana Michalowski, MD, Collaborating Partner, 13 Watford General Hospital, Watford, UK. Vasanta Nanduri, MD, Collaborating Partner, 14 Dana Farber Cancer Institute and Childrens Hospital, Boston, Massachusetts, USA. Carlos Rodriguez-Galindo, MD, Collaborating Partner, 15 Medical University Plovdiv, Bulgaria. Mariya Spasova, MD, PhD, Associate Professor, Collaborating Partner, 16 University Pediatric Hospital, Lublin, Poland. Maria Jolanta Stefaniak, MD, PhD, Collaborating Partner, 17 UZ Leuven, Leuven, Belgium. Stefaan Van Gool, MD, PhD, Collaborating Partner, 18 University Hospitals of Leicester, Leicester Royal Infirmary Childrens Hospital, Leicester, United Kingdom. Johann Visser, MD, Collaborating Partner, 19 Hospital for Sick Children, Toronto, Ontario, Canada. Sheila Weitzman, MD, Collaborating Partner, 20 Newcastle University, Newcastle, United Kingdom. Kevin Patrick Windebank, MD, Collaborating Partner, 21 Clinique Al Madina, Casablanca, Morocco. Saadia Zafad, MD, PhD, Collaborating Partner.

Euro Histio Net Partners—Patient Associations. 1 The Histiocytosis Research Trust, United Kingdom, www.hrtrust.org Associated Partner; 2 Artemis Association on Histiocytoses, Greece, www.histioartemis.gr Collaborating Partner; 3 Asociacion Espanola contra la Histiocitosis de celulas de Langerhans (ACHE), Spain, www.histiocitosis.org Collaborating Partner; 4 Association Histiocytose France (A.H.F.), France, www.histiocytose.org Collaborating Partner; 5 Associazione italiana ricerca istiocitosi (AIRI LCH onlus), Italy, www.istiocitosi.org Collaborating Partner; 6 Erwachsenen Histiozytose X e.V (EHX e.V.)., Germany, www.histiozytose.com Collaborating Partner; 7 Föräldraföreningen För Histiocytos (Ffh), Sweden, www.histiocytos.se Collaborating Partner; 8 Histiocytosis Association of America (HAA), USA, www.histio.org Collaborating Partner; 9 Histiozytosehilfe e.V., Germany, www.histiozytose.org Collaborating Partner; 10 LCH-Belgium, Belgium, www.lch.be Collaborating Partner; 11 The ECD Global Alliance, USA, www.erdheim-chester.org Collaborating Partner.

REFERENCES

1. Guyatt GH, Oxman AD, Vist GE, et al. GRADE: An emerging consensus on rating quality of evidence and strength of recommendations. BMJ 2008;336:924–926.
2. Guyatt GH, Oxman AD, Sultan S, et al. GRADE guidelines: 9. Rating up the quality of evidence. J Clin Epidemiol 2011;64:1311–1316.
3. Chikwava K, Jaffe R. Langerin (CD207) staining in normal pediatric tissues, reactive lymph nodes, and childhood histiocytic disorders. Pediatr Dev Pathol 2004;7:607–614.
4. Lau SK, Chu PG, Weiss LM. Immunohistochemical expression of Langerin in Langerhans cell histiocytosis and non-Langerhans cell histiocytic disorders. Am J Surg Pathol 2008;32:615–619.
5. Swerdlow SH, Campo E, Harris NL, et al. WHO classification of tumours of haematopoietic and lymphoid tissues, 4th edition. Lyon: IARC press; 2008.
6. Valladeau J, Ravel O, zutter-Dambuyant C, et al. Langerin, a novel C-type lectin specific to Langerhans cells, is an endocytic receptor that induces the formation of Birbeck granules. Immunity 2000;12:71–81.

7. Jaffe R. The diagnostic histopathology of Langerhans cell histiocytosis. In: Weitzman S, Egeler M, editors. Histiocytic disorders of children and adults. Cambridge, UK: Cambridge University Press; 2005. pp. 14–39.
8. Gadner H, Grois N, Arico M, et al. A randomized trial of treatment for multisystem Langerhans' cell histiocytosis. J Pediatr 2001;138:728–734.
9. Gadner H, Grois N, Potschger U, et al. Improved outcome in multisystem Langerhans cell histiocytosis is associated with therapy intensification. Blood 2007;111:2556–2562.
10. Minkov M, Grois N, Heitger A, et al. Response to initial treatment of multisystem Langerhans cell histiocytosis: An important prognostic indicator. Med Pediatr Oncol 2002;39:581–585.
11. Ronceray L, Potschger U, Janka G, et al. Pulmonary involvement in pediatric-onset multisystem langerhans cell histiocytosis: Effect on course and outcome. J Pediatr 2012;161:129–133.
12. Tazi A, Soler P, Hance AJ. Adult pulmonary Langerhans' cell histiocytosis. Thorax 2000;55:405–416.
13. Vassallo R, Ryu JH, Colby TV, et al. Pulmonary Langerhans'-cell histiocytosis. N Engl J Med 2000;342:1969–1978.
14. Braier J, Latella A, Balancini B, et al. Outcome in children with pulmonary Langerhans cell histiocytosis. Pediatr Blood Cancer 2004;43:765–769.
15. Donadieu J, Rolon MA, Thomas C, et al. Endocrine involvement in pediatric-onset Langerhans' cell histiocytosis: A population-based study. J Pediatr 2004;144:344–350.
16. Grois N, Potschger U, Prosch H, et al. Risk factors for diabetes insipidus in Langerhans cell histiocytosis. Pediatr Blood Cancer 2006;46:228–233.
17. Haupt R, Nanduri VR, Egeler RM. Late effects of Langerhans cell histiocytosis and the association of LCH with malignancy. In: Egeler RM, Weitzman S, editor. Histiocytic disorders in children and adults. Cambridge, UK: Cambridge University Press; 2005.
18. Grois N, Fahrner B, Arceci RJ, et al. Central nervous system disease in Langerhans cell histiocytosis. J Pediatr 2010;156:873–881, 881.
19. Berry DH, Gresik M, Maybee D, et al. Histiocytosis X in bone only. Med Pediatr Oncol 1990;18: 292–294.
20. Egeler RM, Thompson RC, Jr., Voute PA, et al. Intralesional infiltration of corticosteroids in localized Langerhans' cell histiocytosis. J Pediatr Orthop 1992;12:811–814.
21. Roger G, Dupre M, Leboulanger N, et al. Cholesteatoma secondary to temporal bone involvement by Langerhans cell histiocytosis: A complication amenable to curative surgery. Otol Neurotol 2009;30:190–193.
22. Dimentberg RA, Brown KL. Diagnostic evaluation of patients with histiocytosis X. J Pediatr Orthop 1990;10:733–741.
23. Raney RB, Jr., D'Angio GJ. Langerhans' cell histiocytosis (histiocytosis X): Experience at the Children's Hospital of Philadelphia, 1970–1984. Med Pediatr Oncol 1989;17:20–28.
24. Sessa S, Sommelet D, Lascombes P, et al. Treatment of Langerhans-cell histiocytosis in children. Experience at the Children's Hospital of Nancy. J Bone Joint Surg Am 1994;76:1513–1525.
25. Krafchik B, Pope E, Walsh SRA. Histiocytosis of the skin in children and adults. In: Weitzman S, Egeler M, editors. Histiocytic disorders of children and adults. Cambridge, UK: Cambridge University Press; 2005. pp. 130–153.
26. Hadfield PJ, Birchall MA, Albert DM. Otitis externa in Langerhans' cell histiocytosis—The successful use of topical nitrogen mustard. Int J Pediatr Otorhinolaryngol 1994;30:143–149.
27. Steen AE, Steen KH, Bauer R, et al. Successful treatment of cutaneous Langerhans cell histiocytosis with low-dose methotrexate. Br J Dermatol 2001;145:137–140.
28. Womer RB, Anunciato KR, Chehrenama M. Oral methotrexate and alternate-day prednisone for low-risk Langerhans cell histiocytosis. Med Pediatr Oncol 1995;25:70–73.
29. McClain KL, Kozinetz CA. A phase II trial using thalidomide for Langerhans cell histiocytosis. Pediatr Blood Cancer 2007;48:44–49.
30. Donadieu J, Egeler M, Pritchard J. Langerhans cell histiocytosis: A clinical update. In: Weitzman S, Egeler M, editors. Histiocytic disorders of children and adults. Cambridge, UK: Cambridge University Press; 2005. pp. 95–129.
31. Ottaviano F, Finlay JL. Diabetes insipidus and Langerhans cell histiocytosis: A case report of reversibility with 2-chlorodeoxyadenosine. J Pediatr Hematol Oncol 2003;25:575–577.
32. Broadbent V, Pritchard J. Diabetes insipidus associated with Langerhans cell histiocytosis: Is it reversible? Med Pediatr Oncol 1997;28:289–293.
33. Minehan KJ, Chen MG, Zimmerman D, et al. Radiation therapy for diabetes insipidus caused by Langerhans cell histiocytosis. Int J Radiat Oncol Biol Phys 1992;23:519–524.
34. Rosenzweig KE, Arceci RJ, Tarbell NJ. Diabetes insipidus secondary to Langerhans' cell histiocytosis: Is radiation therapy indicated? Med Pediatr Oncol 1997;29:36–40.
35. Ng Wing TS, Martin-Duverneuil N, Idbaih A, et al. Efficacy of vinblastine in central nervous system Langerhans cell histiocytosis: A nation wide retrospective study. Orphanet J Rare Dis 2011;6:83.
36. Dhall G, Finlay JL, Dunkel IJ, et al. Analysis of outcome for patients with mass lesions of the central nervous system due to Langerhans cell histiocytosis treated with 2-chlorodeoxyadenosine. Pediatr Blood Cancer 2008;50:72–79.
37. Donadieu J, Piguet C, Bernard F, et al. A new clinical score for disease activity in Langerhans cell histiocytosis. Pediatr Blood Cancer 2004;43:770–776.
38. The French Langerhans' Cell Histiocytosis Study Group. A multicentre retrospective survey of Langerhans' cell histiocytosis : 348 cases observed between 1983 and 1993. Arch Dis Child 1996; 75:17–24.
39. Bernard F, Thomas C, Bertrand Y, et al. Multi-centre pilot study of 2-chlorodeoxyadenosine and cytosine arabinoside combined chemotherapy in refractory Langerhans cell histiocytosis with haematological dysfunction. Eur J Cancer 2005;41:2682–2689.
40. Steiner M, Matthes-Martin S, Attarbaschi A, et al. Improved outcome of treatment-resistant high-risk Langerhans cell histiocytosis after allogeneic stem cell transplantation with reduced-intensity conditioning. Bone Marrow Transplant 2005;36:215–225.
41. Weitzman S, Braier J, Donadieu J, et al. 2′-Chlorodeoxyadenosine (2-CdA) as salvage therapy for Langerhans cell histiocytosis (LCH). Results of the LCH-S-98 protocol of the histiocyte society. Pediatr Blood Cancer 2009;53:1271–1276.
42. Idbaih A, Donadieu J, Barthez MA, et al. Retinoic acid therapy in "degenerative-like" neuro-Langerhans cell histiocytosis: A prospective pilot study. Pediatr Blood Cancer 2004;43:55–58.
43. Allen CE, Flores R, Rauch R, et al. Neurodegenerative central nervous system Langerhans cell histiocytosis and coincident hydrocephalus treated with vincristine/cytosine arabinoside. Pediatr Blood Cancer 2009;54:416–423.
44. Gavhed D, Laurencikas E, Akefeldt SO, et al. Fifteen years of treatment with intravenous immunoglobulin in central nervous system Langerhans cell histiocytosis. Acta Paediatr 2011;100:e36–e39.
45. Buchler T, Cervinek L, Belohlavek O, et al. Langerhans cell histiocytosis with central nervous system involvement: Follow-up by FDG-PET during treatment with cladribine. Pediatr Blood Cancer 2005;44:286–288.
46. Haupt R, Nanduri V, Calevo MG, et al. Permanent consequences in Langerhans cell histiocytosis patients: A pilot study from the Histiocyte Society-Late Effects Study Group. Pediatr Blood Cancer 2004;42:438–444.
47. Nanduri VR, Pritchard J, Levitt G, et al. Long term morbidity and health related quality of life after multi-system Langerhans cell histiocytosis. Eur J Cancer 2006;42:2563–2569.
48. GH Research Society. Consensus guidelines for the diagnosis and treatment of growth hormone (GH) deficiency in childhood and adolescence: Summary statement of the GH Research Society. GH Research Society. J Clin Endocrinol Metab 2000;85:3990–3993.
49. Schmahmann JD, Gardner R, MacMore J, et al. Development of a brief ataxia rating scale (BARS) based on a modified form of the ICARS. Mov Disord 2009;24:1820–1828.
50. Trouillas P, Takayanagi T, Hallett M, et al. International Cooperative Ataxia Rating Scale for pharmacological assessment of the cerebellar syndrome. The Ataxia Neuropharmacology Committee of the World Federation of Neurology. J Neurol Sci 1997;145:205–211.
51. Curry HL, Parkes SE, Powell JE, et al. Caring for survivors of childhood cancers: The size of the problem. Eur J Cancer 2006;42:501–508.
52. Kenney LB, Bradeen H, Kadan-Lottick NS, et al. The current status of follow-up services for childhood cancer survivors, are we meeting goals and expectations: A report from the Consortium for New England Childhood Cancer Survivors. Pediatr Blood Cancer 2011;57:1062–1066.
53. Badalian-Very G, Vergilio JA, Degar BA, et al. Recurrent BRAF mutations in Langerhans cell histiocytosis. Blood 2010;116:1919–1923.
54. Satoh T, Smith A, Sarde A, et al. B-RAF mutant alleles associated with Langerhans cell histiocytosis, a granulomatous pediatric disease. PLoS ONE 2012;7:e33891.
55. Haroche J, Charlotte F, Arnaud L, et al. High prevalence of BRAF V600E mutations in Erdheim–Chester disease but not in other non-Langerhans cell histiocytoses. Blood 2012;120:2700–2703.
56. Phillips M, Allen C, Gerson P, et al. Comparison of FDG-PET scans to conventional radiography and bone scans in management of Langerhans cell histiocytosis. Pediatr Blood Cancer 2009;52: 97–101.
57. McClain K, Ramsay NK, Robison L, et al. Bone marrow involvement in histiocytosis X. Med Pediatr Oncol 1983;11:167–171.
58. Minkov M, Potschger U, Grois N, et al. Bone marrow assessment in Langerhans cell histiocytosis. Pediatr Blood Cancer 2007;49:694–698.
59. Favara BE, Jaffe R, Egeler RM. Macrophage activation and hemophagocytic syndrome in Langerhans cell histiocytosis: Report of 30 cases. Pediatr Dev Pathol 2002;5:130–140.
60. Galluzzo ML, Braier J, Rosenzweig SD, et al. Bone marrow findings at diagnosis in patients with multisystem Langerhans cell histiocytosis. Pediatr Dev Pathol 2010;13:101–106.

EXPERT OPINION

Medical management of langerhans cell histiocytosis from diagnosis to treatment

Jean Donadieu†, François Chalard & Eric Jeziorski
†*Centre de Référence des Histiocytoses, Registre Français des Histiocytoses, Service d'Hémato Oncologie Pédiatrique, Hopital Trousseau, Paris, France*

Introduction: Langerhans cell histiocytosis (LCH) is a heterogeneous disease, involving the accumulation of langerhans cells in various organs. The physician's perception of the disease varies considerably depending on their experience, the presentation of the disease or the short-term treatment outcome. As this disease is very rare, only a limited number of large surveys exist in the literature and many aspects of the management of patients remain obscure or controversial.

Areas covered: An expert opinion on the diagnosis and medical management of LCH is presented in this paper. The diagnostic procedures, including differential diagnosis, initial clinical workup and criteria for initiating therapy are reviewed, as well as disease evaluation criteria and therapeutic approaches. Controversial issues in the medical management of LCH patients (aged less than 18 years) are also briefly discussed.

Expert opinion: Further fundamental and clinical research is still needed in this field. Progress may be expected from collaborations organized at national and international levels, among collaborative groups and expert networks. Collections of tissue and blood samples in biobanks must also be organized. New international protocols will be opened to patient accrual and represent an opportunity to further develop global research.

Keywords: clinical workup, diagnosis, follow-up, guidelines, Langerhans cell histiocytosis, therapy

Expert Opin. Pharmacother. (2012) 13(9):1309-1322

1. Introduction

Langerhans cell histiocytosis (LCH) is a heterogeneous disease, involving the accumulation of langerhans cells in various organs. It may affect any organ or system of the body, but those more frequently affected are bone (80% of cases), skin (33%) and the pituitary (25%). Other organs involved are the liver, spleen, the hematopoietic system and the lungs (15% each), lymph nodes (5 – 10%) and the central nervous system (CNS) excluding the pituitary (2 – 4%). The natural history of the disease is also extremely heterogeneous, ranging from a self-healing lesion to a disease involving several organs with life-threatening consequences, while some lesions may be responsible for permanent sequelae. The physician's perception of the disease varies considerably depending on their specialty and experience, the presentation of the disease or the short-term treatment outcome. But whatever the initial point of view of the treating physician, a global approach to the management of LCH is recommended. However, as this disease remains very rare, only a limited number of large surveys exist in the literature [1-5], and many aspects of the management of patients remain obscure or controversial. A multidisciplinary approach is warranted in all cases, to coordinate the care needed for this systemic disease and its associated morbidity. This short text proposes to summarize the major issues related to the medical management of the disease in order to provide a consistent body of data.

informa
healthcare

10.1517/14656566.2012.688028 © 2012 Informa UK, Ltd. ISSN 1465-6566

Article highlights.

- Langerhans cell histiocytosis is a rare multisystemic disease.
- The diagnostic needs a concordance of clinical radiological histological findings.
- Initial workup is a two-step procedure.
- The first step of the workup procedure is a thorough clinical examination followed by few routine tests.
- The second step of initial workup is based on organ evaluation if suspected by the first-step screening.
- Therapy is adapted to the extension of the disease.
- First-line therapy, if necessary, is associated vinblastine and steroid.
- Scoring system helps physicians for therapeutic evaluation.
- B raf mutations have a high frequency in LCH.

This box summarizes key points contained in the article.

2. Diagnosis of langerhans cell histiocytosis

In addition to clinical and radiological features, the diagnosis of LCH is based on histological and immuno-phenotypic examination of a biopsy of lesional tissue. The biopsy should be taken from the most accessible organ: skin if involved. In the case of multiple skeletal involvements, the bony lesion that is most easily accessible and felt to be active and representative should be chosen for biopsy. The main diagnostic feature is the morphologic identification of the characteristic LCH cells, but positive staining of lesional cells with CD1a and/or Langerin (CD207) is required for a definitive diagnosis [6-9]. Electron microscopy is no longer recommended since it has been shown that the expression of Langerin fully correlates with the presence on electron microscopy of Birbeck granules, which was previously one of the criteria required for definitive diagnosis. There are very few exceptions; however, in organs such as the liver, Birbeck granules are not present and CD1a and/or Langerin may be negative [10].

In some rare situations, where the location of the only lesion means that the risk of biopsy may outweigh the need for a definitive diagnosis, the risk versus benefit of biopsy should be carefully considered. This is the case in patients with involvement of a vertebral body without adjacent soft tissue involvement, such as cases of isolated involvement of the odontoid peg, for example. However, if the decision to omit or postpone a biopsy is made, every effort should be made to consider other clinical conditions that might lead to a similar radiological finding and close follow-up is warranted.

3. Differential diagnoses

Diagnosis should always be based on concordant clinical–radiological–pathological evidence, and the physician needs to be aware of possible alternative diagnoses. Thus, typical bone lesions (such as a punch-out lytic lesion on the skull) can mimic a dermoid cyst, a vertebra plana can mimic an Ewing's sarcoma and typical cysts in the lung can be a leiomyosarcoma. Even infiltration of histiocytes on a skin biopsy with CD1a staining can result from scabies rather than LCH. The list of potential alternative diagnosis is long and largely depends on location and the specific organ involved (Table 1). When considering the diagnosis of LCH, the physician must be cautious and keep in mind the necessity to carefully evaluate clinical, radiological and pathological data in order to determine whether the disease presented by the patient is really consistent with LCH.

4. Evaluation of the extent of disease at diagnosis or during episodes of reactivation

Once a diagnosis of LCH has been ascertained, it is important to do a careful clinical workup for each individual patient in order to decide on the therapeutic approach.

The first step of this evaluation is a review of the complete medical history including special reference to the nature and duration of symptoms. Specific symptoms to be actively looked for are pain, swelling, skin rashes, otorrhea, irritability, fever, loss of appetite, diarrhea, weight loss or poor weight gain, growth failure, polydipsia, polyuria, changes in activity level, dyspnea, smoke exposure, and behavioral and neurological changes. Examination should be performed at each follow-up visit in order to assess response to therapy, investigate possible disease progression or reactivation, as well as to detect sequelae.

The second step of this evaluation is a routine paraclinical screening. In the absence of a specific biological marker of disease activity, the list of mandatory paraclinical tests is limited and includes a complete blood count, liver tests (including albumin, bilirubin, gamma glutamyl transpeptidase, serum glutamic-oxaloacetic transaminase (SGOT) and serum glutamic-pyruvic transaminase (SGPT)), erythrocyte sedimentation rate (ESR) or C-reactive protein (CRP) levels, a chest X-ray and bone X-ray. Usually, a radiographic skeletal survey is performed at diagnosis, whereas in cases of disease reactivation, X-rays are focused on the anatomic region(s) with clinical symptoms. Abdominal ultrasound may be useful in babies; however, the liver and spleen size should be evaluated clinically.

Other techniques such as technetium scintigraphy [11], positron emission tomography (PET) scan [12], whole-body magnetic resonance imaging (MRI) [13] have been proposed, but remain not currently recommended. In order to decide which of these techniques to employ, two broad principles may be considered: the principle of parsimony, which advocates for strictly the minimum number of examinations needed in order to make a medical decision; and the principle of exhaustivity, which tends to use all available techniques in order to have an exhaustive count and description of all anatomic involvement in the disease. To resolve this dichotomy, it is important to assess what added value, in terms of patient care and treatment decisions, arises from the detection of

Table 1. Differential diagnosis for manifestations of langerhans cell histiocytosis.

Involvement	Manifestation	Possible other condition
Skin	Vesicles and bullae (most common in early infancy)	Erythema toxicum Herpes simplex Chickenpox infection
	Dermatitis (most frequently scalp, diaper or axilla, may occur up to late infancy)	Seborrheic dermatitis (eczema; usually no petechiae and marked scaling)
	Nodules	Mastocytosis Juvenile xanthogranuloma Neuroblastoma Infant leukemia
	Pruritus (more common), Petechiae (uncommon)	Scabies (other family members may be affected) [62] Dermatopathic nodes and dermatopathic lesions [63]
Bone	Vertebra plana	Ewing sarcoma Septic osteomyelitis Chronic relapsing multifocal osteomyelitis (CRMO) Leukemia Lymphoma Aneurysmal bone cyst Juvenile xanthogranuloma Myeloma (only described in adults) Osteoporosis
	Temporal bone	Chronic otitis media Mastoiditis Cholesteatoma Soft tissue sarcoma
	Orbit	Acute infection (preseptal cellulitis) Dermoid cyst Rhabdomyosarcoma Neuroblastoma Pseudoinflammatory tumor
	Other lytic lesions of the long bones	Parasitosis like difilariosis [64] Osteomyelitis Chronic relapsing multifocal osteomyelitis Aneurysmal bone cyst Bone angiomatosis (Gorham disease) Fibrous dysplasia Atypical mycobacterial infection Osteogenic sarcoma Ewing's sarcoma
Lung	In particular systemic symptoms and cavitated pulmonary nodules	Pneumocystis Carinii cavitated infection Mycobacterial or other pulmonary infections Sarcoidosis Bronchiolar-alveolar carcinoma (only described in adults) Lymphangio-Leiomyosarcoma (only described in young adult women) Septic emboli
Pituitary	Central diabetes insipidus	Dysgerminoma Idiopathic central diabetes insipidus [65,66]
Liver	Jaundice with direct hyperbilirubinemia Hypoalbuminemia	Chronic destructive cholangitis Metabolic disease Hepatitis Neoplasia obstructing biliary tract Inherited deficient conjugation of bilirubin Toxic (Reye syndrome) Chronic inflammatory bowel disease Neonatal hemochromatosis
Anemia Thrombocytopenia	Hematophagocytic syndrome with hepato splenomegaly	Familial Hemophagocytic Lymphohistiocytosis [67]

any given lesion, particularly bone extensions. To our best knowledge, no study has demonstrated that disease outcome is related to the total number of locations of the disease in the body. Indeed, the anatomic site itself (particularly for bone involvement), the volume of associated soft tissue involvement and degree of local destruction have a more clear impact on disease outcome that the actual number of bones involved. Lastly, it is important to consider that all 'new' techniques have a cost for the health system and may add to radiation exposure or inconvenience to the patient, such as general anesthesia for whole-body MRI in young children. The conclusion of this scientific debate has not yet been reached, but so far, the parsimony principle is commonly recommended. The only exception to date is the complete bone X-ray survey, which is still recommended at diagnosis for all patients.

Whatever the final choice to evaluate the bone lesions in a patient with LCH, it is very strongly not recommended to change the method of evaluation during the course of a given patient, as it may lead to discrepancy between assessments. It is important also to consider, during follow-up, limiting the evaluation to the anatomic region initially involved.

The third step of the evaluation process is targeted imaging or specialized clinical assessments for precise evaluation of specific involvement. A history of polyuria or polydipsia requires an early-morning urine sample for determination of specific gravity and osmolality, a blood electrolytes test and a water deprivation test, if possible. Other suspected endocrine abnormalities (i.e., short stature, growth failure, hypothalamic syndromes, precocious or delayed puberty) need a complete endocrine workup.

Bicytopenia, pancytopenia or persistent unexplained single cytopenia requires analysis of hemophagocytic biological features (coagulation, including fibrinogen, triglycerides and ferritin), bone marrow aspiration and trephine biopsy to exclude causes other than LCH.

Liver dysfunction requires abdominal ultrasound and the advice of a hepatologist. Liver MRI currently appears preferable to retrograde cholangiography in cases of frank liver dysfunction (liver enzymes > 5 times normal and/or bilirubin > 5 times normal range). Liver biopsy is only recommended if there is clinically significant liver involvement and if the test results will affect treatment decisions (i.e., to differentiate between active LCH and sclerosing cholangitis).

In case of abnormal chest X-ray or symptoms/signs suggestive of lung involvement, or lung findings not characteristic of LCH, or suspicion of an atypical infection, a lung evaluation is needed using high-resolution computed tomography (HR-CT) or, preferably, low-dose multi-detector HR-CT if available, and also a lung function test (if age appropriate). Bronchoalveolar lavage (BAL) may be useful to exclude other condition such as infections and may offer in addition to HR-CT, a positive argument for LCH involvement if the case of false-positive CD1a staining is excluded [14]. Finally, lung biopsy is useful if the diagnosis is not ascertained by another method. Vertebral lesions require MRI of the spine to exclude spinal cord compression and to assess for soft tissue masses. Any visual or neurological abnormalities need neurological and neuropsychometric assessment. Aural discharge or suspected hearing impairment/mastoid involvement requires a formal hearing assessment, MRI of the head and HR-CT of the temporal bone. Unexplained chronic diarrhea, failure to thrive, or malabsorption requires endoscopy with multiple biopsies.

4.1 Cranial MRI in LCH patients

To date, MRI of the head is not recommended for all patients with LCH, but only for those patients with neurological symptoms, pituitary dysfunction or patients with skull or facial bone lesions. If performed, the MRI protocol must be able to investigate the entire brain, the hypothalamus–pituitary axis and all craniofacial bones. The aim of the MRI is to systematically seek any neurodegenerative involvement and/or tumorous lesions and meningeal involvement [15,16]. The use of an intravenous contrast agent (gadolinium chelate) is mandatory. The following protocol is recommended: axial and sagittal T_1-weighted slices of the entire brain, fine T_1-weighted sagittal slices focused on the pituitary gland (3 mm/ 0.3 mm or below), axial T_2-weighted and fluid attenuated inversion (FLAIR) slices (except in patients aged less than 1 year) of the entire brain. The option 'contrast by magnetic transfer' is not recommended. However, if this is used, the same technique must be used at each subsequent evaluation and this information must be specified on the report. After injection of the gadolinium agent, the MRI scan should be performed according to data obtained from the first series (T_1-weighted slices): fine sagittal slices of the pituitary and coronal slices of the brain. Additional sequences may be taken if indicated.

Regarding the frequency of routine MRI surveillance in cases with positive findings at the initial MRI scan, the following recommendations are offered. If a CNS lesion has been identified, it is suggested to repeat the examination after 6 weeks (in symptomatic patients and those with tumorous lesions) and at 3 months. A decision to conduct further images should be made on the basis of the results of the first two examinations. In case of clinical hypothalamic dysfunction or neurodegenerative findings on MRI, even in the absence of symptoms, it is suggested to perform a second MRI after 1 year and then at 2, 4, 7 and 10 years. If after 10 years there is no clinical deterioration, further MRI is recommended only upon clinical indication.

5. Definition of organ involvement/definition of risk organs, CNS risk organ and special sites in langerhans cell histiocytosis

Once a diagnosis of LCH is determined in one organ by histopathology, it is not mandatory to confirm the involvement of other organs using a pathology method. The definitions

of organ involvement are listed in Table 2. Among all organs potentially involved in LCH, some organs are considered as risk organs. In medicine in general, the term 'risk organ' means that in a patient with disease involvement in one organ, there is a higher risk of complication than in patients who do not have involvement in that 'risk organ.' In LCH, there are two different meanings included in the word 'risk': the risk of death and the risk of a neurodegenerative complication.

The organs or systems in which disease involvement may lead to death are well defined in the literature; in children the main one is the hematological system, which almost always is associated with spleen and liver involvement [2,3,5,17]. The lung has been considered for several years as a 'vital' risk organ, and there is general agreement that lung involvement can considerably worsen the prognosis and is, therefore, a mortality risk for the patient [14,18]. However, lung involvement is, in children, rarely the sole cause of death, and when it is a cause of death, it is almost always for 'mechanical complications' not accessible to any systemic therapy, such as untreatable pneumothorax [19]. This is why lung involvement is no longer considered a 'risk organ' in clinical trials for LCH [20].

The CNS risk lesion, also coined a 'special site,' is a more recent concept [21] and has been used in the Histiocyte Society protocol LCH III. The risk involved here is the development of a neurodegenerative LCH, which is a dramatic and irreversible complication associating a clinical symptomatology and typical MRI features [22,23]. The literature does not define this risk directly, and to date two aspects have been reported. First, diabetes insipidus (DI) – that is, pituitary involvement – is associated with neurodegeneration such that about 95% of clinical neurodegenerative syndrome cases have DI; the risk of neurodegeneration in patients with DI is approximately 15% compared with 1% in patients without DI [24]. Second, there is a statistical association between disease involvement in certain organs and occurrence of DI [21,24,25]. By extension, these organs have been considered as 'CNS risk lesions' based on the assumption that DI is a surrogate marker of neurodegenerative histiocytosis [21]. Among the studies that have addressed this question [21,24,25], head bone involvement was shown to be always associated with the occurrence of DI. However, two studies had considered all skull bones together [24,25], while another study evaluated the facial bones separately from vault bone [21], excluding vault bone from the definition of special sites, even if involvement of the same occipital bone or frontal bone could be considered either as a vault lesion or as a skull base lesion. The association of pneumothorax and sclerosing cholangitis with DI was found in one study [24], but not evaluated in others. Finally, one study excluded patients with inaugural DI (i.e., DI onset before or at the same time as extra-pituitary involvement), despite the fact that they represent 50% of DI cases [21]. Indeed, the definition of CNS risk organ is not consensual and remains an extrapolation of epidemiological studies. So far, neurodegenerative lesion in LCH cannot be predicted at the diagnosis of LCH by any method in a reliable way.

6. Clinical classification

LCH has been classified in several ways and several synonyms have been used such as eosinophilic granuloma, Hand-Schuller-Christian syndrome, Letterer–Siwe syndrome, Hashimoto–Prizker syndrome, all of which are quite frequently used. In actual fact, the border between different disease entities is not strict, and so far, despite the heterogeneous presentation of the disease, it is still pertinent to consider LCH as a unique disease with various extensions and various outcomes. As several reactivations may occur during the course of the disease, the extension of the disease through the body may increase from initial presentation to the maximal extent. The current classification differentiates single system disease and multisystem disease. This classification is applied at diagnosis of the disease, even if the final extent of the disease may be different [26]. In single-system LCH (SS-LCH), one organ or system is involved such as unifocal bone (single bone), multifocal bone (more than one bone), skin, lymph node (not the draining lymph node of another LCH lesion), lungs, hypothalamic–pituitary/CNS or others such as thyroid or thymus. In multisystem LCH (MS-LCH), two or more systems are involved that may include 'risk organs' (hematopoietic system, spleen and/or liver) or not (for example skin and bone, or skin and pituitary).

6.1 Evaluation of disease activity

LCH can cause both acute complications and permanent sequelae. At least 10 separate organs can be directly involved (bone, skin, liver, spleen, lung, hematopoietic system, pituitary, brain, lymph nodes, mucosa) while others can be affected by proximity. Some involvements appear to be almost irreversible once they are observed. Indeed isolated pituitary involvement can constitute both a reactivation of disease, when it occurs late in the course of the disease, and at the same time, a permanent consequence. A single bone involvement can be highly symptomatic, with dramatic local consequences (such as deafness in the case of a massive temporal bone lesion) while multiple bone lytic lesions in silent anatomic areas may have no consequences. Finally, the healing 'speed' of bone lesions depends on the criteria used to evaluate it. Our understanding of this important aspect is based on several studies published in the 1980s [27,28].

Disease activity is currently assessed using the criteria employed in Histiocyte Society randomized trials [2,3]. The more recent assessment system is semi-quantitative, with the following four categories [18]: non-active disease, active disease-better, active disease-stable and active disease-worse. The drawbacks of this system are that, by definition, each assessment is based on a comparison of the situation before and after therapy (or over a 6-week interval) and the lack of reliable definition of the disease activity in involved organs.

A disease activity score system, tested on a sample of 650 patients, has been published [29] and is a useful tool to

Table2. Definition of organ involvement in langerhans cell histiocytosis.

Criteria
Bone involvement
General bone involvement: All radiological documented lesions, usually considered as LCH lesions
An abnormality on Tc Bone scan or an MRI hypersignal, not correlated with symptoms, and not correlated with an X-ray image is not considered bony disease!
Skin involvement
Any rash documented by histological examination
or any lesion (erythematous and crusted macules, papules or nodules, with or without ulceration, or petechiae, or seborrhea-like picture) compatible with the diagnosis, if LCH is confirmed by biopsy of another organ
Mucosae involvement
Oral involvement with lesions in the oral mucosa, gums
Genital or anal involvement
Pituitary involvement
Any pituitary hormone deficiency
or tumor appearance in the hypothalamic pituitary axis
Ear involvement
Ear involvement with external otitis, otitis media or otorrhea
Hematopoietic involvement
Mild
Hemoglobin between 10 and 7 g/dl (not due to other causes, e.g., iron deficiency)
Or thrombocytopenia with platelets between 100,000 and 20,000/mm^3
Severe
Hemoglobin < 7 g/dl. Exclude iron deficiency or other causes
Or platelets < 20,000/mm^3
Liver involvement (the patient can show a combination of these symptoms)
Enlargement > 3 cm below the costal margin at the mid-clavicular line, confirmed by ultrasound
or dysfunction documented by: hyperbilirubinemia > 3 times normal, hypoalbuminemia (< 30 g/dl), γ GT increased > 2 times normal,
ALT(SGPT) - AST(SGOT) > 3 times normal, ascites, edema
or intra hepatic nodular mass
Spleen involvement
> 3 cm below the costal margin at the mid-clavicular line, confirmed by ultrasound
Lung involvement
Typical imaging (nodules or cysts) on CT scan
Any atypical aspect needs to be explored by BAL or biopsy in order to have histopathological/cytological diagnosis
Central nervous system (CNS) involvement
Tumoral: All intracerebral expansive lesions predominantly affecting the brain or meninges
Neurodegeneration on MRI: MRI imaging compatible with neurodegenerative disease[1], i.e., abnormal signal intensity localized in the dentate nuclei or cerebellum or cerebral atrophy *not* explained by corticosteroids
Clinical neurodegeneration: Presence of suggestive symptoms (either cerebellar syndrome or learning difficulty) with compatible MRI imaging
Eye involvement
Orbital involvement with proptosis or exophthalmos
Anatomic involvement of the eye

assess disease response, especially in cases of systemic disease (Table 3a).

However, this scoring system is accurate neither for lung involvement nor for monitoring sequelae. CT scanning is now a very accurate method for evaluating the anatomic extension of the disease although the anatomic lesions, categorized roughly as cysts or nodules, can be disseminated in a various proportion at various locations. In order to offer a simple ranking, a semi-quantitative score has been proposed (Table 3b) [30,31]. In addition to the disease activity score, a sequelae score has been proposed and correlated with quality of life (Table 3c) [32].

Altogether, the use of such scoring systems offer a global and reliable approach to determine the activity of the disease and may aid the physician in making treatment decisions as proposed in Table 3a, 3b and 3c.

Lastly, neurodegenerative presentation must be monitored, using the International Cooperative Ataxia Rating (ICAR) scoring system [33], which has been used in the US, France and UK [32,34,35], while the Japanese cooperative group had used a scale derived from multiple sclerosis named EDSS [36].

7. Treatment: what are the options?

7.1 Local therapy

Bone lesions: The decision regarding orthopedic or physiotherapy treatment options must be taken in conjunction with an orthopedic surgeon. Complete excision of bone lesions (curettage) may be indicated if the bone lesion is small (< 2 cm) and this approach may offer a complete treatment. By contrast, the complete excision of large lesions is not indicated since it may increase the size of the bony defect and the time to healing; it may also result in permanent skeletal defects. Depending on lesion size and aspect, intra-lesional injection of methylprednisolone can be used [37]. Immobilization of a limb has to be considered. Vertebra plana 'per se' is not an indication for orthopedic corset, and only appropriate and expert physiotherapy should be considered.

Skin lesions: Topical steroids are often suggested in standard textbooks but their efficacy has never been proven. Moreover, most LCH patients with cutaneous involvement (either isolated or in the context of MS-LCH) are diagnosed only after unsuccessful treatment with local steroids. Skin involvement may usually be controlled by topical nitrogen mustard (mechlorethamine hydrochloride) application [38]. These topical treatments can be applied to the external auditory tract, in case of local lesion [39].

Lung: Pneumothoraces are treated by standard techniques such as drainage and pleurodesis. Pleurectomy should be avoided in patients for whom lung transplantation may ultimately be an option.

Ear nose and throat: In case of temporal bone lesions and recurrent otorrhea, secondary cholesteatoma can be considered [40].

Table 3a. Langerhans cell histiocytosis – systemic score [29].

Variable	Modality	Score
Bone (a)	Pain	1
	No pain	0
Bone (b)	Compressing other organs (orbit or spine)	2
	No compression	0
Fever (> 38.5 °C)	Yes	1
	No	0
Lung: iconography	Pneumothorax	2
	Interstitial lesion on chest X-ray film or lung CT scan	1
	Normal chest X-ray film or lung CT scan	0
Lung: function	Mechanical ventilation or PFT > 50%	5
	Supplemental oxygen or PFT between 50 to 80%	2
	No dysfunction, no cyanosis, no supp. Oxygen	0
Skin: area	25%	2
	5 – 25%	1
	Below 5%	0
Soft tissue tumor (including CNS)	5 cm max diameter	2
	2 – 5 cm max diameter	1
	0 – 2 cm max diameter	0
Nodes (> 2 cm)	Yes	1
	No	0
Liver	Below umbilicus	2
	Enlarged above umbilicus	1
	Not enlarged	0
Spleen	Below umbilicus	2
	Enlarged above umbilicus	1
	Not enlarged	0
Liver (enzymes)	> 10 N	2
	3 N to 10 N	1
	< 3 N	0
Liver (gamma GT)	> 10 N	2
	3 N to 10 N	1
	< 3 N	0
Albumin	Perfusion required in past week	3
	No perfusion but < 30 g/l	1
	> 30 g/l	0
Platelet: requirements in past week	More than 2 transfusions	4
	1 or 2 transfusions	3
	Low platelet count, no transfusion	2
	Normal count	0
Red cells: requirements in past week	More than 2 units	4
	1 or 2 units	3
	Hb below 10 g/dl, no transfusion	1
	Hb equal or above10 gr/dl	0

The score is calculated after collection of the clinical information, a chest X ray, a complete blood count, albumin level, SGOT, SGOT and gamma GT.
N: Maximal normal value for the laboratory.

7.2 Systemic therapy

Many drugs are used in LCH, from nonsteroidal anti-inflammatory drugs (NSAIDS), steroids, to cytostatic drugs such as vincristine, vinblastine, VP-16 (etoposide), 6 mercaptopurine (6-MP), methotrexate, cytarabine and cladribine. To this list can be added many drugs considered as immuno-therapeutic agents (interferon alpha, anti TNF-alpha, ciclosporin A, thalidomide, etc.) and various other drugs such as imatinib, retinoids and bisphosphonates.

Unfortunately, most of the drugs used in LCH have been evaluated in very low numbers of patients, usually in special, potentially biased, circumstances. The degree of evidence of efficacy is usually poor.

In the last 20 years, a limited number of therapeutic trials have been set up: three in the Western world under the auspices of the Histiocyte Society (LCHI [2], LCHII [3] and LCH III, which are not yet published) and one in Japan [41]. None of these trials had included adults [42].

These studies have provided the following observations:

1) The most frequently reported regimen is the association of vinblastine with a steroid. This therapy has been used

Table 3b. Lung score evaluated by the high-resolution CT scan.

Estimation of the proportion of cysts by field:			Estimation of the proportion of nodules by field:		
0 no nodules			0 no nodules		
1 < 25% or rare			1 < 25% or rare		
2 25 – 50% or intermediate			2 25 – 50% or intermediate		
3 > 50% or high			3 > 50% or high		
	Right	Left		Right	Left
Upper			Upper		
Medium			Medium		
Lower			Lower		

To establish this score, the chest was divided into six fields: upper, medium and lower and left and right. For each field, and both for nodules and for cysts, the score was 0 if no lesion, 1 if the proportion of lesions was between 1 and 25% of the surface (or consider as rare), 2 if the proportion of the lesions was between 26 and 50% (or consider as intermediate) and 3 if the proportion of lesions was above 50% (or consider as high) [30,31]. This score correlates with lung function.

since 1972 and so far all reports have shown that, for most of the cases, it is a safe and efficient therapeutic option. Late effects of this treatment are very limited in children. The use of this combination is more controversial in adults and more frequent short term side effects are reported, such as peripheral neuropathy

2) VP-16 added to a combination of vinblastine, steroid and 6-MP did not provide any additional effect in patients with risk organ involvement or MS-LCH [2,3]
3) Methotrexate, in addition to a combination of Vinblastine steroid and 6-MP did not bring any addition benefit for patients with risk organ involvement or MS-LCH (LCH III protocol, unpublished results)
4) In patients with MS-LCH, a 12-month maintenance therapy period limited the rate of reactivation compared with 6 months of maintenance therapy (LCH III protocol, personal communication)
5) The combination of vincristine, steroid, and cytarabine provides comparable results to the combination of vinblastine, steroid, and 6-MP [41]
6) Cladribine monotherapy is effective for non-risk-organ disease that is refractory to standard therapy except in cases of hematological dysfunction [43]
7) Cladribine in association with cytarabine is effective in patients with hematological dysfunction that is refractory to standard therapy [44].
8) Hematopoietic stem cell transplantation is a therapeutic option if risk organ involvement is present, refractory to other salvage therapeutic approaches [45]

Because of its simplicity and low toxicity, compared with other drugs used in association, the use of NSAIDs has to be emphasized too [46].

7.3 Front-Line treatment

The most frequently used systemic therapy is based on vinblastine 6 mg/m^2 intravenous (i.v.) bolus once every 7 days (once a week) for 6 weeks, along with prednisone at 40 mg/m^2/day given orally in three divided doses for 4 weeks and then tapered over the following 2 weeks. After the first 6 weeks of treatment, disease status should be evaluated and treatment continued accordingly. Usually, in cases of disease progression, patients must switch to salvage therapy. By contrast, in cases of complete response, patients continue with maintenance therapy, while in the intermediate situation, a second course of 6 weeks of vinblastine plus steroid is administered, with a further evaluation undertaken at the end of this second course. Given that the risk of reactivations is high in many forms of LCH, and in line with as-yet-unpublished results of the LCH III protocol, treatment should continue for up to a total of 12 months with vinblastine 6 mg/m^2 i.v. bolus every 3 weeks, along with prednisone at 40 mg/m^2/day given orally in three divided doses for 5 days. The immunosuppressive drug 6-MP at a dose of 50 mg/m^2 is added if a risk organ is present at diagnosis. An acceptable modification to this protocol is to avoid steroids in cases of DI (as steroids interfere with water balance) and to use more frequent vinblastine pulses in the maintenance therapy in case of minor reactivation between pulses provided every 3 weeks. Vinblastine with steroid is efficient as a front-line therapy for tumoral processes of the CNS [47].

The association of vincristine, cytarabine and steroid, as proposed by the Japanese cooperative group [41], represents a therapeutic alternative to the combination of vinblastine and steroid. Whatever the systemic therapy, prophylaxis against *Pneumocystis carinii* is recommended during the treatment period.

7.4 Salvage therapy

Refractory disease in patients with hematological and/or liver dysfunction is a rare but life-threatening situation [5,17]. Such patients need to be referred to a trained team, that is, a team with a medical experience of both intensive chemotherapy and LCH. Therapeutic options (although the evidence is quite

Table 3c. Score sequel [32].

	Score	
Hormones DI	3	Panhypopituitarism and/or hypothalamic syndrome not correctable with hormone replacement
	2	Partial anterior pituitary deficiency *and* diabetes insipidus on replacement therapy
	1	Diabetes insipidus on replacement therapy
	0	No pituitary deficiency
Cerebellar syndrome [33]	3	Severe ataxia (scale > 40) or other motor disability
	2	Moderate ataxia (scale 20–40)
	1	Mild ataxia (scale < 20)
	0	No ataxia
Intellectual deficiency	3	Severe learning difficulty (IQ < 70) and/or severe behavioral/psychological problems impairing function and not correctable by treatment
	2	Moderate learning difficulty (IQ 71–79) and/or behavioral/psychological problems correctable by treatment
	1	Mild learning difficulty (IQ 80–89) and/or mild behavioral/psychological problems not requiring treatment
	0	No intellectual deficiency
Ear function	3	Severe bilateral hearing loss, not correctable with aids
	2	Moderate bilateral hearing loss, partially correctable by aids
	1	Mild bilateral or moderate/severe unilateral loss correctable with aids
	0	No hearing loss or mild unilateral hearing loss, no aids required
Lung = dyspnea NYHA	3	Patients who should be at complete rest, confined to bed or chair; any physical activity brings on discomfort and symptoms occur at rest./requiring lung transplant
	2	Patients with marked limitation of activity; they are comfortable only at rest
	1	Patients with slight, mild limitation of activity; they are comfortable with rest or with mild exertion
	0	Patients with no limitation of activities; they suffer no symptoms from ordinary activities
Dysmorphie facial - teeth	3	Gross facial or orthodontic abnormality and/or scarring requiring repeated or major surgery
	2	Moderate facial or orthodontic abnormality and/or scarring correctable with surgery
	1	Mild facial or orthodontic abnormality and/or scarring not requiring any surgery
	0	No abnormality
Liver	3	Liver function extremely poor/requiring liver transplant
	2	Moderate liver function decrease/jaundice permanent
	1	Mild cholangitis – no liver dysfunction
	0	No liver dysfunction
Obesity	3	Pathological obesity – BMI > 35
	2	Obesity – BMI 30 – 35
	0	BMI < 30
Vision	3	Bilateral blindness – not correctable
	2	Mild bilateral blindness or unilateral severe blindness
	1	Mild unilateral blindness
	0	No abnormality
Other: in text		

This score can be applied at each follow-up visit and is correlated with quality of life.

limited) may include the chemotherapy combination of cladribine and cytarabine [44] as a second-line treatment, and even hematopoietic stem cell transplant after reduced-intensity conditioning regimen as a third-line option [45]. Indications for the combination of cladribine and cytarabine in France have been limited to patients with a systemic disease activity score above 5 and who progress after initial therapy with a classical regimen comprising at least six pulses of vinblastine and 6 weeks of therapy. In this group of patients, the survival rate was very low (about 30%) until the use of cladribine and cytarabine and is now as high as 85% (LCH S 2005 protocol – personal data).

In contrast to the situation of failure in patients with risk organs, the possibility of disease progression in patients without risk organ involvement (e.g., bone or mass lesion in the CNS) can be managed by cladribine monotherapy [43].

7.5 Radiotherapy

Radiotherapy is an efficient method to treat a bony lesion or a CNS mass lesion. However, this method has two limitations: first, it is only a local therapy, which means that the systemic course of the disease is not controlled by this approach; and second, there is a frank increased risk of secondary malignant tumor, as observed in several surveys and case reports. With regard to the ALARA (as low as reasonably achievable) safety principle, there is always an alternative therapy.

7.6 Adults

So far, the medical management of adults is not based on therapeutic trial but on small survey [42]. In adult, the dose of vinblastine is commonly adapted (as the maximum dose per pulse is no more than 10 mg), while peripheral neuropathy is a more frequently observed compare with children.

7.7 Neurodegenerative complications

Neurodegenerative complications are complex situations and such patients need to be managed by a multidisciplinary team, involving a physician trained in LCH, a neurologist, a reeducation specialist and, commonly, a endocrinologist, with the help of social workers.

Several therapeutic approaches have been attempted and can be proposed: retinoic acid (survey of 10 patients [35]), the combination of vincristine and cytarabine (survey of 8 patients [34]), immunoglobulin (4 patients including 2 asymptomatic and a case report [36,48]) and more recently infliximab [49]. The best result that can be expected from such regimens is the stabilization of neurological symptoms. So far, intensive therapy, including autologous bone marrow transplant, radiotherapy, high-dose methotrexate or steroids, has never shown any effect, not even a stabilization of the course of neurodegeneration, and should be avoided.

8. Indications for therapy and evaluation

MS-LCH with risk organ involvement (hematopoietic system/liver/spleen, regardless of additional organs involved). A systemic therapy is always recommended. The use of a systemic scoring system [29] is very useful in this situation in order to objectively determine the response to therapy.

MS-LCH and SS-LCH without risk organ. The indication of systemic therapy should be based on the presence or absence of clinical symptoms and/or patient complaints, and on the size and site of the disease. In the absence of symptoms or threat to organ function, the decision is more controversial. Some may decide that a systemic therapy should be used in all MS-LCH without risk organ involvement and some may even decide to treat all patients with skull lesions, or lesions localized at the skull base (but the latter are commonly responsible for symptoms).

There is no consensus regarding duration of maintenance therapy. However, the results of the unpublished LCH III protocol offer a first answer and demonstrate than a duration of 12 months limits the total number of reactivations.

8.1 Isolated lung involvement

The impact of systemic therapy on the lung is not well documented in children or adults, and pneumologists do not consider systemic therapy as the standard approach [14,18]. In adults, smoking cessation and stopping exposure to cigarette smoke in daily life is always mandatory. This recommendation may be considered for teenagers. There is no information about the impact of passive smoking exposure on children. However, isolated lung involvement can be very challenging due to the risk of severe acute complications such as pneumothorax or acute cardiopulmonary arrest.

8.2 Diabetes insipidus and pituitary involvement

In our experience, as in the experience of several groups [50], DI is almost never reversible even if the needs of desmopressin may change during the life of the patient. However, a case report had shown that cladribine provided soon after DI onset may reverse DI [51]. Diabetes insipidus in our experience, as well as in the conclusion of a UK study [50], is not considered as an indication for systemic therapy, except if it is associated with a mass lesion of the hypothalamus–pituitary axis. However, some authors had recommended to start a systemic therapy in case of isolated CDI [23]. In cases of growth hormone deficiency, there is no contraindication to treat a patient with LCH, even with active disease, using growth hormone therapy, if the latter is fully indicated. Indeed, there is no evidence to link an increased risk of LCH reactivation or any peculiar side effects with growth hormone therapy [52].

8.3 Treatment evaluation

All therapy needs to be carefully monitored. The evaluation needs to be focused on the target organs, those for which the initial therapy was started. Whatever the methods and criteria used to assess the response, a treatment period of 6 weeks is important to respect before assessing response [5,17] but some assessments can be delayed for the lung or for bone.

A general disease activity score (Table 3a) is a clear aid for therapeutic evaluation, in order to check for serious, potentially lethal, threats. If the score remains low (i.e., below 5), the disease is not life-threatening. In case of a high disease activity score (above 5), the possibility of switching to a salvage therapy must be considered within the trained team, associating both the experience of LCH and the management of high-dose chemotherapy, like in acute myeloid leukemia. Persistence of very aggressive local disease, if the local activity of the disease may be ascertained, can justify a switch to monotherapy with cladribine.

Usually, bone reconstruction is a very long process and persistence of X-ray bone lesions is rarely a good reason to modify the therapeutic schedule. Lung involvement is commonly assessed by CT scan although it is important to note that the density of cysts is rarely altered by therapy and should not be used to guide treatment.

9. Treatment options in case of reactivation

The choice of treatment options for disease reactivation is based on the same principles as for initial disease [53]. The options for reactivations of SS-LCH (skin, bone, other) include a 'wait and watch' approach, local therapy (as above), NSAID for bony disease and vinblastine plus steroid. Radiotherapy is no longer recommended due to potential

long-term sequelae. In case of a multisystemic reactivation of a SS-LCH, treatment should follow the options for MS-LCH including systemic therapy.

Reactivation after systemic therapy. If the reactivation is after completion of treatment, re-induction with vinblastine plus steroid may be effective, and there may be no need to switch to an alternative therapy.

9.1 Management of permanent consequences

Although LCH is a mostly benign and treatable disease, it can result in sequelae affecting various involved tissues [25]. Some sequelae may be present at diagnosis or even precede diagnosis, while other may become manifest later. It is thus important to keep monitoring these patients at least until growth is completed and possibly further into adult life. The most common long-term consequences are endocrine and growth, auditory and orthopedic. Neurocognitive, pulmonary and liver sequelae are rare but cause major morbidity. A scoring system for sequelae has been developed in order to observe disease evolution, and its adaptation to incorporate liver sclerosing cholangitis and morbid obesity is proposed [32].

So far, the management of long-term sequelae is not specific to LCH and all therapeutic options, like growth hormone therapy, liver or lung transplantation must be considered according to current medical practice.

9.2 Follow-up; duration and frequency

With regard to the heterogeneity of the disease, a standard follow-up schedule appears difficult to propose and we wish to provide only some principles.

The first principle is the use of a coordinated multidisciplinary approach. This means that each patient needs to be followed by the referring physician during the course of their disease and that evaluation and/or therapy of a particular clinical situation need to be addressed by a competent specialist.

The second principle is to follow the patient for a sufficient duration, which has been considered as at least 5 years after the last therapy or the last activation of the disease in the absence of systemic therapy.

The frequency of the follow-up is necessarily adapted to each particular situation. If the patient is receiving a systematic therapy, this frequency is adapted to the treatment schedule. In the absence of systemic therapy or in the absence of symptomatology, we consider that the routine number of consultations should be 4 during the first year after diagnosis, 2 in the second and third years and 1 each for years 4 and 5.

10. Expert opinion

LCH is a rare disease potentially resulting in death or with permanent sequelae. The burden of therapy may also be extremely heavy: there are still lots of reasons to continue to develop fundamental and clinical research in this field.

Indeed, in 2010 the team of Barrett Rollins reported a very important discovery that about 50% of the tumoral tissues of LCH patients bear a somatic mutation of the B raf oncogenes [54]. A lot of complementary research remains to be done in order to understand how such mutations may lead to disease as observed in many other conditions including malignant disease (melanoma, colon carcinoma, papillary thyroid cancer [55-57]) and benign conditions such as naevi [58]. Nevertheless, this discovery may have a clear potential impact if we consider the possibility of treating LCH with the new class of B raf inhibitors [59]. However, many steps need to be made from this discovery to the clinical use of these new drugs including a determination of the group(s) of patients who may benefit from B raf inhibitor treatment.

Progress may be expected from collaborations organized at national and international levels, among collaborative groups and expert networks. Collections of tissue and blood samples in biobanks have to be organized too. New international protocols will be opened to patient accrual and represent an opportunity to develop global research [60,61].

Acknowledgements

This work is the fruit of the personal and professional experience of authors and is inspired by the work performed in the last 15 years in the French LCH study group, formalized in the guidelines HL2010. An acknowledgement must be paid to the working group of euro histio net, as part of the thoughts were generated in conjunction with our friends, Riccardo Haupt (Gaslini Instituto, Genoa), Milen Minkow (Kinderspital, Vienna, Austria), and Itziar Astirigarra (Hospital de la cruz Bilbao).

Declaration of interest

The authors declare no conflict of interest and have received no payment in preparation of this manuscript. We thank Rod McNab of inScience Communications, Springer Healthcare, who provided native English editing of the manuscript; this Association was funded by a grant from Association Histiocytose France.

Bibliography

Papers of special note have been highlighted as either of interest (•) or of considerable interest (••) to readers.

1. Gadner H, Heitger A, Grois N, et al. Treatment strategy for disseminated Langerhans cell histiocytosis. DAL HX-83 Study Group. Med Pediatr Oncol 1994;23:72-80
   - • **The first report in English literature of the DAL HX group.**
2. Gadner H, Grois N, Arico M, et al. A randomized trial of treatment for multisystem Langerhans' cell histiocytosis. J Pediatr 2001;138:728-34
3. Gadner H, Grois N, Potschger U, et al. Improved outcome in multisystem Langerhans cell histiocytosis is associated with therapy intensification. Blood 2007;111:2556-62
   - • **This study demonstrates that VP16 fails to improve the outcome of multisystemic patients treated with a standard treatment by vinblastine and steroid.**
4. Minkov M, Grois N, Heitger A, et al. Treatment of multisystem Langerhans cell histiocytosis. Results of the DAL-HX 83 and DAL-HX 90 studies. DAL-HX Study Group. Klin Padiatr 2000;212:139-44
   - •• **An overview of the German-Austrian protocols with information about long-term outcome.**
5. The French Langerhans' Cell Histiocytosis Study Group. A multicentre retrospective survey of Langerhans' cell histiocytosis : 348 cases observed between 1983 and 1993. Arch Dis Child 1996;75:17-24
   - •• **An overview of the larger national survey so far with long-term outcome.**
6. Chikwava K, Jaffe R. Langerin (CD207) staining in normal pediatric tissues, reactive lymph nodes, and childhood histiocytic disorders. Pediatr Dev Pathol 2004;7:607-14
7. Lau SK, Chu PG, Weiss LM. Immunohistochemical expression of Langerin in Langerhans cell histiocytosis and non-Langerhans cell histiocytic disorders. Am J Surg Pathol 2008;32:615-19
8. Swerdlow SH, Campo E, Harris NL, et al. WHO Classification of Tumours of Haematopoietic and Lymphoid Tissues. 4th edition. IARC press; Lyon: 2008
9. Valladeau J, Ravel O, zutter-Dambuyant C, et al. Langerin, a novel C-type lectin specific to Langerhans cells, is an endocytic receptor that induces the formation of Birbeck granules. Immunity 2000;12:71-81
10. Jaffe R. The diagnostic histopathology of Langerhans cell histiocytosis. In: Weitzman S, Egeler M, editors. Histiocytic Disorders of Children and Adults. Cambridge University Press; Cambridge: 2005. p. 14-39
    - •• **A very nice overview about the pathology of LCH.**
11. Howarth DM, Mullan BP, Wiseman GA, et al. Bone scintigraphy evaluated in diagnosing and staging Langerhans' cell histiocytosis and related disorders. J Nucl Med 1996;37:1456-60
12. Phillips M, Allen C, Gerson P, McClain K. Comparison of FDG-PET scans to conventional radiography and bone scans in management of Langerhans cell histiocytosis. Pediatr Blood Cancer 2009;52:97-101
    - • **This study shows that FDG-PET scans may be used to monitor disease activity.**
13. Goo HW, Yang DH, Ra YS, et al. Whole-body MRI of Langerhans cell histiocytosis: comparison with radiography and bone scintigraphy. Pediatr Radiol 2006;36:1019-31
    - • **This study shows that whole-body MRI may be used to evaluate disease extension in LCH.**
14. Vassallo R, Ryu JH, Colby TV, et al. Pulmonary Langerhans'-cell histiocytosis. N Engl J Med 2000;342:1969-78
    - • **A comprehensive literature review about pulmonary LCH.**
15. Martin-Duverneuil N, Idbaih A, Hoang-Xuan K, et al. MRI features of neurodegenerative Langerhans cell histiocytosis. Eur Radiol 2006;16:2074-82
    - • **A review of MRI findings in neurodegenerative LCH.**
16. Prayer D, Grois N, Prosch H, et al. MR imaging presentation of intracranial disease associated with Langerhans cell histiocytosis. AJNR Am J Neuroradiol 2004;25:880-91
    - • **A review of MRI finding in all types of CNS-LCH.**
17. Minkov M, Grois N, Heitger A, et al. Response to initial treatment of multisystem Langerhans cell histiocytosis: an important prognostic indicator. Med Pediatr Oncol 2002;39:581-5
18. Tazi A, Soler P, Hance AJ. Adult pulmonary Langerhans' cell histiocytosis. Thorax 2000;55:405-16
    - • **A comprehensive literature review about pulmonary LCH.**
19. Braier J, Latella A, Balancini B, et al. Outcome in children with pulmonary Langerhans cell Histiocytosis. Pediatr Blood Cancer 2004;43:765-9
20. Ronceray L, Potschger U, Janka G, et al. Pulmonary involvement in pediatric-onset multisystem langerhans cell histiocytosis: effect on course and outcome. J Pediatr Jan 26 2012. [Epub ahead of print]
21. Grois N, Potschger U, Prosch H, et al. Risk factors for diabetes insipidus in langerhans cell histiocytosis. Pediatr Blood Cancer 2006;46:228-33
22. Barthez MA, Araujo E, Donadieu J. Langerhans cell histiocytosis and the central nervous system in childhood: evolution and prognostic factors. Results of a collaborative study. J Child Neurol 2000;15:150-6
23. Grois N, Fahrner B, Arceci RJ, et al. Central nervous system disease in Langerhans cell histiocytosis. J Pediatr 2010;156:873-81.881
    - • **The state of the art of CNS LCH.**
24. Donadieu J, Rolon MA, Thomas C, et al. Endocrine involvement in pediatric-onset Langerhans' cell histiocytosis: a population-based study. J Pediatr 2004;144:344-50
    - •• **A detailed prognostic analysis of endocrine involvement in LCH.**
25. Haupt R, Nanduri V, Calevo MG, et al. Permanent consequences in Langerhans cell histiocytosis patients: a pilot study from the Histiocyte Society-Late Effects Study Group. Pediatr Blood Cancer 2004;42:438-44
26. Bernstrand C, Sandstedt B, Ahstrom L, Henter JI. Long-term follow-up of Langerhans cell histiocytosis: 39 years' experience at a single centre. Acta Paediatr 2005;94:1073-84

27. Sartoris DJ, Parker BR. Histiocytosis X: rate and pattern of resolution of osseous lesions. Radiology 1984;152:679-84

• **Quite old but still very interesting report about the duration of bone healing in LCH.**

28. Womer RB, Raney RB Jr, D'Angio GJ. Healing rates of treated and untreated bone lesions in histiocytosis X. Pediatrics 1985;76:286-8

• **Quite old but still very interesting report about the duration of bone healing in LCH.**

29. Donadieu J, Piguet C, Bernard F, et al. A new clinical score for disease activity in Langerhans cell histiocytosis. Pediatr Blood Cancer 2004;43:770-6

•• **A scoring system to monitor disease activity in LCH.**

30. Canuet M, Kessler R, Jeung MY, et al. Correlation between high-resolution computed tomography findings and lung function in pulmonary Langerhans cell histiocytosis. Respiration 2007;74:640-6

31. Tazi A, Marc K, Dominique S, et al. Serial CT and lung function testing in pulmonary Langerhans cell histiocytosis. Eur Respir J 2012;In press

•• **This study demonstrates the correlation between lung anatomic lesions observed by CT and pulmonary functional test.**

32. Nanduri VR, Pritchard J, Levitt G, Glaser AW. Long term morbidity and health related quality of life after multi-system Langerhans cell histiocytosis. Eur J Cancer 2006;42:2563-9

•• **This study shows how the long morbidity correlates with quality of life and provides a global scoring system for sequels in LCH.**

33. Trouillas P, Takayanagi T, Hallett M, et al. International Cooperative Ataxia Rating Scale for pharmacological assessment of the cerebellar syndrome. The Ataxia Neuropharmacology Committee of the World Federation of Neurology. J Neurol Sci 1997;145:205-11

34. Allen CE, Flores R, Rauch R, et al. Neurodegenerative central nervous system Langerhans cell histiocytosis and coincident hydrocephalus treated with vincristine/cytosine arabinoside. Pediatr Blood Cancer 2009;54:416-23

35. Idbaih A, Donadieu J, Barthez MA, et al. Retinoic acid therapy in "degenerative-like" neuro-langerhans cell histiocytosis: a prospective pilot study. Pediatr Blood Cancer 2004;43:55-8

36. Imashuku S, Shioda Y, Kobayashi R, et al. Neurodegenerative central nervous system disease as late sequelae of Langerhans cell histiocytosis. Report from the Japan LCH Study Group. Haematologica 2008;93:615-18

37. Egeler RM, Thompson RC Jr, Voute PA, Nesbit ME Jr. Intralesional infiltration of corticosteroids in localized Langerhans' cell histiocytosis. J Pediatr Orthop 1992;12:811-14

38. Sheehan MP, Atherton DJ, Broadbent V, Pritchard J. Topical nitrogen mustard: an effective treatment for cutaneous Langerhans cell histiocytosis. J Pediatr 1991;119:317-21

39. Hadfield PJ, Birchall MA, Albert DM. Otitis externa in Langerhans' cell histiocytosis–the successful use of topical nitrogen mustard. Int J Pediatr Otorhinolaryngol 1994;30:143-9

40. Roger G, Dupre M, Leboulanger N, et al. Cholesteatoma secondary to temporal bone involvement by Langerhans cell histiocytosis: a complication amenable to curative surgery. Otol Neurotol 2009;30:190-3

41. Morimoto A, Ikushima S, Kinugawa N, et al. Improved outcome in the treatment of pediatric multifocal Langerhans cell histiocytosis: results from the Japan Langerhans Cell Histiocytosis Study Group-96 protocol study. Cancer 2006;107:613-19

42. Arico M, Girschikofsky M, Genereau T, et al. Langerhans cell histiocytosis in adults. Report from the International Registry of the Histiocyte Society. Eur J Cancer 2003;39:2341-8

• **The first large multinational retrospective that provides a description of the disease in adulthood.**

43. Weitzman S, Braier J, Donadieu J, et al. 2'-Chlorodeoxyadenosine (2-CdA) as salvage therapy for Langerhans cell histiocytosis (LCH). results of the LCH-S-98 protocol of the Histiocyte Society. Pediatr Blood Cancer 2009;53:1271-6

•• **A large survey of patients receiving 2-CdA monotherapy as a salvage therapy, both for risk or no-risk organ patients.**

44. Bernard F, Thomas C, Bertrand Y, et al. Multi-centre pilot study of 2-chlorodeoxyadenosine and cytosine arabinoside combined chemotherapy in refractory Langerhans cell histiocytosis with haematological dysfunction. Eur J Cancer 2005;41:2682-9

•• **This short pilot protocol shows that 2-CdA in association with cytosine arabinoside may cure refractory Langerhans cell histiocytosis with hematological dysfunction.**

45. Steiner M, Matthes-Martin S, Attarbaschi A, et al. Improved outcome of treatment-resistant high-risk Langerhans cell histiocytosis after allogeneic stem cell transplantation with reduced-intensity conditioning. Bone Marrow Transplant 2005;36:215-25

46. Munn SE, Olliver L, Broadbent V, Pritchard J. Use of indomethacin in Langerhans cell histiocytosis. Med Pediatr Oncol 1999;32:247-9

•• **A short survey to demonstrate how nonsteroid anti-inflammatory drugs are useful in LCH.**

47. Ng Wing TS, Martin-Duverneuil N, Idbaih A, et al. Efficacy of vinblastine in central nervous system Langerhans cell histiocytosis: a nation wide retrospective study. Orphanet J Rare Dis 2011;6:83

48. Gavhed D, Laurencikas E, Akefeldt SO, Henter JI. Fifteen years of treatment with intravenous immunoglobulin in central nervous system Langerhans cell histiocytosis. Acta Paediatr 2011;100:e36-9

49. Chohan G, Barnett Y, Gibson J, et al. Langerhans cell histiocytosis with refractory central nervous system involvement responsive to infliximab. J Neurol Neurosurg Psychiatry 2012;83:573-5

50. Broadbent V, Pritchard J. Diabetes insipidus associated with Langerhans cell histiocytosis: is it reversible? Med Pediatr Oncol 1997;28:289-93

• **This study shows that DI in LCH is almost always irreversible, so far.**

51. Ottaviano F, Finlay JL. Diabetes insipidus and Langerhans cell histiocytosis: a case report of reversibility with 2-chlorodeoxyadenosine. J Pediatr Hematol Oncol 2003;25:575-7

52. Donadieu J, Rolon MA, Pion I, et al. Incidence of growth hormone deficiency in pediatric-onset Langerhans cell

histiocytosis: efficacy and safety of growth hormone treatment. J Clin Endocrinol Metab 2004;89:604-9

•• **GH deficiency is present in 50% of the patients with CDI. GH is safe for patients with GH deficiency.**

53. Minkov M, Steiner M, Potschger U, et al. Reactivations in multisystem Langerhans cell histiocytosis: data of the international LCH registry. J Pediatr 2008;153:700-5.705

54. Badalian-Very G, Vergilio JA, Degar BA, et al. Recurrent BRAF mutations in Langerhans cell histiocytosis. Blood 2010;116:1919-23

•• **This study demonstrates that B raf mutations are observed in 50% of the patients with LCH. The demonstration is definitive and had changed the paradigm of pathophysiology of LCH.**

55. Davies H, Bignell GR, Cox C, et al. Mutations of the BRAF gene in human cancer. Nature 2002;417:949-54

56. Begum S, Rosenbaum E, Henrique R, et al. BRAF mutations in anaplastic thyroid carcinoma: implications for tumor origin, diagnosis and treatment. Mod Pathol 2004;17:1359-63

57. Ball DW. Selectively targeting mutant BRAF in thyroid cancer. J Clin Endocrinol Metab 2010;95:60-1

58. Poynter JN, Elder JT, Fullen DR, et al. BRAF and NRAS mutations in melanoma and melanocytic nevi. Melanoma Res 2006;16:267-73

59. Flaherty KT, Puzanov I, Kim KB, et al. Inhibition of mutated, activated BRAF in metastatic melanoma. N Engl J Med 2010;363:809-19

60. Available from: www eurohistio net 2012

61. Available from: www histiocytesociety org 2012

62. Talanin NY, Smith SS, Shelley ED, Moores WB. Cutaneous histiocytosis with Langerhans cell features induced by scabies: a case report. Pediatr Dermatol 1994;11:327-30

63. Geissmann F, Nosjean MC, Dezutter C, et al. Accumulation of immature Langerhans cells in human lymph nodes draining chronically inflamed skin. J Exp Med 2002;196:417-30

64. Perret-Court A, Coulibaly B, Ranque S, et al. Intradural dirofilariasis mimicking a Langerhans cell histiocytosis tumor. Pediatr Blood Cancer 2009;53:485-7

65. Maghnie M, Cosi G, Genovese E, et al. Central diabetes insipidus in children and young adults. N Engl J Med 2000;343:998-1007

66. Marchand I, Barkaoui MA, Garel C, et al. Central diabetes insipidus as the inaugural manifestation of Langerhans cell histiocytosis: natural history and medical evaluation of 26 children and adolescents. J Clin Endocrinol Metab 2011;96:E1352-60

67. Favara BE, Jaffe R, Egeler RM. Macrophage activation and hemophagocytic syndrome in langerhans cell histiocytosis: report of 30 cases. Pediatr Dev Pathol 2002;5:130-40

Affiliation

Jean Donadieu[†1] MD PhD,
François Chalard[2] MD &
Eric Jeziorski[3] MD PhD
[†]Author for correspondence
[1]Centre de Référence des Histiocytoses, Registre Français des Histiocytoses, Service d'Hémato Oncologie Pédiatrique, Hopital Trousseau, 26 avenue du Dr Netter, F 75012 Paris, France
E-mail: donadieu.genc@wanadoo.fr
[2]Service de Radiologie, Hopital Trousseau, 26 avenue du Dr Netter, F 75012 Paris, France
[3]Service de Pédiatrie III, CHU de Montpellier, Hopital Arnaud de Villeneuve, Montpellier 34000, France

Orphanet Journal of Rare Diseases

BioMed Central
The Open Access Publisher

Management of adult patients with Langerhans cell histiocytosis: recommendations from an expert panel on behalf of Euro-Histio-Net

Orphanet Journal of Rare Diseases 2013, **8**:72 doi:10.1186/1750-1172-8-72

Michael Girschikofsky (michael.girschikofsky@elisabethinen.or.at)
Maurizio Arico (m.arico@meyer.it)
Diego Castillo (DCastillo@santpau.cat)
Anthony Chu (a.chu@imperial.ac.uk)
Claus Doberauer (Doberauer@evk-ge.de)
Joachim Fichter (j.fichter@t-online.de)
Julien Haroche (julien.haroche@psl.aphp.fr)
Gregory A Kaltsas (gregory.kaltsas@gmail.com)
Polyzois Makras (makras@internet.gr)
Angelo V Marzano (angelovalerio.marzano@policlinico.mi.it)
Mathilde de Menthon (mathilde.de-menthon@cch.aphp.fr)
Oliver Micke (strahlenklinik@web.de)
Emanuela Passoni (emanuela.doc@katamail.com)
Heinrich M Seegenschmiedt (prof.seegenschmiedt@googlemail.com)
Abdellatif Tazi (abdellatif.tazi@sls.aphp.fr)
Kenneth L McClain (klmcclai@txch.org)

ISSN 1750-1172

Article type Review

Submission date 10 February 2013

Acceptance date 2 May 2013

Publication date 14 May 2013

Article URL http://www.ojrd.com/content/8/1/72

Orphanet Journal of Rare Diseases

BioMed Central
The Open Access Publisher

Central journal, go to

http://www.ojrd.com/authors/instructions/

For information about other BioMed Central publications go to

http://www.biomedcentral.com/

Management of adult patients with Langerhans cell histiocytosis: recommendations from an expert panel on behalf of Euro-Histio-Net

Michael Girschikofsky[1*]
* Corresponding author
Email: michael.girschikofsky@elisabethinen.or.at

Maurizio Arico[2]
Email: m.arico@meyer.it

Diego Castillo[3]
Email: DCastillo@santpau.cat

Anthony Chu[4]
Email: a.chu@imperial.ac.uk

Claus Doberauer[5]
Email: Doberauer@evk-ge.de

Joachim Fichter[6]
Email: j.fichter@t-online.de

Julien Haroche[7]
Email: julien.haroche@psl.aphp.fr

Gregory A Kaltsas[8]
Email: gregory.kaltsas@gmail.com

Polyzois Makras[9]
Email: makras@internet.gr

Angelo V Marzano[10]
Email: angelovalerio.marzano@policlinico.mi.it

Mathilde de Menthon[11]
Email: mathilde.de-menthon@cch.aphp.fr

Oliver Micke[12]
Email: strahlenklinik@web.de

Emanuela Passoni[10]
Email: emanuela.doc@katamail.com

Heinrich M Seegenschmiedt[13]
Email: prof.seegenschmiedt@googlemail.com

Abdellatif Tazi[14]
Email: abdellatif.tazi@sls.aphp.fr

Kenneth L McClain[15]
Email: klmcclai@txch.org

[1] Department of Medicine I, Center of Hematology an Stem Cell Transplantation, Hemostasis and Medical Oncology Internal Medicine I, Elisabethinen Hospital, Fadinger Str. 1 4010, Linz, Austria

[2] Department of Pediatric Hematology Oncology, Azienda Ospedaliero Universitaria A. Meyer, Florence, Italy

[3] Departament of Respiratory Medicin, Hospital de la Santa Creu i Sant Pau, Barcelona, Spain

[4] Imperial NHS Trust, London, UK

[5] Clinic for Internal Medicine, Protestant Clinics, Gelsenkirchen, Germany

[6] Paracelsus Klinik, Osnabrück, Germany

[7] Service de Medicine Interne, Groupe Hospitalier Pitie-Salpetiere, Paris, France

[8] Department of Pathophysiology, University of Athens School of Medicine, Athens, Greece

[9] Department of Endocrinology and Diabetes, 251 Hellenic Air Force & VA General Hospital, Athens, Greece

[10] U.O. Dermatologia, Fondazione IRCCS Ca´ Granda-Ospedale Maggiore Policlinico, Milano, Italy

[11] Department of Internal Medicine, Hospital Saint Louis, Paris, France

[12] Department of Radiotherapy and Radiation Oncology, Franziskus Hospital,, Bielefeld, Germany

[13] Radiation Oncology Center, Hamburg, Germany

[14] Pulmonolgy Department, Saint Louis Teaching Hospital, Paris, France

[15] Texas Children's Cancer Center/Hematology Service, Houston, TX, USA

Abstract

Langerhans Cell Histiocytosis (LCH) is an orphan disease of clonal dendritic cells which may affect any organ of the body. Most of the knowledge about the diagnosis and therapy is based on pedriatic studies. Adult LCH patients are often evaluated by physicians who focus on only the most obviously affected organ without sufficient evaluation of other systems, resulting in patients being underdiagnosed and/or incompletely staged. Furthermore they may be treated with pediatric-based therapies which are less effective and sometimes more toxic for adults. The published literature on adult LCH cases lacks a comprehensive discussion on the differences between pediatric and adult patients and there are no recommendations for evaluation and comparative therapies. In order to fill this void, a number of experts in this field cooperated to develop the first recommendations for management of adult patients with LCH. Key questions were selected according to the clinical relevance focusing on diagnostic work up, therapy, and follow up. Based on the available literature up to December 2012, recommendations were established, drafts were commented by the entire group, and redrafted by the executive editor. The quality of evidence of the recommendations is predominantly attributed to the level of expert opinion. Final agreement was by consensus.

Keywords

Langerhans, Adult, Histiocytosis

Background, process of development and restrictions

There are no universally accepted international guidelines available for the diagnosis and treatment of adult LCH patients. The largest number of patients was published in a pooled retrospective analysis from several national registries [1].

Based on the available literature up to December 2012 and personal experience the following recommendations were established by an international group of academic clinicians who are recognized experts in the field of histiocytic disorders. Grading of recommendations based on levels of evidence and agreement between experts is listed in Table 1.

Table 1 Grade of Recommendation

Level of evidence	Level of agreement between experts
A meta-analyses, high quality systematic reviews, or randomized controlled trials	**2** general agreement between all experts
B systematic reviews of case control or cohort studies	**1** discussed recommendation, but no formal objections between experts
C non-analytic studies: for example, case reports, case series, small retrospective studies	**0** divergence of opinion
D expert opinion	

Due to the diversity of clinical course of LCH, even recommendations which are established as standard of care may need to be critically appraised in an individual case and involvement of a LCH expert should be considered. A map of experts, reference centers and additional

information about the disease is available on the web-site of Euro-Histio-Net (http://www.eurohistio.net) and the Histiocytosis Association (https://www.histio.org/).

General consideration

The etiology of LCH is unknown. LCH cells are clonal (except primary pulmonary LCH) [2,3] and a cancer-associated mutation (*BRAFV600E)* was found in more than half of investigated specimens, indicating that LCH may be more a neoplastic (not a malignant!) disease than a reactive disorder, but the pathogenesis is still unclear [4,5]. Although apparent associations between LCH and malignant tumors have been recognized, these cases represent a minority of all LCH patients and the pathophysiologic relationship remains undefined [6].

The disease may affect any organ or system, more frequently bones, skin, and pituitary gland. Lymph nodes, liver, spleen, gut, the central nervous system, pituitary, and the hematopoietic system are less frequently affected. Lungs may be affected simultaneously or consecutively with other organs, but isolated pulmonary LCH (PLCH) occurs frequently in adults and may proceed to multisystem involvement. PLCH requires a different management in contrast to multi-organ involvement and is therefore discussed in a separate section.

Clinical manifestations of LCH vary depending on the organ or system affected, from self-healing disease to chronic recurrences. A rapid progressive form, seen in children, is usually not observed in adults. Langerhans cell sarcoma (malignant histiocytosis) can occur de novo or from an antecedent LCH [7]. This paper will not cover other histiocytic disorders such as Erdheim-Chester disease (ECD), Rosai-Dorfman disease (RDD) or malignant histiocytosis. In cases of occurrence of LCH and ECD or RDD in the same patient, the management is based on the predominant disease.

Treatment options vary depending on disease extent and severity at onset. A uniform diagnostic work-up is necessary (see Figure 1). One of the main problems of LCH in adults is the variety of potentially involved organs resulting in several physicians being consulted. Frequently only the most obviously affected site is considered and a complete examination is not done thus missing other sites of disease.

Figure 1 Management of Langerhans Cell Histiocytosis in adults.

Diagnosis

The diagnosis of LCH should be based on histologic and immunophenotypic examination of a lesional biopsy. Normal Langerhans cells stain positively with CD1a and/or Langerin [8-10]. Misdiagnoses of LCH have occurred, as the presence of normal reactive LCs in skin and regional lymph nodes may be confusing.

The two levels of certainty of LCH diagnosis which are generally agreed upon are shown in Table 2 [11].

Table 2 Diagnostic criteria of LCH

Definitive:	Presumptive (or compatible):
Based on clinic-pathological evidence with microscopic examination and at least one of the following immunological staining: • Langerin (CD 207) positivity • CD1a positivity • Presence of Birbeck granules on electronic microscopy	Based only on clinico-radiological evidence, without biopsy, as in case of: e.g.: Pulmonary lesions on CT scan with typical cysts and nodules in a smoker. (however, biopsy should be considered in order to reach a more definitive diagnosis)

Pretreatment clinical evaluation

Complete history

Patients with LCH are often asymptomatic or show only mild symptoms. The most common symptoms are dyspnea, cough, bone pain, an abnormal growth of soft tissue over the affected bone, rash, pruritus, increased thirst, and lymphadenopathy. Additional signs are fatigue, generalized weakness, weight loss, night sweats, nausea, and fever.

A thorough history should be performed including the questioning about unexplained symptoms in the past such as "idiopathic" eczema, thyroid disease or diabetes insipidus, lung cysts or pneumothorax, or bony lesions, the smoking and family history with special attention to autoimmune disease. A very small number of familial cases are reported [12].

Complete physical examination

A comprehensive physical examination is necessary. The skin and visible mucous membranes should be inspected. Supplemental neurological and/or psychological investigations are useful in patients presenting with neuromyopathy or cognitive impairment.

Laboratory and radiographic evaluation

The laboratory tests to be performed for all patients independently of affected organs include a complete blood count, blood chemistry, coagulation studies, thyroid stimulating hormone (TSH), freeT4 and urine analysis - see Table 3 (Grade D2).

Table 3 Baseline laboratory and radiographic evaluation

Recommendation	Grade
Full Blood Count (Hemoglobin, White blood cell and differential count, Platelet count)	D2
Blood Chemistry (Total protein, Albumin, Bilirubin , ALT (SGPT), AST (SGOT) Alkaline phosphatase (AP), gammaglutamyl transpeptidase (γGT) Creatinine, Electrolytes, CRP (C-reactive Protein)	D2
Erythrocyte Sedimentation Rate (ESR)	D1
Coagulation Studies (INR/PT, Fibrinogen)	D2
Thyroid Stimulating Hormone (TSH), freeT4	D2

Morning Urine Osmolarity	D1
Urine Test Strip	D2
Ultrasound (liver, spleen, lymph-nodes, thyroid gland)	D2
Chest Radiograph (CXR)	D2
Low Dose Whole Body (Bone) CT (if not available: X-Ray Skeletal/Scull Survey)	D2
Optional: Baseline Head-MRI	D2
Optional: PET-CT instead of Ultrasound, CXR and Bone CT	D2

A skeletal survey, skull series (or low dose whole bone CT [13]) and chest x-ray (AP and lateral) are the first radiographic examinations to be done. CT of specific areas of the skeleton are indicated when mastoid, orbital, scapular, vertebral, or pelvic lesions are found by plain x-rays. MRI may detect additional osseous or extraosseous lesions. A skeletal scintigram (bone scan) alone does not suffice.

Any evidence of a pathological thoracic finding should be followed up by high-resolution chest CT. Ultrasonographic examination of the abdomen may reveal hepatic abnormalities. An ultrasound of the neck with attention to the thyroid gland may be indicated if there are thyroid nodules or evidence of thyroid dysfunction. A MRI of head is needed for hypothalamic/pituitary or brain abnormalities. PET-(CT) scan may identify lesions missed by other modalities and documents response to therapy [14].

Further investigations may be indicated based on the patient's symptoms and the findings of the basic diagnostic tests - see Table 3 and 4 (Grade D2).

Table 4 Specific clinical scenarios: recommended additional testing

Recommendation	Grade
History of polyuria or polydipsia:	D2
• Urine and Plasma osmolality	
• Water deprivation test	
• MRI of the head	
Suspected Other Endocrine Abnormality:	D2
• Endocrine assessment (including dynamic tests of the anterior pituitary, MRI of the head)	
Bi- or Pancytopenia, Or Persistent Unexplained Single Cytopenia:	D2
• Any other cause of cytopenia has to be ruled out according to standard medical practice	
• Bone marrow aspirate and trephine biopsy to exclude causes other than LCH	
• In case of morphological signs of hemophagocytosis additional tests like serum-ferritin should be performed (criteria of HLH)	
Liver Or Spleen Abnormalities:	D2
• In case of any unclear sonographically pathology CT, PET-CT, MRI or Scans should be added (the choice is depending on the sonomorphology – discuss with your radiologist)	
• Visuable lesions of the liver should be biopsied if possible	
• Other causes of splenomegaly has to be ruled out before it may be assigned to LCH	

• ERCP (Endoscopic Retrograde Cholangiopancreatography) or MRCP (Magnetic Resonance Cholangiopancreatography) should be performed in case of elevated serum cholestasis markers or sonomorphologically dilatated bile ducts. Primary biliary cirrhosis and primary sclerosing cholangitis have to be ruled out.	
Unexplained Chronic Diarrhea, Weight loss, Evidence Of Malabsorption Or Hematochezia	D2
• GI-Exploration (Endoscopy with biopsies, capsule endoscopy)	
Enlarged Lymph Nodes (LN):	D2
• If found by screening ultrasound or physical examination the best suitable LN should be extirpated. A LN needle biopsy should be avoided.	
• CT scans or a PET-CT should be performed additionally	
Lung Involvement - In case of abnormal Chest X Ray or symptoms/signs suggestive for lung involvement or suspicion of a pulmonary infection:	D2
• Lung high resolution computed tomography (HR-CT)	
• Lung function tests (Spirometry, Diffusing capacity, Oxygen desaturation during exercise (6MWT), blood gases)	
• Bronchoalveolar lavage (BAL): > 5% CD1a + cells in BAL fluid may be diagnostic of LCH	
• Lung biopsy (if BAL is not diagnostic), ideally Video-assisted thoracoscopic surgery (VATS)	
Osseous Disease:	D2
• CT +/- MRI should be performed in case of craniofacial or vertebral lesions or signs of additional soft tissue involvement	
• Biopsies should be taken from the most suitable region in case of multifocal bone disease	
Skin, Oral And Genital Mucosa lesions:	D2
• Biopsies should be taken	
Aural Discharge Or Suspected Hearing Impairment / Mastoid Involvement:	D2
• Formal hearing assessment	
• MRI of head	

Definition of organ involvement

Possibly involved organs

After the diagnosis of LCH has been made, involvement of other organs should be evaluated and defined according to the clinical, biological or radiological criteria.

Risk organs (bone marrow, liver, spleen, CNS)

Involvement in the hematopoietic system (extremely rare in adults), spleen, liver or CNS indicates a less favorable prognosis, with possible mortality if the patient does not respond to therapy. Although this has never been proven for adults, retrospective analyses of national registries and the experts' experience support the existence of the above mentioned "risk organs".

Fever, night-sweats and weight loss combined with poor performance score might predict the rarely observed aggressive course of LCH in adults comparable to that of high grade non-Hodgkin lymphoma [15,16].

"Special Sites" and "CNS-Risk" bone involvement

Vertebral lesions with intraspinal or cranofacial bone lesions with soft tissue extensions (orbit, mastoid, sphenoid or temporal bones) may cause immediate risk to the patient because of the critical anatomical site and the hazards of attempting local therapy. Isolated disease in these "Special Sites" justifies systemic therapy for children because of spinal cord compression and the association of cranio-facial bone lesions with an increased risk of developing diabetes insipidus [17]. It is unclear if this connection might be extrapolated to adults, but most experts treating LCH patient follow the same guidelines for their adult patients as with the pediatric cases. (Grade D2)

Endocrinologic dysfunction

LCH exhibits a predilection for the hypothalamo-pituitary (HP) region leading to permanent posterior and/or anterior pituitary hormonal deficiencies in a subset of patients.

Diabetes Insipidus (DI) is the most common disease-related consequence that can predate the diagnosis or develop anytime during the course of the disease [18,19]. DI is found in up to 30% of patients [1], but may reach to 40% in patients with multisystem disease or 94% in the presence of other pituitary deficiencies [18,20]. Polyuria and polydipsia, and/or structural abnormalities of the HP region dictate investigations to confirm DI.

Anterior pituitary dysfunction (APD) is found in up to 20% of patients, almost always with DI [18,21]. Although APD is not invariably associated with abnormal HP imaging it is almost always encountered in patients with MS LCH who have DI and HP pathology on MR imaging [22]. Growth hormone deficiency (GHD) is the most frequent disease-related APD found in up to 50% of patients with DI [20]. In adults there are no specific GHD-related symptoms that can suggest the diagnosis [23]. Gonadotropin deficiency is the second most common deficiency, presenting with menstrual disturbances in women and decreased libido in men [20]. ACTH deficiency may be partial or complete and present either with non-specific symptoms or as acute adrenal insufficiency following stressful events. TSH deficiency is almost always associated with panhypopituitarism and may present with subtle symptoms or obvious signs of hypothyroidism. Moderately elevated prolactin levels attributed to pituitary stalk infiltration can cause galactorrhoea in females and gonadotropin deficiency in all patients. Established endocrine deficiencies almost never recover over time, although apparent HP abnormal imaging may often regress either in response to treatment or as a result of the "natural course" of the disease [22].

Hypothalamic involvement is less frequent than pituitary involvement and leads to not only pituitary dysfunction, but neuropsychiatric and behavioral disorders, disturbances of thermo-regulation and sleeping pattern, and autonomic and metabolic abnormalities. The most frequent consequence is severe obesity due to increased appetite. Hypothalamic-related adipsia may seriously complicate the management of DI.

Metabolic abnormalities: One study involving 14 adult patients and 42 controls has shown that adults with LCH are at high risk of developing abnormalities of carbohydrate metabolism

(diabetes mellitus, impaired glucose tolerance) and lipid metabolism leading to increased insulin resistance even in the absence of obesity [24].

Bone metabolism: Adults with LCH may present with a lower than expected bone mineral density at any age especially during periods of active disease [25].

Investigation of hormonal deficiencies: Evaluation of TSH, free T4 and morning urine osmolality is recommended in all patients, further procedures (water deprivation test, plasma osmolality, serum cortisol, insulin like growth factor I, gonadal steroids and gonadotropin serum levels) to detect partial DI or anterior pituitary deficiencies should be performed when clinical symptoms are present (Grade D2).

Dermatological involvement

Cutaneous LCH can be the great pretender, mimicking a number of common dermatoses, and may represent the earliest sign of the disease [26]. The typical scalp lesions are small translucent papules, 1-2 mm in diameter, slightly raised and rose-yellow in colour. These lesions frequently show scaling or crusting, often leading to a misdiagnosis of seborrheic dermatitis.

Intertriginous involvement in the axillary, inguinal, vulvar, or anogenital regions with erythema and erosions are frequently misdiagnosed as eczema, psoriasis, Candida infection, or intertrigo. Generalised skin eruptions can mimic guttate psoriasis prurigo nodularis or lichen planus.

Gingival involvement is frequently associated with alveolar bone involvement and loosening of teeth. Tooth extraction should be avoided as with treatment they will embed into the recovering alveolar bone. Nail changes include paronychia, onycholysis, subungueal hyperkeratosis and purpuric striae of the nail bed, suggesting a wide panel of conditions. Dark-brown striae similar to those drug-induced are also seen.

Cutaneous LCH has so many different manifestations that one needs a high level of suspicion and biopsy is essential. Although skin disease may be the primary presentation, one must investigate for systemic disease. (Grade D2)

Gastrointestinal involvement

Gastrointestinal (GI) tract involvement by LCH is rare and may appear as a solitary colorectal polyp or multiple granulomatous lesions of the mucous membrane in the upper and lower GI tract [27]. Patients are often asymptomatic. Multiple infiltrations are associated with abdominal pain, diarrhea, and hypoalbuinemia.

Liver infiltration is characterized sometimes by infiltration of CD1a+ cells in nodules or by lymphocytes alone along the portal tracts which may lead to sclerosing cholangitis. In case of splenomegaly other causes than LCH primarily have to be ruled out. Pancreatic involvement (mainly tumorous) is extremely rare.

Stratification

Single System LCH (SS-LCH): One organ/system involved (uni- or multifocal):

- ➢ Bone: unifocal (single bone) or multifocal (> 1 bone)
- ➢ Skin
- ➢ Lymph node
- ➢ Hypothalamic-pituitary / Central nervous system
- ➢ Lungs (primary pulmonary LCH)
- ➢ Other (e.g. thyroid, gut)

Multisystem LCH (MS-LCH): Two or more organs/systems involved:

- ➢ With involvement of "Risk Organs" (Hematopoietic system, spleen, and/or liver, tumorous CNS)
- ➢ Without involvement of "Risk Organs"

Treatment

Management algorithms (see Figure 1)

Treatment recommendations are based on site and extension of the disease.

Careful Observation, Local or "mild systemic" Therapy

Bone involvement

In case of single system LCH with unifocal bone involvement of "non-CNS-Risk facial bones" local therapy and careful observation is recommended. The modality of treatment depends on location, size, and symptoms of the disease. Biopsy or curettage is suitable for histopathologic diagnosis and initiating a healing process. Complete excision of bone lesions is not indicated as it may increase the size of the bony defect and the time to healing or result in permanent skeletal defects. Intralesional injection of steroid may hasten healing. Dosages of 40 – 160 mg of methylprednisolone have been used [28] (Grade C2). Radiotherapy is indicated if there is an impending neurological deficit and a high surgical risk, e.g. lesion in the odontoid peg or cranial base. For multifocal bone LCH and for bone lesions in "special sites" systemic therapy (see next page under front line treatment) should be given. (Grade D2)

Isolated lymph nodes involvement

Isolated lymph nodes involvement is rare but spontaneous regressions have been observed. Thus extensive surgery (e.g. neck-dissection) and systemic therapy should be omitted [29] (Grade C2).

Skin Involvement

Surgical excision should be limited to solitary lesions, but mutilating surgeries such as hemi-vulvectomy should not be performed (Grade D2). If the patient is being treated for multisystem disease the skin will respond to treatment. In single system skin disease or in the rare instance where the skin fails to respond fully to systemic treatment for multisystem disease there are a number of treatments directed specifically to the skin:

Topical nitrogen mustard: 20% nitrogen mustard applied to the skin is an effective treatment in children [30]. There is no published data on treatment in adults and there are problems with availability in most countries. (Grade C1)

Phototherapy: Psoralen plus ultraviolet A (PUVA) [31] and narrow band ultraviolet (UV) B [32] are effective in treating cutaneous LCH in individual case reports. It is difficult to treat patients with intertriginous or scalp involvement and would be contraindicated in penile disease. (Grade C1)

Thalidomide: is a TNF-α antagonist and has been shown to be effective in treating cutaneous LCH [33] but gives poor responses in high risk multisystem disease [34]. Dose of 100mg/day in adults is generally used but toxicity with peripheral neuropathy must be monitored (Grade C2).

Azathioprine: There are no published reports of the use of azathioprine (or its metabolite 6-mercaptopurine) in adults with cutaneous LCH but it is a useful drug in single system skin as well as multisystem disease [35]. Patients need to be tested for thiopurine methyl transferase, and if normal should be treated at a dose of 2mg/kg/day. The drug takes about 6 weeks to become effective. (Grade D1)

Methotrexate: There are published reports on the use of low dose methotrexate as either single agent treatment or in combination with azathioprine or prednisolone. Methotrexate was used successfully at the dosages of 20mg once weekly [36]. (Grade C1)

Involvement of the oral mucous membranes

These lesions should be treated with "mild systemic" therapy as described above and extraction of teeth should be avoided as much as possible. In refractory cases more intensive systemic treatment is required (see next paragraph). (Grade D2)

Systemic therapy

Front line treatment

Systemic therapy should be considered in case of the following disease category:

- MS-LCH with/without involvement of "risk organs"
- SS-LCH with multifocal lesions
- SS-LCH with "special site" lesions

There is no standard first line therapy like in pediatric LCH. Vinblastine/prednisolone is mentioned in various chemotherapeutic manuals, but has never been proven effective for adults in a prospective study. An international trial failed because of low recruitment rate. Due to lower risk of neurotoxicity and frequently observed unacceptable steroid induced side effects some experts prefer monotherapy with cladribine, cytarabine or etoposide [35]. In a retrospective study evaluating 58 adult patients with bone lesions the authors observed a clear superiority of cytarabine especially to vinblastine/prednisolone but even to 2-CDA in terms of response and toxicity [37]. Intensive combination chemotherapies (e.g. MACOP-B) are

effective [38] but should be used only in rare cases of an aggressive LCH form [15]. (Grade C1)

Until recently, most experts started with 2-CDA in case of risk organ or tumorous cerebral involvement, but cytarabine may be a reasonable alternative. (Grade C2)

Some investigators have used bisphosphonates for multifocal bone disease, but patients have to be advised to the risk of osteonecrosis of the jaw and its prevention [39]. COX-Inhibitors might be more than analgetic drugs and regression of LCH was observed [40]. (Grade C2).

Grade of recommended systemic first line therapy is listed in Table 5.

Table 5 First line systemic therapy

Recommendation	Grade
Mild Symptoms, No Risk Organ Involved:	
• Methotrexate 20 mg per week p.o/i.v.	C1
• Azathioprine 2 mg/kg/d p.o	D1
• Thalidomide 100mg/d p.o in skin or soft tissue multifocal single system LCH	C2
Additionally In Multifocal Bone LCH	
• zoledronic acid 4 mg i.v.	C2
q 1 (- 6) month (depending on extent and response)	C1
Symptomatic, MS-LCH, No Risk Organs involved	
• Cytarabine 100 mg/m^2 d1-5 q4w i.v.	C1
• Etoposide 100 mg/m^2 d1-5 q4w i.v.	D1
• Vinblastin/Prednisolone (like in pediatric studies)	C1
MS-LCH, Risc Organs Involved	
• 2-CDA 6 mg/m^2 d1-5 q4w s.c./i.v.	C2

Evaluation of response

Evaluation is done after 2 to 3 cycles of chemotherapy. If there is disease progression or reactivation, complete evaluation as recommended in the previous section has to be performed. (Grade D2)

Maintenance therapy

Etoposide or 2-CDA are usually administered up to 6 months. Cytarabine can be given at low dose monthly up to a year in most patients (6-12 cycles). (Grade D2)

Salvage therapy

Refractory disease should be treated with drugs not used for the first course. In case of further progression, especially in CNS involvement cytarabine may be added to 2-CDA (both drugs cross the blood brain barrier) [41]. Some cases with response to tyrosine kinase inhibitors (imatinib) have been reported [42,43]. In the rare case of a most aggressive course of disease hematopoietic stem cell transplant has been performed successfully as well [44,45]. Clofarabine has been effective for refractory childhood LCH [46]. (Grade C2)

Treatment options in case of reactivation

Reactivations of LCH in adults occur in about 25-38% of the patients (European national registry data and [37]). Patients may have further reactivations especially those with multisystem disease.

Reactivation of single system disease

The choice of treatment options is based on the same principles as for initial disease.

The options for reactivations of SS-LCH (skin, bone, other) include

I. Wait and watch approach
II. Local therapy including irradiation (as above)
III. Bisphosphonates for bony disease (as above)
IV. Chemotherapy (as above)

In case of a multisystem reactivation of a SS-LCH, treatment should follow the options for MS-LCH including systemic therapy. (Grade D2)

The efficacy of 2-CDA for single and multisystem reactivated LCH has been proved in a phase II trial [47].

Reactivation after systemic therapy

I. If the reactivation is more than one year after completion of treatment, re-induction with the prior chemotherapy may be effective. If however, the disease is not responsive we suggest discussion with the reference centre for your country.
II. If reactivation occurs while on treatment, potentially 2nd line strategies as described above, but should be generally discussed with your reference centre. (Grade D2)

Radiotherapy

In contrast to pediatric recommendations, radiotherapy is an effective treatment option with acceptable side-effects for adult patients with LCH in selected situations [48-52].

Most literature data concerning radiotherapy in adult LCH deal with uni- or multifocal osseous single-system disease. The local control rates ranged from 75-100%, complete remission from 79-100%, respectively [53].

The dose recommendation for radiotherapy is still controversial and an exact dose-effect relationship has not been established. There is a wide dose range of applied total doses from 1,4 Gy up to 45 Gy. In general, a dose range from 10 to 20 Gy is recommended in adults [50,54]). (Grade C2)

Recommended indications for the use of radiotherapy in adults with LCH are listened in Table 6.

Table 6 Possible indications for the use of radiotherapy in adults

Recommendation	Grade
Isolated "Unresectable" lesion: if a resection would significantly compromise anatomic function, e.g. odontoid peg, CNS	C2
Recurrent or progressive lesion: In multifocal or multisystem disease only in case of minor response to standard systemic therapy	C2
Adjuvant treatment following marginal or incomplete resection: especially in single system bone disease with soft tissue involvement	C2

Treatment and hormone replacement of endocrinopathies

DI should be treated with desmopressin. The timing and dosage must be individualized. In proven LCH new onset DI is a sign of active disease and initiation of systemic treatment is recommended to try to prevent the development of further hormonal deficiencies although existing ones usually do not resolve [55]. Adequate replacement of hormonal deficiencies should be initiated as soon the diagnosis is made. (Grade D2)

Central nervous system involvement

Tumorous lesions

These lesions are most frequently observed in the hypothalamic-pituitary region. The tumor size ranges from discrete thickening of the pituitary stalk to larger tumors. Parenchymal, meningeal or choroid plexus lesions occur less frequently [56].

In addition to hormone replacement isolated cerebral tumors should be treated with irradiation or chemotherapy and pituitary/hypothalamic lesions with chemotherapy. Multifocal brain lesions or single brain lesions with multi system disease need to be treated with chemotherapy. The most suitable drugs are Cladribine or Cytarabine as described above. (Grade C2)

Neurodegerative LCH

Non-tumorous MRI findings of the cerebellum, and/or brain stem are histopathologically different than the typical LCH mass lesions. The neurodegenerative lesions lack CD1a+ histiocytes and have infiltrating CD8+ lymphocytes [55]. Some of these patients show no symptoms, others have clinical signs ranging from subtile tremor, dysarthria, dysphagia, and motor spasticity to pronounced ataxia, behavioral disturbances and severe psychiatric disease.

Retinoic acid and intravenous immunoglobulin may stabilize such patients [57,58]. Improvement with infliximab has been observed in one case [59]. Cytarabine with or without Vincristine provided improvement in 5/8 patients of which 4/8 remained stable over more than 7 years of follow-up and one relapsed but is improved after treatment with intravenous Methotrexate. Patients who responded to Cytarabine/Vincristine had symptoms for less than 18 months before starting treatment [60,61]. Thus early onset of Cytarabine is recommended

as first line therapy, but for any case of neurodegenerative LCH we suggest discussion with the reference centre for your country. (Grade C1)

Primary pulmonary LCH

Epidemiology

The incidence of pulmonary LCH (PLCH) is unknown. Reports provided by histopathological studies and interstitial lung diseases registries revealed about 5% of PLCH in this population [62]. Data from a Japanese survey show an estimated prevalence of 0.07-0.27/100000 population in females and males, respectively [63]. The prevalence may be underestimated.

PLCH affects mainly young, predominantly smoking (> 90%) adults with a peak at 20-40 years of age and a slight predominance of women. It is unknown if there are any racial differences in this disease [62].

Clinical features

Patients with PLCH often present with a non-productive cough or dyspnoea, chest pain, associated non-specific symptoms like fatigue, weight loss, night sweats and fever may be observed [62,64]. About 20% of patients with PLCH are initially asymptomatic and an equal percentage of patients present with acute symptoms of a pneumothorax.

It is important to exclude the existence of multi system LCH. Thus, a thorough history, comprehensive physical examination, and baseline radiographic, blood and urine tests should be performed in any patient presenting with PLCH to avoid undertreatment. (see Table 3 and 4).

Diagnosis

X-Ray of the chest shows a reticulo-micronodular pattern. In more advanced cases cysts may be visible within the infiltrates symmetrically in both lungs, but predominating in the middle and upper lung fields and sparing the costophrenic angles [62].

High resolution CT (HRCT) is the most important visualizing tool for PLCH [62]. The typical HRCT pattern is of small nodules, cavitated nodules (both may resolve), and thick- and finally thin-walled cysts. As the disease evolves, cystic lesions become a predominant finding.

Pulmonary lung function tests most frequently show reduced diffusing capacity of the lung for carbon monoxide (DLCO), 70–90% of the patients. Lung volumes are impaired in a majority of patients with decreased vital capacity and air trapping (elevated residual volume). Total lung capacity is within normal values in most cases. An obstructive pattern is observed in a sizeable proportion of patients, particularly in advanced disease. Rarely a restrictive component may appear [65]. A predominantly nodular pattern suggestive of active inflammatory disease can have only moderate functional consequences [65].

Bronchoalveolar lavage (BAL) often shows high alveolar macrophage counts, reflective of smoking. Infection should be systematically ruled out. BAL yielding more than 5% CD1-positive cells has previously reported to support the diagnosis of pulmonary LCH [66]. While this has a high specificity, BAL results lack sensitivity.

Bronchial biopsies are not helpful in the diagnosis of PLCH but are useful in ruling out other diagnoses in patients with atypical manifestations. The diagnostic method of choice is therefore videothoracoscopic lung biopsy after HRCT evaluation (see Table 7). In asymptomatic patients with a typical HRCT pattern and a macrophage alveolitis by BAL, for whom no systemic therapy is required, a presumptive diagnosis may be acceptable with a close follow-up. In patients with extensive cystic lesions, the risk of invasive procedures has to be balanced with the need for a definitive diagnosis. (Grade D2)

Table 7 Diagnostic recommendations in pLCH

Recommendation	Grade
Confirm definitive diagnosis	
• in all patients before start of systemic therapy	D2
• prefer lung biopsy	D2
• HRCT is required in all patients	D2
Exclude Existence Of Multi System LCH	D2

Treatment and prognosis

The natural history of adults with PLCH is widely variable and mostly unpredictable in the individual patient. About 40-50% of patients with PLCH experience a favorable outcome and partial or complete clearance of the radiological abnormalities occurs with or without therapy.

Serial lung function tests are essential for following patients with PLCH. In a recent retrospective multicenter study, lung function (mainly DLCO and FEV_1) deteriorated in approximately 60% of the patients [65]. An isolated decline of DLCO in symptomatic patients should prompt a search for pulmonary hypertension by echocardiography and in case of increased systolic pulmonary arterial pressure should be confirmed by right heart catheterization [67].

Based on the epidemiologic data smoking cessation is essential. Patients with a stable disease despite ongoing smoking should be told about all other known medical reasons for ceasing smoking and enrollment in a support group may be valuable [62,64].

There are no study-based data supporting cortisone therapy for pulmonary LCH. Any possible therapeutic benefit for symptomatic patients should, therefore, be carefully weighed against the potential undesired effects of this form of treatment, because spontaneous remissions do occur. If smoking cessation failed and treatment is required systemic steroid therapy (usually 1mg/kg/day for one month, followed by tapering dosages over months) may be given in patients with the nodular form of pulmonary LCH [62,64].

Lower respiratory tract infection is a common cause of deterioration of PLCH and should lead to prompt treatment. Annual vaccination against influenza as well as anti-pneumococcal is recommended for patients with impaired lung function.

Progressive PLCH despite steroid therapy may be treated with 2-CDA [68,69]. A randomized controlled trial evaluating the effectiveness and tolerance of 2-CDA in this subgroup of patients is ongoing.

Pneumothorax requires drainage and pleurodesis should be considered in case of recurrence [70]. Lung transplantation (LT) may represent a therapeutic option in case of advanced PLCH (severe respiratory failure or major pulmonary hypertension). Recurrence of LCH after transplatation occurs in 20% without impact on the survival rate [71].

Grades of recommendations for therapy in pLCH are listed in Table 8.

Table 8 Therapeutic recommendations in pLCH

Recommendation	Grade
first step is Smoking cessation in all patients	C2
Watchful waiting in a- or minor symptomatic patients	C2
systemic steroid therapy in symptomatic patients	C2
Chemotherapy (e.g. 2-CDA) in progressive disease	C2
consider lung transplantation in case of severe respiratory failure or major pulmonary hypertension	C2

Pregnancy

There are only a few reports about pregnancy and LCH with worsening to no change of clinical symptoms, but even improvement was observed. Deterioration was mainly related to diabetes insipidus. It is unclear if worsening or onset of DI during pregnancy is really caused by LCH. This may also be observed in women not suffering from a histiocytic disorder and is caused by an accelerated degradation of vasopressin through placental enzyme vasopressinase [72].

It is unpredictable if and in which way pregnancy may influence the course of LCH. The scant literature suggests there is no adverse impact of LCH on pregnancy or birth, with exception of need for cesarean section in selected cases [73,74]. (Grade C2)

Follow up

LCH may reactivate and lead to chronic local symptoms or induce organ dysfunction. Rarely LCH is associated with malignant tumors. Therefore, follow-up investigations of disease and monitoring of functional impairments are necessary.

Restaging every 2-3 months is standard. Follow-up intervals depend on the primary extent and activity of disease within 3 to 12 months (see Table 9). In case of affirmed reactivation, clinical evaluation should include all investigations listed above. (Grade D2)

Table 9 Recommendations for follow-up

Test	Frequency	Grade
SS-LCH And No Disease Activity		
History (especially of thirst, polyuria, cough, dyspnea, bone pain, skin changes, neurological symptoms)	• Every clinic visit	D2
Clinical assessment, blood count and blood chemistry (as described in baseline diagnostics), ultrasound	• End of therapy • every 6 month (for the next 2 years) • then once a year (for at least 3 years)	D2
Chest XR	• annually (for at least 3 years)	D2
After MS-LCH And With No Disease Activity		
History (especially of thirst, polyuria, cough, dyspnea, bone pain, skin changes, neurological symptoms)	• Every clinic visit	D2
Clinical assessment, blood count and blood chemistry(as described in baseline diagnostics), ultrasound	• End of therapy • every 3 month (for the next 2 years) • every 6 month (for the next 3 years) • then once a year (for at least 5 years)	D2
Chest XR	• annually (for at least 3 years)	D2
TSH, freeT4	• Once a year (until end of routinely follow up)	D2
Patients With Active Disease		
Diagnostic procedures are depending on the site of organ involvement	Frequency is depending on rates and velocity of recurrences	D2
Patients With pLCH		
History (in case of non-pulmonary symptoms: look for MS LCH, see Table 4)	• Every clinic visit	D2
Diagnostic procedures are depending on symptoms und course of PLCH (baseline: Chest X-ray, lung function (+DCLO)	• End of therapy • every 6 month (for the next 2 years) • then once a year (for at least 5 years)	D2

Competing interest

The authors declare that they have no competing interests.

Authors' contributions

Based on the available literature up to December 2012, recommendations were established, drafts were commented by the entire group, and redrafted by the executive editor. All authors read and approved the final manuscript.

References

1. Arico M, *et al*: **Langerhans cell histiocytosis in adults. Report from the International Registry of the Histiocyte Society.** *Eur J Cancer* 2003, **39**(16):2341–2348.

2. Willman CL, *et al*: **Langerhans'-cell histiocytosis (histiocytosis X)–a clonal proliferative disease.** *N Engl J Med* 1994, **331**(3):154–160.

3. Yousem SA, *et al*: **Pulmonary Langerhans' cell histiocytosis: molecular analysis of clonality.** *Am J Surg Pathol* 2001, **25**(5):630–636.

4. Badalian-Very G, *et al*: **Recurrent BRAF mutations in Langerhans cell histiocytosis.** *Blood* 2010, **116**(11):1919–1923.

5. Badalian-Very G, *et al*: ***Pathogenesis of Langerhans Cell Histiocytosis.*** *Annu Rev Pathol* 2013, **24**(8):1–20.

6. Egeler RM, *et al*: **Association of Langerhans cell histiocytosis with malignant neoplasms.** *Cancer* 1993, **71**(3):865–873.

7. Lee JS, *et al*: **Langerhans cell sarcoma arising from Langerhans cell histiocytosis: a case report.** *J Korean Med Sci* 2006, **21**(3):577–580.

8. Lau SK, Chu PG, Weiss LM: **Immunohistochemical expression of Langerin in Langerhans cell histiocytosis and non-Langerhans cell histiocytic disorders.** *Am J Surg Pathol* 2008, **32**(4):615–619.

9. Swerdlow SHC, *et al*: *International Agency for Research on, Cancer and O. World Health: WHO classification of tumours of haematopoietic and lymphoid tissues.* International Agency for Research on Cancer (IARC); 2008.

10. Valladeau J, *et al*: **Langerin, a novel C-type lectin specific to Langerhans cells, is an endocytic receptor that induces the formation of Birbeck granules.** *Immunity* 2000, **12**(1):71–81.

11. Minkov M, Grois N, McClain K, Nanduri V, Rodriguez-Galindo C, Simonitsch-Klupp I, Visser J, Weitzmann S, Whitlock J, Windebank K: *Langerhans Cell Histiocytosis - Histiocyte Society Evaluation and Treatment Guidelines.* ; 2009. cited; Available from: www.histiocytesociety.org/document.doc?id=290.

12. Arico M, *et al*: **Familial clustering of Langerhans cell histiocytosis.** *Br J Haematol* 1999, **107**(4):883–888.

13. McClain K: *Bone and Soft Tissue Involvement - Oral Presentation at the Annual Meeting of the Histiocyte Society, Vienna.* ; 2011.

14. Phillips M, *et al*: **Comparison of FDG-PET scans to conventional radiography and bone scans in management of Langerhans cell histiocytosis.** *Pediatr Blood Cancer* 2009, **52**(1):97–101.

15. Szturz P, *et al*: **[Lymphoma-like course in aggressive adult multisystem Langerhans cell histiocytosis and the benefit of PET/CT imaging in evaluation of diffuse metabolic activity of lung parenchyma].** *Vnitr Lek* 2010, **56**(11):1177–1193.

16. Teng CL, *et al*: **Rapidly fatal Langerhans' cell histiocytosis in an adult.** *J Formos Med Assoc* 2005, **104**(12):955–959.

17. Grois N, *et al*: **Risk factors for diabetes insipidus in langerhans cell histiocytosis.** *Pediatr Blood Cancer* 2006, **46**(2):228–233.

18. Kaltsas GA, *et al*: **Hypothalamo-pituitary abnormalities in adult patients with langerhans cell histiocytosis: clinical, endocrinological, and radiological features and response to treatment.** *J Clin Endocrinol Metab* 2000, **85**(4):1370–1376.

19. Prosch H, *et al*: **Central diabetes insipidus as presenting symptom of Langerhans cell histiocytosis.** *Pediatr Blood Cancer* 2004, **43**(5):594–599.

20. Makras P, *et al*: **Endocrine manifestations in Langerhans cell histiocytosis.** *Trends Endocrinol Metab* 2007, **18**(6):252–257.

21. Amato MC, *et al*: **Endocrine disorders in pediatric - onset Langerhans Cell Histiocytosis.** *Horm Metab Res* 2006, **38**(11):746–751.

22. Makras P, *et al*: **Evolving radiological features of hypothalamo-pituitary lesions in adult patients with Langerhans cell histiocytosis (LCH).** *Neuroradiology* 2006, **48**(1):37–44.

23. Donadieu J, *et al*: **Incidence of growth hormone deficiency in pediatric-onset Langerhans cell histiocytosis: efficacy and safety of growth hormone treatment.** *J Clin Endocrinol Metab* 2004, **89**(2):604–609.

24. Alexandraki KI, *et al*: **Cardiovascular risk factors in adult patients with multisystem Langerhans-cell histiocytosis: evidence of glucose metabolism abnormalities.** *QJM* 2008, **101**(1):31–40.

25. Makras P, *et al*: ***Reduced bone mineral density in adult patients with Langerhans cell histiocytosis.*** *Pediatr Blood Cancer* 2012, **58**(5):819–822.

26. Caputo R: *A Text Atlas of Histiocytic Syndromes.* Informa HealthCare; 1998.

27. Singhi AD, Montgomery EA: **Gastrointestinal tract langerhans cell histiocytosis: A clinicopathologic study of 12 patients.** *Am J Surg Pathol* 2011, **35**(2):305–310.

28. Yasko AW, *et al*: **Percutaneous techniques for the diagnosis and treatment of localized Langerhans-cell histiocytosis (eosinophilic granuloma of bone).** *J Bone Joint Surg Am* 1998, **80**(2):219–228.

29. Lo WC, *et al*: **Isolated adult Langerhans' cell histiocytosis in cervical lymph nodes: should it be treated?** *J Laryngol Otol* 2009, **123**(9):1055–1057.

30. Hoeger PH, *et al*: **Long term follow up of topical mustine treatment for cutaneous langerhans cell histiocytosis.** *Arch Dis Child* 2000, **82**(6):483–487.

31. Sakai H, *et al*: **Satisfactory remission achieved by PUVA therapy in Langerhans cell hisiocytosis in an elderly patient.** *J Dermatol* 1996, **23**(1):42–46.

32. Imafuku S, *et al*: **Cutaneous Langerhans cell histiocytosis in an elderly man successfully treated with narrowband ultraviolet B.** *Br J Dermatol* 2007, **157**(6):1277–1279.

33. Sander CS, Kaatz M, Elsner P: **Successful treatment of cutaneous langerhans cell histiocytosis with thalidomide.** *Dermatology* 2004, **208**(2):149–152.

34. McClain KL, Kozinetz CA: **A phase II trial using thalidomide for Langerhans cell histiocytosis.** *Pediatr Blood Cancer* 2007, **48**(1):44–49.

35. Chu A: *Dermatological Aspects and Presentation of an Adult Clinic - Oral Presentation at the Annual Meeting of the Histiocyte Society, Vienna.* ; 2011.

36. Steen AE, *et al*: **Successful treatment of cutaneous Langerhans cell histiocytosis with low-dose methotrexate.** *Br J Dermatol* 2001, **145**(1):137–140.

37. Cantu MA, *et al*: **Optimal therapy for adults with Langerhans cell histiocytosis bone lesions.** *PLoS One* 2012, **7**(8):e43257.

38. Derenzini E, *et al*: **MACOP-B regimen in the treatment of adult Langerhans cell histiocytosis: experience on seven patients.** *Ann Oncol* 2010, **21**(6):1173–1178.

39. Montella L, *et al*: **Zoledronic acid in treatment of bone lesions by Langerhans cell histiocytosis.** *J Bone Miner Metab* 2009, **27**(1):110–113.

40. Reichle A, *et al*: **Anti-inflammatory and angiostatic therapy in chemorefractory multisystem Langerhans' cell histiocytosis of adults.** *Br J Haematol* 2005, **128**(5):730–732.

41. McClain KL: **Drug therapy for the treatment of Langerhans cell histiocytosis.** *Expert Opin Pharmacother* 2005, **6**(14):2435–2441.

42. Montella L, Insabato L, Palmieri G: **Imatinib mesylate for cerebral Langerhans'-cell histiocytosis.** *N Engl J Med* 2004, **351**(10):1034–1035.

43. Janku F, *et al*: **Response of histiocytoses to imatinib mesylate: fire to ashes.** *J Clin Oncol* 2010, **28**(31):e633–e636.

44. Ingram W, *et al*: **Reduced-intensity conditioned allogeneic haematopoietic transplantation in an adult with Langerhans' cell histiocytosis and thrombocytopenia with absent radii.** *Bone Marrow Transplant* 2006, **37**(7):713–715.

45. Xicoy B, *et al*: **[Sustained remission in an adult patient with Langerhans cell histiocytosis following T-cell depleted allogenic cell transplantation].** *Med Clin (Barc)* 2006, **127**(18):716.

46. Rodriguez-Galindo C, *et al*: **Clofarabine in refractory Langerhans cell histiocytosis.** *Pediatr Blood Cancer* 2008, **51**(5):703–706.

47. Saven A, Burian C: **Cladribine activity in adult langerhans-cell histiocytosis.** *Blood* 1999, **93**(12):4125–4130.

48. Atalar B, *et al*: **Adult langerhans cell histiocytosis of bones : a rare cancer network study.** *Acta Orthop Belg* 2010, **76**(5):663–668.

49. Gaundong Mbethe GL, *et al*: **[Multifocal Langerhans cell histiocytosis of bone: indications for radiotherapy].** *Cancer Radiother* 2010, **14**(8):759–762.

50. Brady LW, *et al*: **Langerhans Cell Histiocytosis**. In *Langerhans Cell Histiocytosis.* Edited by Olschewski T, Seegenschmiedt MH, Micke O. Springer Verlag; 2008:397–423.

51. Greenberger JS, *et al*: **Radiation therapy in patients with histiocytosis: management of diabetes insipidus and bone lesions.** *Int J Radiat Oncol Biol Phys* 1979, **5**(10):1749–1755.

52. Heyd R, *et al*: **Radiotherapy in Langerhans-cell histiocytosis. 2 case reports and review of the literature.** *Rontgenpraxis* 2000, **53**(2):51–61.

53. Micke O, Seegenschmiedt MH: **Consensus guidelines for radiation therapy of benign diseases: a multicenter approach in Germany.** *Int J Radiat Oncol Biol Phys* 2002, **52**(2):496–513.

54. Cassady JR: **Current role of radiation therapy in the management of histiocytosis-X.** *Hematol Oncol Clin North Am* 1987, **1**(1):123–129.

55. Grois N, *et al*: **Neuropathology of CNS disease in Langerhans cell histiocytosis.** *Brain* 2005, **128**(Pt 4):829–838.

56. Grois N, *et al*: **Central nervous system disease in Langerhans cell histiocytosis.** *J Pediatr* 2010, **156**(6):873–881. 881 e1.

57. Idbaih A, *et al*: **Retinoic acid therapy in "degenerative-like" neuro-langerhans cell histiocytosis: a prospective pilot study.** *Pediatr Blood Cancer* 2004, **43**(1):55–58.

58. Imashuku S, *et al*: **Treatment of neurodegenerative CNS disease in Langerhans cell histiocytosis with a combination of intravenous immunoglobulin and chemotherapy.** *Pediatr Blood Cancer* 2008, **50**(2):308–311.

59. Chohan G, *et al*: **Langerhans cell histiocytosis with refractory central nervous system involvement responsive to infliximab.** *J Neurol Neurosurg Psychiatry* 2012, **83**(5):573–575.

60. Allen CE, *et al*: **Neurodegenerative central nervous system Langerhans cell histiocytosis and coincident hydrocephalus treated with vincristine/cytosine arabinoside.** *Pediatr Blood Cancer* 2010, **54**(3):416–423.

61. Allen CE: **Personal communication about**. In *Neurodegenerative central nervous system Langerhans cell histiocytosis and coincident hydrocephalus treated with vincristine/cytosine arabinoside.*; 2010.

62. Tazi A: **Adult pulmonary Langerhans' cell histiocytosis.** *Eur Respir J* 2006, **27**(6):1272–1285.

63. Watanabe R, *et al*: **Clinico-epidemiological features of pulmonary histiocytosis X.** *Intern Med* 2001, **40**(10):998–1003.

64. Vassallo R, *et al*: **Clinical outcomes of pulmonary Langerhans'-cell histiocytosis in adults.** *N Engl J Med* 2002, **346**(7):484–490.

65. Tazi A, Marc K, Dominique S, de Bazelaire C, Crestani B, Chinet T, Israel-Biet D, Cadranel J, Frija J, Lorillon G, Valeyre D, Chevret S: **Serial CT and lung function testing in pulmonary Langerhans cell histiocytosis.** *Eur Respir J* 2012, **40**(4):905–912.

66. Auerswald U, Barth J, Magnussen H: **Value of CD-1-positive cells in bronchoalveolar lavage fluid for the diagnosis of pulmonary histiocytosis X.** *Lung* 1991, **169**(6):305–309.

67. Lepavec J, Lorillon G, Jaïs X, Tcherakian C, Feuillet S, Dorfmüller P, Simonneau G, Humbert M, Tazi A: **Pulmonary Langerhans Cell Histiocytosis associated pulmonary hypertension: clinical characteristics and impact of pulmonary arterial hypertension therapies.** *Chest* 2012.

68. Lazor R, *et al*: **Progressive diffuse pulmonary Langerhans cell histiocytosis improved by cladribine chemotherapy.** *Thorax* 2009, **64**(3):274–5.

69. Lorillon G, *et al*: **Cladribine is effective against cystic pulmonary Langerhans cell histiocytosis.** *Am J Respir Crit Care Med* 2012, **186**(9):930–2.

70. Mendez JL, *et al*: **Pneumothorax in pulmonary Langerhans cell histiocytosis.** *Chest* 2004, **125**(3):1028–32.

71. Dauriat G, *et al*: **Lung transplantation for pulmonary langerhans' cell histiocytosis: a multicenter analysis.** *Transplantation* 2006, **81**(5):746–50.

72. Ananthakrishnan S: **Diabetes insipidus in pregnancy: etiology, evaluation, and management.** *Endocr Pract* 2009, **15**(4):377–82.

73. DiMaggio LA, Lippes HA, Lee RV: **Histiocytosis X and pregnancy.** *Obstet Gynecol* 1995, **85**(5 Pt 2):806–9.

74. Sharma R, Maplethorpe R, Wilson G: **Effect of pregnancy on lung function in adult pulmonary Langerhans cell histiocytosis.** *J Matern Fetal Neonatal Med* 2006, **19**(1):67–8.

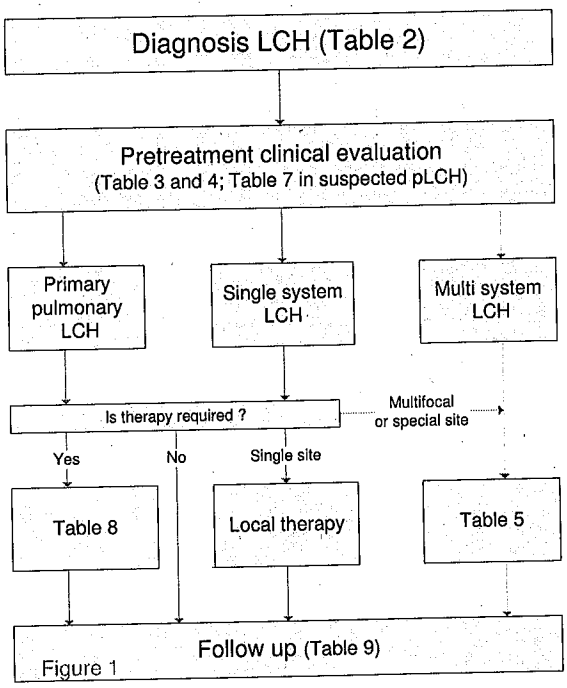
Diagnosis LCH (Table 2)
Pretreatment clinical evaluation
(Table 3 and 4; Table 7 in suspected pLCH)
Primary pulmonary LCH
Single system LCH
Multi system LCH
Is therapy required ?
Multifocal or special site
Yes
No
Single site
Table 8
Local therapy
Table 5
Follow up (Table 9)

Figure 1

Etude LCH A 1 A Tazi St Louis

Eur Respir J 2012; 40: 905–912
DOI: 10.1183/09031936.00210711

Serial computed tomography and lung function testing in pulmonary Langerhans' cell histiocytosis

Abdellatif Tazi, Karima Marc, Stéphane Dominique, Cédric de Bazelaire, Bruno Crestani, Thierry Chinet, Dominique Israel-Biet, Jacques Cadranel, Jacques Frija, Gwenael Lorillon, Dominique Valeyre and Sylvie Chevret

ABSTRACT: **Little is known about longitudinal lung function variation in patients with pulmonary Langerhans' cell histiocytosis (LCH). The contribution of serial lung computed tomography (CT) to managing these patients has not been evaluated.**

This long-term retrospective study included 49 patients who were serially evaluated by lung CT and pulmonary function tests. The lung function variation was categorised as improvement or deterioration. The extent of the CT lesions was correlated with lung function.

Lung function deteriorated in ~60% of the patients. Forced expiratory volume in 1 s (FEV_1) and diffusing capacity of the lung for carbon monoxide ($D_{L,CO}$) were the parameters that most frequently deteriorated. A subgroup of patients experienced a dramatic decline in FEV_1 within 2 yrs of diagnosis. Airway obstruction was the major functional pattern observed. In a multivariate analysis, % predicted FEV_1 at diagnosis was the only factor associated with the incidence of airway obstruction. The increase in cystic lesions on the lung CTs was associated with impaired lung function but did not anticipate the decline in FEV_1 or $D_{L,CO}$.

Serial lung function tests are essential for following patients with pulmonary LCH, who frequently develop airway obstruction. A lung CT at diagnosis is informative, but routine sequential CTs seem less useful. A prospective study is needed to characterise those patients with early progressive disease.

KEYWORDS: **Airway obstruction, diffuse cystic lung disease, multicentre study, smoking cessation**

Pulmonary Langerhans' cell histiocytosis (LCH) is an uncommon disorder that occurs predominantly in young smokers [1–4]. The natural history of pulmonary LCH is widely variable and difficult to predict in an individual patient [5–8]. It has been suggested that older age, evidence of obstruction, air trapping (an increased residual volume (RV)/total lung capacity (TLC) ratio) and a reduced diffusing capacity for carbon monoxide ($D_{L,CO}$) at diagnosis are associated with the development of respiratory failure and increased mortality [5, 6, 9]. However, scant information is available concerning the longitudinal variations in lung function over time, particularly over a long period.

The eventual contribution of high-resolution computed tomography (HRCT) to predicting the outcome of patients with pulmonary LCH has not been evaluated. Nodules may progress over time to cysts that may remain stable or progress [10]. The extent of the cystic lesions present on HRCT has been correlated with impaired $D_{L,CO}$ and an impaired forced expiratory volume in 1 s (FEV_1)/forced vital capacity (FVC) ratio at a given time point [11, 12] and (more recently) during follow-up in a small series of patients [13]. Those authors stated that the patients with declining lung function had severe cystic alterations on lung computed tomography (CT), but few patients in their series progressed [13].

We conducted a long-term retrospective multicentre study of a large cohort of patients with pulmonary LCH who were serially evaluated by HRCT and lung function testing. We had the following objectives:

AFFILIATIONS
For affiliations details, please refer to the Acknowledgements section.

CORRESPONDENCE
A. Tazi
Service de Pneumologie
Hôpital Saint Louis
1 Avenue Claude Vellefaux
75475
Paris cedex 10
France
E-mail: abdellatif.tazi@sls.aphp.fr

Received:
Dec 01 2011
Accepted after revision:
Feb 14 2012
First published online:
March 22 2012

European Respiratory Journal
Print ISSN 0903-1936
Online ISSN 1399-3003

This article has supplementary material available from www.erj.ersjournals.com

1) to evaluate the longitudinal variation in lung function parameters; 2) to compare the HRCT findings and lung function results during follow-up; and 3) to identify the factors that predict eventual outcome in these patients.

MATERIALS AND METHODS

Design of the study, setting and subject selection

This was a retrospective study involving seven French teaching hospital pulmonary departments. All the consecutive patients referred to these centres for pulmonary LCH from June 1989 to January 2005 were sequentially included in this study, provided that they were serially evaluated by two or more HRCTs and lung function tests performed at ⩾6-month intervals.

49 patients with pulmonary LCH were selected to be reviewed retrospectively in the cohort. This study was approved by the institutional review board of Bichat Hospital, Paris, France (number IRB00006477).

Diagnosis of pulmonary LCH

The diagnosis of pulmonary LCH was based on one of the following criteria: 1) disease proven by lung biopsy; 2) a positive biopsy of an extra thoracic localisation of the disease or the presence of diabetes insipidus associated with characteristic lung HRCT findings; or 3) the combination of an appropriate clinical setting, a typical lung HRCT pattern (showing both nodules and cysts) and exclusion of the alternative diagnoses.

Data collection

Data on the patients' demographics, clinical presentation, smoking habits and treatments of interest were retrieved from the medical records.

All of the HRCT scans were centrally analysed by two radiologists (C. de Bazelaire and J. Frija) and a chest physician (A. Tazi), without knowledge of the clinical or functional findings. The lung HRCT lesions were classified as has been previously described [10]. Each lung was divided into three areas, from the lung apices to the domes of the diaphragm, and semi-quantitative CT scores were established for each area to estimate the nodule profusion and the extent of the cysts. The results were obtained by consensus. The global nodular and cystic CT scores were calculated by adding the nodule extent and cyst values obtained from the three areas of the lung (giving maximum values of 18 and 24, respectively). Based on the CT scores, the patients were classified as having low, intermediate and high nodular CT scores, and low, intermediate, high and very high cystic CT scores. Additional details on the methods used to determine the lung CT scores are provided in the online supplement.

Lung volumes were evaluated by plethysmography (except for two patients), and FEV1 and FVC by the flow–volume curve. $D_{L,CO}$ was measured using the single-breath method. The predictive values were determined as has been previously described [14]. Obstruction was defined as FEV1/FVC ratio <70% [15].

End-points of the study

Two outcomes were considered: deterioration or improvement of lung function from the baseline measurements. For each parameter, variations of ⩾10% in the FEV1 or FVC, or of ⩾15% in the $D_{L,CO}$ defined improvement or deterioration [16]. The overall lung function outcome was defined by whether there was an increase or decrease of ⩾10% in the FEV1 and/or FVC, and/or of ⩾15% in the $D_{L,CO}$. In cases of discrepancies, the impaired parameter was used as the overall lung function outcome. If the changes were <10% for FEV1 and FVC, and <15% for $D_{L,CO}$, lung function was considered to be stable.

Times to developing airway obstruction and restriction were also computed.

Statistical analysis

The descriptive statistics of the study groups are presented. Mean±SD or median (interquartile range (IQR)) values are reported. Receiver operating characteristic (ROC) curves for the HRCT scores were plotted to delineate the patients with obstructive or restrictive patterns at diagnosis, with the area under the ROC curve (AUC) used as a measure of discrimination.

Patient follow-up was the interval between the date of the first examination and the date of an event; the patients who neither deteriorated nor improved and who did not develop obstructive or restrictive functional defects were censored at the reference date (September 2005). Thus, the actual follow-up varied according to the patients' date of inclusion in the study and was up to 16 yrs. As the patients were enrolled sequentially from 1989 to 2005 and the study ended in September 2005, statistical methods for time-to-event data were used to account for the censoring of the data. The cumulative incidences of lung function deterioration, lung function improvement and obstructive or restrictive patterns over time were estimated separately. Cox proportional hazards models were used to calculate the relative hazards of lung function deterioration or improvement associated with different population characteristics while fully adjusting for potential confounders. To assess the influence of smoking cessation, a Cox model with a time-dependent covariate was used.

All of the statistical tests were two-sided, with p-values ⩽0.05 denoting statistical significance.

RESULTS

Study population

The demographic characteristics, clinical features, lung function tests and HRCT score subgroups at diagnosis are shown in table 1. Among the 47 patients evaluated by plethysmography, 23 (49%) patients had normal lung volumes, 21 (45%) had air trapping and three (6%) patients had a mild restriction (TLC 78.7±0.6% predicted), either isolated (n=2) or associated with obstruction (mixed pattern, n=1). Among the whole study population (n=49), 15 (31%) had an obstructive pattern (FEV1 74.4±13.7% pred; FEV1/FVC 65.1±3.4%). The $D_{L,CO}$ was decreased in 35 (81%) of the 42 patients in whom it was initially measured.

46 patients had both nodules and cysts in their lung HRCTs and three patients had an isolated cystic pattern. At the time of diagnosis, the mean HRCT nodular score was 6.6±3.4 and the mean cystic score was 11.9±6.1.

Nine patients received steroids for 22.9±11.7 months and one received vinblastine alone for 19 months, while two were treated with both prednisone and vinblastine for 19 and 40 months, respectively.

TABLE 1 The characteristics of the patients at the time of their pulmonary Langerhans' cell histiocytosis diagnosis

Characteristic	Subjects
Subjects n	49
Age yrs	30.5±7.2
Male sex	24 (49)
Smoking status	
Current smokers	46 (94)
Ex-smokers	3 (6)
Exposure pack-yrs	22±19
Symptoms	38 (77.5)
Cough	25 (51.0)
Dyspnoea (NYHA II/III)	10/1 (22.5)
Pneumothorax	9 (18.5)
Respiratory + constitutional	11 (22.5)
No symptoms	11 (22.5)
Histological confirmation	35 (71)
Surgical lung biopsy	30 (61)
Extra-pulmonary biopsy	5 (10)
TLC# % pred	100.4±16.5
FVC % pred	89.1±18.6
RV# % pred	129.4±47.8
RV/TLC# % pred	126.5±38.0
FEV_1 % pred	77.6±21.9
FEV_1/FVC %	72.8±12.6
$D_{L,CO}$ % of pred (n=42)	62.8±22.6
HRCT nodular score subgroup	
Low	31 (63)
Intermediate	16 (33)
High	2 (4)
HRCT cystic score subgroup	
Low	14 (29)
Intermediate	15 (31)
High	10 (20)
Very high	10 (20)

Data are presented as mean±SD or n (%), unless otherwise stated. NYHA: New York Heart Association; TLC: total lung capacity; % pred: % predicted; FVC: forced vital capacity; RV: residual volume; FEV_1: forced expiratory volume in 1 s; $D_{L,CO}$: diffusing capacity of the lung for carbon monoxide; HRCT: high-resolution computed tomography. #: n=47.

Correlation between HRCT and lung function at diagnosis

At diagnosis, the HRCT nodular score was not correlated with any lung function parameters or with a restrictive or an obstructive pattern. By contrast, the HRCT cystic score was inversely correlated with the FEV_1, FEV_1/FVC ratio (r= -0.7, p<0.0001), and $D_{L,CO}$ (r= -0.38, p=0.01) and positively correlated with air trapping (RV/TLC % pred; r=0.63, p<0.0001). The 15 patients with airway obstruction had higher HRCT cystic scores than the patients without obstruction (17.6±5.9 and 9.4±4.1, respectively; p<0.001). The HRCT cystic score at diagnosis discriminated between the patients with and without an obstructive lung function pattern, with AUC of 0.86 (95% CI 0.73–0.99). A cut-off value of 14 for the HRCT cystic score predicted an obstructive pattern with a sensitivity of 80% and a specificity of 91.2%. There was no difference in tobacco consumption at diagnosis among these patients (p=0.51).

Evolution of lung function and HRCT findings during follow-up

The median follow-up was 36 months (IQR 17–67 months), with a median of two longitudinal and lung function evaluations (IQR 1–3 months). Six (12.2%) patients were lost to follow-up before any deterioration of their lung function after a median time of 3 yrs of follow-up. Table 2 shows the lung function outcomes for the study population. These results were confirmed when estimating the cumulative incidence of patients with either deteriorated or improved lung function over time (fig. 1).

The changes in the different lung function parameters varied considerably, with the $D_{L,CO}$ being the parameter that improved the least frequently (table 2 and fig. 1). It is noteworthy that among the 19 patients who had an impaired FEV_1 during follow-up, 10 (52.6% or 20.5% of the study population) had deteriorated soon after their diagnoses. The median FEV_1 decrease within the first 2 yrs for these 10 patients was -235 mL (IQR -340– -200 mL; -18% compared to the values at diagnosis, IQR -21– -11%), whereas it was -30 mL (IQR -195–100 mL) for the nine patients whose FEV_1 deteriorated later (-6% of the value at diagnosis, IQR -13– -4%).

Six patients developed a new-onset airflow obstruction, among whom one patient displayed a mixed pattern (TLC 83% and 79% pred, respectively, at diagnosis and at 68 months of follow-up). Thus, 21 (43%) patients had an obstructive pattern at some point (mean FEV_1 1,900±655 mL (54.4±16.8% pred) at the time of last follow-up). Conversely, the three patients who had mild restriction at diagnosis had normal TLCs at their last evaluations.

The variations in the nodular and cystic CT scores over time were inversely correlated (p<0.05). Overall, the mean nodular score decreased during the follow-up. At the final follow-up, 45 (92%) of the patients had a low nodular CT score, and four (8%) of the patients had an intermediate CT nodular score. By contrast, the mean value of the cystic HRCT score increased over time (p<0.01). At the last evaluation, 26 (53%) patients had a high or very high CT cystic score.

The effects of smoking cessation on the variations in the lung function and HRCT findings

Of the 46 patients who were current smokers at diagnosis, 16 stopped smoking during the follow-up, with a median time to cessation of 11 months (IQR 0–24.5 months). The lung function results and HRCT nodular and cystic scores of these patients at diagnosis were similar to those who continued to smoke (not shown). No statistical differences in lung function outcomes, including decline *versus* improvement of FEV_1, were observed between the two groups of patients (table 3). The hazard ratio (HR) for developing airflow obstruction during follow-up was not significantly different after smoking cessation (p=0.66). No significant differences were observed between the mean nodular and cystic CT scores of the patients who ceased smoking and the scores of those who continued to smoke.

Correlation between HRCT and lung function during follow-up

The variations in the HRCT nodular score over time and lung function outcomes were not correlated (p=0.91). Conversely, the variations in the HRCT cystic score were inversely correlated

TABLE 2 Lung function outcomes in the complete study population

Lung function	Improvement	Deterioration	Cumulative incidence of deterioration at 5 yrs %
Overall	10 (20.5)	28 (57)	59.4
FVC	9 (18.3)	11 (22,5)	24.7
FEV1	8 (16)	19 (39)	42.6
***D*L,CO#**	2/40 (5)	18/40 (45)	47.9

Data are presented as n (%), unless otherwise specified. For each parameter, changes of ⩾10% in forced expiratory volume in 1 s (FEV1) or forced vital capacity (FVC) or of ⩾15% in diffusing capacity of the lung for carbon monoxide (*D*L,CO) constituted improvement or deterioration. The overall lung function outcome was defined based on increases or decreases of ⩾10% in FEV1 and/or FVC and/or of ⩾15% in *D*L,CO. In case of discrepancies, the impaired parameter was used. The patients whose lung function was stable (neither improved nor deteriorated) are not shown. The estimated cumulative incidences of deterioration in lung function parameters at 5 yrs were calculated considering the competing risks framework for overall lung function and according to each lung function parameter. #: serial *D*L,CO results were available for 40 patients.

with variations in *D*L,CO (p=0.0001), FVC (p=0.0001) and FEV1 (p=0.002). Among the 19 patients whose FEV1 deteriorated, 10 (52.6%) had higher HRCT cystic scores, as compared to two (25%) among the eight patients whose FEV1 improved. Once the HRCT cystic score increased, however, the HR for a deteriorating FEV1 was not significantly increased (HR 2.1, 95% CI 0.47–9.64; p=0.32). The increase in the HRCT cystic score did not precede the deterioration in the FEV1 or the *D*L,CO (fig. 2).

Prognostic analyses

None of the factors evaluated at diagnosis was significantly associated with FEV1 deterioration. Notably, the FEV1 at

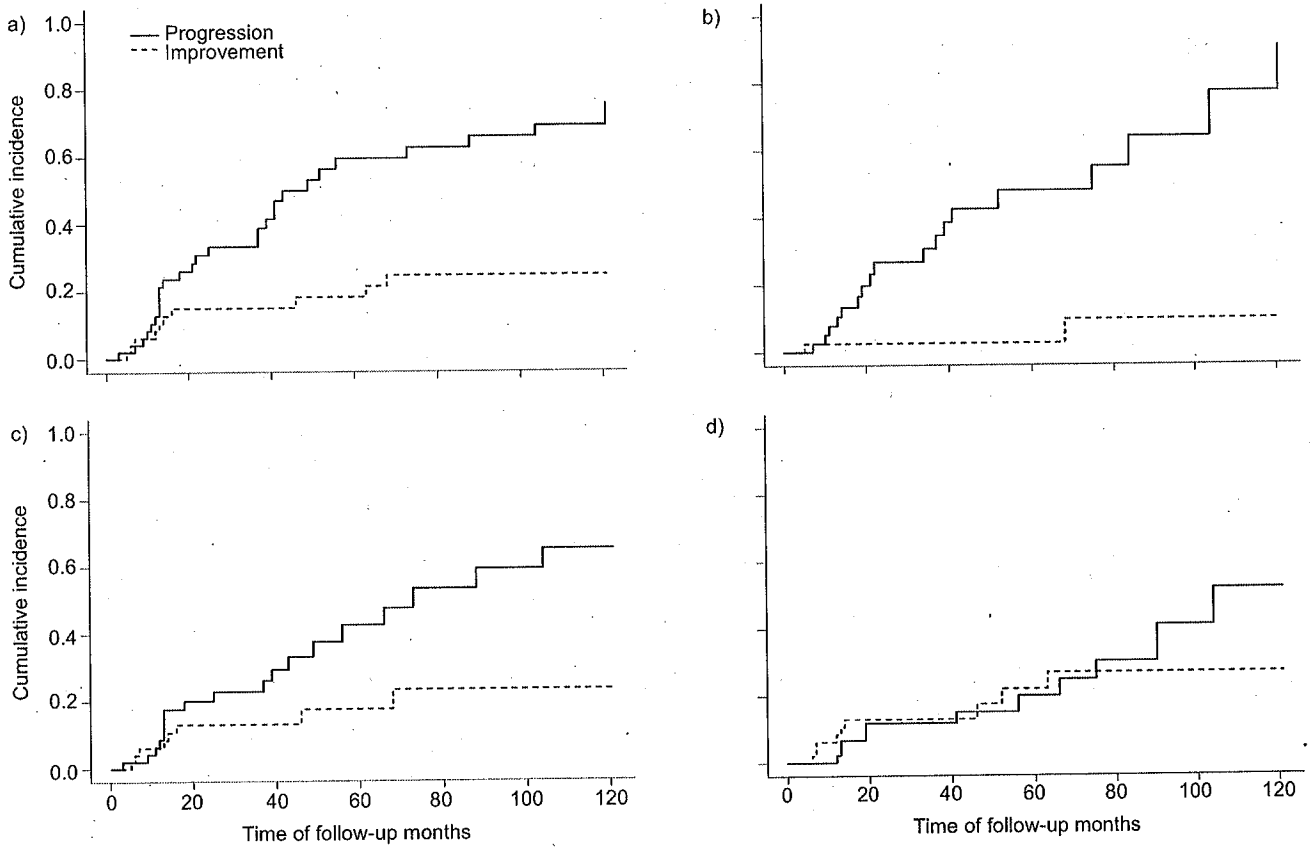

FIGURE 1. The estimated cumulative incidences of deterioration or improvement in the lung function of the study population over time. a) Overall lung function. Increase or decrease of ⩾10% in forced expiratory volume in 1 s (FEV1) and/or forced vital capacity (FVC) and/or of ⩾15% in diffusing capacity of the lung for carbon monoxide (*D*L,CO). In case of discrepancies, the impaired parameter was used; b) *D*L,CO; c) FEV1; d) FVC.

TABLE 3 Lung function outcomes according to continued smoking or smoking cessation in pulmonary Langerhans' cell histiocytosis patients who were current smokers at the time of diagnosis

Lung function	Improvement		Deterioration	
	Continued smoking	Smoking cessation	Continued smoking	Smoking cessation
Subjects	30	16	30	16
Overall	5 (17)	5 (31)	17 (56)	8 (50)
FVC	5 (17)	4 (25)	7 (23)	2 (12.5)
FEV_1	5 (17)	3 (19)	13 (43)	4 (25)
$D_{L,CO}$	1/25 (4)	1/13 (8)	13/25 (52)	4/13 (31)

Data are presented as n or n (%). n=46. The lung function parameters represent all patients, unless otherwise specified. For each parameter, changes of ⩾10% in forced expiratory volume in 1 s (FEV_1) or forced vital capacity (FVC), or of ⩾15% in diffusing capacity of the lung for carbon monoxide ($D_{L,CO}$) constituted improvement or deterioration. The overall lung function outcome was defined based on increases or decreases of ⩾10% in FEV_1 and/or FVC and/or of ⩾15% in $D_{L,CO}$. In case of discrepancies, the impaired parameter was used. p-values were not significant for any of the comparisons.

diagnosis did not differ between the patients who deteriorated (2,456±987 mL; 71±24% pred) and the patients who did not (2,840±796 mL; 82±20% pred). No factor at diagnosis could distinguish the subgroup of 10 patients whose FEV_1 deteriorated within the first 2 yrs of follow-up except that, surprisingly, their mean cumulative tobacco consumption was lower compared with the remaining patients (table 4). However, the hazard of early decline of FEV_1 was not statistically modified by tobacco consumption, either unadjusted (HR 0.94, 95% CI 0.88–1.02; p=0.1) or adjusted for age and sex (HR 0.94, 95% CI 0.86–1.02; p=0.11). Furthermore, no factor at diagnosis could differentiate between the patients whose FEV_1 decreased within the first 2 yrs and those in whom it declined later. Finally, smoking cessation had no influence on whether the FEV_1 decreased within the first 2 yrs (p=0.90).

A significant difference in the cumulative incidence of airflow obstruction according to the HRCT cystic score at diagnosis was observed (p<0.0001; table 5). In the multivariate model, however, only the FEV_1 % pred at diagnosis remained significantly associated with the incidence of airflow obstruction (p=0.0006). Thus, a smaller FEV_1 % pred at diagnosis was associated with a greater risk of developing airflow obstruction.

DISCUSSION

This is the largest cohort study evaluating the long-term variations in lung function and HRCT findings in patients with pulmonary LCH. We determined the rate and lung function deterioration profile of these patients and identified a sizeable group of patients who experienced dramatic declines in their FEV_1 values early in the course of the disease. We also provided additional information concerning the prognostic value of lung HRCTs, both at diagnosis and during follow-up.

Overall, lung function deteriorated in ~60% of the patients and improved in 20%. The evolution of the different lung function parameters was heterogeneous. $D_{L,CO}$ deteriorated in approximately half of the patients, and FEV_1 deteriorated in 40% of them, while FVC significantly decreased during follow-up in a minority of the patients. Strikingly, we identified two populations of

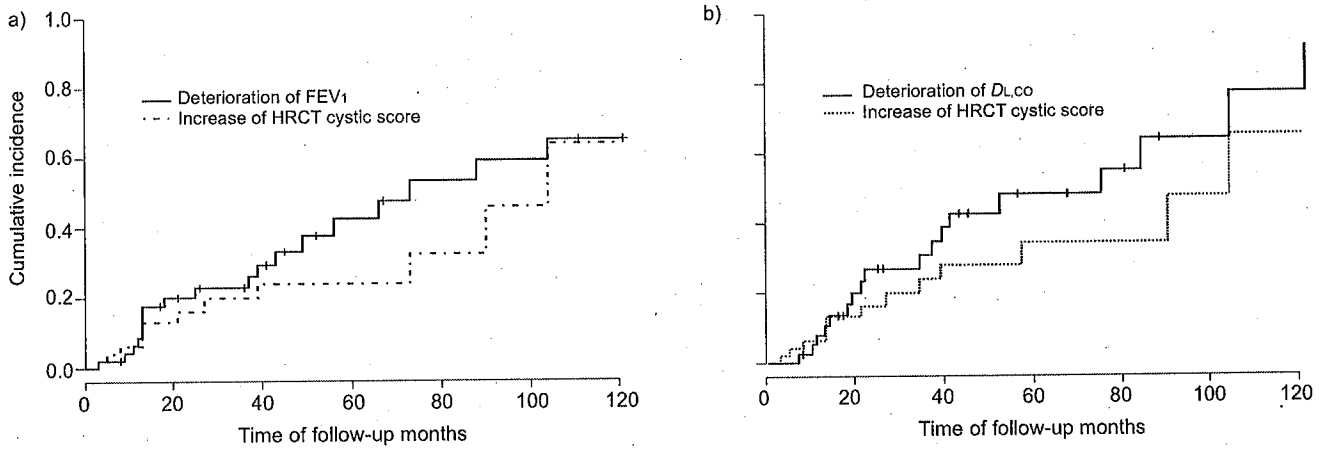

FIGURE 2. A comparison of the study population's estimated cumulative incidences of deterioration of lung function and high-resolution computed tomography (HRCT) cystic score variation over time. a) forced expiratory volume in 1 s (FEV_1); b) diffusing capacity of the lung for carbon monoxide ($D_{L,CO}$). Although the two curves follow parallel courses, note that the increase in the extent of the cystic lesions did not precede either the FEV_1 or the $D_{L,CO}$ impairment.

TABLE 4 Characteristics of the patients whose forced expiratory volume in 1s (FEV_1) decreased within the first 2 yrs after their pulmonary Langerhans' cell histiocytosis diagnosis compared with the remaining study population

Characteristic	Decline of FEV_1 within 2 yrs	No decline of FEV_1 within 2 yrs	p-value
Subjects n	10	39	
At diagnosis			
Age yrs	28.1±8.6	31.5±7.5	0.24
Male sex	4 (40.0)	20 (51.3)	0.73
Smoking status			
Current smokers	8 (80.0)	38 (97.4)	0.10
Ex-smokers	2 (20.0)	1 (2.6)	
Exposure pack-years	11.0±9.4	24.4±20.0	0.02
TLC % pred[#]	99.4±15.9[+]	100.6±16.9	0.90
FVC % pred	86.3±18.9	89.8±18.7	0.79
FEV_1 % pred	74.7±21.6	78.3±22.2	0.65
FEV_1/FVC %	71.1±11.3	73.2±13.0	0.48
RV % pred[#]	137.1±52.4[+]	127.3±47.1[##]	0.69
RV/TLC % pred[#]	137.0±48.1[+]	123.6±35.0[##]	0.64
$D_{L,CO}$ % pred[#]	70.9±27.9[§]	60.6±20.9[¶¶]	0.39
HRCT nodular score	6.4±4.8	6.7±3.0	0.65
HRCT cystic score	13.1±7.4	11.6±5.7	0.61
During follow-up			
$D_{L,CO}$ deterioration[¶]	5/8 (62.5)[/]	13/32 (40.6)[++]	0.43
Smoking cessation	1/8 (12.5)	15/38 (39.5)	0.23

Data are presented as mean±SD or n (%), unless otherwise stated. The lung function parameters represent all patients, unless otherwise specified. TLC: total lung capacity; % pred: % predicted; FVC: forced vital capacity; RV: residual volume; $D_{L,CO}$: diffusing capacity of the lung for carbon monoxide; HRCT: high-resolution computed tomography. [#]: at diagnosis. TLC and RV results were available for 47 patients and $D_{L,CO}$ for 42 patients; [¶]: serial $D_{L,CO}$ results were available for 40 patients; [+]: n=10; [§]: n=9; [/]: n=8; [##]: n=37; [¶¶]: n=33; [++]: n=32.

TABLE 5 Univariate prognostic analyses of the factors measured at diagnosis that were candidates for predicting the incidence of airway obstruction[#]

Characteristic	HR (95% CI)	p-value
Age per 10 yrs	0.93 (0.52–1.67)	0.81
Smoking per 10 pack-yrs	1.06 (0.87–1.28)	0.56
Dyspnoea	1.01 (0.42–2.39)	0.99
TLC % pred[¶]	1.17 (0.91–1.50)	0.22
FVC % pred[¶]	0.75 (0.57–0.99)	0.04
FEV_1 % pred[¶]	0.59 (0.45–0.77)	0.0001
FEV_1/FVC %[¶]	0.54 (0.42–0.69)	0.0001
RV % pred[¶]	1.16 (1.08–1.26)	0.0002
RV/TLC % pred[¶]	1.24 (1.11–1.39)	0.0002
$D_{L,CO}$ % pred[¶]	0.04 (0.03–0.47)	0.01
HRCT nodular score	0.91 (0.80–1.03)	0.13
HRCT cystic score	1.13 (1.05–1.21)	0.0009

HR: hazard ratio; TLC: total lung capacity; % pred: % predicted; FVC: forced vital capacity; FEV_1: forced expiratory volume in 1 s; RV: residual volume; $D_{L,CO}$: diffusing capacity of the lung for carbon monoxide; HRCT: high-resolution computed tomography. [#]: A total of 21 (43%) out of 49 patients had an obstructive pattern (FEV_1/FVC <70%) at any time during the study; [¶]: the HR is calculated for 10% variations in the predicted values.

patients with different FEV_1 impairment profiles over time. Approximately half of these patients experienced a dramatic decline in their FEV_1 within the 2 yrs following diagnosis. The median rate of FEV_1 decline in these patients was markedly more pronounced than that reported for smokers and patients with chronic obstructive pulmonary disease (COPD) [17]. Unfortunately, we were unable to identify a predictive factor at diagnosis that identified this subgroup of patients.

Airway obstruction was the salient pattern of lung function defect observed both at diagnosis and during the course of the disease. This finding is consistent with the bronchiolar localisation of pulmonary LCH lesions [18] and with the functional pattern observed in other diffuse cystic lung diseases, such as lymphangiomyomatosis [19].

The $D_{L,CO}$ decline was isolated in some of the patients, which may suggest the development of pulmonary hypertension (PH), a known complication of pulmonary LCH [20–24]. Although echocardiography or right heart catheterisation results were not available for these patients, this assumption is consistent with a recent study we performed in patients with pulmonary LCH and PH, in whom isolated declines in $D_{L,CO}$ were associated with the development of PH [24].

In this large cohort, we confirmed that the extent of the HRCT cystic lesions is correlated with various lung function parameters [11–13]. Additionally, we found that the HRCT cystic score was both sensitive and specific for discriminating between

the patients with and without airflow obstruction, both at diagnosis and during follow-up. However, although the hazard for having airway obstruction was strikingly increased in the patients with high cystic CT scores, only the FEV1 % pred at diagnosis remained a predictive factor for the incidence of airway obstruction in the multivariate analysis.

The extent of the nodular lesions decreased during follow-up, whereas the extent of the cystic lesions increased, as has been previously reported for smaller series [10, 13]. No patients had high nodular CT scores at the time of the last evaluation, whereas half the patients had a high or very high cystic CT score. Although this increase in the cystic CT score was correlated with deterioration in several lung function parameters, it did not precede the FEV1 or the $D_{L,CO}$ decrease over time. Thus, the initial lung HRCT findings are useful for both the diagnosis and prognosis of pulmonary LCH, but our results suggest that routine serial CT scans add limited information to lung function measurements during patient follow-up.

Surprisingly, smoking cessation did not modify the pulmonary LCH outcomes. As this study was retrospective and no surrogate marker was available to ascertain smoking cessation, definitive conclusions should not be drawn from these results. The relatively small sample size (and thus, the limited statistical power) could also explain this negative finding. Obviously, continuing to smoke has several deleterious consequences for these patients, such as increased risk of COPD and lung cancer [25]. It should be stressed, however, that although improved pulmonary LCH has been reported in patients who have stopped smoking, the effect of smoking cessation on the outcome of the disease has not been rigorously evaluated [26].

This retrospective study has several limitations. As the patients were sequentially included during the study period, the follow-up time was variable. Although adequate statistical methods for time-to-event data were used, we cannot exclude a bias toward an over-representation of patients with unfavourable outcomes. It is also possible that the patients selected for this study may not have been fully representative of the general pulmonary LCH population, although the lung function at diagnosis of our patients was similar to the lung function reported in previous studies [5–8]. Finally, as systemic treatments were prescribed according to the physicians' discretion, we could not evaluate their effects on the pulmonary LCH outcomes. In a previous study, corticosteroid therapy was associated with poorer outcomes, probably as a result of selection bias towards more severe forms of the disease [6].

In summary, this study provides important clinical insights into the long-term lung function outcomes of patients with pulmonary LCH. In practice, serial lung function tests are important during follow-up. Lung function should be closely monitored during the first 2 yrs after diagnosis. A lung HRCT at diagnosis is informative, but routine serial CT scans seem less useful for managing these young patients, in whom the radiation burden is a concern. Prospective studies are needed to better characterise the patients who progress soon after diagnosis and to assess the effects of controlled smoking cessation on pulmonary LCH outcomes.

STATEMENT OF INTEREST

A statement of interest for D. Valeyre can be found at ww.erj.ersjournals.com/site/misc/statements.xhtml

ACKNOWLEDGEMENTS

Author affiliations are as follows. A. Tazi, K. Marc and G. Lorillon: Reference Centre for Langerhans Cell Histiocytosis, University Paris Diderot, Sorbonne Cité, Assistance Publique Hôpitaux de Paris, Pulmonary Dept, Saint-Louis Hospital, Paris, France; S. Dominique: University of Rouen, Pulmonary Dept, Charles Nicolle Hospital, Rouen, France; C. de Bazelaire and J. Frija: University Paris Diderot, Sorbonne Cité, Assistance Publique Hôpitaux de Paris, Radiology Dept, Saint-Louis Hospital, Paris, France; B. Crestani: University Paris Diderot, Sorbonne Cité, Assistance Publique Hôpitaux de Paris, Pulmonary Dept, Bichat Hospital, Paris, France; T. Chinet: University of Versailles Saint Quentin en Yvelines, Assistance Publique Hôpitaux de Paris, Pulmonary Dept, Ambroise Paré Hospital, Paris, France; D. Israel-Biet: University Paris 5, Sorbonne Cité, Assistance Publique Hôpitaux de Paris, Pulmonary Dept, European Georges Pompidou Hospital, Paris, France; J. Cadranel: University Paris 6, Assistance Publique Hôpitaux de Paris, Pulmonary Dept, Tenon Hospital, Paris, France; D. Valeyre: University Paris 13, Sorbonne Cité, Assistance Publique Hôpitaux de Paris, Pulmonary Dept, Avicenne Hospital, Paris, France; S. Chevret: INSERM U 717, University Paris Diderot, Sorbonne Cité, Assistance Publique Hôpitaux de Paris, Biostatistics Dept, Saint-Louis Hospital, Paris, France.

The authors thank M. Mao (Assistance Publique Hôpitaux de Paris, Pulmonary Dept, Saint-Louis Hospital, Paris, France) and E. Savariau (Institut Universitaire d'Hématologie, Service d'Infographie, Saint-Louis Hospital, Paris, France) for their technical assistance.

REFERENCES

1 Abbott GF, Rosado-de-Christenson ML, Franks TJ, *et al.* From the archives of the AFIP: pulmonary Langerhans cell histiocytosis. *Radiographics* 2004; 24: 821–841.
2 Sundar KM, Gosselin MV, Chung HL, *et al.* Pulmonary Langerhans cell histiocytosis: emerging concepts in pathobiology, radiology, and clinical evolution of disease. *Chest* 2003; 123: 1673–1683.
3 Tazi A. Adult pulmonary Langerhans' cell histiocytosis. *Eur Respir J* 2006; 27: 1272–1285.
4 Vassallo R, Ryu JH, Colby TV, *et al.* Pulmonary Langerhans'-cell histiocytosis. *N Engl J Med* 2000; 342: 1969–1978.
5 Basset F, Corrin B, Spencer H, *et al.* Pulmonary histiocytosis X. *Am Rev Respir Dis* 1978; 118: 811–820.
6 Delobbe A, Durieu J, Duhamel A, *et al.* Determinants of survival in pulmonary Langerhans' cell granulomatosis (histiocytosis X). Groupe d'Etude en Pathologie Interstitielle de la Societe de Pathologie Thoracique du Nord. *Eur Respir J* 1996; 9: 2002–2006.
7 Schonfeld N, Frank W, Wenig S, *et al.* Clinical and radiologic features, lung function and therapeutic results in pulmonary histiocytosis X. *Respiration* 1993; 60: 38–44.
8 Travis WD, Borok Z, Roum JH, *et al.* Pulmonary Langerhans cell granulomatosis (histiocytosis X). A clinicopathologic study of 48 cases. *Am J Surg Pathol* 1993; 17: 971–986.
9 Vassallo R, Ryu JH, Schroeder DR, *et al.* Clinical outcomes of pulmonary Langerhans'-cell histiocytosis in adults. *N Engl J Med* 2002; 346: 484–490.
10 Brauner MW, Grenier P, Tijani K, *et al.* Pulmonary Langerhans cell histiocytosis: evolution of lesions on CT scans. *Radiology* 1997; 204: 497–502.
11 Canuet M, Kessler R, Jeung MY, *et al.* Correlation between high-resolution computed tomography findings and lung function in pulmonary Langerhans cell histiocytosis. *Respiration* 2007; 74: 640–646.
12 Moore AD, Godwin JD, Muller NL, *et al.* Pulmonary histiocytosis X: comparison of radiographic and CT findings. *Radiology* 1989; 172: 249–254.

13 Abbritti M, Mazzei MA, Bargagli E, *et al.* Utility of spiral CAT scan in the follow-up of patients with pulmonary Langerhans cell histiocytosis. *Eur J Radiol* 2011; [Epub ahead of print DOI: 10.1016/j.ejrad.2011.04.018].
14 Standardized lung function testing. Official statement of the European Respiratory Society. *Eur Respir J* 1993; 6: Suppl. 16, 1–100.
15 Pauwels RA, Buist AS, Calverley PM, *et al.* Global strategy for the diagnosis, management, and prevention of chronic obstructive pulmonary disease. NHLBI/WHO Global Initiative for Chronic Obstructive Lung Disease (GOLD) Workshop summary. *Am J Respir Crit Care Med* 2001; 163: 1256–1276.
16 Bradley B, Branley HM, Egan JJ, *et al.* Interstitial lung disease guideline: the British Thoracic Society in collaboration with the Thoracic Society of Australia and New Zealand and the Irish Thoracic Society. *Thorax* 2008; 63: Suppl. 5, v1–v58.
17 Kohansal R, Martinez-Camblor P, Agusti A, *et al.* The natural history of chronic airflow obstruction revisited: an analysis of the Framingham offspring cohort. *Am J Respir Crit Care Med* 2009; 180: 3–10.
18 Kambouchner M, Basset F, Marchal J, *et al.* Three-dimensional characterization of pathologic lesions in pulmonary langerhans cell histiocytosis. *Am J Respir Crit Care Med* 2002; 166: 1483–1490.
19 McCormack FX. Lymphangioleiomyomatosis: a clinical update. *Chest* 2008; 133: 507–516.
20 Chaowalit N, Pellikka PA, Decker PA, *et al.* Echocardiographic and clinical characteristics of pulmonary hypertension complicating pulmonary Langerhans cell histiocytosis. *Mayo Clin Proc* 2004; 79: 1269–1275.
21 Dauriat G, Mal H, Thabut G, *et al.* Lung transplantation for pulmonary Langerhans' cell histiocytosis: a multicenter analysis. *Transplantation* 2006; 81: 746–750.
22 Fartoukh M, Humbert M, Capron F, *et al.* Severe pulmonary hypertension in histiocytosis X. *Am J Respir Crit Care Med* 2000; 161: 216–223.
23 Hamada K, Teramoto S, Narita N, *et al.* Pulmonary veno-occlusive disease in pulmonary Langerhans' cell granulomatosis. *Eur Respir J* 2000; 15: 421–423.
24 Le Pavec J, Lorillon G, Jais X, *et al.* Pulmonary arterial hypertension associated with pulmonary Langerhans cell histiocytosis: impact of pulmonary hypertension therapy. *Am J Respir Crit Care Med* 2011; 183: A5916.
25 Sadoun D, Vaylet F, Valeyre D, *et al.* Bronchogenic carcinoma in patients with pulmonary histiocytosis X. *Chest* 1992; 101: 1610–1613.
26 Vassallo R, Ryu JH. Tobacco smoke-related diffuse lung diseases. *Semin Respir Crit Care Med* 2008; 29: 643–650.

The present study shows that detection of influenza viral RNA by rRT-PCR is more efficient in EA than in NTS, probably because of the higher viral load in EA specimens.

Data comparing the yield of NTS and EA specimens for the diagnosis of influenza in adults are scarce. Using rRT-PCR, Rello and colleagues (7) reported false-negative results in 10% of NTS from patients admitted to the ICU. However, the authors did not take the samples simultaneously, and viral load was not quantified. Therefore, it is not possible to know whether the false negatives were due to low viral load, poorly collected specimens, inappropriate handling, delayed transport, or technical problems (12). Other authors present case reports or small series showing false-negative NTS specimens in patients with lower respiratory tract infection, although, once again, samples were not selected simultaneously (13). Rice and colleagues (10) recently reported better sensitivity for LRT specimens than for upper airway specimens; however, they collected their specimens within a 3-day period.

We demonstrated that EA is more sensitive than NTS (90.9% vs. 63.6%) for the diagnosis of 2009 pandemic influenza A H1N1 virus by real-time rRT-PCR. However, 10% of cases can go undetected if only EA specimens are investigated. The explanation for this difference in the yield of both specimens could be the higher viral load in lower respiratory tract secretions. In an experimental model of pandemic influenza H1N1 in ferrets, Munster and coworkers (14) demonstrated that viral replication is more efficient in the trachea, bronchi, and bronchioles than in the upper respiratory tract. In our patients, viral load was 3.75 times greater in EA specimens.

Our study is limited in that the small number of patients diminishes the power of the data analysis. In addition, we only enrolled intubated ICU patients, frequently with suspected pneumonia during the postpandemic period (2010–2011), when the prevalence of the pandemic influenza A H1N1v strain was still high. Therefore, we cannot be sure that our data can be extrapolated to non-ICU patients or to viruses other than H1N1.

In conclusion, our recommendation for an optimal diagnosis of influenza in ICU patients is to use mainly EA, but to include NTS where possible in order not to miss cases.

Author disclosures are available with the text of this letter at www.atsjournals.org.

Acknowledgment: The authors would like to thank Thomas O'Boyle for his help with the preparation of the manuscript.

PAULA LÓPEZ ROA, PHARM.D.
BELEN RODRÍGUEZ-SÁNCHEZ, B.SC., PH.D.
PILAR CATALÁN, PHARM.D.
MADDALENA GIANNELLA, M.D., PH.D.
LUIS ALCALÁ, PHARM.D.
BELÉN PADILLA, M.D.
Hospital General Universitario Gregorio Marañón
Madrid, Spain

DAVID GARCÍA VIEDMA, B.SC., PH.D.
Hospital General Universitario Gregorio Marañón
Madrid, Spain
and
CIBER de Enfermedades Respiratorias (CIBERES)
Madrid, Spain

PATRICIA MUÑOZ, M.D., PH.D.
EMILIO BOUZA, M.D., PH.D.
Hospital General Universitario Gregorio Marañón
Madrid, Spain
CIBER de Enfermedades Respiratorias (CIBERES)
Madrid, Spain
and
Universidad Complutense

References

1. Muller MP, McGeer A. Febrile respiratory illness in the intensive care unit setting: an infection control perspective. *Curr Opin Crit Care* 2006;12:37–42.
2. Sandrock C, Stollenwerk N. Acute febrile respiratory illness in the ICU: reducing disease transmission. *Chest* 2008;133:1221–1231.
3. Sandrock CE. Severe febrile respiratory illnesses as a cause of mass critical care. *Respir Care* 2008;53:40–53; discussion 53–57.
4. Rodriguez A, Diaz E, Martin-Loeches I, Sandiumenge A, Canadell L, Diaz JJ, Figueira JC, Marques A, Alvarez-Lerma F, Valles J, *et al.* Impact of early oseltamivir treatment on outcome in critically ill patients with 2009 pandemic influenza A. *J Antimicrob Chemother* 2011;66:1140–1149.
5. Hiba V, Chowers M, Levi-Vinograd I, Rubinovitch B, Leibovici L, Paul M. Benefit of early treatment with oseltamivir in hospitalized patients with documented 2009 influenza A (H1N1): retrospective cohort study. *J Antimicrob Chemother* 2011;66:1150–1155.
6. Ling LM, Chow AL, Lye DC, Tan AS, Krishnan P, Cui L, Win NN, Chan M, Lim PL, Lee CC, *et al.* Effects of early oseltamivir therapy on viral shedding in 2009 pandemic influenza A (H1N1) virus infection. *Clin Infect Dis* 2010;50:963–969.
7. Rello J, Rodriguez A, Ibañez P, Socias L, Cebrian J, Marques A, Guerrero J, Ruiz-Santana S, Márquez E, Del Nogal-Saez F, *et al.* Intensive care adult patients with severe respiratory failure caused by influenza A (H1N1)v in Spain. *Crit Care* 2009;13:R148.
8. Yeh E, Luc RE, Dyner L, Hong DK, Banaei N, Baron EJ, Pinsky BA. Preferential lower respiratory tract infection in swine-origin 2009 A (H1N1) influenza. *Clin Infect Dis* 2010;50:391–394.
9. Ngaosuwankul N, Noisumdaeng P, Komolsiri P, Pooruk P, Chokephaibulkit K, Chotpitayasunondh T, Sangsajja C, Chuchottaworn C, Farrar J, Puthavathana P. Influenza a viral loads in respiratory samples collected from patients infected with pandemic H1N1, seasonal H1N1 and H3N2 viruses. *Virol J* 2010;7:75.
10. Rice TW, Rubinson L, Uyeki TM, Vaughn FL, John BB, Miller RR III, Higgs E, Randolph AG, Smoot BE, Thompson BT. Critical illness from 2009 pandemic influenza A virus and bacterial coinfection in the United States. *Crit Care Med* 2012;40:1487–1498.
11. López-Roa P. Viral load relative quantification of influenza virus in paired lower respiratory tract (LRT) and nose-throat swabs (NTS) samples from patients admitted in intensive care units. Presented at the European Congress of Clinical Microbiology and Infectious Diseases. March 31 to April 3, 2012, London, UK. Abstract P-2328.
12. Singh K, Vasoo S, Stevens J, Schreckenberger P, Trenholme G. Pitfalls in diagnosis of pandemic (novel) A/H1N1 2009 influenza. *J Clin Microbiol* 2010;48:1502–1503.
13. Blyth CC, Iredell JR, Dwyer DE. Rapid-test sensitivity for novel swine-origin influenza A (H1N1) virus in humans. *N Engl J Med* 2009;361:2493.
14. Munster VJ, de Wit E, van den Brand JM, Herfst S, Schrauwen EJ, Bestebroer TM, van de Vijver D, Boucher CA, Koopmans M, Rimmelzwaan GF, *et al.* Pathogenesis and transmission of swine-origin 2009 A(H1N1) influenza virus in ferrets. *Science* 2009;325:481–483.

Cladribine Is Effective against Cystic Pulmonary Langerhans Cell Histiocytosis

Pulmonary Langerhans cell histiocytosis (PLCH) is a rare disease of unknown etiology characterized by the infiltration and destruction of the walls of distal bronchioles by Langerhans cell granulomas (1–3). In patients with progressive disease and impaired lung

Author Contributions: A.T. contributed to the study design, revising the paper, and the final approval of the manuscript. G.L. contributed to the data acquisition, drafting the article, and the final approval of the manuscript. A.B. contributed to drafting the article and the final approval of the manuscript. L.D., S.J., and B.W. contributed to the manuscript revision and the final approval of the manuscript. J.F. contributed to the radiological analysis and the final approval of the manuscript.

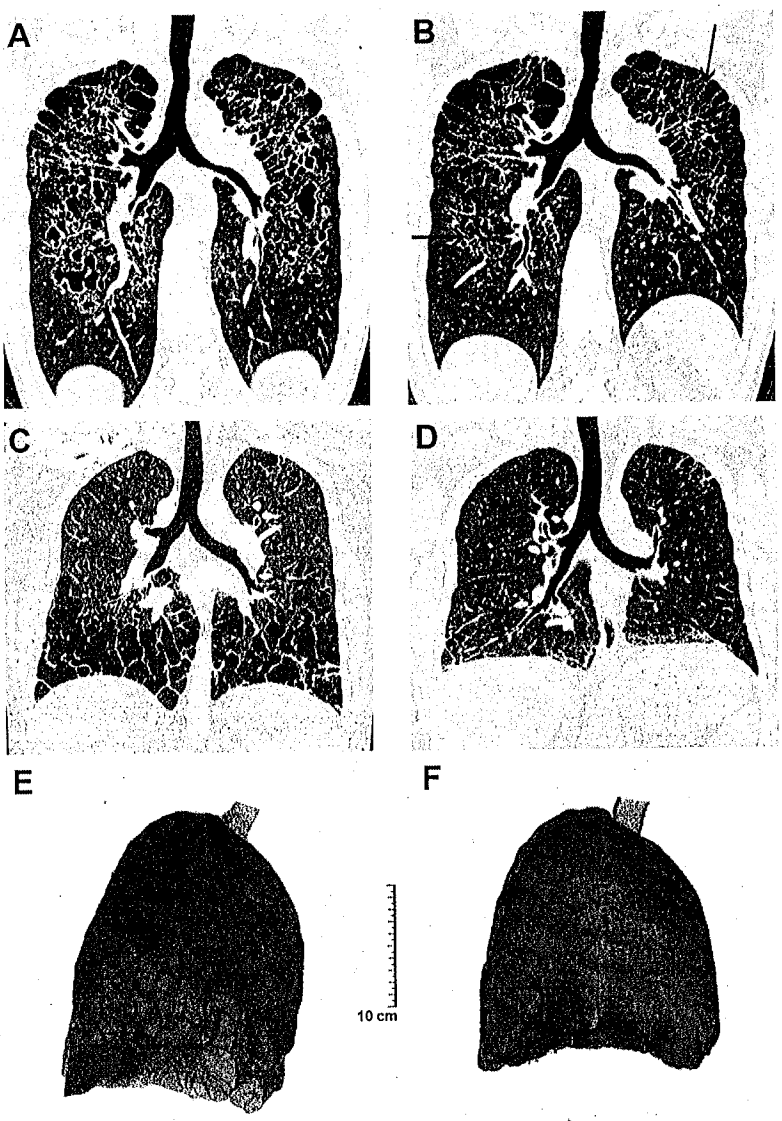

Figure 1. Comparative lung high-resolution computed tomography scans performed before and after treatment with cladribine in patients with pulmonary Langerhans cell histiocytosis. Thin coronal sections through the tracheal bifurcation are shown. (*A* and *B*) Patient 2. The thick-walled cysts were resolved with a fibrous local scar. Note the presence of increased traction emphysema and reduced lung volume in areas where the cystic lesions improved (*arrows*). (*C* and *D*) Patient 3. The bullocystic lesions dramatically collapsed, and lung volume decreased after treatment with cladribine. (*E* and *F*) Three-dimensional reconstruction of the serial lung high-resolution computed tomography scans from patient 3, performed before (*E*) and after (*F*) treatment with cladribine. The bullous subpleural lesions dramatically collapsed after cladribine treatment and were replaced by irregular linear scars. Note the reduction of lung volume after treatment, the retraction of the right inferior lobe, and the minimal dilation of the right upper and middle lobes. Smaller bullae remained present in the inferior part of the lung. *Scale bar* = 10 cm.

function, extensive cystic lesions are the main finding on high-resolution computed tomography (HRCT) scans (4–6), a radiological pattern usually considered end-stage disease. With the exception of lung transplantation, no treatments have been shown to be effective for these patients (7).

We report the cases of three patients, all current smokers, with progressive cystic PLCH who were significantly improved after treatment with cladribine, a purine nucleoside analog. After written informed consent, the patients received four to five courses of subcutaneous cladribine at 0.1 mg/kg/d for 5 consecutive days every month, as a salvage therapy (8). Oral trimethoprim/sulfamethoxazole and valaciclovir were administered to prevent opportunistic infections. In all cases, the treatment was well tolerated.

A 21-year-old male was referred for PLCH associated with diabetes insipidus and a biopsy-proven osteolytic lesion of the skull. Despite treatment with vinblastine and corticosteroids, his lung condition worsened to stage III World Health Organization (WHO) functional class dyspnea and his lung function deteriorated (FVC: 52%; FEV_1: 40% of predicted values; FEV_1/FVC: 71%). After treatment with cladribine, his dyspnea improved to stage II WHO functional class. The lung HRCT showed a partial resolution of both the nodular and cystic lesions. His FVC and FEV_1 values increased by 41 and 24%, respectively, compared with the pretreatment values.

Patient 2, a 32-year-old male, was diagnosed with PLCH on the presence of a combination of small nodules and thick-walled cysts on lung HRCT. He received oral corticosteroids for 18 months for stage II WHO functional class dyspnea. Despite this treatment, his dyspnea worsened to stage III, and his lung function revealed worsening of the diffusing capacity of carbon monoxide (D_{LCO}) value (24% of predicted), although the other parameters remained stable. No pulmonary hypertension was evidenced on two successive echocardiographs. The lung HRCT scan showed extensive thick-walled cysts (Figure 1A). After treatment with cladribine, his dyspnea improved to a class II WHO functional status. The lung HRCT showed that numerous thick-walled cysts had resolved and that the lung tissue initially containing these cysts had retracted and was surrounded by traction emphysema (Figure 1B). In addition, the D_{LCO} value significantly improved (+46% compared with the pretreatment value).

Patient 3, a 23-year-old man, had a long history of histologically proven multisystem LCH, which was diagnosed during his childhood and treated by corticosteroids and vinblastine with a good response. At 22 years of age, his LCH relapsed and

he complained of stage III WHO functional class dyspnea. Of note, he had begun smoking 5 years earlier. A lung HRCT scan demonstrated extensive bullocystic lesions predominantly in the lower regions of the lung (9). Despite treatment with vinblastine and corticosteroids, his lung function deteriorated (total lung capacity [TLC]: 77%; FVC: 47%; FEV_1: 37%; residual volume [RV]: 163%; D_{LCO}: 37% of predicted; FEV_1/FVC: 68%). After treatment with cladribine, his dyspnea improved to stage II. Strikingly, on serial lung HRCT scan, the confluent bullocystic lesions had almost completely resolved, whereas the lung volume had decreased (Figures 1C–1F). In parallel, his RV and TLC values decreased (respectively to 100 and 67% of predicted). In contrast, his FEV_1 and FVC levels had, respectively, increased by 71 and 40% compared with the pretreatment values.

These results clearly demonstrate that an isolated cystic pattern observed on lung HRCT in patients with PLCH does not necessarily represent end-stage disease (10, 11). A randomized controlled trial is strongly needed to assess the effectiveness and tolerance of cladribine in a larger population of patients with progressive PLCH.

Author disclosures are available with the text of this letter at www.atsjournals.org.

Acknowledgment: The authors thank Malika Mao and Elisabeth Savariau for their technical assistance.

GWENAEL LORILLON, M.D.
Assistance Publique Hôpitaux de Paris, Reference Center for Langerhans Cell Histiocytosis, Saint Louis Hospital
Paris, France

ANNE BERGERON, M.D., PH.D.
University Paris Diderot, Reference Center for Langerhans Cell Histiocytosis, Saint Louis Hospital
Paris, France

LAURENCE DETOURMIGNIES, M.D.
Roubaix Hospital
Roubaix, France

STÉPHANE JOUNEAU, M.D., PH.D.
University of Rennes 1, Pontchaillou Hospital
Rennes, France

BENOIT WALLAERT, M.D.
University of Lille 2, Calmette Hospital
Lille, France

JACQUES FRIJA, M.D., PH.D.
University Paris Diderot, Saint Louis Hospital
Paris, France

ABDELLATIF TAZI, M.D., PH.D.
University Paris Diderot, Reference Center for Langerhans Cell Histiocytosis, Saint Louis Hospital
Paris, France

References

1. Tazi A. Adult pulmonary Langerhans' cell histiocytosis. *Eur Respir J* 2006;27:1272–1285.
2. Kambouchner M, Basset F, Marchal J, Uhl JF, Hance AJ, Soler P. Three-dimensional characterization of pathologic lesions in pulmonary Langerhans cell histiocytosis. *Am J Respir Crit Care Med* 2002;166: 1483–1490.
3. Vassallo R, Ryu JH, Colby TV, Hartman T, Limper AH. Pulmonary Langerhans'-cell histiocytosis. *N Engl J Med* 2000;342:1969–1978.
4. Tazi A, Marc K, Dominique S, de Bazelaire C, Crestani B, Chinet T, Israel-Biet D, Cadranel J, Frija J, Lorillon G, *et al.* Serial CT and lung function testing in pulmonary Langerhans cell histiocytosis. *Eur Respir J* 2012;40:905–912.
5. Abbritti M, Mazzei MA, Bargagli E, Refini RM, Penza F, Perari MG, Volterrani L, Rottoli P. Utility of spiral CAT scan in the follow-up of patients with pulmonary Langerhans cell histiocytosis. *Eur J Radiol* 2011;81:1907–1912.
6. Canuet M, Kessler R, Jeung MY, Metivier AC, Chaouat A, Weitzenblum E. Correlation between high-resolution computed tomography findings and lung function in pulmonary Langerhans cell histiocytosis. *Respiration* 2007;74:640–646.
7. Dauriat G, Mal H, Thabut G, Mornex JF, Bertocchi M, Tronc F, Leroy-Ladurie F, Dartevelle P, Reynaud-Gaubert M, Thomas P, *et al.* Lung transplantation for pulmonary Langerhans' cell histiocytosis: a multicenter analysis. *Transplantation* 2006;81:746–750.
8. Robak T, Korycka A, Robak E. Older and new formulations of cladribine: pharmacology and clinical efficacy in hematological malignancies. *Recent Patents Anticancer Drug Discov* 2006;1:23–38.
9. Seely JM, Salahudeen S Sr, Cadaval-Goncalves AT, Jamieson DH, Dennie CJ, Matzinger FR, Souza CA. Pulmonary Langerhans cell histiocytosis: a comparative study of computed tomography in children and adults. *J Thorac Imaging* 2012;27:65–70.
10. Kim HJ, Lee KS, Johkoh T, Tomiyama N, Lee HY, Han J, Kim TS. Pulmonary Langerhans cell histiocytosis in adults: high-resolution CT-pathology comparisons and evolutional changes at CT. *Eur Radiol* 2011;21:1406–1415.
11. Soler P, Bergeron A, Kambouchner M, Groussard O, Brauner M, Grenier P, Crestani B, Mal H, Tazi A, Battesti JP, *et al.* Is high-resolution computed tomography a reliable tool to predict the histopathological activity of pulmonary Langerhans cell histiocytosis? *Am J Respir Crit Care Med* 2000;162:264–270.

Erratum: Alterations of the Arginine Metabolome in Asthma

The authors would like to correct errors they discovered in their 2008 *American Journal of Respiratory and Critical Care Medicine* article (1). They have found errors in the units that are listed for arginase activity and for amino acid concentrations. On page 675, the paragraph under the heading "Arginase Activity" contains several instances in which units of arginase activity are measured in mmol/ml/h; throughout this paragraph, these units should be corrected to "μmol/ml/h." On page 676, the first line of the first paragraph, and throughout Table 3, all instances of "mM" should be changed to "μM."

Reference

1. Lara A, Khatri SB, Wang Z, Comhair SAA, Xu W, Dweik RA, Bodine M, Levison BS, Hammel J, Bleecker E, *et al.*; National Heart, Lung, and Blood Institute's Severe Asthma Research Program. Alterations of the arginine metabolome in asthma. *Am J Respir Crit Care Med* 2008;178: 673–681.

Utilisation de VLB et stéroide chez les adultes G Lorillon St Louis

Utilisation du 2 cda chez l'adulte A Neel CHU Nantes

Diphosphonates Aracytine et autres traitements / Revue de la littérature M De Menthon St Louis

Radiothérapie chez l'adulte J Donadieu Trousseau

Thalidomide (équipe St Louis)

Euro Histio net E Schaefer Trousseau & Association Histiozytosehilfe e.V. Allemagne

Coopération France / Egypte M Sedlki

Atteintes neurologiques Enfants et Adultes Recommandations pour le diagnostic et la prise en charge des: A Idbaih K Hoang Xuan E Bayen / propositions de recommandations

2 Cda Arac - Mise à jour. Trop toxicité ? Recommandations thérapeutiques version 2013 J Donadieu Trousseau

Les recommandations HL 2010 offre une base pour la prise en charge des patients, dans la démarche diagnostique, l'évaluation, la thérapeutique.

Les propositions d'amendement concernent les points suivants:

* L'absence durable de caryolysine nous oblige à nous adapter. L'aldara a été suggéré mais ne semble pas consensuel. Une proposition, en cas d'échec au stéroïde local serait de recommander le purinethol.

* Généralisation de l'étude de l'oncogène B Raf pour tous nouveaux diagnostics des atteintes sévères.

* Association 2 cda Aracytine et aussi 2 Cda : Les modifications a introduire seraient de limiter à 3 cures maximum les cures de 2 Cda Arac, de recommander des mesures de prophylaxie anti bactérienne plus stringentes: Immunoglobulines IV / Bactrim à viser anti bactérienne et aussi anti Herpés.